David Alexandre Micael Pereira

METABOLITE PROFILING OF MARINE ORGANISMS : MODULATION OF ER-STRESS IN CANCER AND INFLAMMATION

Tese do 3º Ciclo de Estudos Conducente ao Grau de Doutor em Ciências Farmacêuticas

Especialidade de Fitoquímica e Farmacognosia

Trabalho realizado sob a orientação da

Professora Doutora Paula Cristina Branquinho de Andrade

e co-orientação da

Professora Doutora Natércia Aurora Teixeira

PORTO, Outubro de 2013

Trabalho apoiado financeiramente através da atribuição de uma bolsa de doutoramento pela Fundação para a Ciência e Tecnologia, no âmbito do POPH – QREN – Tipologia 4.1 – Formação Avançada, comparticipada pelo Fundo Social Europeu e por fundos nacionais do MCTES

É AUTORIZADA A REPRODUÇÃO PARCIAL DESTA TESE, APENAS PARA EFEITOS DE INVESTIGAÇÃO, MEDIANTE DECLARAÇÃO ESCRITA DO INTERESSADO QUE A TAL SE COMPROMETE.

Publicações:

Dos trabalhos descritos nesta dissertação resultaram as seguintes publicações:

Publicações em revistas indexadas no Journal Citation Reports da ISI Web of Knowledge:

1. Federico Ferreres, **David M. Pereira**, Angel Gil-Izquierdo, Patrícia Valentão, João Botelho, Teresa Mouga, Paula B. Andrade. Metabolite profiling of cytotoxic carotenoids from the echinoderm *Marthasterias glacialis* (spiny sea-star). Journal of Separation Science, 2010, 33, 2250-2257.

2. **Pereira, D.M.**, Vinholes, J., Correia-da-Silva, G., Valentão, P., Teixeira, N., Andrade, P.B. Fatty acids in marine organisms: In the pursuit of bioactive agents. Current Pharmaceutical Analysis, 2011, 7, 108-119.

3. **David M. Pereira**, Juliana Vinholes, Paula Guedes de Pinho, Patrícia Valentão, Teresa Mouga, Natércia Teixeira, Paula B. Andrade. A gas chromatography-mass spectrometry multi-target method for the analysis of three classes of metabolites in marine organisms. Talanta, 2012, 100, 391-400.

4. Lilian R. B. Mariutti, **David M. Pereira**, Adriana Zerlotti Mercadante, Patrícia Valentão, Natércia Teixeira, Paula B. Andrade. Further insights on the carotenoid profile of the echinoderm *Marthasterias glacialis*. Marine Drugs, 2012, 10, 1498-1510.

5. **David M. Pereira**, Patrícia Valentão, Natércia Teixeira, Paula B. Andrade. Amino acids, fatty acids and sterols profile of some marine organisms from Portuguese waters. Food Chemistry, 2013, 141, 2412-2417.

6. **David M. Pereira**, Georgina Correia-da-Silva, Patrícia Valentão, Teresa Mouga, Natércia Teixeira, Paula B. Andrade. GC-MS/MS Lipidomic Profiling of the Echinoderm *Marthasterias glacialis* and Screening for Bioactivity Against Human Cancer and Non-cancer Cell Lines. Submitted.

7. **David M. Pereira**, Georgina Correia-da-Silva, Patrícia Valentão, Natércia Teixeira, Paula B. Andrade. The anti-inflammatory effect of unsaturated fatty acids and ergosta-

7,22-dien-3-ol from the echinoderm *Marthasterias glacialis* involves prevention of CHOP pathway-mediated ER-stress and NF-κB activation. Submitted.

8. **David M. Pereira**, Georgina Correia-da-Silva, Patrícia Valentão, Natércia Teixeira, Paula B. Andrade. Palmitic acid and ergosta-7,22-dien-3-ol contribute to the ER-stress-mediated apoptotic effect and cell cycle arrest of an extract from *Marthasterias glacialis* L. in neuroblastoma cells. Submitted.

Capítulos de livros

1. **David M. Pereira**, Georgina Correia da Silva, Patrícia Valentão, Natércia Teixeira, Paula B. Andrade. Marine Metabolomics in Cancer Chemotherapy. *In* OMICS: Biomedical Prospective and applications", CRC Press. Edited by Debmalya Barh. pp. 377-398, 2011.

2. **David M. Pereira**, Patrícia Valentão, Paula B. Andrade. Lessons from the Sea: Distribution, SAR and Molecular Mechanisms of Anti-inflammatory Drugs from Marine Organisms. *In* Studies in natural products chemistry, vol. 40. Edited byAtta-ur-Rahman (Ed.). Elsevier Science Publishers, Amsterdam, The Netherlands, 2013, pp. 205-228, 2013.

Resumos publicados em revistas indexadas no Journal Citation Reports da ISI Web of Knowledge:

1. **D. Pereira**, G. Correia-da-Silva, P. Valentão, N. Teixeira, P. B. Andrade. Biological properties of a lipophilic extract of sea-star *Marthasterias glacialis* L. upon several cancer cell lines. The FEBS Journal, 279 (Supplement 1), 2012.

2. **D. Pereira**, G. Correia-da-Silva, P. Valentao, N. Teixeira, P. B. Andrade. Modulation of Cox-2 and iNOS expression in macrophages by a lipophylic extract of the sea-star *Marthasterias glacialis*: cooperative effect of fatty acids and ergosta-7,22-dien-3-ol. The FEBS Journal, 280 (Supplment 1), 2013.

Comunicações em congressos que foram submetidas a revisão pelas respectivas Comissões Científicas e ficaram registadas nos livros de actas

Comunicações orais

1. **David M. Pereira**, Federico Ferreres, Angel Gil-Izquierdo, Patrícia Valentão, Paula B. Andrade. Bioguided HPLC-PAD-APCI-MS metabolite profiling of cytotoxic carotenoids from the marine echinoderm *Marthastherias glacialis* (spiny sea-star). 3rd Meeting of Young Researchers of University of Porto. Porto, 17th-19th February 2010, Portugal.

2. **David M. Pereira**, Patrícia Valentão, Federico Ferreres, Angel Gil-Izquierdo, Georgina Correia da Silva, Natércia Teixeira, Paula B. Andrade. Marine organisms as a source of bioactive molecules: A case study with *Marthasterias glacialis* (spiny sea-star). International Meeting On Marine Resources, Peniche, 16th-18th November, 2010, Portugal.

3. **David M. Pereira**, Juliana Vinholes, Patrícia Valentão, Natércia Teixeira, Paula B. Andrade. A GC-MS multi-target method for the simultaneous analysis of three classes of metabolites in marine organisms. 3rd Portuguese Young Chemists Meeting. Porto, 11th May, 2012, Portugal

Comunicações sob a forma de painel

1. **David M. Pereira**, Federico Ferreres, Angel Gil-Izquierdo, Patrícia Valentão, Teresa Mouga, Paula B. Andrade. HPLC-PAD-APCI-MS analysis of carotenoids: a case study with the marine equinoderm *Marthasterias glacialis.* 2nd Portuguese Meeting of Young Chemists, Aveiro, 21st-23rd April, 2010, Portugal.

2. **David M. Pereira**, Federico Ferreres, Angel Gil-Izquierdo, Patrícia Valentão, Paula B. Andrade. *Marthasterias glacialis*: cytotoxic carotenoids metabolite profiling by HPLC-PAD-APCI-MS. Metabolomics 2010, Amsterdam, 27th June-1st July, 2010, The Netherlands.

3. **David Pereira,** G. Correia-da-Silva, P. Valentão, T. Mouga, N. Teixeira, P. B. Andrade. Biological effects of the carotenoid extract of *Marthasterias glacialis* (spiny

sea-star) against the cancer cell lines MCF-7 and SH-SY5Y. XVII National Congress of Biochemistry, Porto, 15-17th December, 2010, Portugal.

4. **D. Pereira**, G. Correia-da-Silva, P. Valentão, N. Teixeira, P. B. Andrade. Biological properties of a lipophilic extract of sea-star *Marthasterias glacialis* L. upon several cancer cell lines. Young Scientist Program (FEBS/IUBMB), Cádiz, 1st-4th September, 2012, Spain.

5. **D. Pereira**, G. Correia-da-Silva, P. Valentão, N. Teixeira, P. B. Andrade. Biological properties of a lipophilic extract of sea-star *Marthasterias glacialis* L. upon several cancer cell lines. 22nd IUBMB and 27th FEBS Congress. Seville, 4th-9th September, 2012, Spain.

6. **D. Pereira**, G. Correia-da-Silva, P. Valentão, N. Teixeira, P. B. Andrade. Modulation of COX-2 and iNOS expression in macrophages by a lipophylic extract of the sea-star *Marthasterias glacialis*: cooperative effect of fatty acids and ergosta-7,22-dien-3-ol. 37th FEBS Congress. St. Petersburg, 6th-11th July, 2013, Russia.

7. **D. Pereira**, G. Correia-da-Silva, P. Valentão, N. Teixeira, P. B. Andrade. The synergic anti-inflammatory effect of fatty acids and ergosta-7,22-dien-3-ol from *M. glacialis* involves prevention of CHOP pathway-mediated ER-stress and NF-κB activation. EMBO Young Scientists' Forum, Lisbon, 15th-16th July, 2013, Portugal.

O autor declara que participou ativamente na recolha e estudo do material incluído em todos os trabalhos, tendo redigido os textos com a colaboração dos restantes coautores.

Agradecimentos

Uma das maiores alegrias em atingir a meta que um Curso de Doutoramento constitui é a constatação do caminho percorrido, relembrando e agradecendo às pessoas sem as quais o percurso não teria sido possível:

À Profª Doutora Paula Andrade, por ter acreditado e apostado em mim quando era um aluno do 2º Ano do Mestrado Integrado em Ciências Farmacêuticas, aceitando-me como aluno de investigação no Laboratório de Farmacognosia. Agradeço-lhe a paixão incutida pela pela áreas da Farmacognosia e da Química, bem como pela actividade científica em que me iniciou e na qual representa para mim uma referência e exemplo a seguir, tendo a minha total admiração. Não tenho hoje qualquer dúvida que o contacto e convivência que tivemos nos primeiros anos de trabalho conjunto marcaram de forma profunda e irreversível a construção da minha personalidade, da minha identidade científica e da minha postura face à Ciência. E ainda bem. Agradeço ainda à Dra Paula, motor do Laboratório de Farmacognosia, por todo o percurso científico que me possibilitou percorrer e que culminou no currículo científico que hoje tenho e cujas origens e raízes nunca esquecerei. O que hoje tenho devo-o principalmente a si. Por isto, e muito mais, muito obrigado.

À Prof Doutora Natércia Teixeira, co-orientadora desta dissertação o meu agradecimento e admiração por ter sempre a porta aberta e disponibilidade para me receber, conversar, discutir e pensar. Agradeço-lhe por ser sempre uma fonte de serenidade, calma, reflexão e amizade. Estou igualmente muito grato por me ter recebido e dados as boas vindas no Laboratório de Bioquímica e pelo facto de, desde o primeiro momento, me ter feito sentir parte da equipa. Muito obrigado.

À Prof. Doutora Georgina Correia-da-Silva, por todo o apoio prestado e ajuda na execução da tese, pela sua paixão e fascínio contagiantes pela Ciência e pela sua curiosidade inata, com a qual me identifico. Agradeço-lhe profundamente por todo o apoio dado na realização desta tese e por me ter acolhido na sua equipa, bem como pelo seu incentivo constante a não tomar nenhum conhecimento como adquirido e a questionar continuamente tudo o que sabemos.

À Prof. Doutora Patrícia Valentão, pelos ensinamentos e paciência que sempre teve aquando da minha estadia no Laboratório de Farmacognosia ainda como aluno de

investigação. Agradeco-lhe todo o apoio que tornou esta tese possível, nomeadamente todas as diligências administrativas, bem como a sua ajuda indispensável aquando da escrita e revisão dos trabalhos e submissão dos mesmos, tarefa para a qual muito contribui a sua capacidade de pensamento analítico e atenção aos pormenores verdadeiramente únicas e que muito admiro.

À Prof. Doutora Teresa Mouga, da Escola Superior de Turismo e Tecnologias do Mar de Peniche, pela colaboração e fornecimento das amostras indispensáveis à realização deste trabalho.

À Fátima Fernandes, Andreia Oliveira e Marcos Taveira do Laboratório de Farmacognosia, ao qual tanto devo, pelo percurso que partilhámos durante anos, pelos bons momentos que passámos e também pela ajuda e apoio fundamentais para ultrapassar os maus momentos. Obrigado a todos.

À Engª Carla Sousa, por ter sido a primeira pessoa com quem trabalhei quando me iniciei no mundo da investigação, o meu reconhecimento por todos os ensinamentos e paciência.

A todos os meus colegas do Laboratório de Bioquímica, pelo ambiente acolhedor, divertido e crítico que sempre me proporcionariam. Um agradecimento especial ao Henrique Nascimento e João Fernandes, meus amigos, sócios e cúmplices, pelo seu apoio e amizade constantes e por terem tornado a minha experiência no Laboratório de Bioquímica tão rica. À Cristina Amaral, pela sua amizade, camaradagem e ajuda com os trabalhos de citometria de fluxo desenvolvidos ao longo desta tese. Ao Bruno Fonseca, companheiro de congressos, de bancada e amigo. À Marta Almada, pela sua irreverência que sempre constitui uma lufada de ar fresco. Não posso também deixar de agradecer à Susana Rocha pela disponibilidade e apoio demonstrados sempre que procurei o seu conselho e ajuda na condução de procedimentos laboratoriais. Obrigado a todos.

Um agradecimento também a todo o pessoal técnico que tornou este trabalho possível, nomeadamente o Rui Gonçalves do Laboratório de Farmacognosia e ainda o Luís Daniel, Ana Paula e D. Casimira do Laboratório de Bioquímica.

Aos meus amigos, por todo o apoio que sempre me deram, por terem sempre acreditado em mim e acima de tudo por toda a paciência demonstrada ao longo dos últimos 8 anos em todas as situações em que não pude estar com eles tantas vezes como gostaria. Valeu a

pena. Um agradecimento especial ao Telmo Oliveira, por ter sempre acreditado em mim cegamente e por todo o apoio prestado na prossecução dos meus objectivos.

A todos os meus Professores, pelo seu contributo para a minha formação científica e pelo apoio e curiosidade manifestados no decorrer desta dissertação.

À Cláudia Silva, pela sua amizade e presença na minha vida.

Um agradecimento especial aos meus pais, que desde sempre apoiaram e incentivaram a minha paixão pela Ciência, pelo apoio constante e por terem criado condições para que eu pudesse percorrer um percurso que agora culmina numa Curso de Doutoramento. Muito obrigado. Um agradecimento também ao meu irmão, por ser o meu maior fã. O sentimento é recíproco.

À Fundação para a Ciência e Tecnologia, pelo suporte financeiro da atribuição da bolsa de doutoramento SFRH/BD/62663/2009 no âmbito POPH – QREN – Tipologia 4.1 – Formação Avançada, comparticipada pelo Fundo Social Europeu e por fundos nacionais do MCTES.

RESUMO

RESUMO

Atualmente, a Natureza permanece uma fonte importante de moléculas com atividades biológica e interesse para a saúde humana.

Durante vários anos as plantas constituíram a única fonte de produtos naturais, no entanto este paradigma tem vindo a mudar em função da atenção dada a fontes alternativas de produtos naturais, tal como os organismos marinhos.

Neste trabalho foram conduzidos estudos de caracterização metabolómica em várias espécies de organismos marinhos obtidos em ecossistemas de Portugal, sendo que o equinoderme *Marthasterias glacialis* L. (estrela-do mar de espinhos) foi selecionada para subsequentes estudos biológicos.

Inicialmente, um extrato nativo foi obtido a partir de *M. glacialis* e analisado quando à sua composição em carotenóides. A análise por HPLC-DAD e APCI-LC-MS revelou vários isómeros destes compostos, tendo-se encontrado a astaxantina, zeaxantina e luteína como compostos mais relevantes. Esta fração do extrato mostrou exercer um forte efeito anti-proliferativo na linha celular cancerígena RBL-3H3 (leucemia basofílica de rato), enquanto que contra a linha celular não-cancerígena V79 (fibroblastos de pulmão de rato), a toxicidade foi marcadamente inferior.

De forma a caracterizar outros metabolitos com relevância biológica, foi desenvolvido um método de GC-MS/MS para a análise simultânea de três classes de metabolitos: aminoácidos, ácidos gordos saturados/insaturados e esteróis. Este método provou ser rápido, reprodutível e depende da extração dos metabolitos com etanol, evitando assim solventes orgânicos mais perigosos e poluentes. Bons parâmetros analíticos foram obtidos para os 40 compostos sob a análise, incluindo 15 aminoácidos, 16 ácidos gordos, 6 esteróis e 3 lupanos. Para validação da técnica foram utilizados extratos etanólicos de vários indivíduos de *M. glacialis* colhidos em diferentes pontos geográficos e em diferentes meses do ano. Este método foi posteriormente aplicado a outros organismos marinhos, nomeadamente os equinodermes *Paracentrotus lividus* Lamarck (ouriço-do-mar), *Holothuria forskali* Chiaje (pepino-do-mar) e os moluscos gastrópodes *Aplysia fasciata* Poiret e *Aplysia punctata* Cuvier (lesmas-do-mar). Todas as espécies apresentaram os aminoácidos estudados, com a exceção de *H. forskali*, onde não foi possível encontrar glicina, prolina, *trans*-4-hidroxi-prolina ou fenilalanina e *A. fasciata*, a qual não apresentou prolina. Com a excepção de *A. fasciata*, os ácidos gordos insaturados eram os ácidos gordos predominantes, em particular os pertencentes à série omega-6. No caso dos esteróis, os únicos compostos encontrados foram o colesterol, o β-sitoesterol e um derivado não identificado do colesterol. A espécie *P. lividus* foi aquela que apresentou maior quantidade de esteróis.

Em trabalhos subsequentes foi obtido um extrato purificado de *M. glacialis*, o qual continha principalmente os ácidos palmítico, *cis* 11-eicosenoico e *cis* 11,14-eicosadienoico e o esterol ergosta-7,22-dieno-3-ol e que foi usado nos estudos biológicos. Este extracto, bem como os seus compostos predominantes, foram avaliados pela sua atividade anti-inflamatória na linha de macrófagos de ratinho RAW 264.7, usando o LPS como estímulo pró-inflamatório e avaliando os níveis de expressão da COX-2, iNOS, IκB-α e CHOP. O composto ergosta-7,22-dieno-3-ol foi o composto mais potente, no entanto a atividade máxima foi atingida apenas quando todos os compostos foram utilizados em combinação. Os resultados demonstraram que a atividade anti-inflamatória do extrato e dos seus principais componentes envolve a prevenção da via de stress reticular mediado pela CHOP e ativação do NF-κB.

De seguida, foi avaliado o impacto deste extrato purificado na viabilidade, integridade membranar e densidade celular de 3 linhas celulares humanas cancerígenas (SH-SY5Y, neuroblastoma; MCF-7, cancro da mama recetor do estrogénio positivo; Caco-2, cancro do cólon) e 2 linhas humanas não-cancerígenas (HDF, fibroblastos da derme; HFF, fibroblastos do antebraço). Os resultados demonstraram a atividade distinta do extrato de acordo com a linha celular testada, sendo a linha SH-SY5Y a mais sensível. As células não-cancerígenas revelaram ser menos sensíveis que as cancerígenas. Estes resultados preliminares foram posteriormente confirmados ao estudar o mecanismo de ação responsável pelo efeito anticancerígeno encontrado. Foram utilizadas as linhas celulares MCF-7 e SH-SY5Y e a avaliação da síntese de DNA mostrou uma diminuição significativa, sendo a linha celular SH-SY5Y a mais suscetível. Observou-se paragem do ciclo celular na fase G0/G1, um efeito atribuído ao esterol ergosta-7,22-dieno-3-ol. Estudos morfológicos mostraram que o extrato causava o aparecimento de vesículas citoplasmáticas de conteúdo lipídico e condensação de cromatina compatível com apoptose, tendo este processo de morte celular sido confirmado por avaliação da atividade da caspase-9 e da caspase-3/7. O ácido palmítico revelou ser o principal responsável por este efeito pro-apoptótico, o qual foi demonstrado ser independente da ceramida e envolvendo a ativação da via de stress do reticulo endoplasmático.

Com esta tese de doutoramento, a composição química de vários macroorganismos marinhos de Portugal foi elucidada. O equinoderme *M. glacialis* foi selecionado para subsequentes estudos biológicos, tendo a sua atividade anticancerígena e anti-inflamatória demonstrada, estabelecendo assim este organismo como uma potencial fonte de moléculas bioativas com aplicação em várias patologias.

Palavras-chave: *Marthasterias glacialis*; Ácidos Gordos; Inflamação; Apoptose; Stress reticular

ABSTRACT

ABSTRACT

Nowadays, Nature still remains a very important source of biologically active molecules with application in human health.

For many years, plants have been the only natural products being studied, however this paradigm is being shifted towards alternative source of natural products, of which marine organism are a good example.

In this work, metabolite profiling was conducted in several species of marine macroorganisms obtained in Portuguese ecosystems, with *Marthasterias glacialis* (spiny sea star) being selected for further biological evaluation.

Initially, a crude extract obtained from *M. glacialis* was analyzed for its carotenoid composition. By employing HPLC-DAD and APCI-LC-MS, identification and differentiation of carotenoids isomers was achieved, with astaxanthin, zeaxanthin and lutein being the most important compounds. This carotenoid-enriched fraction displayed a strong cell proliferation inhibition against the rat basophilic leukemia cell line RBL-2H3, while against non-cancer rat lung fibroblasts the effect was weaker.

In order to evaluate other biologically-relevant metabolites in *M. glacialis*, a GC-MS/MS method for the simultaneous analysis of three classes of metabolites, amino acids, saturated/unsaturated fatty acids and sterols, was developed. This method was shown to be fast, reproducible and relied on extraction with ethanol without using organic solvents such as chloroform and ether. Good analytical parameters were obtained for the 40 compounds under analysis (15 amino acids, 16 fatty acids, 6 sterols and 3 lupanes). Crude ethanolic extracts of several individuals of *M. glacialis*, collected in different temporal and geographical points, were used for validating this technique. This method was later used in other marine organisms from Portuguese waters, the echinoderms *Paracentrotus lividus* Lamarck (sea urchin) and *Holothuria forskali* Chiaje (sea cucumber) and the gastropod mollusks *Aplysia fasciata* Poiret and *Aplysia punctata* Cuvier (sea hares). In general, all species presented the amino acids covered by the method, with the exceptions of *H. forskali*, in which no glycine, proline, *trans* 4-hydroxy-proline or phenylalanine were found, and of *A. fasciata* which did not contain proline. In what regards fatty acids, among all species studied 14 compounds were detected and 12 could be quantified. Apart from *A. fasciata*, unsaturated fatty acids were predominant compounds in all species, with those from the ω-6 series being in higher amounts than their ω -3 homologues. In the case of sterols, the only compounds found were cholesterol, β-sitosterol and one unidentified cholesterol derivative. *P. lividus* was the species with the highest sterol content.

After a deeper knowledge of the chemical composition of *M. glacialis* was achieved, a purified lipophilic extract containing mainly palmitic, *cis* 11-eicosenoic and *cis* 11,14-

eicosadienoic acids, as well as ergosta-7,22-dien-3-ol was evaluated for its biological properties. Initially, attention was given to the anti-inflammatory activity of the extract and its components. The purified extract, as well as the predominant compounds *cis* 11-eicosenoic and *cis* 11,14-eicosadienoic acids and the unsaturated sterol ergosta-7,22-dien-3-ol were evaluated for anti-inflammatory activity in the macrophage cell line RAW 264.7 challenged with LPS, as assessed by the expression levels of COX-2, iNOS, IκB-α and CHOP. Ergosta-7,22-dien-3-ol was the most active compound, although maximum activity was obtained only when all compounds were tested in combination. In addition, the anti-inflammatory activity of the extract from *M. glacialis* and its compounds was shown to involve prevention of CHOP pathway-mediated ER stress and NF-κB activation.

After the anti-inflammatory activity of the extract and its compounds was established, the anticancer activity of the same matrix was evaluated. Initial studies evaluated the impact of this purified extract (78-625 μg/mL) on cell viability, density and membrane integrity of three human cancer cell lines (SH-SY5Y, human neuroblastoma; MCF-7, human oestrogen receptor-positive breast cancer; Caco-2, human colon cancer) and two human non-cancer cell lines (HDF, human dermal fibroblasts; HFF, human foreskin fibroblasts). Differential activity towards the cell lines was found, being SH-SY5Y cell line the most susceptible. No activity was found for Caco-2 cell line and the non-cancer cell lines revealed to be less susceptible than cancer ones. These preliminary results were further investigated by studying the mechanism of action behind this activity. MCF-7 and SHSY-5Y cell lines were selected and evaluation of DNA synthesis revealed that both cell lines were markedly affected in a concentration-dependent way, being SH-SY5Y cell line more susceptible. G0/G1 cell cycle arrest was observed, an effect induced by the sterol ergosta-7,22-dien-3-ol present in the extract. Morphological studies showed that incubation with the extract caused the advent of lipid droplets and chromatin condensation, the latter compatible with apoptosis, which was confirmed by the evaluation of caspase-3/7 and -9 activities. Palmitic acid was the main compound responsible for this apoptotic effect by a ceramide-independent mechanism that involved activation of the CHOP-mediated ER stress pathway.

With the doctoral thesis presented herein, the chemical composition of several marine macroorganisms from Portuguese waters was established. The echinoderm *M. glacialis* was further studied and its anticancer and anti-inflammatory capacity was demonstrated, thus establishing this organism as a potential source of bioactive molecules with application in several pathologies.

Keywords: *Marthasterias glacialis*; Fatty acids; Inflammation; Apoptosis; ER stress

GENERAL INDEX

THESIS INDEX

FIGURE INDEX

ABREVIATIONS

$\Delta_{\psi m}$	Mitochondrial membrane potential
5-HETE	5-Hydroxyeicosatetraenoic acid
5-HPETE	5-Hydroperoxyeicosatetraenoic acid
ACP	Acyl carrier protein
AIF	Apoptosis inducing factor
ALA	α-Linolenic acid
Apaf-1	Apoptotic protease-activating factor 1
APCI	Atmospheric pressure chemical ionization
APCI-MS	Atmospheric pressure chemical ionization-mass spetrometry
ATF6	Activating transcription factor 6
ANT	Adenine nucleotide translocase
ATP	Adenosine-5'-triphosphate
Bak	Bcl-2 antagonis killer 1
Bax	Bcl-2 associated protein x
Bcl-xL	Bcl-2 long isoform
BH4	Tetrahydrobiopterin
BHT	Butylated hydroxytoluene
C/EBP	CCAAT-enhancer-binding proteins
Caco-2	Human colon adenocarcinoma cell line
CAT	Catalase
CHOP	C/EBP homologous protein
CLA	Conjugated linoleic acid
cPLA$_2$	Cytosolic PLA2s
CoA	Coenzyme A
COX	Cyclooxigenases
COX-2	Cyclooxigenase 2
CypD	Cyclophilin A
DAD	Diode array detector
DHA	Docosahexaenoic acid
DISC	Death-inducing signalling complex
DOXP	1-Deoxy-D-xylulose-5-phosphate
DMAPP	Dimethylallyl pyrophosphate
DMOX	4,4-Di-methyloxazoline
DR	Death receptor
dsRNA	Double stranded ribonucleic acid

EDEM	ER degradation-enhancing α-mannosidase-like protein
eIF2α	Eukaryotic translation-initiation factor 2α
EPA	Eicosapentaenoic acid
eNOS	Endothelial nitric oxide synthase
ER	Endoplasmic reticulum
ERO1	Endoplasmic reticulum oxidoreductin 1
ERSE	Endoplasmic reticulum stress responsive element
ESI	Electrospray ionization
FA	Fatty acids
FAD	Flavon adenine dinucleotide
FADD	Fas-associated death domain
FAME	Fatty acid methyl ester
FAK	Focal adhesion kinase
FasL	Fas ligand
FID	Flame ionization detector
FMN	Flavin mononucleotide
GADD153	DNA-damage inducible gene 153
GC	Gas chromatography
GC-MS	Gas chromatography-mass spectrometry
GPrx	Gluthatione peroxidase
GTP	Guanosine-5'-triphosphate
HDF	Human dermal fibroblasts
HFF	Human foreskin fibroblasts
HIF	Hypoxia inducing factor
HMG-CoA	3-Hydroxy-3-methylglutaryl-CoEnzyme A
HPLC	High pressure liquid chromatography
IFN-γ	Interferon gamma
IL	Interleukin
IκB-α	Nuclear factor kappa-light-chain-enhancer of activated B cells inhibitor alpha
IKK	IκB kinase complex
iPLA$_2$	Calcium-independent PLA$_2$
IPP	Isopentenyl pyrophosphate
iNOS	Inducible nitric oxide synthase
IRE1α	Inositol-requiring 1α
JNK	c-Jun N-terminal kinase
LA	Linolenic acid
LC-MS	Liquid chromatography-mass spectrometry

LOX	Lipoxygenase
$LpPLA_2$	Lipoprotein associated PLA_2
LPS	Lipopolysaccharide
LTA_4	Leukotriene A_4
LTB_4	Leukotriene B_4
LTC_4	Leukotriene C_4
LTD_4	Leukotriene D_4
LTE_4	Leucotriene E_4
MAP	Microtubule-associated proteins
MAPK	Mitogen-activated protein kinases
MCF-7	Human estrogen receptor positive breast cancer cell line
Mcl-1	Myeloid cell leukemia sequence 1
MEF	Mouse embrionyc fibroblasts cell line
MEP	2C-Methyl-D-erythritol-4-phosphate
miRNA	Micro RNA
MS	Mass spectrometry
MSTFA	N-methyl-*N*-(trimethylsilyl)-trifluoroacetamide
MTA	Microtubule targeting agents
MTT	(3-(4,5-dimethylthiazol-2-yl)-2,5-diphenyltetrazolium bromide
MUFA	Mono unsaturated fatty acids
MyD88	Myeloid differentiation factor 88
MuLV	Murine leukemia virus
NADPH	Nicotinamide adenine dinucleotide phosphate
NF-κB	Nuclear factor kappa-light-chain-enhancer of activated B cells
NMIFA	Non-methylene-interrupted fatty acids
nNOS	Neuronal nitric oxide synthase
NO	Nitric oxide
NOS	Nitric oxide synthase
nNOS	Neuronal nitric oxide synthase
PAF	Platelet-activating factor
PDI	Protein disulphide isomerase
PERK	Double-stranded RNA-dependent protein kinase (PKR)-like ER kinase
PGD_2	Prostaglandin D_2
PGE_2	Prostaglandin E_2
PGG_2	Prostaglandin G_2
PGH_2	Prostaglandin H_2
PGI_2	Prostaglandin I_2

PGF2	Prostaglandin F_2
PLA_2	Phospholipase A_2
PMA	Phorbol myristate acetate
PP2A	Protein phosphatase 2A
PPAR	Peroxisome proliferator-activated receptor
PTP	Permeability transition pores
PUFA	Polyunsaturated fatty acids
OMM	Outer mitochondrial membrane
Rnase	Ribonuclease
RNS	Reactive nitrogen species
ROS	Reactive oxygen species
RP-HPLC	Reversed phase high pressure liquid chromatography
SH-SY5Y	Human neuroblastoma cell line
SOD	Superoxide dismutase
SPE	Solid phase extraction
$sPLA_2$	Secreted PLA_2
TBARS	Thiobarbituric acid reactive substances
tBid	Truncated Bid
TG	Triglycerides
TIR	Toll/IL-1 receptor
TLC	Thin layer chromatography
TLR	Toll-like receptor
TLR4	Toll-like receptor 4
TMS	Trimethylsilyl
TNF-α	Tumor necrosis factor α
TNFR	Tumor necrosis factor receptor
TPA	12-*O*-Tetradecanoylphorbol-13-acetate
TXA_2	Thromboxane A_2
UPR	Unfolded protein response
UV	Ultraviolet
VDA	Vascular disrupting agents
VEGF	Vascular endothelial growth factor
VEGFR	Vascular endothelial growth factor receptor
VEGFR2	Vascular endothelial growth factor receptor 2
VLCFA	Very long chain fatty acids
VDAC	Voltage-dependent anionic chanel
WHO	World Health Organization

WT Wild type

PART I
INTRODUCTION AND OBJECTIVES

1.1. Nature as a source of bioactive molecules

Even in the periods of pre-technical medicine, humans have always pursued to counter diseases with medicines. For thousands of years, natural products have been the sole option for treating a number of pathological conditions in the form of tinctures, powders and decocts, among others (1). This happens due to the fact that Nature is, and has been, an undeniable source of bioactive molecules. In recent History, the development of medicine and chemotherapy led to an obvious convergence to the use of isolated molecules within a formulation rather than chemically complex mixtures, thus providing us with molecules such as morphine, codeine, digitoxin and vincristine.

The interest in natural products is a consequence of the success of natural molecules as biologically active agents, which, in turn, arises from their complex chirality and ring systems and the number of heteroatoms and aromatic rings, thus allowing them to bind to complex proteins and other three-dimensional biological targets (2). For this reason, natural products have been addressed as "privileged structures", as their molecular scaffolds are able to accommodate several pharmacophores, hence displaying multiple biological activities by fitting biological targets that are frequently conserved across species (3).

As it has been reviewed by Cragg and Newman in 2009, between 1981 and 2006, 66% of the 974 small molecule drugs introduced in clinical practice were synthetic. However, deeper insights revealed that 17% of these molecules contained a pharmacophore directly derived from natural products and 12% were derived from natural products. Thus, directly or indirectly, Nature remains a very important source of bioactive molecules (4). Nevertheless, it is undeniable that in the last 15 years there has been a decline in the approvals of Nature-derived molecules and many pharmaceutical industries have terminated their natural drug discovery pipeline (5). However, more than a threat this constitutes an opportunity, as the paradigm of drug discovery from natural products is changing with new hotspots of bioactivity under study and techniques for structure elucidation and target characterization.

Marine environment remains, to this day, the most diversified ecosystem on Earth and simultaneously the least studied. Marine organisms have to cope with the several challenges that marine life represents, including high pressures, low temperatures and light availability. In addition, many organisms have primitive immune systems and soft bodies and, for this reason, what they lack in physical defences is frequently balanced with remarkable chemical defences. In fact, organisms with lower physical defences, such as sponges and molluscs, are usually the ones with the most bioactive molecules. Marine natural products have proved to be an amazing source of chemical diversity and,

consequently, many sea-derived molecules were shown to exhibit a number of different pharmacological activities and are currently under clinical trials to treat various pathological conditions, such as cancer, inflammation and pain (6-9). Among the several classes of marine natural products described, the most relevant in a biological context are terpenes, alkaloids, peptides, fatty acids and sterols. In the next chapters, the chemical classes relevant for this thesis will be presented from a chemical, analytical, biosynthetic and biological point of view.

1.2. Fatty acids

1.2.1. Chemistry

Fatty acids (FA) are a class of lipophilic molecules that can be found in all living organisms. They can occur in their free form or, alternatively, integrate more complex lipids, such as triglycerides (TG), phospholipids or glycolipids, as presented in **Figure 1**. In addition, FA can be part of lipoproteins, lipopolysaccharides and alkaloids.

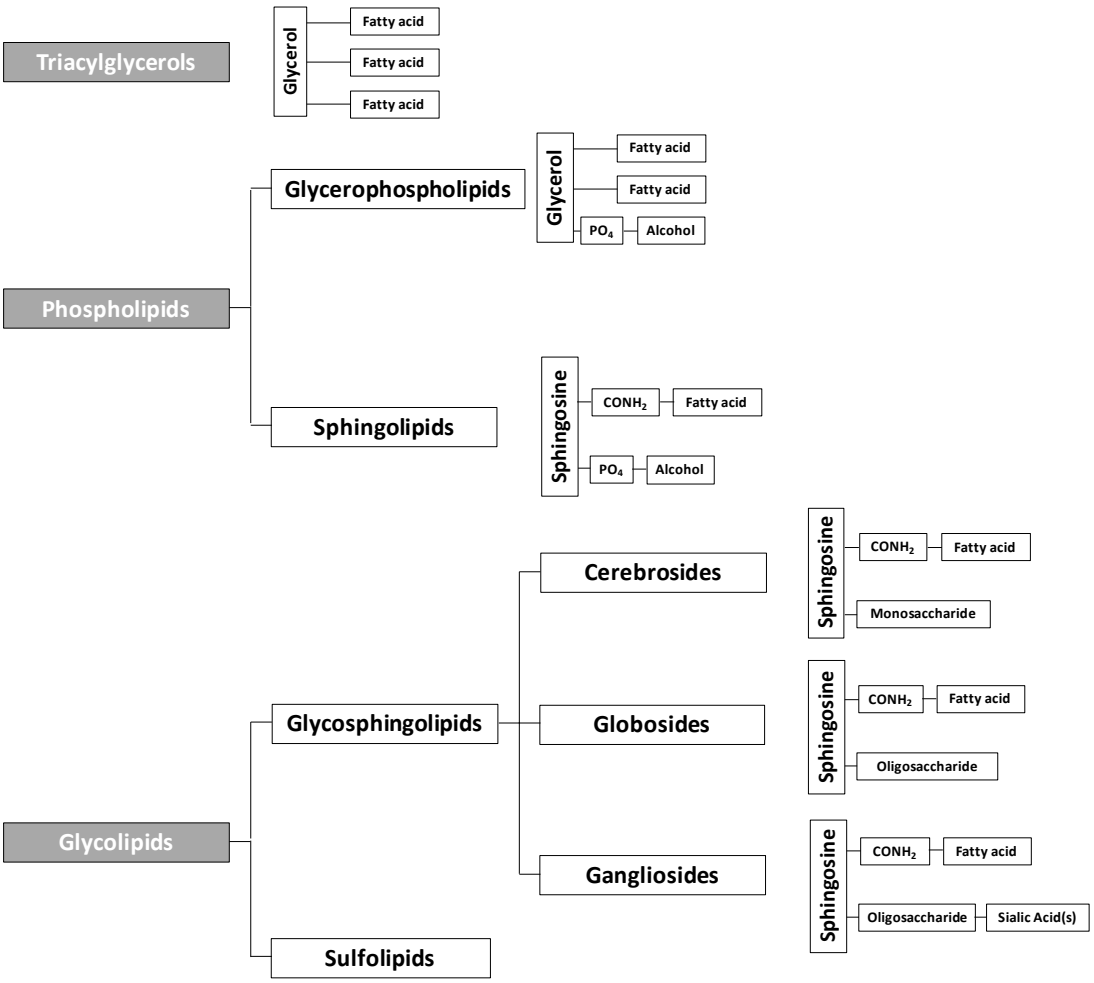

Figure 1 – Lipid classes.

FA exhibit a very diversified chemistry, which results in several possible structures such as saturated/unsaturated, branched and cyclic, which can, in turn, display distinct functional groups, such as hydroxyl, keto and epoxy, hence adding to the diversity of these molecules.

Classical nomenclature for FA indicates chain length, number and position of double bonds when present (example: 20:2 Δ5,11. In this example, there are 20 atoms of carbon, with 2 double bonds, which are located in the position 5 and 11). The carbon associated with the methyl end group is designated ω carbon and, accordingly,

unsaturated FA in which the position of the first double bond is located 3, 6 and 9 carbons away from the ω carbon are named ω-3 (omega-3), ω-6 (omega-6) and ω-9 (omega-9).

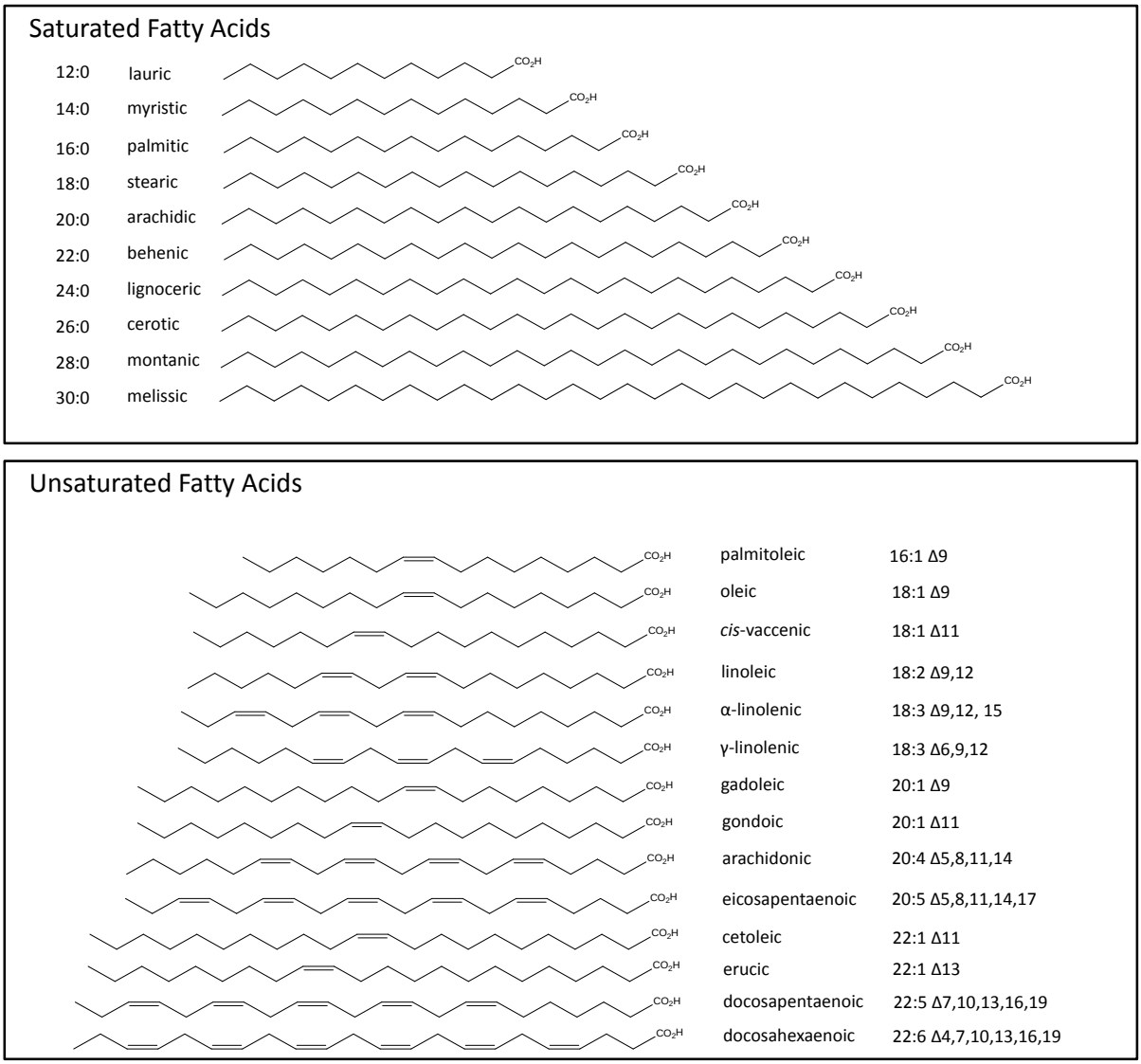

Figure 2 – Most common saturated and unsaturated fatty acids. Image obtained from (10).

In mammals, FA with a maximum chain length of 16-18 carbons constitute about 90% of total FA (11). FA consisting of 20 or more carbon atoms are referred as Very Long Chain Fatty Acids (VLCFA).

Saturated FA, as the name indicates, are molecules with no double bonds. These compounds usually have between 12 and 24 carbon atoms (12) (**Figure 2**). On the other hand, when unsaturation is present the compounds are called either mono unsaturated fatty acids (MUFA) or polyunsaturated fatty acids (PUFA). In the case of the latter, double bonds are frequently in an non-conjugated arrangement, with —$(CH=CHCH_2)_n$—

repeating units (**Figure 2**), although some exceptions are known, as it will be presented later.

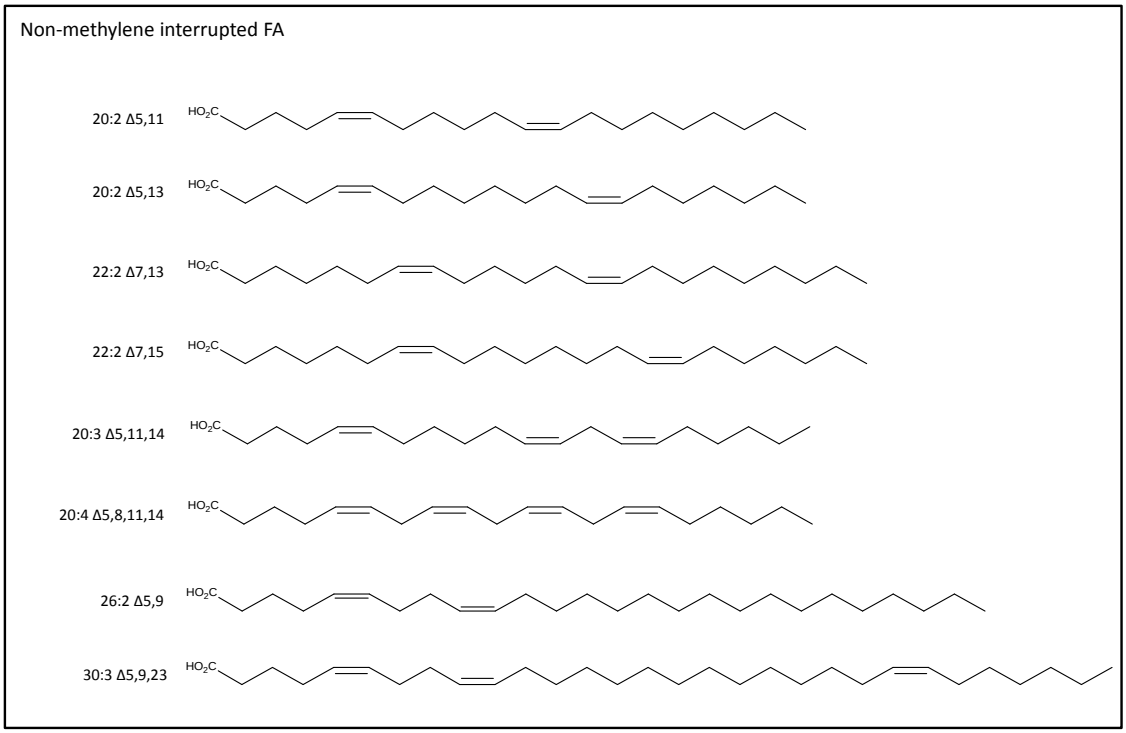

Figure 3 – Non-methylene interrupted FA. Image obtained from (10).

The *cis* (*Z*) stereochemistry of the double bond causes a kink in the alkyl chain that has consequences in the physical properties of the molecules, like fluidity, which is important in a biological context, namely in cellular membranes.

In the last few years, great advances have been made in the study of the chemistry of FA. In particular, the study of marine organisms has led to the discovery of new and less conventional classes of FA with remarkable chemistry, such as halogenated FA, acetylenic FA, non-methylene interrupted FA (NMIFA, **Figure 3**) and methoxylated FA (**Figure 4**). NMIFA are compounds that display unusual unsaturation features, namely double bonds with more than one methylene group between ethylenic bonds. These compounds are, in general, of marine origin and have been described in algae, mollusks and sponges (10, 13). A review on the chemistry of marine FA has been published recently (10).

Methoxylated FA are rare compounds, presenting limited distribution in Nature and described recently. These compounds are frequently found in cyanobacteria, bacteria and sponges (10, 14-16).

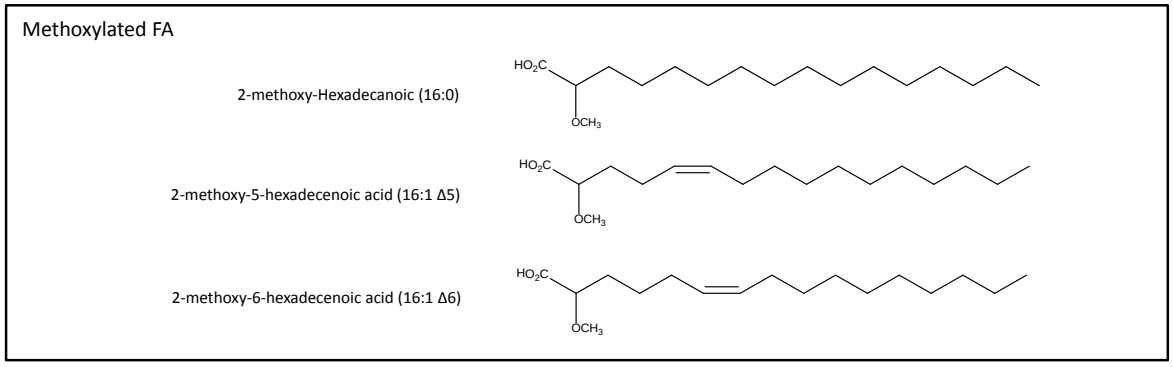

Figure 4 – Methoxylated FA. Image obtained from (10).

1.2.2. Biosynthesis

Biosynthesis of FA, as it happens in most biological reactions, is not simply a reversal of its degradative pathway, of which β-oxidation is the most relevant. In general terms, FA biosynthesis takes place in cytosol and requires the action of fatty acid synthase, which comprises several enzymes pivotal to the synthesis. The building block of FA is acetic acid in the form of acetyl-S-Coenzyme A (CoA), which is exported from mitochondrion and acts as the direct initiator. Further elongation is assured by malonyl-CoA which, in turn, derives from acetyl-CoA by the action of acetyl Co-A carboxylase.

Sequential elongation of the growing FA chain takes place by two units of carbon. Elongation stops when C14-C18 FA are obtained, typically in the C16:C18:C14 proportion of 7:1:2 (17). FA with higher carbon number, VLCFA, can be synthesized, however additional enzymes are required. In all cases, intermediates are covalently linked to the sulfhydryl groups of an acyl carrier protein (ACP). A four-step repeating cycle, which comprises condensation, reduction, dehydration and reduction once again, results in the addition of 2 carbons. While these steps are, in general, sufficient for saturated FA, biosynthesis of the unsaturated homologues requires additional steps, frequently microsomal dehydrogenation. A long-standing question has been whether or not multiple microsomal elongation systems exist in the cell with different saturation and/or chain length specificities (18). The simplest ω-3 FA is α-linolenic acid (18:3 ω-3) and its biosynthesis differs according to the organism. In plants, α-linolenic acid is synthesized from linoleic acid (18:2 ω -6) *via* desaturation, catalysed by delta-15 desaturase.

Animals, however, do not possess this enzyme and, for this reason, cannot synthesize α-linolenic acid, which must be obtained from the diet. Despite this fact, animals are still able to metabolize α-linolenic acid, mainly by the means of further desaturation and elongation. In particular, α-linolenic is an important source of eicosapentaenoic acid (EPA), as depicted in **Figure 5**.

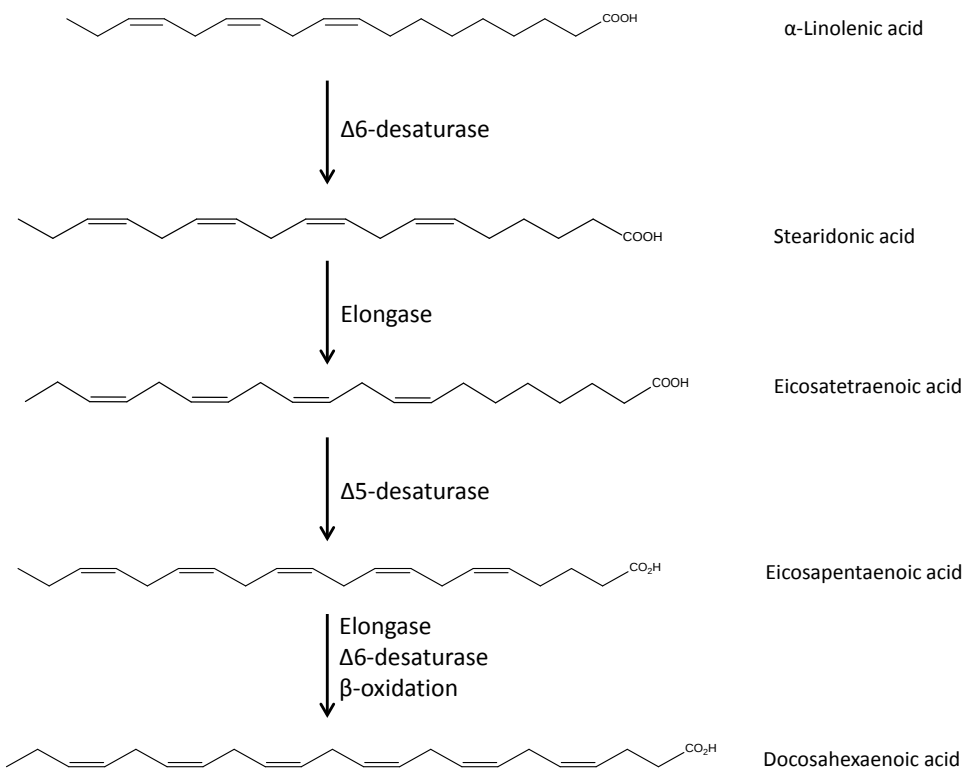

Figure 5 – Biosynthesis of DHA.

When it comes to the biosynthesis of VLCFA, it is well accepted that the major site for biosynthesis of these molecules is the membranes of the endoplasmic reticulum (ER) (19).

1.2.3. Analysis

Extraction

Given the high chemical diversity in FA, extraction and analysis must be optimized to each class. In the case of free FA, soft and quick extraction procedures are required and they should minimize autoxidative degradation and formation of artefacts. Two reference methods are largely used for FA extraction, namely those of Folch (20) and of Bligh & Dyer (21), both of them based on the mixture of two immiscible solvents, one polar and one non-polar. In the case of the Bligh & Dyer method, lower final volumes are used (approximately 2 mL) and, for this reason, is considered a green method and adaptation of the Folch procedure. In this method, the fat fraction in the sample is extracted by the polar solvent mixture of chloroform, methanol and water, which gives a one-phase system. After

extraction, the one-phase system is separated into chloroform and methanol/water phases by addition of more chloroform and water. The non-polar phase, containing both neutral and polar lipids, can be further divided into the different lipid classes, by applying techniques like preparative thin-layer chromatography (TLC), high pressure liquid chromatography (HPLC) and silicic acid or alumina chromatography. Moreover, the extraction and enrichment of specific classes of FA can be also attained by several techniques: solid-phase extraction (SPE) for the extraction and purification of free FA (22), formation of silver ion complex for the enrichment in halogenated FA (23) and by the separation of molecules with different degrees of unsaturation by partial hydrogenation of their concentrates with hydrazine hydrate and subsequent isolation of the monoenoate products by argentation TLC (24).

Derivatization and analysis

Nowadays, gas chromatography (GC) is one of the most widely used analytical techniques for the analysis of FA. Although GC can render very efficient separation of FA, one of its drawbacks resides in the need of a derivatization step prior to the analysis that improves the volatility of the analytes. Several derivatization agents can be used. The most frequent FA derivatized form is the fatty acid methyl ester (FAME), which requires a methylation reaction, sometimes called transesterification or transmethylation. Several different procedures can be found in literature, namely multistep or direct methylation methods.

In multistep methods, FA are extracted and subsequently methylated into FAMEs, which are then re-extracted and analysed by GC (24-29). Differently, in direct methylation methods, extraction and derivatization is combined in one single step, thus reducing some of the drawbacks of multistep methods, such as high volumes of solvents or loss of analyte (30).

Nowadays silylation is widely used as derivatization method for gas chromatography-mass spectrometry (GC-MS) metabolic profile studies, since it allows the determination of metabolites from different classes. Among silylation agents, *N*-methyl-*N*-(trimethylsilyl)-trifluoroacetamide (MSTFA) has been increasingly used due to its ability to react with primary amines and amides, alcohols, phenols, carbohydrates and carboxylic groups (31, 32). Another type of derivatizing agents are nitrogen-bearing molecules, of which pyrrolidides, 4,4-di-methyloxazoline (DMOX) and piconyl ester derivatives are the most representative (33). Several reviews can be found in literature regarding each of these compounds (34-36), with each technique having its advantages and disadvantages. The technique of choice should be adapted to the type of sample and compounds under study. Piconyl esters frequently use mild temperatures, while DMOX derivatization

usually requires temperatures around 180 °C, which can be a problem in the case of some labile compounds. Also, the MS spectra of DMOX derivatives can be more informative regarding the location of the double bond in conjugated dienes, such as in conjugated linoleic acid (CLA) (36). Many other differences between the two methods are found in the above referred reviews.

1.2.4. Biological properties

Lipids in general, FA in particular, serve three major roles in an organism: they are structural components of biological membranes, provide energy reserves and serve as biologically active molecules exerting a wide range of functions.

FA are endogenous ligands of several nuclear receptors, which in part play important roles in controlling a number of metabolic pathways. Unsaturated FA with 18-20 carbon atoms are precursors of prostaglandins, thromboxanes and leucotrienes, which display several autocrine and paracrine effects and have a number of regulatory properties. These mediators will be discussed in **Section 2.4** when inflammation is addressed. FA with 20 and 22 carbon atoms are precursors of other biologically important molecules, such as non-classic eicosanoids, which include resolvins, lipoxins and neuroprotectins (37). For example, sphingolipids and glycerolipids are involved in DNA replication, cell recognition, signaling and transduction pathways and cell trafficking. In combination with diacylglycerols they can be involved in processes such as conformational changes of enzymes, cell division and apoptosis (38).

The number of biological properties attributed to FA and their derivatives has been increasing (8). There is a growing body of evidence that FA can be successful in the treatment of cancer, as it will be discussed later. Antimicrobial properties, not addressed herein, have also been extensively studied (39-41).

In the last few years we have assisted the rising importance of lipid rafts, membrane microdomains, in several biological processes, including infectious diseases, signal transduction and cytoskeleton reorganization (42-45). These microdomains are rich in cholesterol as well as saturated lipids such as sphingolipids. They also include a characteristic protein composition which can be important for signal transduction or even targeted membrane trafficking. In this regard, sterols have been increasingly regarded as pivotal for the formation of these structures (46, 47), as it will be presented later.

1.2.4.1. Fatty acids in inflammation

The effect of FA on the onset and maintenance of inflammatory conditions is highly dependent on their chemistry. In this regard, it is important to highlight that saturated and unsaturated FA frequently exhibit opposing activities.

Several studies have shown that some saturated FA are able to induce the expression of pro-inflammatory markers such as cyclooxygenase-2 (COX-2), inducible nitric oxide synthase (iNOS) and interleukin-1α (IL-1α) as a consequence of the activation of Toll-like receptor 4 (TLR4). Among saturated FA, lauric and palmitic acids have been described as some of the most potent pro-inflammatory FA (48).

Differently, unsaturated FA are increasingly regarded as molecules that may exhibit anti-inflammatory properties, an effect that often results from several mechanisms of action. Among FA or their derivatives, with anti-inflammatory properties, PUFAs are particularly important (49).

Regarding FA necessary for the equilibrium of the human organism, with the exception of two compounds, linoleic acid (LA, C18:2 ω-6) (precursor of the ω-6 series of FA) and α-linolenic acid (ALA, C18:3 ω-3) (precursor of the ω-3 series of FA), all compounds are produced by humans.

Many inflammatory conditions result from an excessive production of pro-inflammatory mediators like eicosanoids, prostaglandin E_2 (PGE_2) and leukotriene B4 (LTB_4). At this point, it is important to highlight that these molecules are synthesized in the organism from the ω-6 FA arachidonic acid (C20:4 ω-6). If we consider that western diet results in high ω-6 and low ω-3 ratio of PUFA (50), it may be postulated that correction of these proportions, by increasing the consumption of ω-3 FA like EPA (C20:5 ω-3) and docosahexaenoic acid (DHA, C22:6 ω-3) may change this trend (51), as they may replace arachidonic acid as an eicosanoid substrate in cell membranes (52). In addition, several works have shown that the anti-inflammatory properties of FA can also occur downstream of phospholipase A_2 (PLA_2)-mediated production of arachidonic acid. In particular, C22:6 ω-3, C20:5 ω-3, C20:4 ω-6, C18:2 ω-6 and C18:1 ω-9 have proved to be able to prevent saturated FA-induced increase in the expression levels of COX-2 at 5 μM (48). Another work evaluated the effect of a mixture containing high concentrations (200 μM) of oleic and palmitic acids in mouse peritoneal macrophages. Results showed that, in wild type (WT) macrophages, nuclear factor of kappa light polypeptide gene enhancer in B-cells inhibitor (IκB), a marker of Nuclear factor kappa-light-chain-enhancer of activated B cells (NF-κB) activation, was degraded, while in macrophages obtained from $TLR4^{-/-}$ animals no effect was noticed. A similar trend was found for other inflammatory markers, namely tumor necrosis factor α (TNF-α) and IL-6 mRNA (53).

In addition to NF-κB pathway inhibition, activation of peroxisome proliferator-activated receptors (PPAR) is referred as another mechanism for the anti-inflammatory activity of FA. Several PUFAs have been shown to activate PPAR (54-56), however the precise mechanism of cross-talk between this transcription factor and NF-κB is still not completely understood.

1.2.4.2. Fatty acids in cancer

The fact that populations of eskimos, which consume substantial amounts of long chain ω-3 polyunsaturated FA, EPA and DHA, exhibit lower incidence of cancer (57), launched the debate about the potential interest of these compounds as anti-carcinogenic molecules. Subsequent epidemiological studies showed an inverse relationship between blood levels of EPA and DHA and the risk of prostate (58) and colon (59, 60) cancers. These epidemiological data have been further confirmed by experimental models that showed the ability of some marine lipids to prevent the conversion of healthy cells to cancerous cells (61).

In a study by Hossain et al. (62) several FA (arachidonic acid, EPA and DHA) were tested for their ability to inhibit the growth and induce apoptosis in three colon cancer cell lines, HT-29, Caco-2 and DLD-1, both in their free form and as constituents of phospholipids. DHA was the most effective compound in the HT-29 cell line, especially when in the phospholipid form, with 100 μM causing a loss of 60 % in cell viability. The antioxidant butylated hydroxytoluene (BHT) was able to prevent DHA-mediated toxicity, suggesting that the mechanism of action of that FA may be related with the induction of oxidative stress. The finding of increased levels of thiobarbituric acid reactive substances (TBARS), a marker of lipid peroxidation, after incubation with DHA confirmed that hypothesis (62).

The effect of EPA on the human leukemia cell line HL60 was also evaluated (63). EPA inhibited cell growth, though in the econazole (Ec)-resistant HL60 clone E2R2 this compound was not so effective. Econazole is known to deplete calcium from the ER and to inhibit calcium influx in mammalian cells, thus leading to the activation of the unfolded protein response (UPR) and apoptosis. Gene expression analysis of HL60 cells revealed extensive changes in transcripts related to ER homeostasis, calcium homeostasis and cell cycle/apoptosis (63).

In addition to the above mechanism of action, which frequently involve pro-apoptotic mechanisms, FA can also exert their anti-cancer effect *via* inhibition of topoisomerase I, a key enzyme in the breaking and repair of DNA strands (64-66). While saturated FA seem to be devoid of interest as topoisomerase I inhibitors, several

unsaturated FA have proved to be active (64, 66, 67), including oleic acid (66), EPA (68, 69), very long chain (C_{26}-C_{30}) $\Delta 5,9$ FA (70) and phospholipids containing unsaturated FA (65). FA with one double bond strongly inhibit this enzyme (66), an activity that is even higher in the case of conjugated FA (68). Palmitic acid has also been reported to be cytotoxic to several leukemic cell lines in the range of 10–15 μg/ml, an effect mainly attributed to its ability to inhibit topoisomerase I (71).

1.3. Sterols

1.3.1. Chemistry

Sterols are, typically, C27 steroid alcohols that are widespread in Nature, being synthesized by higher plants, algae, virtually all fungi and also vertebrates, although through different biosynthetic pathways. Curiously, insects are unable to synthesize these molecules and obtain them from diet. While sterols can exist in their free form, the presence of the C3 hydroxyl group turns esterification a possibility and, hence, sterols can be esterified with FA, hydroxycinnamic acids, hexoses or 6-fatty acyl hexoses.

From a chemical point of view, the general structure of sterols comprises a 4 ring system comprising cyclopenta[a]phenanthrene in *trans* junctures, methyl groups at C18 and C19 with β-stereochemistry and a carbon side chain at C17 (**Figure 6**). In a general way, the hydroxyl group at C3 also displays β-stereochemistry. Saturated derivatives of sterols are known as stanols and they usually occur in trace amounts in plants, with the exception of cereal grains where they are present in considerable levels (12, 72).

Major sterols in plants include campesterol (24-methyl cholesterol), β-sitosterol (24-ethyl cholesterol) and stigmasterol (22-dehydro sitosterol) and they all have a double bond in position 5. They are similar to cholesterol, differing in the side chain. The additional unsaturation in the side-chain, trans Δ^{22}, is trait common in plants sterols but not in mammalian, as well as a one- or two-carbon substituent with variable stereochemistry in the side chain at C-24 which is conserved during metabolism.

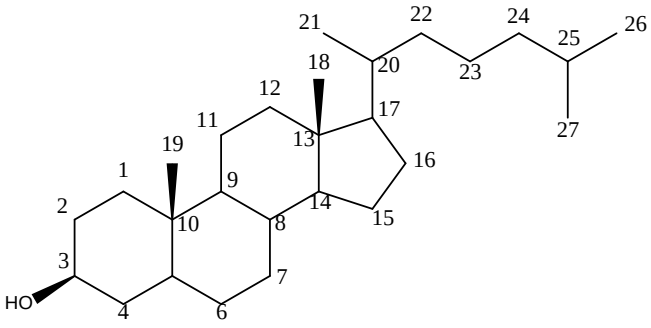

Figure 6 – General structure and numeration of sterols.

Ergosterol, a sterol with a β-24-methyl group, a *trans* Δ^{22} double bond and another unsaturation in Δ^{7} is the predominant sterol found in fungi. If we take a structural criteria, plant sterols can be divided into 4-desmethyl sterols (no substituent on C4), 4-α-monomethyl sterols and 4,4-dimethyl. The first family, in turn, can be categorized as Δ^{5}, Δ^{7} and $\Delta^{5,7}$, according to the position of double bonds in the B ring.

1.3.2. Biosynthesis

Plant sterols are biosynthesized *via* the isoprenoid pathway. In this pathway, isoprene is not directly used in the biosynthesis, instead two C5 derivatives are possible: 3,3'-dimethylallyl diphosphate (DMAPP) and 3-isopentenyl diphosphate (IPP). For a long time, the mevalonate pathway, which starts with the production of acetoacetyl-CoA from two molecules of acetyl-CoA, was believed to be the sole and universal route leading to the production of IPP and DMAPP. Nowadays, this pathway is known to occur in a large number of animal species, eubacteria as well as in the cytosol and mitochondria of plants, fungi and some parasites. In fact, the pathway used can be highly dependent of the cellular compartment, as depicted in **Figure 7**.

An alternative pathway for IPP and DMAPP formation was described recently. This route, usually addressed as the non-mevalonate, 1-deoxy-D-xylulose-5-phosphate (DOXP) or 2-C-methyl-D-erythritol-4-phosphate (MEP) pathway, occurs in plant and algae chloroplasts, cyanobacteria and apicomplexan parasites (73, 74).

Mevalonic acid arises from the condensation of three molecules of acetyl-SCoA, thus originating β-hydroxy-β-methylglutaryl-CoA (HMG-CoA). Hydrolysis and enzymatic reduction will eventually yield mevalonic acid.

Differently, in the 1-deoxy-D-xylulose-5-phosphate pathway, two products of glycolysis, pyruvic acid and glyceraldehyde are responsible for the synthesis of the intermediate 1-deoxy-D-xylulose-5-phosphate *via* the enzyme thiamine diphosphate.

In the case of sterols, mevalonate is the biosynthetic precursor. Biosynthesis of sterols differs between animals and plants. While in animals (75, 76) and fungi (77, 78) the tetracycle backbone is obtained from lanosterol, in the case of plants, the pentacycle cycloartenol is used instead. An additional enzyme, cycloeucalenol-obtusifoliol isomerase, opens the cyclopropyl ring, thus yielding a tetracycle moiety (79) (**Figure 8**).

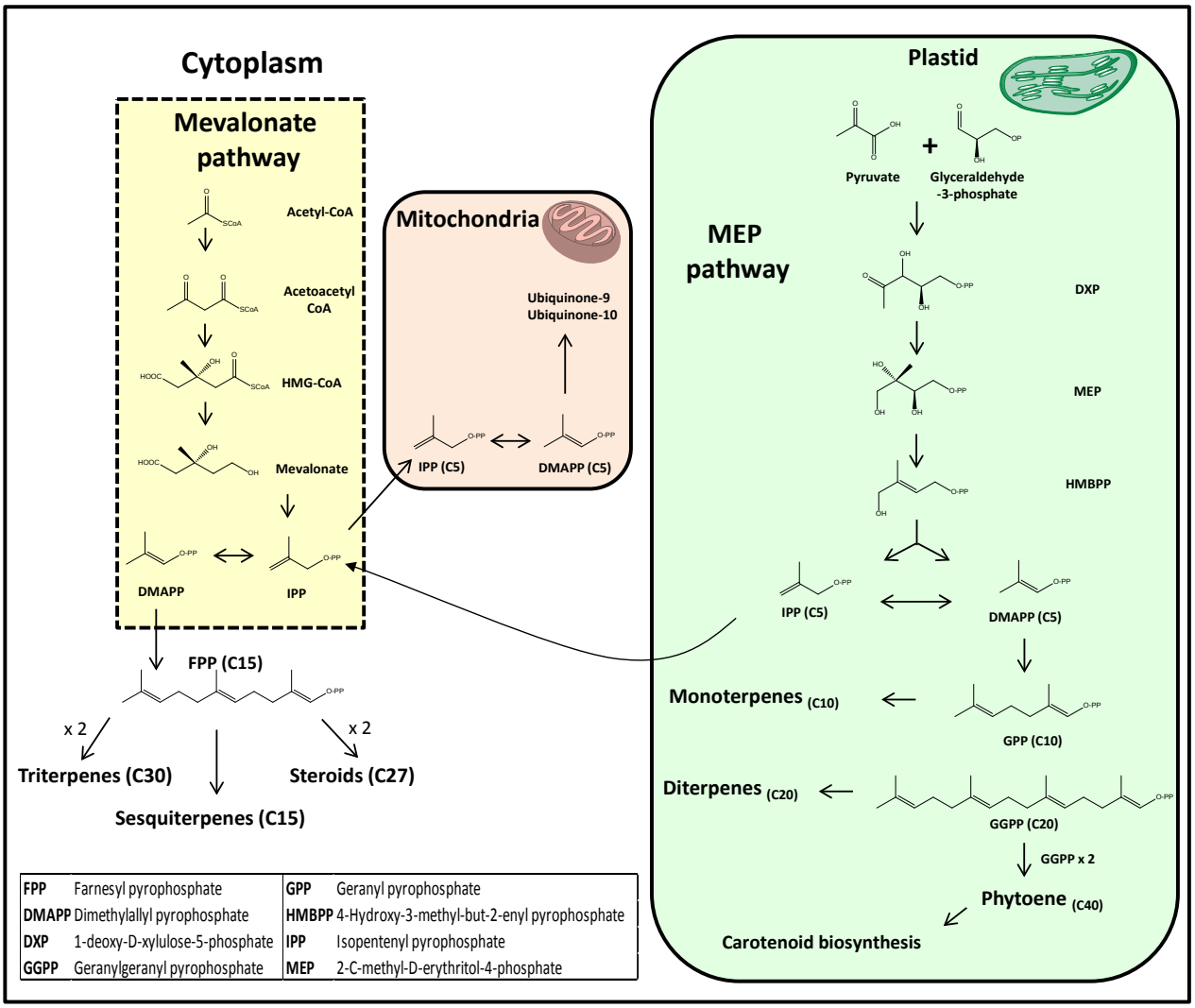

Figure 7 - Major biosynthetic steps of the mevalonate / 1-deoxy-D-xylulose-5-phosphate pathways and their cellular compartments.

In animals, lanosterol originates cholesterol in a process that requires the loss of three methyl groups, reduction of the carbon side-chain double bond and generation of a $\Delta^{5,6}$ double bond instead of $\Delta^{8,9}$. The precise order by which the reactions take place are thought to be species-dependent and cytochrome P450 enzymes participate in these reactions (12).

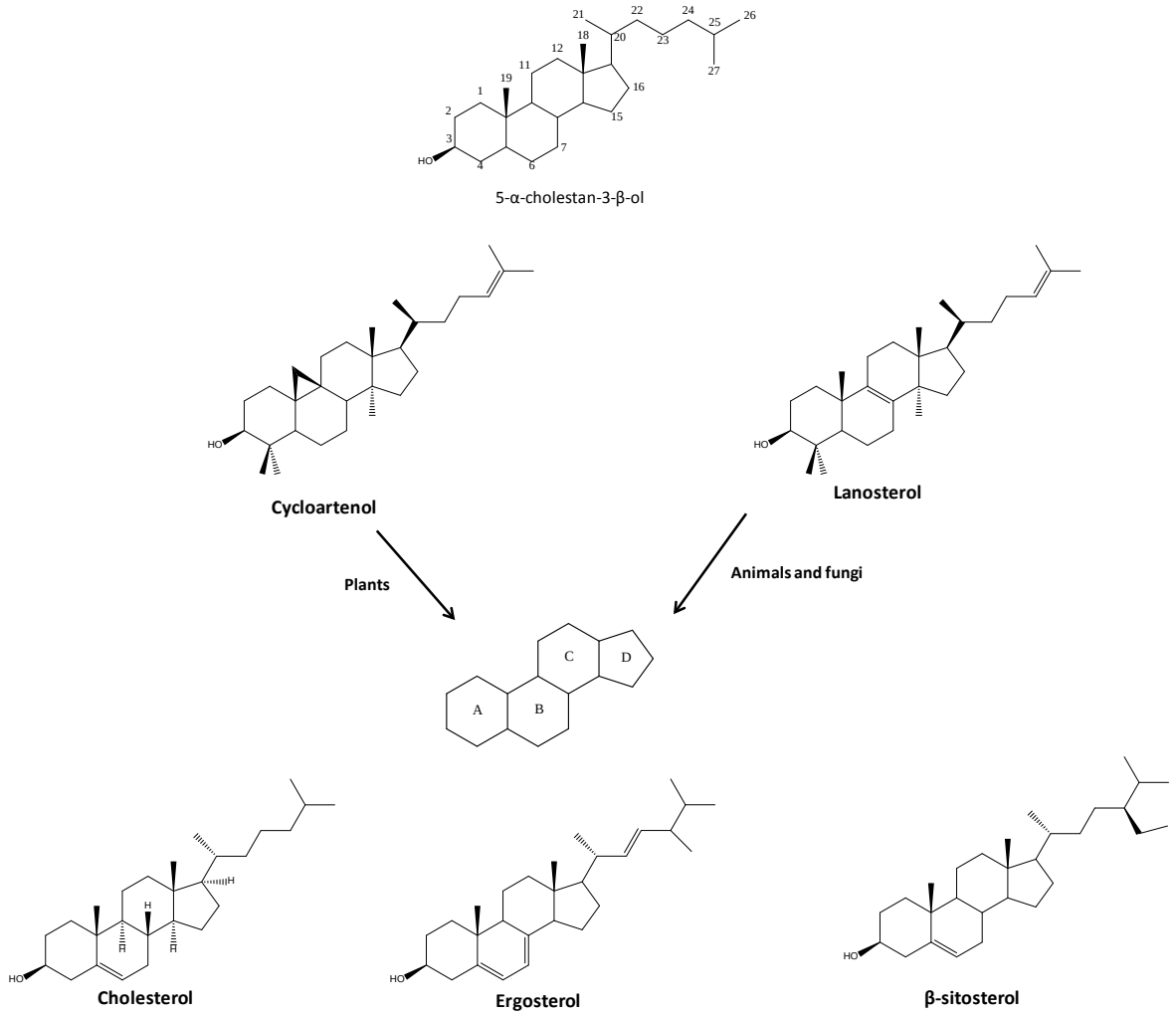

Figure 8 – Origin of the sterol backbone in animals and plants.

1.3.3. Analysis

Nowadays, most common techniques involve the extraction of the lipid fraction, saponification, extraction of non-saponifiables, derivatization, separation and detection by GC using a capillary quantification. Extraction is mainly performed by employing mixtures of different solvents, frequently chloroform-methanol, chloroform-methanol-water, hexane, methylene chloride or acetone (80). SPE using neutral alumina has also been reported (81, 82), as well as the combination of SPE with supercritical CO_2 (83).

Traditionally, GC is the main technique for the separation of sterols and detection is conducted by either flame ionization detector (FID) (84) or mass spectrometry (MS) (85). The latter has been increasingly used as a powerful tool to the identification of many sterols given the extensive information provided by the mass fragmentation spectra. In

these regards, GC analysis of trimethylsilyl (TMS) derivatives of sterols is a highly used technique for their study (80, 86, 87).

HPLC is also an option, in which case detection by ultraviolet (UV) (88, 89) or diode array detector (DAD) (90) is usually the most common option for detection due to their absorption maxima in the 190-230 nm range.

Recently, liquid chromatography-mass spectrometry (LC-MS) has been increasingly regarded as an excellent source for the analysis of sterols due to its low detection limits and the possibility of analyzing complex biological matrices. In this area, the widespread use of electrospray ionization (ESI) has been hindered by the difficulty of neutral sterols to be ionized and, therefore, achieve the sensitivity that can be obtained by using atmospheric pressure chemical ionization-mass spectrometry (APCI-MS) (91) or APCI-MS/MS (92). Recent works have addressed these drawbacks in ESI and have successfully enhanced the efficiency by including charged moieties in the 3β-hydroxyl group *via* derivatizing agents (93).

1.3.4. Biological properties

For the study of the biosynthesis and biological functions of sterols, the discovery of *Arabidopsis thaliana* L. sterol mutants has been fundamental, as has been reviewed before (94, 95).

Sterols play a pivotal role in most organisms, mainly due to their function as membrane constituents. Membrane dynamics is essential for cell survival. A delicate balance between a highly fluid membrane with great permeability and a rigid membrane that yields any transfer across the bilayer impossible could only be achieved through millions of years of evolution. Sterols are one of the mechanisms by which eukaryotic cells are able to control and modulate the properties of biological membranes, such as fluidity. Even organisms that lack sterols, such as some bacteria, have developed surrogates that play the same role, in this case hopanoids like bacteriohopanetetrol (96, 97).

The barrier properties of cell membranes and other lipid bilayer are strongly affected by the qualitative and quantitative profile of sterols included, which are frequently addressed as membrane-active sterols. The knowledge that all membrane active-sterols share similar chemical and physical properties allowed the identification of the minimum requirements for membrane-active sterols, which includes a polar group in C3, virtually always an hydroxyl, a C17 side-chain similar to that of cholesterol, a flat fused ring system and low area (<40 A/molecule) (98).

In the case of plants, several genetic and functional studies showed the involvement of these molecules in processes as diverse as cell division and growth, embryonic formation and cellulose accumulation (99-102).

Without a doubt, the most explored biological property of sterols in humans is related to their well-established capacity to lower total cholesterol and low density lipoproteins without major effects on high density lipoprotein, an effect described over 40 years ago (103, 104). Several studies show that the effect is dose-dependent, with a dose in the range of 2-2.5 g/day eliciting a reduction of about 10%-15% (105) . This value, albeit low, can have a positive impact both in individual patients and populations and has been shown to equally lower the risk of coronary heart disease when used in primary prevention (106). When higher reduction values are required, supplementation with sterols has been shown to act synergically with pharmacotherapy involving cholesterol-lowering agents, such as statins (107).

One of the most widely studied mechanisms involved in cholesterol-lowering capacity of sterols is their ability to interfere with intestinal absorption of dietary cholesterol, which has been quantified in an extent around 30-50% (106). Dietary cholesterol is known to be absorbed in the intestinal lumen in the form of bile salt/phospholipid micelles. Both *in vivo* and *in vitro* studies have shown the ability of several plant sterols to compete with cholesterol and displace them from these micelles (106).

Yet another approach involving sterols can be used for the modulation of blood cholesterol levels. While the above-mentioned treatment targets the absorption of dietary sterols, modulation of the biosynthetic pathway of sterols is also a widely used strategy to reduce blood cholesterol of endogenous origin. In this regard, the inhibition of HMG-CoA reductase is widely exploited by drugs of the statin family, of which lovastatin, a natural product isolated from the Red yeast rice (the yeast *Monascus purpureus* grown on rice) was a lead drug. Nowadays, lovastatin and other members of this group such as atorvastatin, rosuvastatin and simvastatin are first line options in cholesterol-lowering pharmacotherapy, both in monotherapy and in association with other drugs.

1.3.4.1. Sterols in inflammation

Due to their chemical similarity with glucocorticoids, it has been hypothesized that sterols could retain some of the anti-inflammatory properties of that class of drugs. Sterols have already proved to be associated to the reduction of inflammatory conditions both in animal and human models (108-110), with the advantage of not causing significant side-effects and toxicity. Sterols have been implicated in decreased levels of the pro-

inflammatory cytokines IL-6 and TNF-α and increased levels of the anti-inflammatory IL-10 in LPS-stimulated spleen cells from mice (110).

Sterols extracted from transgenic *Panax ginseng* C. A. Meyer successfully inhibited the synthesis of TNF-α and other pro-inflammatory interleukins, as well as the expression of COX-2 in phorbol-myristate acetate (PMA) plus calcium ionophore-stimulated human mast cells (111). The fungal-derived ergosterol and ergosterol peroxide have also been studied for their anti-inflammatory properties in macrophage-like cells, and showed their ability to inhibit LPS-induced TNF-α secretion, IL-1α/β expression and binding of NF-κB to DNA (112).

A mixture of β-sitosterol and its corresponding sterolin, β-sitosterol glucoside was shown to enhance the cellular response of T lymphocytes both *in vivo* and *in vitro* (113). In endotoxin-activated monocytes, the same mixture was able to completely prevent IL-6 and TNF-α release. In addition, a purified sterol fraction (1 mg/mL) obtained from *Sideritis foetens* Clemente ex Lag consisting of campsterol, stigmasterol and β-sitosterol prevented 12-O-Tetradecanoylphorbol-13-acetate (TPA)-induced mouse ear oedema by about 50% (114).

A review on the anti-inflammatory properties of sterols and their derivatives has been published recently (115).

1.4. Carotenoids

1.4.1. Chemistry

Carotenoids constitute a class of natural products widely distributed in Nature, mainly in lower levels of trophic systems. They can be found both in terrestrial and aquatic environments and they are present in several taxonomical groups. The most common carotenoids in Nature include fucoxanthin, neoxanthin, violaxanthin and lutein (116). The presence of these molecules in animals usually arises from diet.

The designation carotenoid includes two different groups: carotenes, which are hydrocarbons, and xanthophyls or oxycarotenoids, which are oxygenated derivatives. Another division can be made between primary carotenoids, which are required for photosynthesis (β-caroten, violaxanthin, neoxanthin, among others), and secondary carotenoids, which are compounds present in fruits and flowers (α-caroten, zeaxanthin, antheraxanthin, β-cryptoxanthin, among others) (117).

Due to the long system of conjugated double bonds, which constitutes the chromophore (**Figure 9**), nearly all carotenoids absorb light in the 400-500 nm range. This chromophore, however, turn carotenoids unstable in the presence of light, heat or oxidative atmosphere and they are prone to isomerization from all-*trans* (all-E) to *cis* (Z) isomers, although *cis* forms are also known to occur naturally, albeit in low amounts (118-120). The effect of storage and processing techniques on carotenoid content in several foodstuffs has been reviewed before (121). The chemical differences between the two isomer forms have biological consequences: while all-t*rans* carotenoids are linear and rigid molecules, their *cis* isomers display a kink in the chain with marked consequences in their ability to interact with enzymes, assemble in supramolecular structures and fit cellular structures. For example, in a biological context, *cis* carotenoids display lower tendency to aggregate and thus influencing parameters such as solubilization, chemical reactivity and light absorption (122, 123).

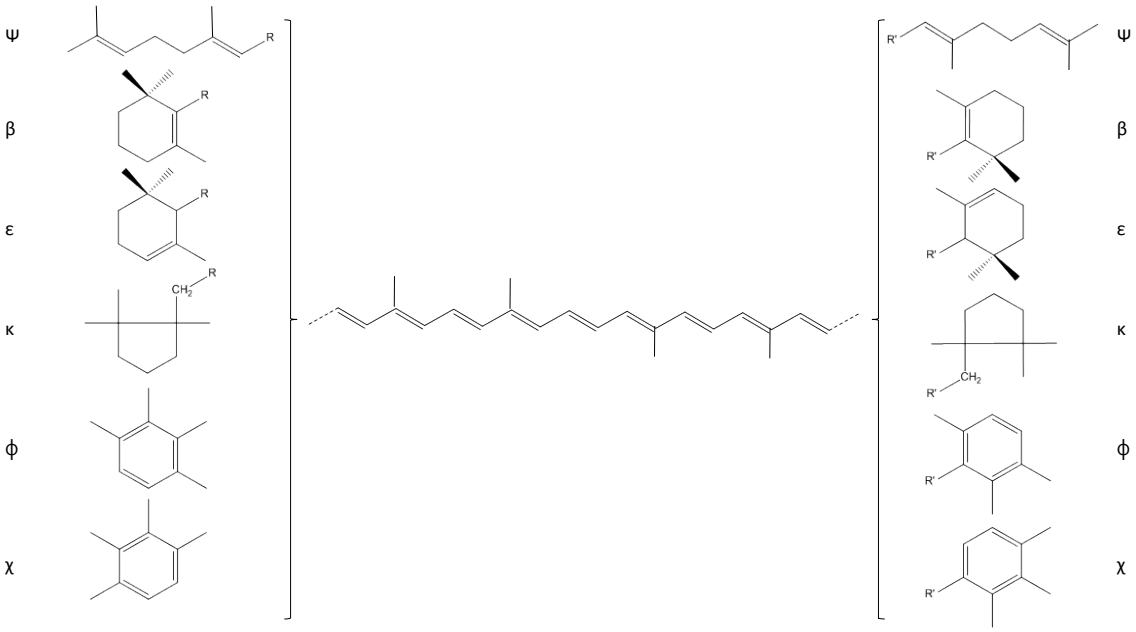

Figure 9 – General chemical structure of carotenoids, including end-group classification. Adapted from (124).

Taking into account the diverse chemistry of carotenoids, which usually display 40 atoms of carbon (C_{40}), these compounds can be sorted in different sub-classes.

Apo/diapo carotenoids are derivatives in which one or two terminal fragments, respectively, have been removed, and include compounds such as crocetin (**Figure 10**) and bixin (124).

Homocarotenoids are compounds that result from the addition of more than 8 units of isoprene. As it will be presented later, carotenoids arise from the condensation of, normally, 8 units of isoprene, which present 5 atoms of carbon each. The designation of homocarotenoids includes all the compounds with over 40 atoms of carbon, as in the case of C_{50} carotenoids (124).

Norcarotenoids display an unusual number of carbons, such as C_{37}, C_{38} and C_{39}. (124) Differently, norisoprenoids are frequently C_{13} fragments, although other carbon numbers are possible.

Given the presence of free hydroxyl groups, carotenoids can also be esterified with other molecules, notably FA. These FA-esterified carotenoids have been described in several taxonomical groups (125-127). Other compounds can be used in the esterification, for example sugars. One of the most widely known carotenoid ester is crocin, the pigment responsible for the color of saffron and that corresponds to the diester of the disaccharide gentiobiose and the carotenoid carboxylic acid crocetin, responsible for the color of crocus flowers (**Figure 10**).

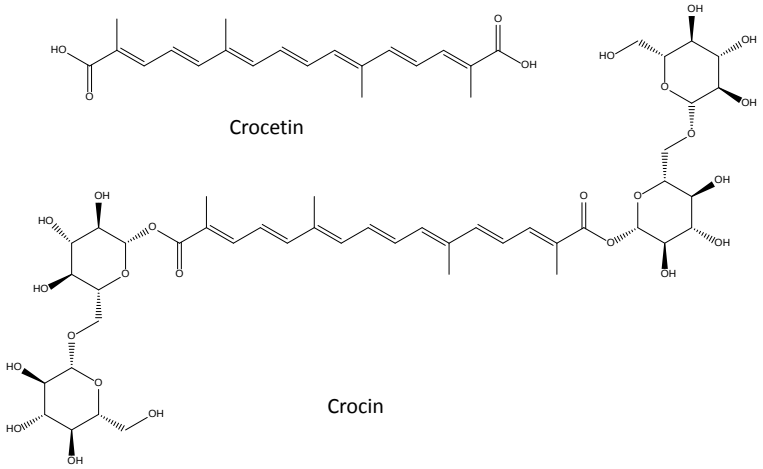

Figure 10 – Crocetin and its gentiobioside diester, crocin.

1.4.2. Biosynthesis

Carotenoids are terpenes, in particular tetraterpenes (C_{40} terpenes). Biosynthesis of carotenoids begins with the 5 carbon molecule DMAPP, which is successively conjugated with further DMAPP building blocks, thus originating molecules with 10, 15 and 20 atoms of carbon (geranyl diphosphate, farnesyl diphosphate and geranylgeranyl diphosphate, respectively) (**Figure 11**).

Several molecules can be obtained from geranylgeranyl diphosphate, namely diterpenes, chlorophyls, geranylgeranylated proteins and carotenoids. In the case of carotenoids, biosynthesis proceeds by condensing 2 molecules of the C_{20} geranylgeranyl into a C_{40} molecule called phytoene. Phytoene is considered by some authors the first true carotenoid, although its incomplete chromophore renders it colorless, thus being devoid of one of the characteristics of true carotenoids. From this point, a number of enzymes perform dehydrogenation reactions, originating sequentially phytofluoene, ζ-carotene, neurosporene and lycopene (**Figure 11**). Starting with lycopene, all the remaining carotenoids can be obtained through a number of reactions that include, but are not limited to: dehydrogenation, hydrogenation, cyclization, double bond migration, chain elongation and chain shortening (128).

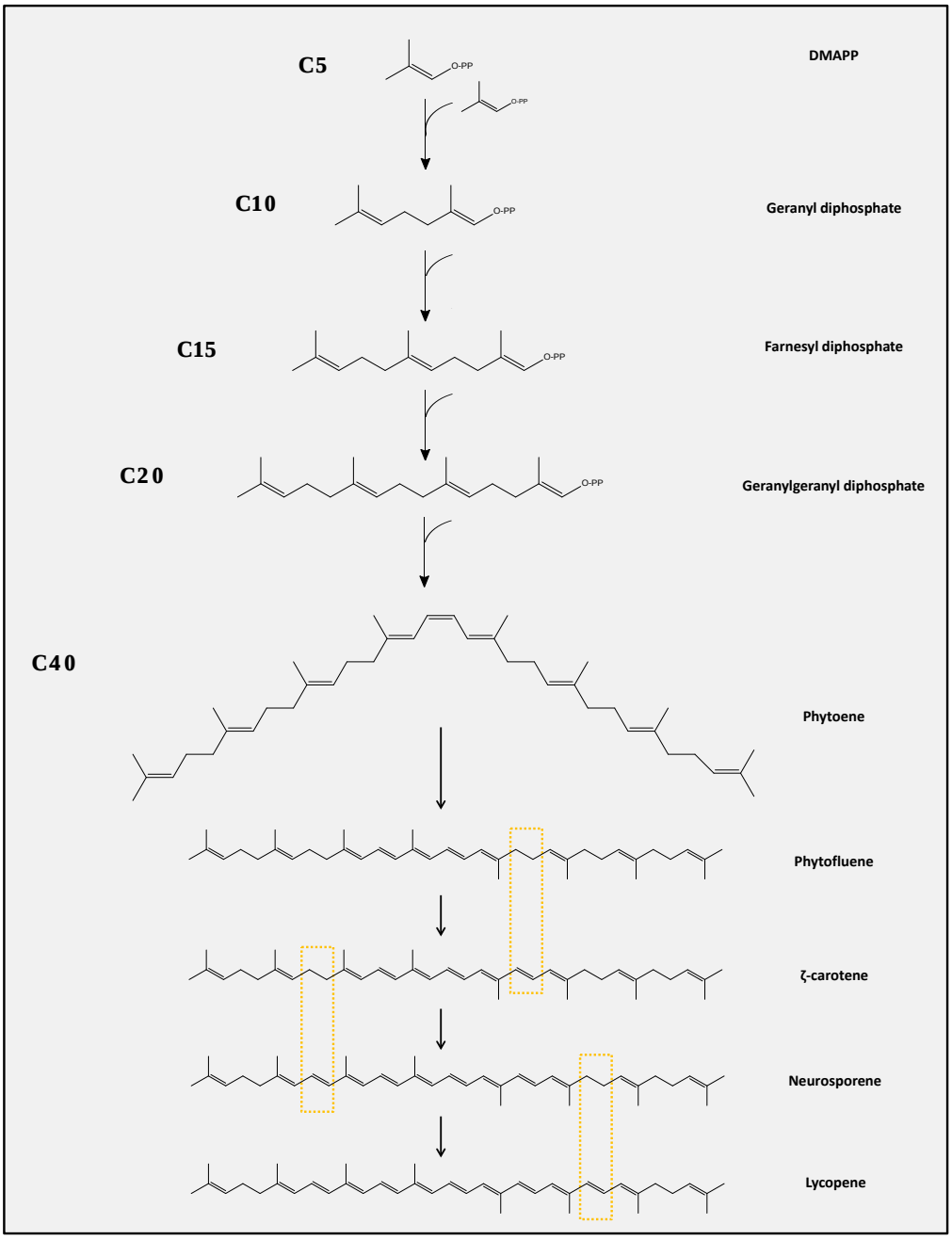

Figure 11. – Biosynthesis of carotenoids from DMAPP. Major differences through the biosynthesis are highlighted in yellow.

1.4.3. Analysis

The diversity of carotenoids can render their analysis challenging. When studying this class of compounds, several levels of information can be obtained. Nowadays, the study of carotenoids should include: UV-vis spectrum (spectral fine structure, peak *cis* intensity), chromatographic properties verified in two systems, co-chromatography with an authentic standard and mass spectrum. When differentiation of stereoisomers is intended, NMR must be used (129, 130).

Chromatographic techniques are widely used for the analysis of carotenoids. GC-MS is regarded as not suitable to this class of metabolites due to their heat-lability. Differently, HPLC is the technique more widely reported in literature. The most commonly used detectors are DAD and MS as they provide very useful spectroscopic and mass information, respectively. The very rich chemistry of carotenoids results in several different isomers possible for each compound.

The separation of carotenoids mixtures can be attained both by normal and reversed phase column, although the latter are preferred owing to their excellent resolution, reproducibility and column stability. In the case of reversed phase-high pressure liquid chromatography (RP-HPLC), C_{18} and C_{30} columns are widely reported in literature. In the case of C_{18} columns, different carotenoids can be separated although, in general, no isomer differentiation is possible and, for this reason, it is usually employed in screening studies where the identification of isomeric forms is not required. On the other hand, C_{30} columns render the separation of geometrical and structural isomers possible. In addition, the C_{30} stationary phase is uniquely capable of resolving geometrical carotenoids in which *cis* bonds are present at the same carbon number but at opposite ends of the molecule (131). In a general way, polar xanthophylls elute first and are followed by the less polar carotenes (132, 133).

Within natural products, some classes of secondary metabolites display optical properties that render the analysis of their UV-vis spectra a very important tool. In the case of carotenoids, both the shape and maxima of the spectrum can provide, to some extent, information regarding their chemical structure. For instance, the number of conjugated double bonds is known to affect the position of long-wave absorbance bands and thus, an increase in this number results in an increase in the wavelength of maximal absorption (124).

In most carotenoids, the UV-spectrum displays three maxima, as depicted in **Figure 12-A** and is commonly addressed as the fine structure. Apart from the maxima of each peak, which can lead to the identification of the compound, the relative proportion between the peak with the highest wavelength (band III) and the middle peak (band II) is a valuable tool for identifying these molecules.

When a carbonyl group is present in a cyclic end-group in conjugation with the polyene chain, the spectra suffer marked changes. The most evident one is the loss of the fine structure, resulting in a single, sometimes symmetrical, peak (**Figure 11-B**). A bathochromic shift can also be found.

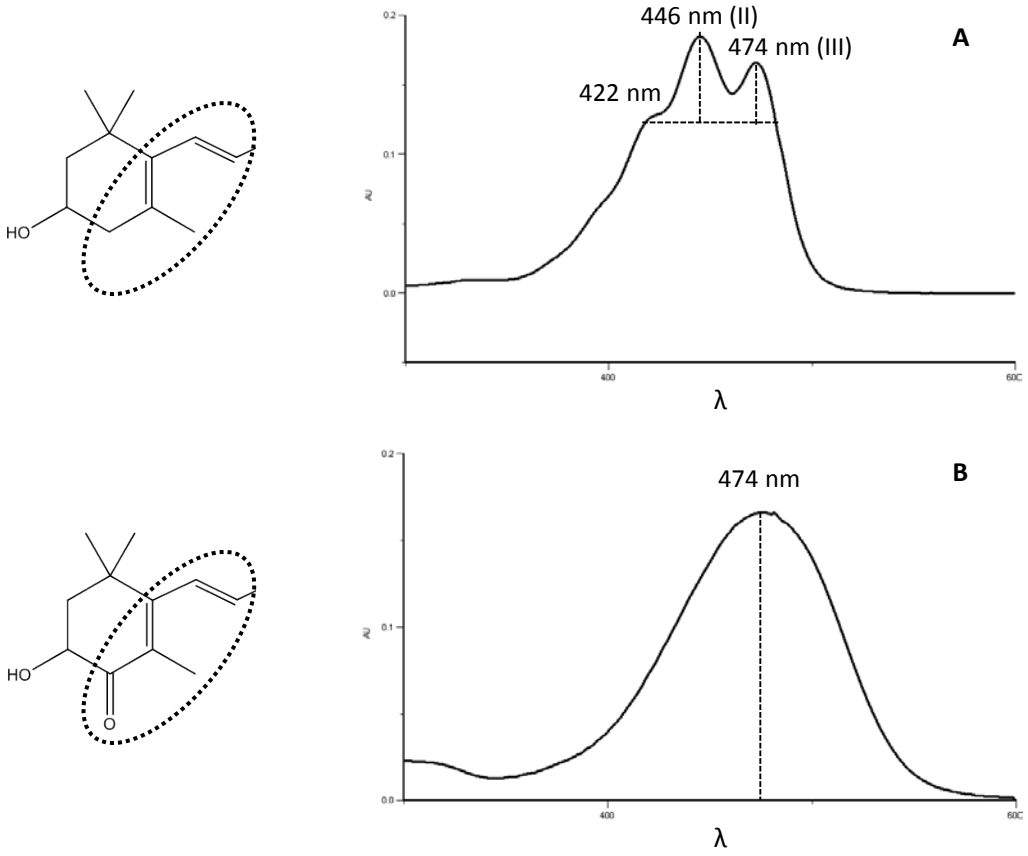

Figure 12 – Spectrum and maxima of (**A**) lutein and (**B**) astaxanthin. In these compounds, the effect of a carbonyl group in conjugation with the polyene chain on the fine structure is visible. This functional group is present in astaxanthin and absent in lutein.

The use of MS renders two levels of information, equally important: molecular weight and fragmentation pattern. Molecular weight, although limited can be useful for ruling out compounds that do not fit the expected molecular weight for a given compound. In the case of fragmentation patterns, much richer information is provided, which can help identify functional groups and the type of chemical linkages present.

Several ionization sources are available for MS analysis and, in the case of carotenoids, they are particularly important, with APCI and ESI being the most relevant to this class of molecules. As it happens in the case of ESI, in APCI ionization takes place at atmospheric pressure. However, in the case of APCI a heated nebulizer is used, while in ESI ionization is obtained *via* an electromagnetic field that facilitates solvent evaporation.

In positive-mode APCI molecular ions and protonated molecules are observed, while molecular ions and deprotonated molecules are found in negative-mode APCI. As it happens with other ionizations processes, in APCI the solvent and mobile phases used affect the abundance and proportion of the several fragments detected. In the particular

case of carotenoids, polar solvents such as alcohols increase the abundance of protonated carotenoids, while apolar solvents facilitate the advent of molecular ions (133).

Other analytical parameters are equivalent between ESI and APCI. The latter has the advantage of yielding higher linearity of detector response over carotenoid concentrations, frequently achieving three orders of magnitude, which is particularly relevant when quantification is intended (133). For obvious reasons, no analytical technique is without drawbacks and, in the case of APCI, abundant fragmentation is known to occur, which may lead to reduced abundance of molecular ions.

1.4.4. Biological properties

Apart from their physical properties, mainly color, carotenoids exert several physiological functions in organisms across different trophic levels.

In a general way, carotenoids exhibit different functions in plants and animals. In photosynthetic organisms carotenoids are used in light harvesting processes in cooperation with chlorophyll and as protectors against photooxidative processes (134). This happens as a consequence of the marked antioxidant capacity of many carotenoids, a characteristic also exploited by animals. In humans, carotenoids can be found in plasma and also in the eye, were they integrate the macular antioxidant system, where a xanthophyll-binding protein has been reported (135).

Biological properties exhibited by carotenoids are often a consequence of several bioactivities, namely the pro-vitamin A activity of some of these compounds, their antioxidant activity, modulation of immune responses and their ability to induce gap-junction communications (136, 137). In order to exhibit pro-vitamin A activity, a carotenoid must display at least one unsubstituted β-ionone ring and a correct number and position of methyl groups in the polyene chain.

Carotenoid absorption and metabolism have been extensively reviewed (138-140).

Several works address the effect of carotenoid-enriched diets in cancer prevention. Although there seems to be enough evidence to support these claims, it should be highlighted that in some situations, high intakes of carotenoids can lead to the opposite effect, that is, increased changes of developing cancer. As it has been reviewed recently, high intakes of carotenoids in individuals with lung damage, such as smokers or workers exposed to asbestos, can result in an increase in the probability of developing cancer up to 30% (141).

1.5. Inflammation

Inflammation is a complex process that constitutes one of the first lines of defense against a number of *stimuli* that are perceived as harmful, such as bacteria, trauma and irritants. While acute inflammatory processes may serve to protect the organism, chronic inflammation is the base of a number of pathological conditions that include asthma, rheumatoid arthritis, inflammatory bowel diseases, atherosclerosis, among many others (142).

Inflammation is a process tightly regulated by several chemical mediators that include cytokines, eicosanoids, platelet-activating factor (PAF), nitric oxide (NO) and neuropeptides, among others. Eicosanoids, comprising prostaglandins, prostacyclins, thromboxanes and leukotrienes, play a major role in inflammation. These molecules are active at very low concentrations and constitute a family of oxygenated FA derivatives obtained from arachidonic acid *via* COXs and lipoxygenases (LOX). While COXs are mainly responsible for the production of prostaglandins and thromboxanes, LOXs mediate the synthesis of 5-hydroperoxyeicosatetraenoic acid (5-HPETE), which, in turn, originates leukotrienes and other mediators.

Several different approaches for the management of inflammatory conditions can be designed, ranging from upstream inhibition of arachidonic acid synthesis *via* PLA_2 inhibition, to downstream modulation of pro-inflammatory cytokines.

1.5.1. Targets in inflammation

Phospholipases A_2

PLA_2s are a group of enzymes responsible for the hydrolysis of membrane phospholipids into arachidonic acid and have been increasingly regarded as an interesting target for anti-inflammatory drug discovery (143-148).

These enzymes can be found in almost all types of cells and hydrolyze the 2-acyl ester bond of 1,2-diacyl-sn-3-glycerophospholipids, of which arachidonic acid is an example. The several PLA_2s described so far (over 15) are divided into four families: cytosolic PLA_2s ($cPLA_2$s), secreted PLA_2s ($sPLA_2$s), lipoprotein associated PLA_2s ((Lp)PLA_2s) and calcium-independent PLA_2s ($iPLA_2$s). Notably, (Lp)PLA_2s display anti-inflammatory properties, as they are able to degrade pro-inflammatory molecules, such as PAFs (143). In the particular case of inflammation, $cPLAS_2$ are very important for the synthesis of eicosanoids, being critical for the signaling pathways involving these bioactive lipids.

cPLA$_2$s are calcium-dependent enzymes activated by extra-cellular *stimuli*, like pathogens, tissue injury, physical or chemical stress. Noteworthy, cPLA$_2$s are the only PLA$_2$s with specificity for arachidonic acid at the phospholipase sn-2 position.

Although the role of sPLA$_2$s in inflammation remains poorly understood, it has been suggested that sPLA$_2$s induce an increase of cPLA$_2$-dependent eicosanoid release and that they synergize with other pro-inflammatory mediators (143).

As referred, arachidonic acid is formed after PLA$_2$-mediated hydrolysis of membrane phospholipids. After this point several different routes can be followed, like metabolization by COX or LOX. In addition to the above mentioned arachidonic acid, the action of PLA$_2$ on membrane phospholipids originates yet another set of molecules, the lysophospholipids. These compounds, precursors of PAFs, are not deprived of biological activity, as they are involved in the secretion of histamine by mast cells and in the activation of leukocytes (149-151).

COX Enzymes and Prostanoids

Arachidonic acid is a ω-6 polyunsaturated FA with an important role in both homeostasis and pathological conditions. In its free form, arachidonic acid is a substrate to COX, also known as prostaglandin H synthases, being readily oxidized and originating prostaglandin G$_2$ (PGG$_2$) and subsequently prostaglandin H$_2$ (PGH$_2$) (**Fig 13**).

Three isoforms of cyclooxygenase are known: COX-1, COX-2 and COX-3. While COX-1 is constitutively expressed in most mammalian tissues, being responsible for the physiological production of prostanoids, COX-2 is usually not detectable in normal tissues. It can be induced by either mitogenic and/or pro-inflammatory *stimuli* (152), causing an elevated production of prostanoids, thus triggering inflammatory effects (153). For this reason, COX-2 is widely targeted for the treatment of inflammation, while non-specific inhibition of COX-1 is usually responsible for the side-effects of anti-inflammatory drugs. In fact, the first generation of non-steroidal anti-inflammatory drugs suffer from strong side-effects as consequence of their inability to distinguish between the two isoforms. Nowadays, COX-2-selective drugs are able to prevent most of these side-effects. Recently, a third isoform of COX was described: COX-3. In fact, this isoform results from the same gene of COX-1, but with alternative splicing that leads to the retention of intron 1 in its mRNA. For this reason, some authors claim that it should be named COX-1b (153).

Regardless the COX isoform, arachidonic acid is converted into PGG$_2$, which subsequently originates PGH$_2$ *via* COX peroxidase activity. From this point forward, several different molecules can be synthesized according to the enzymes involved in the reaction (**Figure 13**). Given the fact that these enzymes are heterogeneously distributed

in tissues, distinct biological effects are possible, including vasodilatation (PGD_2, PGE_2, PGI_2), gastric cytoprotection (PGI_2), as well as fever mediation, pain sensitivity, and inflammation (PGE_2) (154, 155). Other functions include involvement in the contraction of bronchial airways and regulation of platelet aggregation (TXA_2) (155).

As it will be presented later, arachidonic acid can also be metabolized by LOX, thus originating hydroxyeicosatetraenoic acids, leukotrienes and lipoxins.

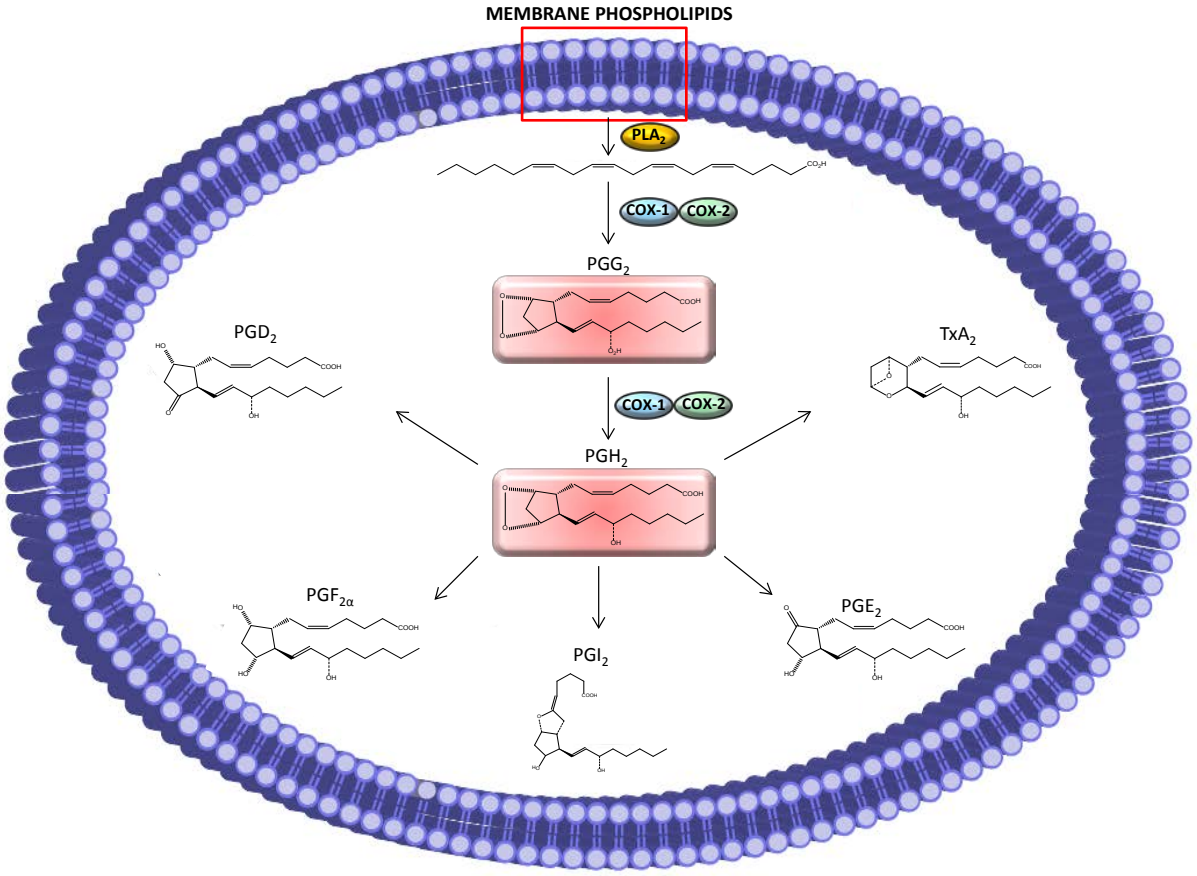

FIGURE 13 – COX pathway. PLA_2 hydrolyzes membrane phospholipids, originating arachidonic acid, which is further metabolized by COX. Tissue-specific enzymes are responsible for the end-products formed.

Lipoxygenase

LOX belong to a super family of enzymes that have polyunsaturated FA as substrates. These enzymes are responsible for several biological functions in cells, which include signaling as well as structural and pathological changes, according to the products obtained. LOXs can be found in plants and animals and are absent in yeast, while their presence in insects is not yet consensual. Nowadays, several LOXs are known to occur in humans, 5-LOX, 12-LOX and 15-LOX being the most important in physiological and pathological processes (156).

In the particular case of inflammatory processes, arachidonic acid is a substrate for LOX, originating 5-HPETE, which is spontaneously converted to 5-hydroxyeicosatetraenoic acid (5-HETE) that, in turn, is converted in LTA_4 and then sequentially to LTC_4, LTD_4 and LTE_4 (**Figure 14**).

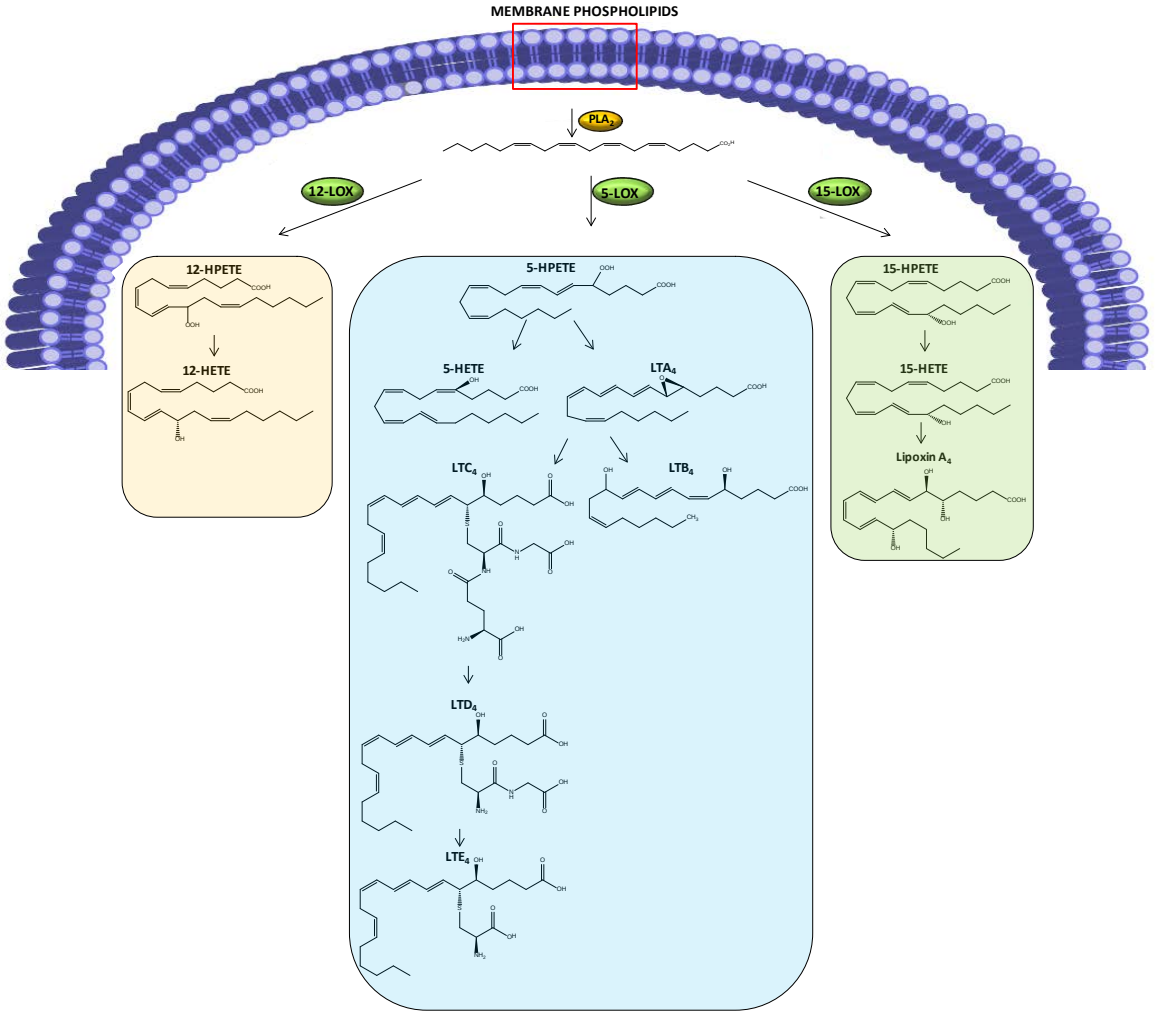

FIGURE 14 – LOX pathway. PLA_2 hydrolyzes membrane phospholipids, originating arachidonic acid. According to the LOX isoform involved, different metabolites are obtained.

Nitric oxide synthases

Nitric oxide synthase (NOS) is the main enzyme involved in the synthesis of NO, whereas NO is synthesized from L-arginine in a reaction that also yields L-citrulline. It requires nicotinamide adenine dinucleotide phosphate (NADPH) and oxygen as co-substrates and (6R)-tetrahydrobiopterin (BH_4), flavin adenine dinucleotide (FAD), flavin mononucleotide (FMN) and iron protoporphyrin IX as co-factors. Three different NOS isoforms are known. The neuronal NOS (nNOS, NOS I) is expressed predominantly in the

brain and peripheral nervous system (157). Other tissue-dependent isoform of this enzyme is the endothelial NOS (eNOS, NOS III) that, as it can be easily inferred by the name, is found mainly in endothelial cells. Both NOS I and NOS III isoforms are usually described as being constitutively expressed in resting cells, where they exert physiological actions. When certain *stimuli* are triggered, mostly related with an increase of the intracellular concentration of calcium, the enzymes are activated and the synthesis of NO takes place (158). The third isoform is inducible (iNOS) and is responsible for many of the deleterious effects experienced in some pathological conditions, such as inflammation (158, 159). The exposure to microbial products, such as lipopolysaccharide (LPS) and double-stranded RNA (dsRNA), or to pro-inflammatory cytokines, like IL-1, TNF-α and interferon-γ (IFN-γ), induces the expression of *iNOS* gene in various cell types in different tissues. Binding of calmodulin to iNOS is tight even at low calcium concentrations, and, therefore, iNOS is also called calcium-independent NOS and it can produce high levels of NO for prolonged periods (158, 159).

The biological properties of NO can result from a direct effect or, instead, as a consequence of the formation of reactive nitrogen species (RNS), of which peroxynitrite, generated by reaction with superoxide anion, is the best example. Several physiological processes are regulated by NO, including blood pressure, host defense and platelets function.

In the particular case of inflammation, NO can enhance the production of TNF-α (160) and IL-1β (161) and hence acts synergically in the production of inflammatory mediators. In addition, NO is cytotoxic and can react with proteins and nucleic acids and be responsible for the onset of the so called NO-induced apoptosis. This is known to occur in several cells such as microglia, macrophages and β-pancreatic cells, and for which ER-stress has been shown to contribute (162-164). Thus, the ability to prevent NO production following a pro-inflammatory stimulus is commonly used to screen compounds for anti-inflammatory activity.

NF-κB

NF-κB is an ubiquitous and inducible transcription factor. It is one of the most important regulators of the inflammatory response and immune system, being conserved across several species. It is also involved in cell proliferation and apoptosis (165).

Under basal conditions, this transcription factor is located in the cytosol, in an inactive form that is a consequence of the binding to a group of inhibitory proteins, named IkB, which include IkBα, IkBβ, IkBε and IkBγ.

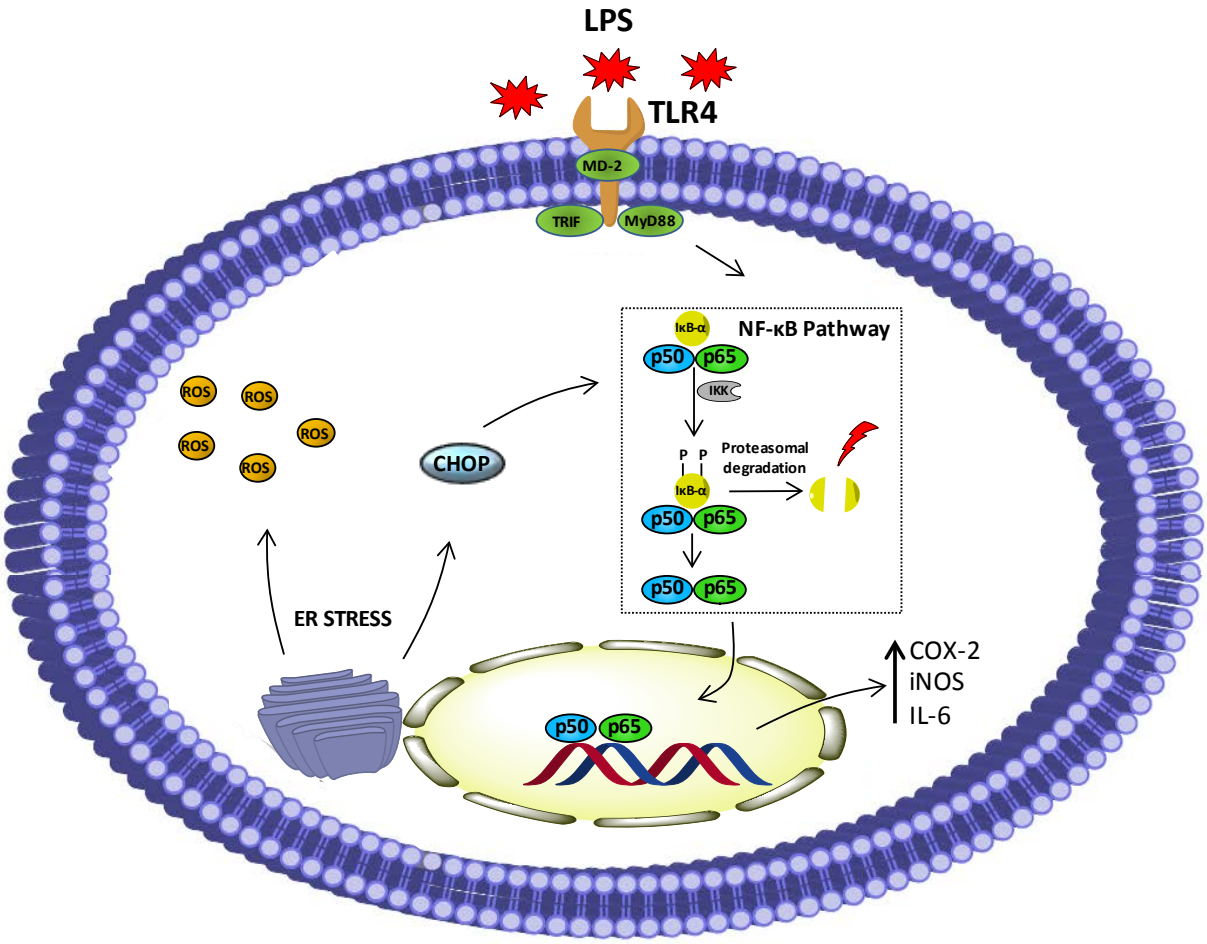

Figure 15 - Representation of NF-κB activation and crosstalk with ER stress. Under basal conditions NF-κB is inhibited by IκB-α which, upon phosphorylation by IKK, is marked for degradation by 26s proteasome complex, thus leaving NF-κB free to be translocated to the nucleus where it modulates gene expression.

In the particular case of mammalian cells, five NF-κB family members are known: RelA/p65, RelB, c-Rel, p50/p105 (NF-κB1) and p52/p100 (NF-κB2). In turn, NF-κB is composed by homodimers and heterodimers of different proteins of the Rel family; however, the most common forms of NF-κB are dimeric complexes of p50/RelA (p50/p65) (166, 167).

Following phosphorylation by the IκB kinase complex (IKK), IκB is marked for degradation *via* the proteasome, thus leaving NF-κB free. Once free, NF-κB translocates to the nucleus, where it binds to the promoter region of several genes, thus exerting a number of actions (**Figure 15**) (168). Target genes include cytokines, *COX-2*, *iNOS*, proteases and many others. At this point it is important to highlight that nowadays, two different activation pathways for NF-κB are known: the canonical and the alternative pathways. The proteasome degradation of the inhibitor complex IκB takes place in both cases, but different *stimuli* trigger this action. While in the classical canonical pathway

NF-κB can be activated by several pro-inflammatory signals, such as cytokines and activation of toll-like receptors (TLRs), in the alternative pathway the activation of B-cells is required (169, 170).

The knowledge of the events that take place in NF-κB activation allows the identification of distinct mechanisms by which inhibition can occur: prevention of the IKK complex activation, modulation of proteasome activity and modulation of NF-κB translocation to the nucleus/prevention of binding to DNA. In the case of molecules of marine origin, several mechanisms of action have been already referred (9).

PPAR

PPARγ is a transcription factor that belongs to the nuclear receptor family of ligand-activated transcription factors. Nowadays, three members of this family are known: PPARα, PPARδ and PPARγ. Contrary to PPARδ and PPARγ, PPARα is indeed a transcription factor whose activation results in proliferation of peroxisomes. PPARγ forms heterodimers with the retinoid X receptor and then exerts its effects by binding to a DNA element, known as the PPAR response element (PPRE). This transcription factor was initially linked to the regulation of adipocyte differentiation and lipid metabolism (171). Nowadays, however, several physiological and pathological events are known to be PPAR-mediated, the effect depending on the cell type (172).

In what concerns the involvement of PPAR in inflammatory pathways, it is known that the activation of this transcription factor in macrophages results in anti-inflammatory effects, such as decreased cytokine production or iNOS expression. These effects can be the result of direct negative modulation of target genes or, alternatively, of the prevention of NF-κB activation (172-174). In fact, PPAR activators have been shown to prevent NF-κB activation *via* physical interaction with both p65 and p50 (175, 176). Activation or increased levels of PPAR-γ have been linked to decreased levels of intracellular reactive oxygen species (ROS) in several cells types (177, 178).

1.6. Cancer

Cancer is a pathological condition with increasing incidence and prevalence, being the leading cause of death in economically developed countries and the second leading cause of death in developing countries (179). Taking into account the numbers from the World Health Organization (WHO), in 2008 13% of all deaths were due to cancer, which represents 7.6 million people (180).

From a physiopathological point of view, cancer is a complex genetic disease involving changes in metabolic pathways and gene expression. For many years carcinogenesis has been primarily attributed to abnormalities in oncogenes and tumor-suppressing genes, however in recent years other players, such as micro RNA (miRNA), have been recognized for their importance in cancer onset and progression (181).

Carcinogenesis, a process by which normal cells are transformed into cancer cells, is a multi-step process that includes initiation, promotion and progression. In all cases, a number of epigenetic and genetic alterations affecting both oncogenes and tumor suppressor genes take place (182).

While the initiation stage can be inhibited by agents that either prevent the action or inactivate carcinogens or act as antioxidants, later stages are prone to inhibition by drugs that suppress tumor growth or stimulate apoptosis. In fact, defects in apoptosis are common traits found across several types of cancer, being one of the critical steps in tumorigenesis and resistance to therapy. For this reason, apoptotic pathways are important targets in cancer therapy (183).

1.6.1. Targets in cancer

Apoptosis

Many of the drugs used in chemotherapy are able to elicit apoptosis, as the loss of the ability to undergo apoptosis is currently accepted as one of the most important changes that mark the onset of cancer cells (184).

Apoptotic cell death displays a number of morphological and biochemical traits that are typical in this type of programmed cell death. From a morphological point of view, cells undergoing apoptosis display condensed chromatin and, in later stages, chromatin fragmentation. The plasma membrane is also affected and, although it never loses its integrity, protrusions commonly referred as “blebs” are usually present. In later stages, apoptotic bodies, which are membrane-bound vesicles that contain several cellular contents, from cytosolic organelles to fragments of condensed nuclei, are formed (185).

This type of cell death can be induced by the intrinsic/mitochondrial pathway, in which mitochondrion play a pivotal role, and by the extrinsic/death receptors (DR) pathway, which involve the activation of DR.

In the mitochondrial pathway, formation of permeability transitions pores (PTP) is critical for the subsequent chain of events. These pores are formed across the mitochondrial membranes and are constituted mainly by 3 protein components: voltage-dependent anionic channel (VDAC), cyclophilin A (CypD) and adenine nucleotide translocase (ANT) (186). Upon several *stimuli*, including high calcium levels and ROS, formation of PTP is triggered and leads to a loss of mitochondrial membrane potential ($\Delta_{\psi m}$) (187). These events result in the leakage of pro-apoptotic molecules, such as cytochrome *c*, Smac/DIABLO, HtrA2/Omi, apoptosis inducing factor (AIF) and endonuclease G. Once in cytosol, cytochrome *c* triggers the assembly of apoptotic protease-activating factor 1 (Apaf-1) and procaspase-9 into a complex called apoptosome, which in turn induces activation of the initiator caspase-9 (188) and subsequently, of the effector caspase-3 and/or -7, depending on the cell type. These caspases trigger some of the above referred hallmarks of apoptosis, like oligonucleosomal DNA fragmentation. However, it should be highlighted that different expression of caspases in different cell types may result in distinct apoptotic traits.

At the same time, the Bcl-2 family proteins also play an important role in this pathway. Bcl-2 family members can act either as anti-apoptotic or as pro-apoptotic factors. Proteins with anti-apoptotic activity are predominantly found within the outer mitochondrial membrane (OMM) or in the ER, while the pro-apoptotic molecules exist in the cytosol or loosely bound to the OMM as monomers. The major anti-apoptotic factors are Bcl-2, Bcl-2 long isoform (Bcl-xL), Bcl-2-related gene A1, and myeloid cell leukaemia 1 (Mcl-1) (189). In what concerns pro-apoptotic proteins, one further division includes effector proteins (Bcl-2 antagonist killer 1 – Bak; Bcl-2 associated protein x- Bax) and BH3-only proteins (Bid, Bim, Bad).

In the extrinsic pathway, membrane receptors with pro-apoptotic activity that belong to the TNF superfamily, are activated by ligands such as TRAIL, TNF-α or Fas ligand (FasL), which activate DR 4/5, tumor necrosis factor receptor (TNFR) and Fas, respectively (190). Following activation, these receptors undergo conformational changes that lead to the assembly of death-inducing signaling complex (DISC). After this point, the receptors recruit Fas-associated death domain (FADD) and procaspase-8. The association of procaspase-8 to DISC results in its autoproteolytic cleavage, releasing two subunits that form the active enzyme (191). After this point, two different pathways may occur, depending on the cell type. In type I cells, the activity of caspase-8 *per si* is enough to activate effector caspase-3, -6 and -7, thus triggering the apoptotic response. Differently,

in type II cells, caspase-8 cleaves Bid giving rise to truncated Bid (tBid) which promotes the oligomerization of Bax/Bak found in the mitochondrial membrane. These proteins will then cause the release of cytochrome c and smac/DIABLO that activate the intrinsic pathway and increase even more the active caspase-8 by a positive feedback (190-192).

Due to the fact that production of superoxide is a physiological process, cells have developed a number of strategies to counter its deleterious effects. One of these strategies relies on conversion of superoxide to hydrogen peroxide by superoxide dismutase (SOD). Two isoforms are found in cells: Mn-SOD in the matrix and Cu/Zn-SOD in the cytoplasm. The hydrogen peroxide formed is then converted to oxygen and water by either catalase (CAT) or glutathione peroxidase (GPrx) (193). Although very efficient, these antioxidant systems are not perfect and there are several points when ROS may leak: superoxide itself can escape from SOD and thus cause oxidative stress *per si* or, alternatively, the less reactive hydrogen peroxide can form the highly reactive hydroxyl radical *via* the Fenton reaction that can initiate lipid peroxidation, particularly in membranes. Taken together these ROS can cause several cellular damage by oxidizing lipids, proteins and DNA, eventually triggering apoptosis (193).

Tubulin

Tubulin-containing structures are important for several cellular functions, including chromosome segregation during cell division, intracellular transport, development and maintenance of cell shape, cell motility, and, in some cases, localization of molecules on cell membranes (194).

Several anticancer drugs exert their effect by affecting microtubules dynamics *via* interactions with tubulin, either as tubulin polymerization inhibitors or promoters, (195). The microtubule cytoskeleton environment is highly dynamic due to the transitions between growing and shrinking phases, caused by exchanges of tubulin dimmers at microtubule end (2, 196). This equilibrium, tightly regulated by microtubule-associated proteins (MAPs), can be disturbed by microtubule targeting agents (MTAs). As a consequence of their effect on microtubules dynamics and activity, these molecules act as stabilizer or destabilizers, which ultimately can lead to cell cycle arrest or cell death.

Four tubulin binding sites are currently known, namely the taxane/epithilones site, the laulimalide/peloruside A site, the colchicine site and the vinca alkaloids site. According to the binding site involved, different mechanisms of interference with tubulin take place. Drugs that bind to the first two sites stabilize microtubules while binding to the latter two results in tubulin depolymerization (196).

Protein kinases

Protein kinases are enzymes that act as key regulators of several intracellular signal transduction pathways. These enzymes are frequently involved in cascades of signal amplification and transduce most extracellular signals, either by receptor-activated tyrosine phosphorylations or by receptor coupling to guanosine-5'-triphosphate (GTP)-binding proteins (197). In normal conditions, several cellular processes are tightly regulated by the appropriated function of protein kinases, however, abnormal protein kinase activity has been increasingly identified in cancer. In fact, an increasing number of kinases have been associated to processes that ultimately lead to tumor proliferation and survival, frequently due to the fact that they become refractory to the regulatory mechanisms by either genetic mutation or translocation (198). Given the fact that normal cells usually tolerate inhibition of these enzymes, a therapeutic opportunity for the selective killing of cancer cells was established (199). About 600 protein kinases and 150 phosphatases are known, all of which can be grouped in 3 main categories: tyrosine-specific, serine/threonine specific and those specific for both tyrosine and serine/threonine.

The factors that affect protein kinase function, as well as the state-of the art in what regards new drugs have been reviewed elsewhere (199, 200), however, it is worth mentioning that natural products have also given their contribution to this new area of research (201-204). Given the widespread presence of protein kinases in nearly all cellular processes, their inhibition can ultimately result in modifications of other targets, such as cell cycle, apoptosis and angiogenesis.

Angiogenesis

Angiogenesis, the process by which new blood vessels are formed, is a very important phenomenon both in physiological and pathological processes (205, 206). Vascular endothelial growth factor (VEGF) is one of the most important proteins that stimulate vasculogenesis and angiogenesis. One of the major *stimulus* that trigger VEGF, and hence angiogenesis, is hypoxia (oxygen levels below 1%), a common trait in tumors given their high metabolic rate and increasing distance from the blood vessels (207). Hypoxia inducible factor 1 (HIF-1) is a heterodimer that comprises two subunits, HIF-1α and HIF-1β, and one of the key modulators of the transcription of *VEGF* gene. While HIF-1β is constitutively expressed, HIF-1α is oxygen dependent and, thus, highly influenced by

hypoxia. Several studies have shown that HIF-1α is over-expressed in many human tumor cells including pre-invasive and invasive breast cancer (201, 208).

Due to the fact that malignant neoplasms require a constant supply of nutrients and oxygen, they cannot grow beyond a limited size without an adequate blood supply. Thus, inhibition of tumor-associated neoangiogenesis represents a promising target for antineoplastic therapy. In particular, the critical role of VEGF (209-211) has turned it a successful strategy for therapeutic intervention (211). In addition to treatment, tumor vasculature has also been increasingly regarded as a valuable marker for tumor grading and metastasis (212).

The major receptor and mediator for VEGF is vascular endothelial growth factor receptor 2 (VEGFR2), also named Flk1, and is involved in several signaling pathways that regulate angiogenesis, like mitogen-activated protein kinases (MAPK) (213), focal adhesion kinase (FAK) (214), AKT8 virus oncogene cellular homolog 8 (215) and the JAK/STAT signaling pathway, especially STAT3. All these targets are currently being studied for drug discovery.

Upon binding to its receptor(s), VEGF activates the MAPK and Akt signaling pathways, which induce endothelial cell growth, migration, homeostasis and microtubules formation. Therefore, many anti-angiogenic agents, currently used clinically and/or under clinical trials, are either antibodies against VEGF or target VEGF signaling by inhibiting VEGF receptor (VEGFR) tyrosine kinase activity (216, 217). Although several natural compounds have shown to inhibit tumor angiogenesis (4, 201, 218-221), at the moment their use is still very limited.

Another approach to target vasculature is the vascular disrupting approach. Vascular disrupting agents (VDA) mainly target the established tumor blood vessels of larger, solid tumors with a major effect on the central part of the tumor, causing vessel occlusion and necrosis (222).

1.7. ER stress in inflammation and apoptosis

Though the involvement of ER stress in different biological processes is not totally clarified, the crosstalk between ER stress and inflammation/apoptosis has been described.

The ER is constituted by a network of branching tubules and sacs that is present in all eukaryotic cells and is contiguous with the nuclear envelope. From a functional point of view, ER is mainly responsible for the synthesis, folding and modification of several proteins (223). The newly ER-synthesized proteins fold into their correct tridimensional structure, after which they are targeted to several cellular organelles or to the extracellular matrix.

Several signals can alter ER homeostasis, from physiological states that increase the demand for protein folding to *stimuli* that disrupt protein folding, originating an imbalance between the protein-folding load and the capacity of the ER (224, 225). The results are misfolded or unfolded proteins that accumulate in the ER lumen, a condition referred to as ER stress.

To this moment, three major proteins are known to act as stress sensors in the ER: double-stranded RNA-dependent protein kinase PKR-like ER kinase (PERK), inositol-requiring 1α (IRE1α) and activating transcription factor 6 (ATF6). Each of these proteins display an ER-luminal domain that senses unfolded proteins, a transmembrane domain and a cytosolic domain that communicates with translational and transcriptional pathways (224, 226, 227). Two of these sensor proteins have also catalytic activity: PERK has a protein-kinase activity and phosphorylates eukaryotic translation-initiation factor 2α (eIF2α). On the other hand, IRE1α has both protein-kinase activity and endoribonuclease (RNase) activity and it removes a 26-nucleotide intron from the ATF6-induced XBP1 mRNA, thus originating the sXBP1 splice which will be further discussed in the next section. In cells that are not undergoing stress, these ER stress sensors are in their inactive form *via* association with an ER chaperone, immunoglobulin-heavy-chain-binding protein (BiP/HSPA5/GRP78). Dissociation of GRP78 from PERK triggers the dimerization and subsequent autophosphorylation of the kinase, thus yielding the active form of PERK. After this point, phosphorylation of eIF2α inhibits protein translation (**Figure 16**) as demonstrated by experiments with $PERK^{-/-}$ mouse embryonic fibroblasts that failed to inhibit protein translation following an ER stress elicitor (228).

Due to the deleterious effect of ER stress, eukaryotic cells have developed sensor pathways, such as the UPR that allow detection of ER stress and trigger response pathways. When the UPR is activated, several emergency systems can be activated in order to cope with stressful and potentially harmful consequences of protein folding

impairment, including induction of ER chaperones, such as BiP/GRP78 and GRP94, degradation of unfolded proteins *via* ER degradation-enhancing α-mannosidase-like protein (EDEM), translational attenuation and NF-κB activation (224-226, 229, 230). The activation of the latter appears to be associated to the above-mentioned attenuation in protein translation, which results in decreased levels of the NF-κB inhibitor, IκB-α. Increased levels of calcium have also been linked with NF-κB activation in ER-stressed cells. This is related with another physiological role of ER, namely to act as the cell's calcium store. Several studies show that antioxidants and calcium chelators can mitigate the activation of the NF-κB as a consequence of ER stress (231).

ROS are an important link between ER stress and inflammation. Increased levels of ROS are a common trait found in inflammatory condition and it is now believed that they, too, can be a consequence of ER dysfunction. In order to carry its folding functions, two proteins are involved in the formation of intra and intermolecular disulphide bridges and serve as electron transporters in ER: protein disulphide isomerase (PDI) and ER oxidoreductin 1 (ERO1) (232). In this process ROS are frequently generated. Although this is a controlled mechanism, in situations involving ER stress the amounts of ROS produced increase, thus triggering the activation of antioxidant mechanisms that involve several defense factors, such as glutathione S-transferase and NAD(P)H-quinone oxidoreductase (227, 233). When these defenses are not enough to counter the deleterious effects of ROS, they can oxidize several proteins in the ER and leak to the cytoplasm where they can attack several cellular targets. In addition, ROS-mediated activation of the NF-κB pathway has also been described.

Several ER-stress inducers are known, although their mechanisms of action are distinct. The *Streptomyces* sp.-derived nucleoside antibiotic tunicamycin acts by blocking protein glycosylation and inducing ROS as presented above, the lactone sesquiterpene thapsigargin causes depletion of ER calcium reserves and dithiothreitol disrupts disulfide bond formation (230).

In certain cellular stress factors, notably ER stress, DNA-damage-inducible gene 153 (GADD153), also known C/EBP homologous protein (CHOP, a member of the C/EBP transcription factor family that heterodimerizes with other C/EBPs) is induced and is responsible for several biological functions, from apoptosis to inflammation (234). In a general way, CHOP is ubiquitously expressed in most cells, albeit at very low levels (230). ER stress causes the proteolytic degradation of the ER transmembranar protein p90ATF6, thus releasing p50ATF6 which is then transported into the nucleus where it binds to the ER stress responsive element (ERSE) of *CHOP* gene and, hence, upregulates the levels of the protein (235, 236) .

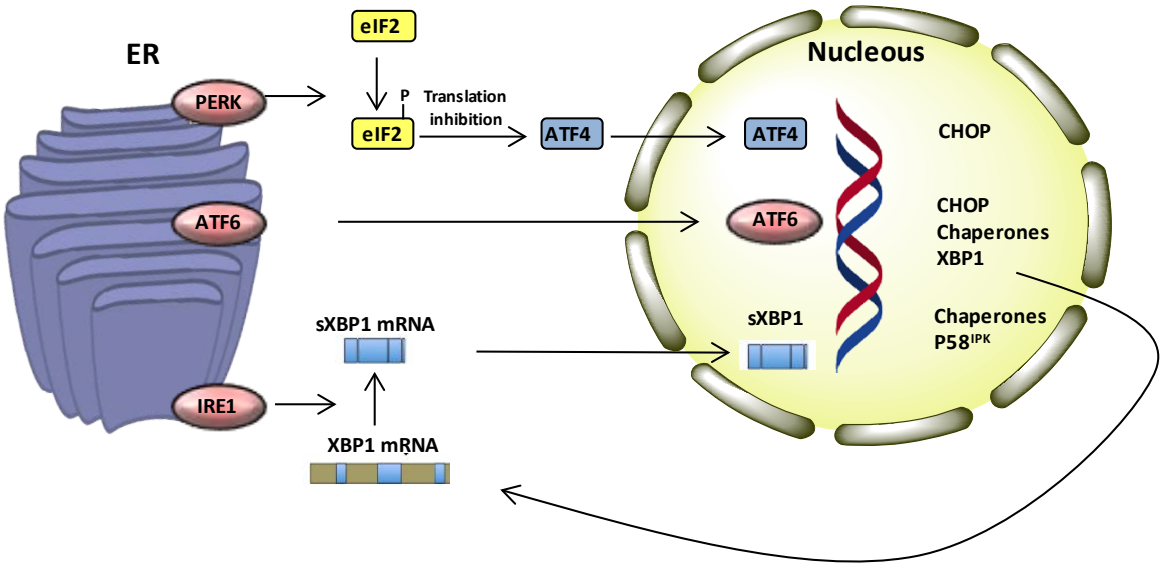

Figure 16 - Major proteins involved in ER stress sensing and signal transduction.

In the particular case of LPS-induced inflammation, several studies have demonstrated that LPS causes an increase of CHOP and NO levels. Deeper insights on the subject showed that, although LPS can elicit several molecules involved in NO-induced apoptosis, they were detected only after the upregulation of the protector molecules BiP, EDEM, Derlin-1 and Derlin-2. Differently, when other *stimuli* are used that are able to trigger an increase in CHOP and NO before the defense mechanisms can be activated, apoptosis takes place (237).

Nowadays, the role of ER stress in apoptosis is well established, however the precise mechanisms linking these two events are not fully understood. The characteristic attenuation of protein translation found in ER-stressed cells is not absolute as some genes can bypass this eIF2-α-mediated translational block. Such is the case of ATF4, which encodes C/EBP and is involved in several survival pathways that include amino acid metabolism, stress response and protein secretion, however ATF4 is also involved in pro-apoptotic pathways *via* upregulation of CHOP (**Figure 17**).

In the case of ATF6, after dissociation from GRP78 it is cleaved to its active form by site-1 and site-2 proteases and moves the nucleus, where it modulates genes that are part of the ERSE (**Figure 16**) (224, 238). At the moment it seems that there is no direct link between ATF6 and ER stress induced apoptosis. However, ATF6 seems to be related with pro-survival pathways and activation of mechanisms to cope with ER stress (224, 228).

As presented before, IRE1α originates the sXBP1 splice form XBP1. This molecule targets ER chaperones and the $P58^{IPK}$, a HSP40 family member. After this point, $P58^{IPK}$ inhibits PERK and provides a negative feedback signal that attenuates PERK-mediated blockage of translation. At this point it is important to highlight that upregulation of $P55^{IPK}$ is not an immediate event, taking place only several hours after phosphorylation of PERK and eIF2a. At the moment, it is believed that upregulation of $P58^{IPK}$ marks the end of the UPR. If this time-gap is enough to correct the factors that triggered UPR, then the cell survives. If, however, the stress is maintained, then apoptotic cell death is triggered by activating death cascades that include CHOP,c-Jun N-terminal kinase (JNK) and the Bcl2 family proteins (**Figure 17**).

Several studies show that activation of UPR is responsible for the activation of caspase-12, which in turn triggers the intrinsic pathway of apoptosis by downstream activation of caspase-9 and -3 (239, 240). It is important to highlight that in this ER-mediated apoptosis, although the intrinsic pathway is initiated, some of the common traits present in this type of controlled cell death, such as cytochrome c release, may not be found. While the contribution of caspase-12 to ER-mediated apoptosis is fairly understood in mice, in humans some controversy remains, mainly due to the fact that most humans do not express active caspase-12, with only a small part of the population being able to express the full-fledged active enzyme (241, 242). For this reason, caspase-4 is believed to fulfill in humans many of the functions of caspase-12 in mice. Similarly to caspase-12, caspase-4 is also part of the caspase-1 subfamily and is bound to the ER membrane, being cleaved following ER stress (243).

ER stress-mediated apoptosis can be inhibited by increased levels of Bcl-2 or one of its homologues, thus indicating that this process is started by pro-apoptotic BH3-only proteins (243). Some studies refer Bim as the sole responsible for this process, without involvement of Puma or Bid, and a calcium-independent mechanism involving Bim dephosphorylation is proposed (244). Although Bim mRNA levels are known to be increased in ER-stressed cells, the most relevant mechanism that results in increased expression involves changes in the protein turnover. In cells that are not undergoing ER stress, Bim is phosphorylated by ERK1/2 and thus marked for ubiquitination and proteasomal degradation. In the case of ER stress, phosphatase 2 A (PP2A) is activated and results in Bim dephosphorylation and consequent changes in the protein turnover. In fact, PP2A-mediated dephosphorilation prevents ubiquitination and proteosomal degradation of Bim. This result was further confirmed by studying the effect of ER-stressers in Bim-deficient cells, which showed a higher survival rate (244).

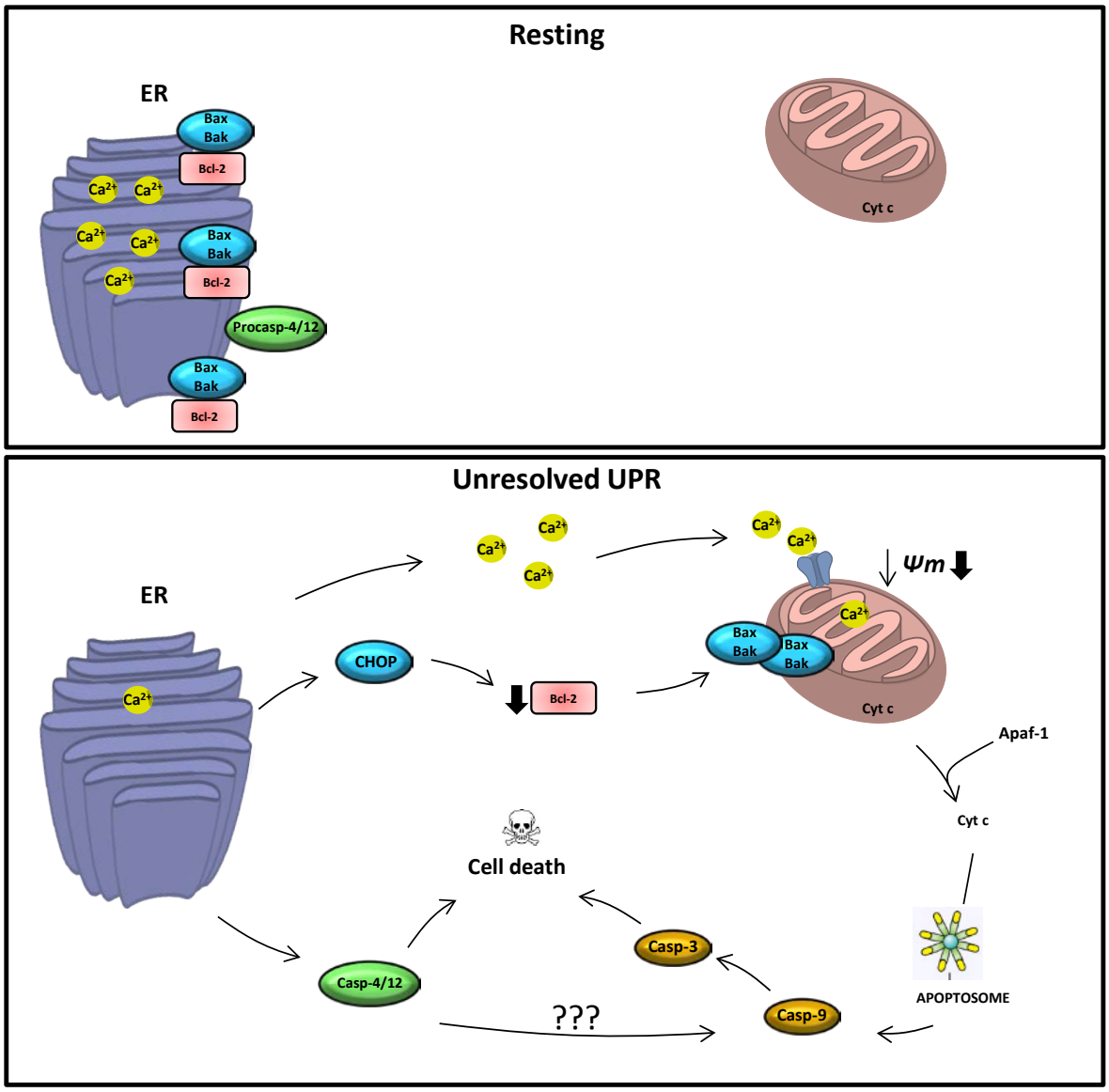

Figure 17 – Major pathways connecting ER stress and apoptosis.

Differently, in studies using the estrogen receptor positive human breast cancer cell line (MCF-7), Puma was found to be the most important pro-apoptotic protein (245) while in the mouse embryonic fibroblast cell line (MEF) Puma and Noxa were the predominant pro-apoptotic proteins (246). Taken together these results show that there is a cell type-specificity regarding ER stress induction of BH3-only proteins. Regardless of the proteins involved, in most cases Bim, Bid, Noxa or Puma are not enough to trigger apoptosis. Instead, they interact with other pro-apoptotic proteins which in turn are responsible for the effective part of cell death. Among these proteins, Bax and Bak are pivotal to this process, as demonstrated by early reports in which deficient levels of these

proteins conferred protection against ER-mediated apoptosis (247). In resting cells, Bax and Bak proteins can be found in the ER-membrane where they are inhibited by the anti-apoptotic protein Bcl-2. In situations when the UPR is not sufficient to restore homeostasis, several events take place. Bcl-2 levels drop, which disturbs the equilibrium between pro- and anti-apoptotic proteins. As so, Bak and Bax are freed from the ER and translocated to the mitochondria membrane where they induce the formation of pores that leads to a loss of $\Delta\Psi_m$ (228) **(Figure 17)**. This event results in the leakage of cytochrome *c* which, in turn, will trigger the classical intrinsic pathway presented in section **2.5.1.** Although the role of Bcl2 proteins to ER-mediated apoptosis is clear, the precise link between the ER-insult and the apoptotic trigger remained elusive for a long time. Nowadays, CHOP and JNK are thought to be this link. When CHOP is expressed *via* the above-mentioned ER-stress sensors, it represses Bcl2 gene family, thus favoring the referred pro-apoptotic proteins. At the same time JNK, which is critical for the phosphorylation of Bcl2 proteins, is activated by the IRE1α-TRAF2-ASK1 pathway of the UPR. This results in phosphorylation of Bcl2 which, in turn, prevents Bax and Bak inhibition and ultimately leads to mitochondrial translocation and activation of the intrinsic pathway of apoptosis (228).

It is also important to refer that, following an unresolved UPR, other function of the ER are lost, such as its ability to store calcium. Calcium levels within the ER are about 500 times higher than in cytosol, with calcium fluxes being largely controlled by dephosphorylated BCL2. When this protein is phosphorylated by JNK, it loses the ability to modulate calcium levels which, upon translocations to mitochondrion, *via* uniport transporters can further aggravate the loss the mitochondrial potential and accelerate the intrinsic pathway of apoptosis.

2. Objectives

The role of Nature as a source of bioactive molecules is undeniable and, recently, marine organisms have been increasingly regarded as a remarkable source of new chemical entities, most of them displaying several biological properties. In this regard, only fully characterized molecules can be further used for biological studies and thus adequate instrumental techniques and methods are required. At the same time, cancer and inflammatory conditions are among the most prevalent diseases in developed countries. Taking into account that many marine-derived products have already been proved to be effective in these diseases, the main objectives of this research project include:

1. The development of instrumental techniques for the analysis of natural products of marine origin with potential application in human health.

2. Contribute to the knowledge of the chemical composition of several marine macro-organisms of Portuguese ecosystems, namely *Marthasterias glacialis*, *Holothuria forskali*, *Paracentrotus lividus* and *Aplysia* sp.

3. Investigate the potential use of *M. glacialis* as a source of pro-apoptotic molecules with application in cancer.

4. Investigate the potential use of *M. glacialis* as a source of anti-inflammatory molecules and the mechanism of action involved.

5. Contribute to the growing body of proof that establishes marine organisms as an interesting source of bioactive molecules with application in human health.

PART II
RESULTS

Paper 1

HPLC-PAD-atmospheric pressure chemical ionization-MS metabolite profiling of cytotoxic carotenoids from the echinoderm *Marthasterias glacialis* (spiny sea-star).

Federico Ferreres, ***David M. Pereira****, Angel Gil-Izquierdo, Patrícia Valentão, João Botelho, Teresa Mouga, Paula B. Andrade.*

Journal of Separation Science, **2010, 33, 2250–2257**

Federico Ferreres[1]
David M. Pereira[2]*
Angel Gil-Izquierdo[1]
Patrícia Valentão[2]
João Botelho[2]
Teresa Mouga[3]
Paula B. Andrade[2]

[1]Research Group on Quality, Safety and Bioactivity of Plant Foods, Department of Food Science and Technology, CEBAS (CSIC), Murcia, Spain
[2]REQUIMTE/Department of Pharmacognosy, Faculty of Pharmacy, Porto University, Porto, Portugal
[3]GIRM – Marine Resources Research Group, School of Tourism and Maritime Technology, Polytechnic Institute of Leiria, Santuário Na. Sra. Dos Remédios, Peniche, Portugal

Received March 23, 2010
Revised May 10, 2010
Accepted May 11, 2010

Research Article

HPLC-PAD-atmospheric pressure chemical ionization-MS metabolite profiling of cytotoxic carotenoids from the echinoderm *Marthasterias glacialis* (spiny sea-star)

An HPLC-PAD-atmospheric pressure chemical ionization-MS metabolite profiling analysis was conducted on the marine echinoderm *Marthasterias glacialis* (spiny sea-star). Bio-guided purification of the methanolic extract led to the isolation of several carotenoids, namely zeaxanthin, astaxanthin and lutein. These compounds were characterized using both UV–Vis characteristics and MS spectra interpretation. No previous works addressed the MS analysis of carotenoids present in this organism. The purified carotenoid fraction displayed a strong cell proliferation inhibition against rat basophilic leukemia RBL-2H3 ($IC_{25} = 268$ μg/mL) cancer cell line. Against healthy V79 (rat lung fibroblasts ($IC_{25} = 411$ μg/mL)) cell line, however, toxicity was lower, as it is desired for anti-cancer molecules. This study suggests that *M. glacialis* may constitute a good source of bioactive compounds that can be used as lead compounds for the pharmaceutical industry.

Keywords: Carotenoids / Cytotoxic / HPLC-PAD-atmospheric pressure chemical ionization-MS / *Marthasterias glacialis*
DOI 10.1002/jssc.201000197

1 Introduction

Carotenoids are a class of hydrocarbons (carotenes) and their oxygenated derivatives (xanthophylls). Their basic structure reflects their biosynthetic pathway and consists of eight isoprenoid units. A series of conjugated double bonds constitute the characteristic chromophore. Carotenoids are quite widespread in nature and marine organisms are no exception. In fact, the higher degree of diversity seems to be in the aquatic environment [1].

These compounds can play an important role in human health by acting as antioxidants, protecting cells and tissues from the damaging effects of reactive species. Lutein and zeaxanthin and xanthophylls found in corn and in leafy greens, such as kale and spinach, are believed to function as protective antioxidants in the macular region of the human retina, to protect against cataract formation, coronary heart diseases and stroke. Astaxanthin, a xanthophyll found in several marine organisms, is another naturally occurring compound with potent antioxidant properties. Other health benefits of carotenoids that may be related to their anti-oxidative potential include enhancement of immune system function and inhibition of the development of certain types of cancers [2]. The most well-known physiological role of carotenoids is provitamin A activity, although not all compounds exhibit this property [3].

Marthasterias glacialis (spiny sea-star) is an asteroid echinoderm, a group that has demonstrated to play one of the most influential roles in benthic ecosystems on a variety of scales [4]. During the period 1940–1950s, this species received great attention, mainly due to its asterosaponins [5]. At the same time, carotenoids in this organism were also studied by means of the analytical techniques common at the time, namely absorption spectrum, comparison of Rf values by TLC and partition coefficient [6]. To our knowledge, no previous study provided the LC-MS analysis of the carotenoid fraction of *M. glacialis* and its biological potential.

Due to the heat-lability of carotenoids, GC-MS is not suitable for their analysis, the most convenient method being HPLC with UV–Vis detection or, if possible, MS detection. Xanthophylls and carotenes form both molecular ions and protonated molecules during positive-ion atmospheric pressure chemical ionization (APCI). APCI is an ideal method of ionization for low to medium polar compounds, which also include carotenoids and related compounds. Since their molecular mass does not exceed 2000 u, even in the case of glycosides or esters, this method is suitable for their analysis, as has been recently reviewed by Rezenka *et al.* [7].

Correspondence: Professor Paula B. Andrade, REQUIMTE/Department of Pharmacognosy, Faculty of Pharmacy, Porto University, R. Aníbal Cunha 164, 4050-047 Porto, Portugal
E-mail: pandrade@ff.up.pt
Fax: +351-222003977

Abbreviations: APCI, atmospheric pressure chemical ionization; **FBS,** fetal bovine serum; **RBL,** rat basophilic leukemia; **SRB,** sulphorhodamine B

*Additional correspondence: Dr. David M. Pereira
E-mail: david.ffup@gmail.com

In this study, an HPLC-PAD-APCI-MS metabolite profiling analysis of the marine organism *M. glacialis* was carried out. A methanol extract was used in order to extract a wide range of metabolites. A bio-guided purification of this extract led to the finding of a fraction rich in carotenoids, which were further confirmed by applying the extraction techniques usually used for these compounds, namely extraction with acetone. The cytotoxic effect of this fraction was tested against both the cancer cell line rat basophilic leukemia (RBL)-2H3 and the healthy cell line V79.

2 Materials and methods

2.1 Chemicals

Lutein, zeaxanthin, β-carotene, sulphorhodamine B (SRB), methanol and ether were from Sigma-Aldrich (St. Louis, MO, USA). Cryptoxanthin was from Extrasynthese (France) and astaxanthin from CaroteNature (Switzerland).

DMEM, fetal bovine serum (FBS), PBS and antibiotic were from GIBCO (Invitrogen, UK). Tris-base, acetic acid and trichloroacetic acid were from Merck (Germany).

2.2 Sample

M. glacialis individuals were collected at the rocky coast at Cabo Carvoeiro, West Portugal, in March 2009, placed on ice and immediately transported to the laboratory in ice-boxes. The macro-invertebrates were then cleaned and washed with sea water and kept at -20°C, prior to their lyophilization in a Labconco 4.5 Freezone apparatus (Kansas City, MO, USA). The dried material was powdered before extraction. The sample corresponded to a mixture of three individuals.

2.3 Extract preparation

Methanol extracts were prepared by exhaustively extracting two to three powdered individuals (*ca.* 22.5 g each) of *M. glacialis* with methanol (3×100 mL of methanol, orbital shaker at 250 rpm for 15 min) and subsequent evaporation. Acetone extracts were prepared by exhaustively extracting 5 g of powdered specimen with 3×100 mL of acetone (orbital shaker at 250 rpm for 15 min). The extract was then evaporated to dryness.

All procedures were conducted in the dark in order to prevent photodegradation of the compounds.

2.4 Lobar column separation

A preliminary separation was achieved by injecting the extract in a Lobar LiChroPrep RP18 (40–63 μm) column (Merck). The mobile phase was methanol and separation was monitored by means of a UV lamp set to 365 nm. Carotenoid fraction corresponded to the orange one.

2.5 HPLC-PAD-APCI-MS/MS analysis

Chromatographic separations were carried out on a 250×4.6 mm, 5 μm, Luna RP-C18 (2) (Phenomenex, UK) column at room temperature. Elution was performed with acetonitrile at a flow rate of 0.5 mL/min isocratic conditions and the injection volume was 40 μL. The HPLC system was equipped with an Agilent 1100 Series diode array and a mass detector in series (Agilent Technologies, Waldbronn, Germany). It consisted of a G1312A binary pump, a G1313A autosampler, a G1322A degasser and a G1315B photo-diode array detector, controlled by ChemStation software (Agilent, v. 08.03). Spectroscopic data from all peaks were accumulated in the range of 300–650 nm, and chromatograms were recorded at 420, 440, 460 and 480 nm. The mass detector was a G2445A ion-trap mass spectrometer equipped with an APCI interface system and controlled by LCMSD software (Agilent, v. 4.1). Nitrogen was used as nebulizing gas at a pressure of 15 psi and the flow was adjusted to 5 L/min. The heated capillary, voltage and current corona were maintained at 350°C, 4 kV and 4000 nA, respectively. The full scan mass covered the range from *m/z* 200 to 1500. Collision-induced fragmentation experiments were performed in the ion trap using helium as collision gas, with voltage ramping cycles from 0.3 up to 2 V. MS data were acquired in the positive and negative ionization modes. MS2 was carried out in the automatic mode.

2.6 HPLC-PAD analysis

Twenty microlitres of either methanolic or acetonic extract redissolved in methanol were analysed using an HPLC unit (Gilson) and a Luna RP-C18 (2) (Phenomenex) 4.6×250 mm, 5 μm particle size column. Elution was performed with a flow of 0.5 mL/min and isocratic acetonitrile. Compounds' elution was monitored at 280, 320 and 450 nm with a Gilson diode array detector. The data were processed on a Unipoint Software system (Gilson Medical Electronics, Villiers le Bel, France).

Quantification was achieved by using calibration curves for each compound, with at least five different concentrations. Lutein ($y = 9.527 \times 10^6 x$) and zeaxanthin ($y = 1.148 \times 10^7 x$) were quantified at 450 nm and astaxanthin ($y = 3.586 \times 10^8 x$) at 475 nm.

2.7 Screening for epoxide carotenoids

The procedure described by Davies [8] was followed. An ether solution of carotenoid fraction was shaken with

aqueous 20% hydrochloric acid. In this situation, 5,6- and 5,8-epoxides react to yield a blue colour; more stable colours are formed in the case of di-epoxides.

2.8 Screening for carotenoid esters

For carotenoid ester screening we followed a described procedure [9]. Briefly, the carotenoids fraction re-dissolved in methanol was incubated in 1 mL of either 0.2 or 0.02 NaOH for 6 h, in the dark, at room temperature (~22°C). After incubation, we added 1 mL of saturated sodium chloride in deionised water to each tube and shook the tubes vigorously by hand for 30 s. We then added 2 mL of deionised water to each of the tubes and shook them. Finally, we added 3 mL of 1:1 hexane/ether to each of the tubes and shook them again. The tubes were centrifuged for 5 min at 3000 rpm. The organic layer was transferred to a 9 mL culture tube, evaporated to dryness under a stream of nitrogen and prepared for HPLC analysis.

2.9 Cell culture

Rat basophile leukemia (RBL-2H3) cell line was acquired from American Type Culture Collection (ATCC). V79 cell line was a kind gift from Professor Fernando Remião, (Laboratory of Toxicology of the Faculty of Pharmacy, Porto University). RBL-2H3 and V79 cells between passages 5–15 and 89–98, respectively, were used. RBL-2H3 cells were maintained in DMEM with 15% FBS and 2% penicillin and V79 cells were cultured in DMEM with 10% FBS and 2% penicillin and in an incubator with 5% CO_2.

2.10 SRB assay

We followed the method described by Houghton *et al.* [10], with modifications. Cells were plated with a density of 1×10^4 cells/well and allowed to attach for 24 h at 37°C, with 5% CO_2. On the following day, medium was removed and cells were gently washed with warm PBS. Samples were redissolved in methanol, diluted with medium, added to wells in several concentrations and incubated for 48 h. Three independent assays were conducted, each one of them in triplicate. Vehicle was used as control.

After the 48 h incubation period, medium was removed, 100 μL of cold 40% trichloroacetic acid was added, and plates maintained at 4°C for 60 min. After this time, plates were washed five times with tap water and allowed to dry in the air. Afterwards, 50 μL of 0.4% SRB in 1% acetic acid was added and plates were incubated for 30 min.

After the incubation period, plates were quickly washed with 1% acetic acid in order to remove unbound dye and plates were allowed to dry in the air. 100 μL of tris-base was added and shaken for 15 min.

Absorbance was read in a multi-plate reader at 492 nm. OD values were plotted against concentration and the IC_{50} and IC_{25} determined using GraphPad Prism.

3 Results and discussion

3.1 HPLC-PAD analysis

HPLC-PAD analysis of carotenoids is a precious tool for a preliminary study of this class of compounds, due to the fact that the chemical characteristics responsible for UV spectra shape and maxima are fairly understood.

The position of long-wave absorbance bands is a function of the number of conjugated double bonds. An increase in this number results in an increase in the wavelength of maximal absorption, an effect that may be modified by cyclization [8].

The introduction of a carbonyl group in a cyclic end group in conjugation with the polyene chain bears two effects: for one, there is a marked loss of persistence, resulting in rounded, sometimes symmetrical, shape. Second, a bathochromic shift takes place.

In the screening of carotenoids from *M. glacialis*, two kinds of UV spectra could be noticed: spectra with rounded shape with just one maximum and spectra with a fine structure with three UV absorption maxima.

Taking into account that a carbonyl group that is not in conjugation with the polyene chain does not result in loss of fine structures, compound 1 (Fig. 1), with no fine structure and a maximum at 474 nm (Table 1), had to be a xanthophyll with a carbonyl group in conjugation with the chromophore.

Due to the presence of a fine structure and multiple UV maxima for the remaining compounds (2 and 3), these were thought to be either carotenes or xanthophylls with no conjugated carbonyl groups. Their UV maxima are listed in Table 1.

UV spectra can also provide information regarding the compound's fine structure. The spectra of most carotenoids show not just a single absorption band but three distinct peaks. The value of %III/II indicates the relationship between the peak heights of the longest-wavelength absorption band (III) and the middle absorption band (II) [11]. Although compounds 2 and 3 exhibited similar spectra (Fig. 1), with three maxima, they could be distinguished by their different %III/II, as summarized in Table 1, while the round shape of compound 1 UV spectrum renders that no such value can be calculated.

3.2 HPLC-PAD-APCI-MS/MS analysis

The HPLC-PAD-APCI-MS/MS study of the acetone and methanol extracts of *M. glacialis* originated similar qualitative results, although the proportion of the several

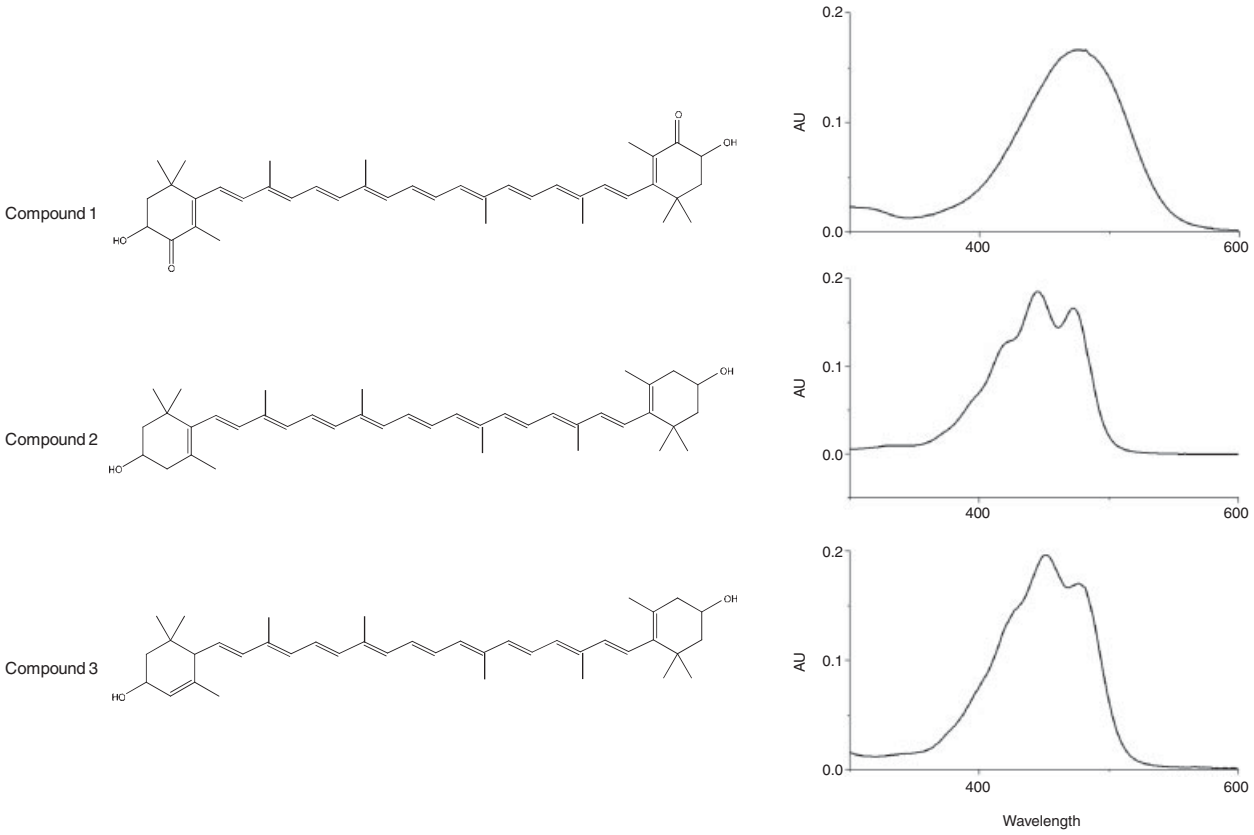

Figure 1. Structures and UV spectra of (**1**) astaxanthin, (**2**) lutein; (**3**) zeaxanthin. UV data as in Table 1.

Table 1. Rt, UV, %III/II and MS data of carotenoids from *M. glacialis*[a)]

Compounds		Rt min	UV nm	%III/II	$[M+H]^+$	MS2$[M+H]^+$					
						−18	−18–18	−56	−18–56	−92	18–80
1	Astaxanthin	15.1	474	–	597.5	579.3(100)	561.4(16)				
2	Lutein	20.3	422, 446, 474	55	551.6[b)]	533.4(100)		495.3(23)	477.1(8)	459.3(14)	453.4(6)
3	Zeaxanthin	21.8	428, 452, 478	27	569.6[c)]	551.3(100)	533.4(19)	513.3(21)		477.1(8)	

a) Main observed fragments. Other ions were found but they have not been included.
b) The ion observed is not the protonated molecule of lutein ([M+H]+: 569.6) but instead 551.6 $(M+H-18]^+$).
c) *m/z* 551.6 $[569.6-18]^+$ was also observed as parent ion.

compounds was different. The major compounds had been described previously [6].

The characterization of the compounds was done by comparison of their UV and MS spectra, and also by co-chromatography with authentic standards. As so, the xanthophylls detected in the acetone and methanol extracts were astaxanthin (1), lutein (2) and zeaxanthin (3) (Figs. 1–4, Table 1).

With the MS conditions used herein, it was noticed that in the process of ion transfer a loss of water occurred in compounds 2 and 3, thus originating the ion $[M+H-18]^+$, being very abundant in the case of lutein (*m/z* 551.6), with the protonated molecule being frequently absent (Figs. 3B and 4B).

In the MS2$[M+H]^+$ fragmentation of all detected carotenoids, a base peak corresponding to the loss of water from the protonated molecular ion ($[M+H)-18]^+$) was observed, as well as another ion, less abundant, arising from the loss of two molecules of water ($[M+H)-36]^+$) (Figs. 3 and 4, Table 1). This ion was not observed in the MS2 fragmentation of the ions at *m/z* 551.6 from lutein (Fig. 3B), probably because they arise from the protonated molecule that had already lost one molecule of water in the ion transfer process, as stated before.

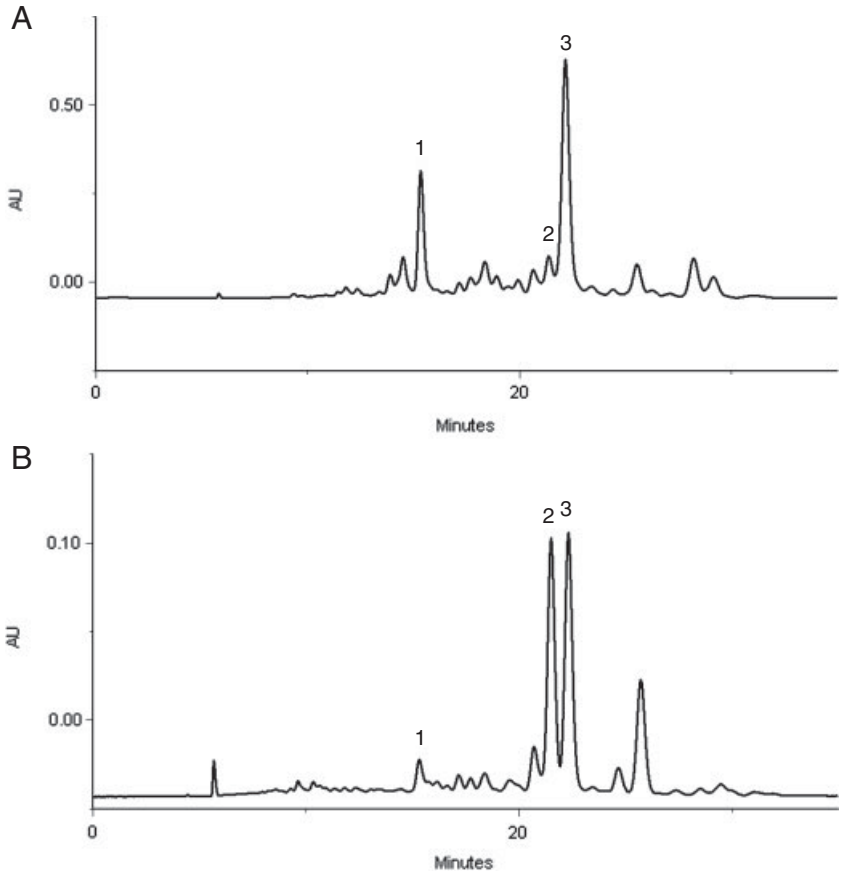

Figure 2. HPLC-PAD chromatographic profile of *M. glacialis* (A) methanol and (B) acetone extract. Detection at 450 nm.

Other observed ions are those resulting from the loss of fragments 56 u and/or 56+18 u and 80+18 u (Table 1), typical of the fragmentation of this class of compounds [12, 13].

It should be highlighted that some minor carotenoids, previously described for this species [6], were not noticed in the individuals studied herein, namely β-carotene, cryptoxanthin, echinenone and lutein 5,6-epoxide. The main ions corresponding to these compounds were searched, but no compounds were found. This result could be explained by the different geographical origin of *M. glacialis*, which in this study was collected in the Atlantic Ocean and in the work of Czeczuga [6] were from the Adriatic Sea. Taking into account that in sea-stars carotenoids arise from the diet, it is plausible that different diets result in different carotenoid compositions of these echinoderms. Regarding lutein 5,6-epoxide, a quick screening for the detection of epoxide carotenoids was conducted, with a negative result being found.

Another compound, 2,4-didehydro-α-carotene was previously described [6]. However, according to Britton *et al*. [11] to this day this is the only reference to this compound in nature, which, together with the fact that no MS or NMR studies were conducted in this compound, turns that its occurrence cannot be confirmed.

Likewise, one carotenoid ester has been previously described in *M. glacialis* [6]. We performed two different saponification procedures in order to identify the presence of these compounds, but no such compounds were found.

In the fractionation of the methanol extract by Lobar chromatography assisted with a UV lamp, a green–white fluorescent spot was noticed. This behavior was compatible with the presence of phytofluene and its derivatives [8]. For this reason, the green fluorescent fraction was isolated and subjected to HPLC-PAD analysis. The characteristic UV spectra of phytofluene and its derivatives include three main absorption bands, located at around 331, 347 and 367 nm (phytofluene, 1,2-dihydrophytofluene). Although some peaks were found in the isolated fraction, no compound presented a UV spectrum compatible with phytofluene or its derivatives.

From a quantitative point of view, the sum of the identified carotenoids accounted for some 945.06 mg/100 g (dry basis, Table 2) in the acetone extract. The major compound was zeaxanthin, both in methanol and in acetone extracts, whereas lutein was in considerably lower amounts in the methanolic one (Table 2). Astaxanthin was a minor compound in both extracts.

In general, the differences between using methanol or acetone affected mainly astaxanthin, detected in considerable amounts only when methanol was used, and lutein, which was detected in higher quantity in acetone extracts, being almost as high as zeaxanthin. In both extracts, the

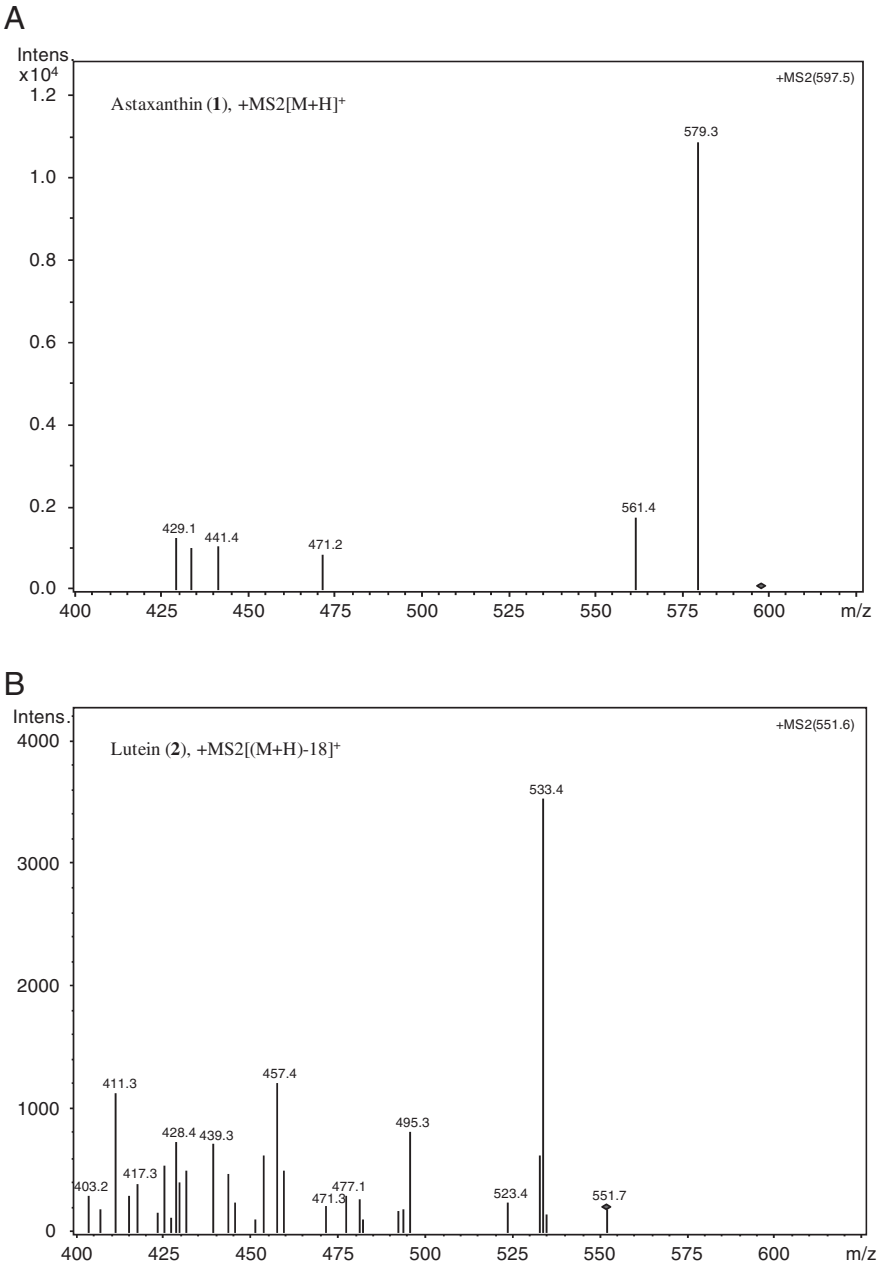

Figure 3. MS2 spectra of (A) astaxanthin (**1**) ($+MS2[M+H]^+$) and (B) lutein (**2**) ($+MS2[(M+H)-18]^+$).

presence of cryptoxanthin, echinenone, β-carotene and carotenoids esters, described before, was not confirmed.

3.3 Cell assays

The native methanol extract was tested against the cancer cell line RBL-2H3. At the highest tested concentration, 2.5 mg/mL, the extract was able to inhibit cell proliferation *ca.* 79.41 ± 1.88% (Fig. 5). These results led us to the purification of the extract by the means described above in order to elucidate the role of carotenoids in the displayed activity.

The IC_{50} obtained for this carotenoid fraction was 575 μg/mL, and a concentration-dependant activity was found (Fig. 6). Given the fact that compounds with anti-cancer properties are only interesting for therapeutics if their toxicity is higher toward cancer cells than healthy ones, we tested the same carotenoid fraction against the cell line V79. The toxicity against this cell line was much lower than that observed for RBL-2H3, with the highest tested concentration presenting *ca.* 50% inhibition (Fig. 6). Given the weak activity in healthy V79 cells, it was not possible to calculate the IC_{50} and compare it with that of RBL-2H3. For this reason, IC_{25} was calculated and the value found, 411 μg/mL, was higher than that obtained for RBL-2H3 cells, 268 μg/mL (Figs. 5 and

Table 2. Quantification of carotenoids in *M. glacialis* purified methanol extract and native acetone extract (mg/100 g, dry sea-star)[a)]

	Compound	Extract	
		Methanol	Acetone
1	Astaxanthin	10.49 ± 0.06	1.40 ± 0.035
2	Lutein	151.33 ± 2.44	427.06 ± 9.13
3	Zeaxanthin	761.53 ± 0.06	516.60 ± 13.78
	Σ	923.35	945.06

a) Results are expressed as means ± standard deviations of three determinations.

6). The ideal anticancer compound should have no toxicity against healthy cells. However, this requisite cannot always be fulfilled, and sometimes compounds that show some degree of toxicity against healthy cells are used, as long as this effect is more pronounced against cancer cells. A good example of this fact is vincristine or paclitaxel [14].

Carotenoids constitute a class of compounds well known for their positive impact on human health, mainly as antioxidants and, for those compounds with pro-vitamin A activity, in the prevention of age-related macular degeneration. Among natural molecules, carotenoids usually are not among the most cytotoxic ones. However, the cytotoxic

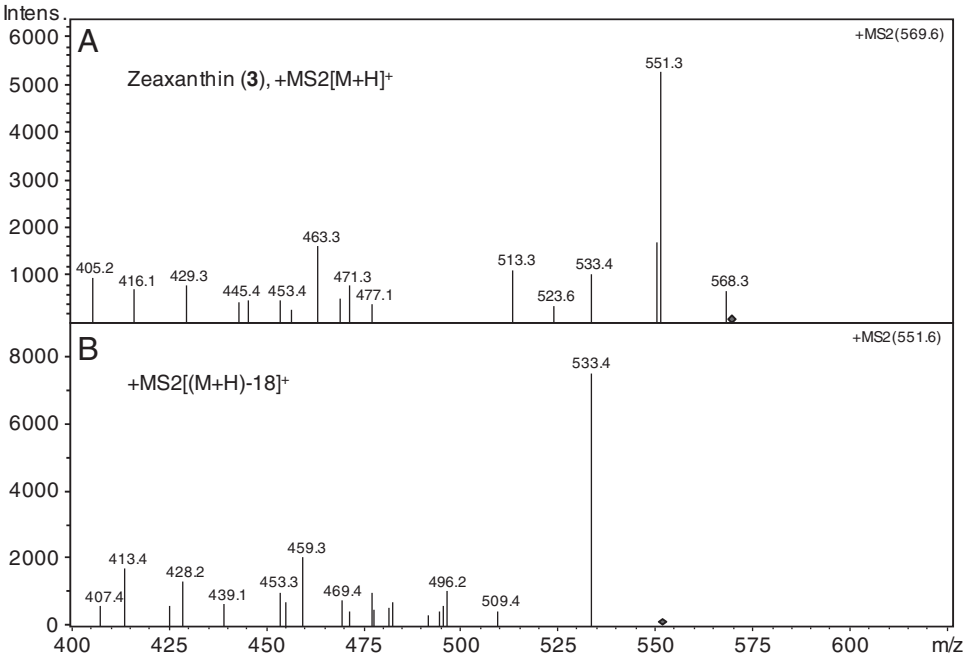

Figure 4. MS2 spectra of zeaxanthin (**3**): (A)+MS2[M+H]$^+$ and (B)+MS2[(M+H)−18]$^+$.

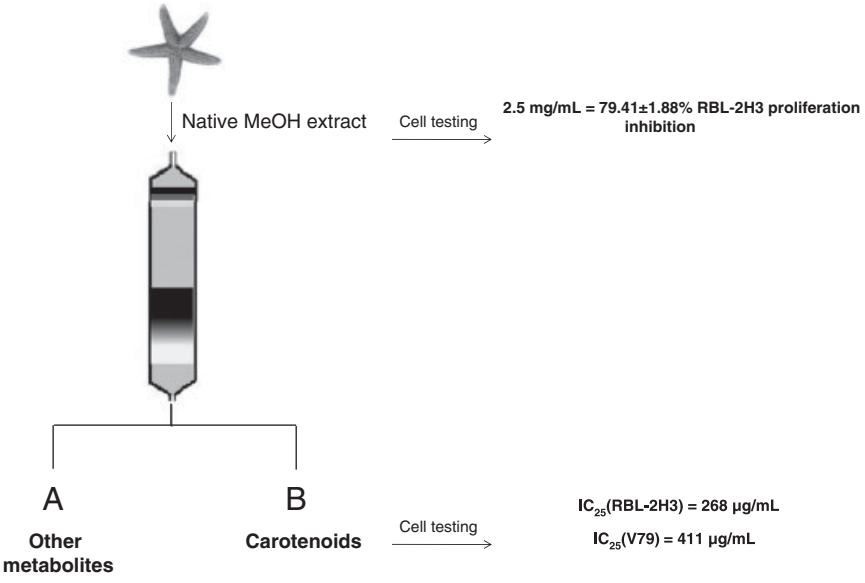

Figure 5. Experimental design for the purification of *M. glacialis* methanol extract and values for cell cytotoxicity.

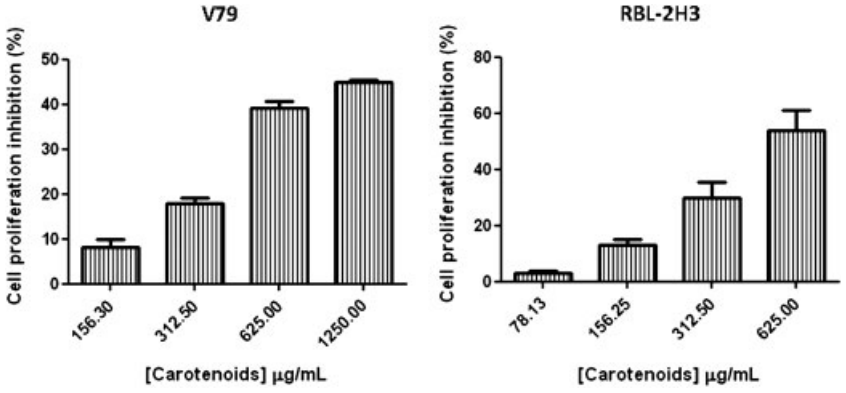

Figure 6. Cell proliferation inhibition of V79 and RBL-2H3 cells by *M. glacialis* carotenoids, assessed with the SRB assay. Values show mean and standard deviation of three different assays, each one in triplicate.

activity of carotenoids, in particular xanthophylls, has been described in the literature and, in line with the findings that we present herein, this activity is usually higher against cancer cells than against healthy ones [15, 16].

The activity found for *M. glacialis* cannot be attributed to single compounds, and, given the chemical diversity of the matrix, synergy between several compounds is likely to occur. Among the identified compounds, astaxanthin has been implied in cytotoxicity against cancer cells [17, 18]. However, it should be highlighted that some compounds found in this study, although presenting UV spectra characteristic of carotenoids, could not be fully identified by LC-MS and could be new compounds that contribute to the displayed activity. In addition, although the extraction procedures used, as well as the purification process by means of Lobar column chromatography, enabled to obtain a carotenoid fraction, minimizing the contribution of other compounds to the displayed activity, the presence of other nonpolar components in the extract cannot be excluded.

4 Concluding remarks

Overall, in this study HPLC-PAD-APCI-MS was used for the first time to study carotenoids from the echinoderm *M. glacialis*. Methanol and acetone extracts yielded a very similar carotenoid profile, although in different amounts.

The purified methanol extract proved to be cytotoxic, an activity that was higher against the cancer cell line RBL-2H3 than against the healthy cell line V79, a trend that could be useful in the development of new bioactive compounds for use in human health.

In both methanol and acetone extracts, the identified carotenoids accounted for almost 1% of sea-star (dry weight), a value that is underestimated due to the fact that only identified carotenoids were included. With this data, we proved that *M. glacialis* could be a good source of bioactive carotenoids to be used in human health, which merits further studies.

David M. Pereira (SFRH/BD/62663/2009) acknowledges FCT for the grant.

The authors have declared no conflict of interest.

5 References

[1] Liaaen-Jensen, S., *Pure Appl. Chem.* 1981, *63*, 1–12.

[2] Maiani, G., Castón, M. J. P., Catasta, G., Toti, E., Cambrodón, I. G., Bysted, A., Granado-Lorencio, F., Olmedilla-Alonso, B., Knuthsen, P., Valoti, M., Böhm, V., Mayer-Miebach, E., Behsnilian, D., Schlemmer, U., *Mol. Nutr. Food Res.* 2009, *53*, S194–S218.

[3] Stahl, W., Sies, H., *Acta. Mol. Bas. Dis.* 2005, *1740*, 101–107.

[4] Verling, E., Crook, A. C., Barnes, D. K. A., Harrison, S. S. C., *J. Mar. Biol. Assoc. UK* 2003, *83*, 583–592.

[5] Minale, L., Pizza, C., Riccio, R., Zollo, F., *Pure Appl. Chem.* 1982, *54*, 935–950.

[6] Czeczuga, B., *Hydrobiologia* 1977, *54*, 177–180.

[7] Rezenka, T., Olsovska, J., Sobotka, M., Sigler, K., *Curr. Anal. Chem.* 2009, *5*, 1–25.

[8] Davies, B. H., in: Goodwin, T. W. (Ed.), *Chemistry and Biochemistry of Plant Pigments*, Vol. 2, Academic Press, New York 1976, pp. 38–165.

[9] Toomey, M. B., McGraw, K. J., *Invest. Ophth. Vis. Sci.* 2007, *48*, 3976–3982.

[10] Houghton, P., Fang, R., Techatanawat, I., Steventon, G., Hylands, P. J., Lee, C. C., *Methods* 2007, *42*, 377–387.

[11] Britton, G., Liaaen-Jensen, S., Pfander, H., *Carotenoids – Handbook*, Birkhäuser, Basel 2004.

[12] Maoka, T., Hashimoto, K., Akimoto, N., Fujiwara, Y., *J. Nat. Prod.* 2001, *64*, 578–581.

[13] Maoka, T., Fujiwara, Y., Hashimoto, K., Akimoto, N., *Lipids* 2004, *39*, 179–183.

[14] Bruneton, J., *Pharmacognosie: Phytochimie, Plantes Médicinales*, 3rd Edn, Editions TEC & DOC, Paris 1999.

[15] Molnár, P., Kawase, M., Satoh, K., Sohara, Y., Tanaka, T., Tani, S., Sakagami, H., Nakashima, H., Motohashi, N., Gyémánt, N., Molnár, J., *Phytother. Res.* 2005, *19*, 700–707.

[16] Rogers, E. W., Molinski, T. F., *J. Nat. Prod.* 2005, *68*, 450–452.

[17] Jyonouchi, H., Sun, S., Iijima, K., Gross, M. D., *Nutr. Cancer* 2000, *36*, 59–65.

[18] Chew, B. P., Park, J. S., Wong, M. W., Wong, T. S., *Anticancer Res.* 1999, *19*, 1849–1853.

Paper 2

Further Insights on the Carotenoid Profile of the Echinoderm *Marthasterias glacialis* L.

Lilian R. B. Mariutti, ***David M. Pereira****, Adriana Zerlotti Mercadante, Patrícia Valentão, Natércia Teixeira, Paula B. Andrade*

Marine Drugs, 2012, 10, 1498-1510

Mar. Drugs **2012**, *10*, 1498-1510; doi:10.3390/md10071498

OPEN ACCESS

Marine Drugs

ISSN 1660-3397

www.mdpi.com/journal/marinedrugs

Article

Further Insights on the Carotenoid Profile of the Echinoderm *Marthasterias glacialis* L.

Lilian R. B. Mariutti [1], David M. Pereira [2], Adriana Zerlotti Mercadante [1,*], Patrícia Valentão [2], Natércia Teixeira [3,4] and Paula B. Andrade [2,*]

[1] Department of Food Science, Faculty of Food Engineering, University of Campinas (UNICAMP), Rua Monteiro Lobato, 80, CEP 13083-862, Campinas, São Paulo, Brazil; E-Mail: lilianmariutti@gmail.com

[2] REQUIMTE/Laboratory of Pharmacognosy, Department of Chemistry, Faculty of Pharmacy, University of Porto, R. de Jorge Viterbo Ferreira, 228, 4050-313 Porto, Portugal; E-Mails: david.ffup@gmail.com (D.M.P.); valentao@ff.up.pt (P.V.)

[3] Laboratory of Biochemistry, Department of Biological Sciences, Faculty of Pharmacy, University of Porto, R. de Jorge Viterbo Ferreira, 228, 4050-313 Porto, Portugal; E-Mail: natercia@ff.up.pt

[4] IBMC—Institute for Cell and Molecular Biology, University of Porto, 4150-180 Porto, Portugal

* Authors to whom correspondence should be addressed; E-Mails: azm@fea.unicamp.br (A.Z.M.); pandrade@ff.up.pt (P.B.A.); Tel.: +55-19-35212163 (A.Z.M.); Fax: +55-19-35212153 (A.Z.M.); Tel.: +351-220428654 (P.B.A); Fax: +351-226093390 (P.B.A).

Received: 24 April 2012; in revised form: 13 June 2012 / Accepted: 28 June 2012 / Published: 12 July 2012

Abstract: In this study, the carotenoid profile of the echinoderm *Marthasterias glacialis* L. was established using HPLC-DAD-APCI-MS/MS equipped with a C_{30} column. This approach rendered the identification of 20 compounds, eight of them reported for the first time in this marine organism. Differentiation of carotenoid isomers was also achieved.

Keywords: *Marthasterias glacialis* L.; carotenoids; isomers; echinoderm; HPLC-DAD-APCI-MS/MS

1. Introduction

Carotenoids constitute a class of isoprenoids widespread in nature, with over 700 compounds documented to this day [1]. These metabolites are responsible for the colors of some plants, algae, microbes and also some animals. For many years, this class of molecules was thought to be present in

animals solely as a result of predation upon organisms from lower trophic levels. However, in 2010 the first carotenoid-synthesizing animal, the pea aphid, was described and is thought to be a result of lateral gene transfer in a context of co-evolution [2].

In plants, carotenoids act as antioxidants, regulators of membrane fluidity and as light-harvesting molecules in photosynthetic systems [3]. In terms of human health, these metabolites are very important due to their strong antioxidant [4] and provitamin A activity displayed by some compounds of this group [5]. A recent meta-analysis showed that a diet rich in carotenoids was effective in the prevention of late age-related macular degeneration [6], although the contribution of these molecules to the treatment of this pathology requires further study.

The presence of carotenoids in the echinoderm *Marthasterias glacialis* L. (spiny sea star) was reported in the 1970's [7]. At the time, several carotenoids had been identified, such as lutein, zeaxanthin and astaxanthin. While the presence of these compounds was recently confirmed, other compounds that have been previously reported, such as echinenone and 5,6-epoxy lutein, were not found [8]. In both works, no characterization of carotenoid isomers was attempted.

Atmospheric pressure chemical ionization (APCI) forms abundant positively or negatively charged molecular ions or protonated and deprotonated molecules of both carotenes and xanthophylls, and their fragmentation pattern can also help with the identification of this type of compounds. In the present work, we deepen the study of the carotenoid composition of *M. glacialis* using a C_{30} column in a high performance liquid chromatography-diode array detector-mass spectrometry detector (HPLC-DAD-APCI-MS/MS) system. Using this type of column, it is possible to separate some of the carotenoid isomers that cannot be resolved with most C_{18} columns. Furthermore, given the fact that some carotenoid isomers are not commercially available, we have conducted isomerization and reduction procedures starting from available standards, in order to be able to confirm the identity of some peaks.

2. Results and Discussion

The carotenoids, extracted from the echinoderm *M. glacialis*, were chromatographically separated and subsequently tentatively identified, based on the combined information obtained from chromatographic elution, UV-vis and mass spectra characteristics (Table 1). The HPLC chromatogram (Figure 1) demonstrates the presence of 20 carotenoids in the extract of the spiny sea star. Since a detailed description of carotenoid identification using the above information is available in literature [9], only considerations regarding carotenoids not identified in previous reports, along with the mass spectroscopy data obtained by negative APCI, are discussed in the present work.

Table 1. Chromatographic, UV-vis and mass spectrometry characteristics of carotenoids from *Marthasterias glacialis* (spiny sea star), obtained by HPLC-DAD-MS/MS.

Peak [a]	Carotenoid	t_R [b] (min)	λ_{max} [c] (nm)	% III/II	$[M + H]^+$ (*m/z*)	MS/MS fragment ions (positive mode) (*m/z*)	$M^{-\bullet}$ or $[M - H]^-$ (*m/z*)	MS/MS fragment ions (negative mode) (*m/z*)
1	not identified 1	8.7–8.8	419, 445, 469	nc [d]	597	579 $[M + H - 18]^+$, 561 $[M + H - 18 - 18]^+$, 505 $[M + H - 92]^+$	595 [f]	577 $[M - H - 18]^-$, 559 $[M - H - 18 - 18]^-$
2	crustaxanthin	9.1–9.2	422, 449, 470	nc	601	583 $[M + H - 18]^+$	599 [f]	581 $[M - H - 18]^-$, 563 $[M - H - 18 - 18]^-$, 507 $[M - H - 92]^-$
3	13-*cis*-astaxanthin	10.4–10.5	371, 466	0	597	579 $[M + H - 18]^+$, 561 $[M + H - 18 - 18]^+$, 379, 285, 173	596 [g]	581 $[M - 15]^-$, 578 $[M - 18]^-$, 504 $[M - 92]^-$, 429 $[M - 167]^-$, 389, 363 $[M - 233]^-$, 337 $[M - 167 - 92]^-$, 323, 297, 233
4	all-*trans*-astaxanthin	11.2–11.6	475	0	597	579 $[M + H - 18]^+$, 561 $[M + H - 18 - 18]^+$, 505 $[M + H - 92]^+$, 379, 285	596 [g] 595 [f]	581 $[M - 15]^-$, 577 $[M - H - 18]^-$, 559 $[M - H - 18 - 18]^-$, 541 $[M - H - 18 - 18 - 18]^-$, 504 $[M - 92]^-$, 429 $[M - 167]^-$, 490 $[M - 106]^-$, 389, 363 $[M - 233]^-$, 337 $[M - 167 - 92]^-$, 323, 297, 233, 203
5	all-*trans*-lutein	11.9–12.2	421, 445, 472	67–71	nd [e]	551 [h] $[M + H - 18]^+$, 533 $[M + H - 18 - 18]^+$, 495 $[M + H - 18 - 56]^+$, 459 $[M + H - 18 - 92]^+$, 430, 175	568 [g] 567 [f]	549 $[M - H - 18]^-$, 531 $[M - H - 18 - 18]^-$, 535 $[M - 18 - 15]^-$, 429
6	astaxanthin derivative 1	13.0–13.2	472	0	597	579 $[M + H - 18]^+$, 561 $[M + H - 18 - 18]^+$, 379, 285, 173	596 [g]	581 $[M - 15]^-$, 578 $[M - 18]^-$, 542 $[M - 18 - 18 - 18]^-$, 429 $[M - 167]^-$, 490 $[M - 106]^-$, 389, 363 $[M - 233]^-$, 337 $[M - 167 - 92]^-$, 323, 297, 233, 203
7	all-*trans*-zeaxanthin	13.8–14.2	423, 451, 476	25–40	569	551 $[M + H - 18]^+$, 533$[M + H - 18 - 18]^+$, 459, 416, 175	567 [f]	549 $[M - H - 18]^-$, 534 $[M - H - 18 - 15]^-$, 531 $[M - H - 18 - 18]^-$, 465, 201, 187
8	astaxanthin derivative 2	14.8–15.0	459	nc	597	579 $[M + H - 18]^+$, 561 $[M + H - 18 - 18]^+$, 285, 173	595 [f] 596 [g]	581 $[M - 15]^-$, 577 $[M-H - 18]^-$, 429 $[M - 167]^-$, 389, 363 $[M - 233]^-$, 337 $[M - 167 - 92]^-$, 323, 297, 233, 203
9	9-*cis*-astaxanthin	15.5	470	0	597	579 $[M + H - 18]^+$, 561 $[M + H - 18 - 18]^+$	596 [g]	581 $[M - 15]^-$, 578 $[M - 18]^-$, 560 $[M - 18 - 18]^-$, 504 $[M - 92]^-$, 429 $[M - 167]^-$, 490 $[M - 106]^-$, 363 $[M - 233]^-$, 337 $[M - 167 - 92]^-$, 323, 297, 233, 203
10	astaxanthin derivative 3	16.2–16.4	454, 475	nc	597	579 $[M + H - 18]^+$, 379, 285	596 [g]	581 $[M - 15]^-$, 578 $[M - 18]^-$, 504 $[M - 92]^-$, 429 $[M - 167]^-$, 490 $[M - 106]^-$, 389, 337 $[M - 167 - 92]^-$, 233
11	not identified 2	16.8	422, 452, 472	nc	565	nd	564 [g]	nd
12	all-*trans*-canthaxanthin	18.3	470	0	565	nd	564 [g]	nd
13	5,6-epoxy-β-cryptoxanthin	19.2	419, 447, 472	67	569	551 $[M + H - 18]^+$, 221	567 [f]	549 $[M - H - 18]^-$
14	not identified 3	20.5–20.7	423, 452, 478	20–25	601	585, 548, 507, 441, 413	600 [g]	581, 543, 416
15	all-*trans*-β-cryptoxanthin	22.6	422, 450, 476	25	nd	nd	552 [g]	534 $[M - 18]^-$, 519 $[M - 18 - 15]^-$, 269, 243
16	not identified 4	23.3	422, 450, 472	25	nd	nd	nd	nd
17	15-*cis*-β-carotene	25.4	420, 448, 471	nc	537	413 $[M + H - 124]^+$	536 [g]	295, 269, 189
18	13-*cis*-β-carotene	26.5	418, 447, 471	nc	537	269	536 [g]	444 $[M - 92]^-$, 295, 269
19	all-*trans*-β-carotene	33.1–34.7	422, 451, 477	20	537	444 $[M + H - 92]^+$, 413 $[M + H - 124]^+$, 400 $[M + H - 137]^+$, 269, 177	536 [g]	444 $[M - 92]^-$, 295, 269
20	9-*cis*-β-carotene	35.1–36.8	419, 448, 472	nc	537	444 $[M + H - 92]^+$, 269	535 [f]	295, 269

[a] Numbered according to Figure 1; [b] Retention time on the C_{30} column; [c] Linear gradient methanol/MTBE; [d] Not calculated; [e] Not detected; [f] $[M - H]^-$; [g] $M^{-\bullet}$; [h] Fragmentation in source.

Figure 1. Chromatogram (processed at 450 nm), obtained by HPLC-DAD, of the carotenoids from *Marthasterias glacialis*. See text for chromatographic conditions. Peak identification and characterization are given in Table 1.

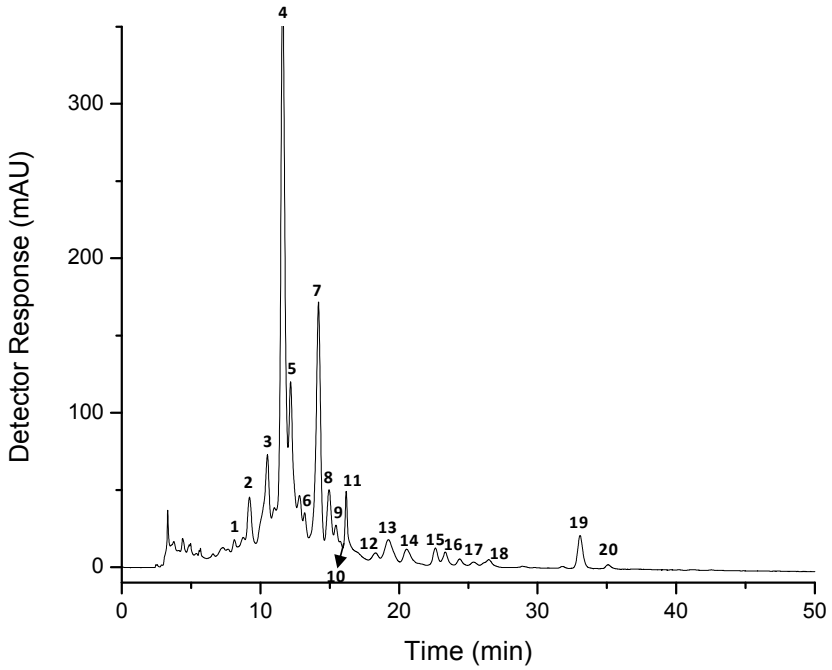

As carotenoids are well-known to form stable protonated molecules ($[M + H]^+$) upon positive ionization, the sample was firstly analyzed in the positive ion mode. As expected, for most of the peaks, the protonated molecule, as well as the respective fragment ions formed, both from the polyene chain and functional groups, were generated. However, an extremely high background noise, probably originating from residual lipids present in the sample also forming positive ions, impaired the identification of the protonated molecules or the interpretation of the fragmentation pattern even by MS/MS. As an example, a very intense signal at *m/z* 369, which corresponds to cholesterol $[M + H]^+$, could be observed from 16 to 20 min. Therefore, the sample was also analyzed in the negative mode and under this condition, negatively charged molecular ions ($M^{-\bullet}$) were formed, whilst deprotonated molecules $[M - H]^-$ were formed in just a few cases. The formation of $M^{-\bullet}$ in the negative mode has previously been described for lutein, α-carotene, β-carotene [10] and astaxanthin esters [11].

The thermal-induced isomerization of all-*trans*-astaxanthin standard solution was carried out in order to indicate the presence of *cis* isomers in the sample. The chromatographic separation of the heated astaxanthin standard solution on the C_{30} column is shown in Figure 2. The relative amounts of the eight compounds derived from all-*trans*-astaxanthin were 1.0% of apo-10′-astaxanthinal, 2.8%, 1.7% and 0.6% of different di-*cis*-isomers of astaxanthin, 3.2% of mono-*cis*-astaxanthin, 29.2% of 13-*cis*-astaxanthin, 50.2% of all-*trans*-astaxanthin and 3.9% of 9-*cis*-astaxanthin. The peaks were tentatively identified based on spectral features, chromatographic elution, mass spectra characteristics (Table 2) and literature data [12–15]. Moreover, four oxidation products of astaxanthin were detected by the extracted ion chromatograms obtained at *m/z* 315, *m/z* 341, *m/z* 381 and *m/z* 447, corresponding to apo-15′-astaxanthinal (13.3 min), apo-14′-astaxanthinal (6.7 min), apo-12′-astaxanthinal (4.2 min) and apo-8′-astaxanthinal (5.6 min), respectively. When the *trans*-form of carotenoids is isomerized to

the *cis*-isomers, a small and large hypsochromic shift in the absorption maximum for, respectively, mono-*cis* carotenoids and di-*cis* carotenoids occurs, as well as the intensity of the *cis*-peak, which increases as the *cis* double bond approaches the centre of the molecule [16]. Peak 4 corresponds to all-*trans*-astaxanthin and the two main isomers formed were assigned as 13-*cis*-astaxanthin (peak 3) and 9-*cis*-astaxanthin (peak 9), with hypsochromic shifts of 8 and 5 nm, respectively, whilst an additional absorption band was present at 370 nm for the 13-*cis* isomer. These characteristics are in agreement with the data presented by Holtin *et al.* [14], which confirmed the identity of these two isomers by nuclear magnetic resonance (NMR). Peak 25 was identified as a *cis*-astaxanthin and presents similar UV-vis characteristics to 13-*cis*-astaxanthin, *i.e.*, hypsochromic shift of 7 nm and a *cis*-peak at 368 nm, but it is probably not a 15-*cis* isomer since it should present a more intense *cis*-peak than 13-*cis* isomer. Apart from peak 21 (*m/z* 406) and 23 (no molecular ion was detected), all the other compounds presented in Figure 2 (peaks 3, 4, 9, 22, 24 and 25) showed the molecular ion ($M^{-\bullet}$) at *m/z* 596 when analyzed by negative ion APCI. However, by positive ion mode, the protonated molecule at *m/z* 597 was present only in the mass spectra of peaks 3, 4, 9 and 25. Peaks 22 to 24 presented hypsochromic shifts between 17 and 21 nm, relative to the absorption maxima of the all-*trans* isomer, and were identified as di-*cis*-astaxanthin, based on comparison with literature data [14]. Peak 21 was identified as apo-10′-astaxanthinal, which is an oxidation product of astaxanthin with a molecular weight of 406 Da. The MS spectra of apo-10′-astaxanthinal presented the protonated molecule at *m/z* 407 $[M + H]^+$ in positive ion mode and the molecular ion at *m/z* 406 ($M^{-\bullet}$) in negative ion mode. In addition, in both ionization modes, the MS/MS fragments corresponded to the loss of one hydroxyl group (18 u).

Figure 2. Chromatogram (processed at 450 nm), obtained by HPLC-DAD, of astaxanthin standard submitted to heat under reflux. See text for chromatographic conditions. Peak identification and characterization are given in Table 2.

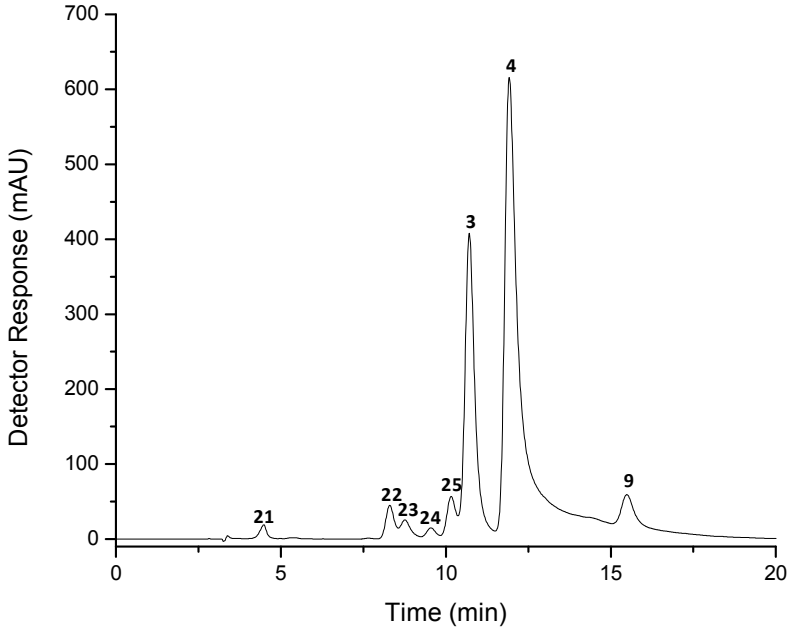

Table 2. Chromatographic, UV-vis and mass spectrometry characteristics of astaxanthin standard submitted to heat under reflux, obtained by HPLC-DAD-MS/MS.

Peak [a]	Carotenoid	t_R [b] (min)	λ_{max} [c] (nm)	Δλ	% III/II	% A_B/A_{II}	$[M + H]^+$ (*m/z*)	MS/MS fragment ions (positive mode) (*m/z*)	$M^{-\bullet}$ (*m/z*)	MS/MS fragment ions (negative mode) (*m/z*)
21	apo-10′-astaxanthinal	4.4–4.5	428	48	0		407	389 $[M + H - 18]^+$	406	388 $[M - 18]^-$
22	di-*cis*-astaxanthin 1	8.2–8.3	457	19	0		nd [d]	nd	596	578 $[M - 18]^-$, 564 $[M - 18 - 18]^-$, 504 $[M - 92]^-$
23	di-*cis*-astaxanthin 2	8.6–8.8	455–457	21	0		nd	nd	nd	nd
24	di-*cis*-astaxanthin 3	9.5	459–457	17	0		nd	nd	596	nd
25	*cis*-astaxanthin	10.2–10.3	368, 469	7	0	58	597	285	596	581 $[M - 15]^-$, 578 $[M - 18]^-$, 504 $[M - 92]^-$, 429 $[M - 167]^-$, 389, 363 $[M - 233]^-$, 337 $[M - 167 - 92]^-$, 233
3	13-*cis*-astaxanthin	10.7–10.8	370, 468	8	0	51	597	579 $[M + H - 18]^+$, 561 $[M + H - 18 - 18]^+$, 379, 285, 173	596	581 $[M - 15]^-$, 578 $[M - 18]^-$, 504 $[M - 92]^-$, 429 $[M - 167]^-$, 389, 363 $[M - 233]^-$, 337 $[M - 167 - 92]^-$, 233
4	all-*trans*-astaxanthin	11.8–11.9	476		0		597	579 $[M + H - 18]^+$, 505 $[M + H - 92]^+$, 379, 285, 173	596	581 $[M - 15]^-$, 578 $[M - 18]^-$, 504 $[M - 92]^-$, 429 $[M - 167]^-$, 389, 363 $[M - 233]^-$, 337 $[M - 167 - 92]^-$, 297, 233, 167
9	9-*cis*-astaxanthin	15.5–15.7	471	5	0		597	579 $[M + H - 18]^+$, 561 $[M + H - 18 - 18]^+$, 379, 285	596	581 $[M - 15]^-$, 578 $[M - 18]^-$, 504 $[M - 92]^-$, 429 $[M - 167]^-$, 389, 363 $[M - 233]^-$, 337 $[M - 167 - 92]^-$, 233

[a] Numbered according to Figure 2; [b] Retention time on the C_{30} column; [c] Linear gradient methanol/MTBE; [d] Not detected.

Table 3. Chromatographic, UV-vis and mass spectrometry characteristics of astaxanthin standard submitted to reduction with $NaBH_4$, obtained by HPLC-DAD-MS/MS.

Peak [a]	Carotenoid	t_R [b] (min)	λ_{max} [c] (nm)	% III/II	% A_B/A_{II}	$[M + H]^+$ (*m/z*)	MS/MS fragment ions (positive mode) (*m/z*)	$[M - H]^-$ (*m/z*)	MS/MS fragment ions (negative mode) (*m/z*)
26	crustaxanthin	7.9	422, 449, 476	40	0	601	583 $[M + H - 18]^+$, 565 [d] $[M + H - 18 - 18]^+$, 547 $[M + H - 18\text{-}18\text{-}18]^+$, 509 $[M + H - 92]^+$	599	581 $[M - 18]^-$, 563 $[M - 18 - 18]^-$, 545 $[M - 18 - 18 - 18]^-$, 507 $[M - 92]^-$, 493 $[M - 106]^-$
27	crustaxanthin	8.5	422, 449, 476	35	0	601	583 $[M + H - 18]^+$, 565 $[M + H - 18 - 18]^+$, 547 [d] $[M + H - 18 - 18 - 18]^+$, 509 $[M + H - 92]^+$	599	581 $[M - 18]^-$, 563 $[M - 18 - 18]^-$, 545 $[M - 18 - 18 - 18]^-$, 507 $[M - 92]^-$
28	*cis*-crustaxanthin	9.0	337, 422, 449, 476	40	6	601	583 $[M + H - 18]^+$, 565 $[M + H - 18 - 18]^+$, 547 $[M + H - 18 - 18 - 18]^+$, 509 $[M + H - 92]^+$	599	581 $[M - 18]^-$, 563 $[M - 18 - 18]^-$, 545 $[M - 18 - 18 - 18]^-$, 507 $[M - 92]^-$
29	*cis*-crustaxanthin	9.3	337, 420, 444, 470	20	39	601	583 $[M + H - 18]^+$, 565 $[M + H - 18 - 18]^+$, 547 $[M + H - 18 - 18 - 18]^+$, 509 $[M + H - 92]^+$	599	581 $[M - 18]^-$

[a] Numbered according to Figure 3; [b] Retention time on the C_{30} column; [c] Linear gradient methanol/MTBE; [d] Fragmentation in source.

Crustaxanthin was synthesized by astaxanthin reduction with $NaBH_4$, and the result of this reaction was separated on C_{30} column, as shown in Figure 3. Four crustaxanthin isomers were separated; however, by chromatographic and MS data we could only tentatively differentiate among *trans* and *cis* isomers, since this carotenoid has four asymmetric carbons and thus 10 different optical *R*/*S* isomers. The peaks were tentatively identified, based on spectral features, chromatographic elution, mass spectra characteristics (Table 3) and literature data [1]. The four peaks presented protonated molecule at *m/z* 601 and deprotonated molecule at *m/z* 599, which indicates that both keto groups of astaxanthin were reduced to hydroxyl groups. The fragmentation pattern was also similar for all the crustaxanthin isomers with fragments corresponding to the loss of one (18 u), two (36 u) and three (54 u) hydroxyl groups, as well as toluene (92 u) and xylene (106 u) from the polyene chain, both in the positive and negative fragmentation ion modes. Peaks 28 and 29 were assigned as *cis*-crustaxanthin due to the presence of a *cis*-peak at 337 nm.

Figure 3. Chromatogram (processed at 450 nm), obtained by HPLC-DAD, of astaxanthin standard submitted to reduction with $NaBH_4$. See text for chromatographic conditions. Peak identification and characterization are given in Table 3.

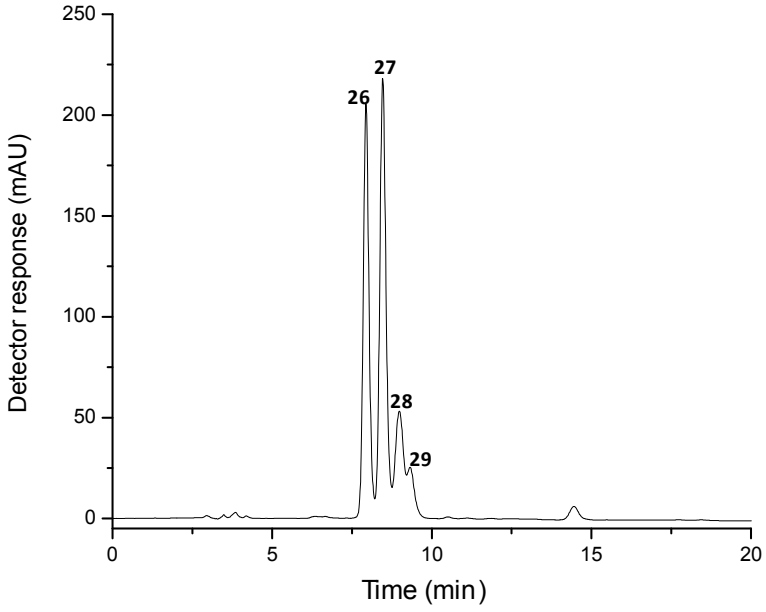

In the spiny sea star (Figure 1, Table 1), the astaxanthin isomers, all-*trans*-astaxanthin (peak 4), 13-*cis*-astaxanthin (peak 3) and 9-*cis*-astaxanthin (peak 9) were identified considering the UV-vis spectra characteristics, chromatographic behavior, co-elution with isomerized standard (Table 2), and mass spectra. The mass spectra of all isomers of astaxanthin obtained in the positive ion mode showed the protonated molecule at *m/z* 597 and fragment ions in the MS/MS at *m/z* 579 $[M + H - 18]^+$ and *m/z* 561 $[M + H - 18 - 18]^+$, corresponding to the loss of one and two hydroxyl groups, respectively. However, the fragment at *m/z* 505 $[M + H - 92]^+$, resulting from the loss of toluene from the polyene chain, was detected only in the all-*trans*-astaxanthin spectra of both sample and standard. In the low mass region of the positive ion APCI tandem mass spectra of astaxanthin isomers, fragment ions corresponding to cleavages of the polyene chain were detected at *m/z* 173, *m/z* 285 and *m/z* 379 [15]. In the negative ion mode, the molecular ion at *m/z* 596 was present in the MS spectra of all the isomers

and only all-*trans*-astaxanthin presented the deprotonated molecule at *m/z* 595 with the same intensity as the molecular ion. In addition, the MS/MS showed the presence of fragments at *m/z* 581 $[M - 15]^-$, *m/z* 578 $[M - 18]^-$, *m/z* 560 $[M - 18 - 18]^-$, *m/z* 504 $[M - 92]^-$ or *m/z* 490 $[M - 106]^-$, resulting from the losses of a methyl radical, one and two hydroxyl groups, toluene and xylene, respectively, and also the presence of other fragments from the polyene chain cleavage previously reported by van Breemen *et al.* [15] at *m/z* 203, *m/z* 233, *m/z* 297, *m/z* 323, *m/z* 337 $[M - 167 - 92]^-$, *m/z* 363 $[M - 233]^-$, *m/z* 389 and *m/z* 429 $[M - 167]^-$. The fragment ion at *m/z* 233 and its complementary ion at *m/z* 363 $[M - 233]^-$ were detected in all the MS/MS spectra of the astaxanthin isomers, and correspond to the cleavage of the 11,12 carbon-carbon bond with hydrogen transfer from the leaving group to the ion. The fragment at *m/z* 167, corresponding to the cleavage of the 7,8-bond with hydrogen transfer from the leaving group to the ion, was not detected; however, its complementary ion at *m/z* 429 $[M - 167]^-$ and the ion at *m/z* 337 $[M - 167 - 92]^-$, which corresponds to the loss of toluene from the ion of *m/z* 429, were detected in all the MS/MS spectra of the astaxanthin isomers.

Peak 2 (Figure 1, Table 1) was identified as crustaxanthin (3,4,3′,4′-tetrahydroxy-β,β-carotene), an astaxanthin metabolite, since it presented the same mass spectra of characteristics peaks 28 and 29 and UV-vis characteristics of peak 29 of the reduced astaxanthin chromatogram (Figure 3, Table 3). All-*trans*-canthaxanthin (peak 12) (Figure 1, Table 1), a carotenoid commonly used as a fish and poultry feed supplement, was identified, based on its UV-vis characteristics, molecular weight (564 Da) obtained from mass spectroscopic data, elution order on the C_{30} column and co-elution with an authentic standard. Peaks 6, 8 and 10 (Figure 1, Table 1) possess the same molecular weight and lack the fine structure as does astaxanthin (596 Da), thus they were assigned as astaxanthin derivative 1, 2 and 3, respectively. The lack of a fine structure is an indicator for the conjugation of a carbonyl group with the chromophore.

All-*trans*-lutein (peak 5) and all-*trans*-zeaxanthin (peak 7) (Figure 1, Table 1) have the same chemical formula ($C_{40}H_{56}O_2$) and, consequently, identical protonated (*m/z* 569), deprotonated (*m/z* 567) molecules and molecular ions (*m/z* 568). The structural difference between these carotenoids is that zeaxanthin has two β-ring end-groups, while lutein has one β-ring and one ε-ring. Therefore, zeaxanthin has both double bonds in the β-ring conjugated to the polyene chain, resulting in a chromophore with eleven conjugated double bonds, and lutein has one hydroxyl allylic to the double bound in the ε-ring that is not conjugated to the polyene chain, resulting in a chromophore with 10 conjugated double bonds. These characteristics allow differentiation between these two carotenoids, based on both UV-vis and mass spectra. As expected, zeaxanthin showed higher λ_{max} values than lutein. In addition, zeaxanthin mass spectrum in positive ion mode presented higher intensity of the protonated molecule peak (569 u) in comparison to the fragment at *m/z* 551 $[M + H - 18]^+$, which indicates that the hydroxyl group is not allylic to the double bond, whilst in the lutein spectrum the fragment at *m/z* 551 was more intense than the protonated molecule at *m/z* 569, as previously reported in the literature [1,9,17]. The MS/MS spectra obtained in the positive ion mode showed fragments at *m/z* 533 $[M + H - 18 - 18]^+$, *m/z* 495 $[M + H - 18 - 56]^+$, *m/z* 459 $[M + H - 18 - 92]^+$, similarly to data reported in the literature [1,9,17]. In the negative ion mode, the MS/MS spectrum of lutein presented a fragment at *m/z* 429, which corresponds to the elimination of the terminal ring containing the unconjugated carbon-carbon double bond, and consequently can be used to distinguish between

lutein and zeaxanthin [15]. The identity of both lutein and zeaxanthin was confirmed by co-elution with authentic standards.

All-*trans*-β-cryptoxanthin (peak 15) (Figure 1, Table 1) presented a similar UV-vis spectrum than that of all-*trans*-β-carotene and that of all-*trans*-zeaxanthin, since they possess the same chromophore. The identification of this carotenoid was also based on its molecular ion at *m/z* 552 obtained in the negative ion mode and the MS/MS fragments at *m/z* 534 $[M - 18]^-$, *m/z* 519 $[M - 18 - 15]^-$, *m/z* 269 and *m/z* 243, since the protonated molecule was not detected in the positive ion mode. The identification was confirmed by co-elution with authentic standard. Peak 13 was assigned as 5,6-epoxy-β-cryptoxanthin, considering the UV-vis, the MS characteristics and comparison with literature data [1,9,18]. The presence of a mass fragment at *m/z* 221 in the positive ion mode, which corresponds to the location of the epoxide group in the 3-hydroxy-β-ring, allowed the identification of this carotenoid as the 5,6-epoxide and not the 5′,6′-epoxide.

Peaks 17, 18, 19 and 20 (Figure 1, Table 1) were identified as 15-*cis*-, 13-*cis*-, all-*trans*- and 9-*cis*-β-carotene, respectively, based on the elution order on the C_{30} column, UV-vis and mass spectra characteristics and literature data [1,9,15,17]. The mass spectra of β-carotene isomers, which were obtained in the negative ion mode, showed the molecular ion at *m/z* 536, except for 9-*cis*-β-carotene, that presented the deprotonated molecule at *m/z* 535. The β-carotene isomers were present in very low concentrations, so the typical fragment ion in the MS/MS resulting from the loss of toluene ($[M - 92]^-$) was observed only for 13-*cis*- and all-*trans*-β-carotene; other fragments in the low mass range described in the literature at *m/z* 269 and *m/z* 295 [15] were detected for all isomers. The identity of all-*trans*-β-carotene was confirmed by co-elution with authentic standard.

Although it was not possible to identify the peaks 1, 11, 14 and 16 (Figure 1), these unknown compounds presented UV-vis spectra with characteristic typical for carotenoids, as can be seen in Table 1.

Astaxanthin monoesters or diesters were not detected, since in the chromatographic conditions used, they should, respectively, elute between 20 min and all-*trans*-β-carotene elution (33.1 to 34.7 min) and after all-*trans*-β-carotene to 50 min. The protonated molecules or main mass ions from carotenoid esters where searched in the range of *m/z* 100 and *m/z* 1500, but not detected. In addition, previous studies have conducted alkaline hydrolysis in the extract of this organism, with no esters being found [8]. Other carotenoids usually found in marine echinoderms and algae, such as 7,8-didehydroastaxanthin, 7,8,7′,8′-tetradehydroastaxanthin, fucoxanthin and echinenone, were also searched by observing the UV-vis spectra and the main ions of the mass spectra, but were not detected. Short chain products of astaxanthin, *i.e.*, apo-8′-, apo-10′-, apo-12′-, apo-14′- and apo-15-astaxanthinal, were not noticed in the sea star.

Recently, all-*trans*-astaxanthin, all-*trans*-lutein and all-*trans*-zeaxanthin were found in methanol and acetone extracts from *M. glacialis* and the purified methanol extract was able to inhibit cell proliferation against rat basophilic leukemia RBL-2H3 cancer cell line [8]. Both β-carotene and cryptoxanthin derivatives were searched, however they were not found. The fact that the work presented herein confirmed the presence of β-carotene and cryptoxanthin points to a possible inter-individual variation of this organism's chemical composition.

Among the 20 carotenoids found in this study, this was the first time that the occurrence of crustaxanthin, all-*trans*-canthaxanthin, two astaxanthin and three β-carotene *cis*-isomers and 5,6-epoxy-β-cryptoxanthin was reported in *M. glacialis*.

3. Experimental Section

3.1. Reagents and Standards

HPLC grade solvents, methanol and methyl *tert*-butyl ether (MTBE) were obtained from Merck (Darmstadt, Germany) or Mallinckrodt Baker (Philipsburg, NJ, USA). Ethyl acetate, methanol, methylene chloride, hexane and chloroform, all analytical grade, were from Synth (Diadema, SP, Brazil). The solvents and samples were filtered through Millipore membranes (Bedford, MA, USA) of 0.22 and 0.45 μm, respectively.

The standards of all-*trans*-astaxanthin, all-*trans*-canthaxanthin and all-*trans*-β-carotene were acquired from Sigma-Aldrich (St. Louis, MO, USA). Standards of all-*trans*-lutein, all-*trans*-zeaxanthin and all-*trans*-β-cryptoxanthin were provided by DSM Nutritional Products (Basel, Switzerland). All standards showed at least 95% purity, determined by HPLC-DAD.

3.2. Sample

M. glacialis individuals were collected from the rocky coast at Cabo Carvoeiro, west Portugal, in March 2009, placed on ice and immediately transported to the laboratory in ice-boxes. The macro-invertebrates were then cleaned and washed with sea water and kept at −20 °C, prior to their lyophilization in a Labconco 4.5 Freezone apparatus (Kansas City, MO, USA). The dried material was powdered before extraction. The sample corresponded to a mixture of three individuals.

3.3. Carotenoid Extraction

In order to avoid carotenoid degradation during analysis, the manipulation of samples and extracts was carried out under dim light and at a controlled room temperature (22 ± 3 °C). The carotenoids were extracted from 2 g of freeze-dried samples using a mortar and a pestle with the aid of glass beads (Sigma-Aldrich, 150–212 μm) to break the cell walls. A total of nine consecutive extractions were performed: four with 10 mL of ethyl acetate, three with 10 mL of methanol and two with 10 mL of methylene chloride. The solvent was separated from the sample using a refrigerated centrifuge (Allegra 64R, Beckman Coulter, Palo Alto, CA, USA) at 10 °C and 1100 *g* for 10 min. To avoid the possible presence of glass beads in the final extract, each extract was filtered through a 0.45 μm membrane and the solvent was immediately evaporated at room temperature under nitrogen flux to avoid isomerization. The further extracts were added to the same tube. The dry extract was stored in darkness and under a nitrogen atmosphere (99.9% purity) at −80 °C until HPLC analysis. The extraction was carried out in triplicate. Immediately before HPLC analysis, the extracts were dissolved in 500 μL of methanol/MTBE (70:30, v/v) and sonicated for 3 min.

3.4. Preparation of Reference Compounds

About 1 mg of all-*trans* astaxanthin authentic standard was dissolved in 4 mL of chloroform and hexane was used to make up the volume to 25 mL. The work solution was prepared by diluting a 10 mL aliquot to 100 mL in a volumetric flask with 4 mL of chloroform with the volume being made up with hexane. The concentration of the work solution, 2.5 μM, was spectrophotometrically (Agilent, Palo Alto, CA, USA) determined using the absorption coefficient for astaxanthin ($E\ ^{1\%}_{1cm}$ = 2100; 470 nm) [19].

To obtain the astaxanthin *cis* isomers, the work solution was mixed with 100 mL hexane and heated under reflux at boiling temperature (~69 °C) for 5 h. The solvent was evaporated in a rotary evaporator (Buchi, Flawil, Switzerland) and the isomerized dry standard was stored in darkness and under a nitrogen atmosphere (99.9% purity) at −36 °C until HPLC analysis.

To synthesize crustaxanthin, the all-*trans* astaxanthin work solution was dried under nitrogen flux, redissolved in 10 mL of anhydrous ethanol and reduced with $NaBH_4$ for 1h at room temperature [20]. The reaction was ended by adding saturated NaCl solution after which the carotenoids were extracted with dichloromethane. The solvent was removed under nitrogen flux and the dry crustaxanthin standard was stored in darkness and under a nitrogen atmosphere (99.9% purity) at −36 °C until HPLC analysis.

3.5. HPLC-DAD-MS/MS Analysis

A Shimadzu HPLC (Kyoto, Japan) equipped with quaternary pumps (model LC-20AD), on-line degasser and a Rheodyne (Rheodyne LCC, Robert Park, USA) injection valve with a 20 μL loop, connected in series to a DAD detector (Shimadzu) and to a mass spectrometer with an ion trap analyzer and atmospheric pressure chemical ionization source (Bruker Daltonics, model Esquire 4000, Bremen, Germany) was used for all analysis.

The carotenoids were separated on a C_{30} YMC column (3 μm, 250 × 4.6 mm i.d.) (Waters, Wilmington, USA) using as mobile phase a linear gradient of methanol/MTBE from 95:5 to 70:30 in 30 min, followed by 50:50 in 20 min. The flow rate was 0.9 mL·min^{-1} and column temperature was set at 29 °C. The UV-vis spectra were obtained between 250 and 650 nm and the chromatograms were processed at 450 nm. The MS parameters were set as follows: positive or negative mode; current corona: 4000 nA; source temperature: 450 °C; dry gas (nitrogen) temperature: 350 °C, flow: 5 L·min^{-1}; nebulizer: 60 psi. The MS/MS was set in automatic mode, applying 1.4 V fragmentation energy. The mass spectra were acquired with an *m/z* range from 100 to 700 [9].

The identification of the carotenoids was performed, considering the combination of the following parameters: elution order on the C_{30} column, UV-vis spectrum features (maximum absorption wavelength (λ_{max}), spectral fine structure (%III/II) and peak *cis* intensity (%A_B/A_{II})), MS spectrum characteristics as compared to standards analyzed under the same conditions, co-chromatography with standards and data available in the literature. In addition, the assignment of the protonated molecule ($[M + H]^+$) and the molecular ions ($M^{-\bullet}$) or deprotonated molecule ($[M - H]^-$) was confirmed by second order MS fragmentation.

4. Conclusions

In this study, HPLC-DAD-APCI-MS/MS allowed the characterization of 20 carotenoids in the echinoderm *M. glacialis*, eight of them reported for the first time. Isomers of the main compounds identified before were reported. Overall, it seems that *M. glacialis* could be an interesting matrix for further studies as a source of antioxidant carotenoids with a positive impact in human health.

Acknowledgments

This work has been supported by Fundação para a Ciência e a Tecnologia (FCT) through grant no. PEst-C/EQB/LA0006/2011. David M. Pereira is grateful to FCT for the grant (SFRH/BD/62663/2009) and Lilian R. B. Mariutti to FAPESP for the grant (2010/16522-8).

References

1. Britton, G.; Liaaen-Jensen, S.; Pfander, H. *Carotenoids Handbook*; Birkhauser Publishing: Basel, Switzerland, 2004.
2. Moran, N.A.; Jarvik, T. Lateral transfer of genes from fungi underlies carotenoid production in aphids. *Science* **2010**, *328*, 624–627.
3. Umeno, D.; Tobias, A.V.; Arnold, F.H. Diversifying carotenoid biosynthetic pathways by directed evolution. *Microbiol. Mol. Biol. Rev.* **2005**, *69*, 51–78.
4. Muller, L.; Frohlich, K.; Bohm, V. Comparative antioxidant activities of carotenoids measured by ferric reducing antioxidant power (FRAP), ABTS bleaching assay (alpha TEAC), DPPH assay and peroxyl radical scavenging assay. *Food Chem.* **2011**, *129*, 139–148.
5. Harrison, E.H. Mechanisms of digestion and absorption of dietary vitamin A. *Annu. Rev. Nutr.* **2005**, *25*, 87–103.
6. Ma, L.; Dou, H.L.; Wu, Y.Q.; Huang, Y.M.; Huang, Y.B.; Xu, X.R.; Zou, Z.Y.; Lin, X.M. Lutein and zeaxanthin intake and the risk of age-related macular degeneration: A systematic review and meta-analysis. *Br. J. Nutr.* **2012**, *107*, 350–359.
7. Czeczuga, B. Investigations of carotenoids in some animals of the Adriatic Sea V. Echinodermata. *Hydrobiologia* **1977**, *54*, 177–180.
8. Ferreres, F.; Pereira, D.M.; Gil-Izquierdo, A.; Valentão, P.; Botelho, J.; Mouga, T.; Andrade, P.B. HPLC-PAD-atmospheric pressure chemical ionization-MS metabolite profiling of cytotoxic carotenoids from the echinoderm *Marthasterias glacialis* (spiny sea-star). *J. Sep. Sci.* **2010**, *33*, 2250–2257.
9. De Rosso, V.V.; Mercadante, A.Z. Identification and quantification of carotenoids, by HPLC-PDA-MS/MS, from Amazonian fruits. *J. Agric. Food Chem.* **2007**, *55*, 5062–5072.
10. Van Breemen, R.B.; Huang, C.R.; Tan, Y.; Sander, L.C.; Schilling, A.B. Liquid chromatography/mass spectrometry of carotenoids using atmospheric pressure chemical ionization. *J. Mass Spectrom.* **1996**, *31*, 975–981.

11. Breithaupt, D.E. Identification and quantification of astaxanthin esters in shrimp (*Pandalus borealis*) and in a microalga (*Haematococcus pluvialis*) by liquid chromatography-mass spectrometry using negative ion atmospheric pressure chemical ionization. *J. Agri. Food Chem.* **2004**, *52*, 3870–3875.
12. Etoh, H.; Suhara, M.; Tokuyama, S.; Kato, H.; Nakahigashi, R.; Maejima, Y.; Ishikura, M.; Terada, Y.; Maoka, T. Auto-oxidation products of astaxanthin. *J. Oleo Sci.* **2012**, *61*, 17–21.
13. Hayakawa, T.; Kulkarni, A.; Terada, Y.; Maoka, T.; Etoh, H. Reaction of astaxanthin with peroxynitrite. *Biosci. Biotechnol. Biochem.* **2008**, *72*, 2716–2722.
14. Holtin, K.; Kuehnle, M.; Rehbein, J.; Schuler, P.; Nicholson, G.; Albert, K. Determination of astaxanthin and astaxanthin esters in the microalgae *Haematococcus pluvialis* by LC-(APCI)MS and characterization of predominant carotenoid isomers by NMR spectroscopy. *Anal. Bioanal. Chem.* **2009**, *395*, 1613–1622.
15. Van Breemen, R.B.; Dong, L.L.; Pajkovic, N.D. Atmospheric pressure chemical ionization tandem mass spectrometry of carotenoids. *Int. J. Mass. Spectrom.* **2012**, *312*, 163–172.
16. Zechmeistee, L. *Cis-trans* isomerization and stereochemistry of carotenoids and diphenylpolyenes. *Chem. Rev.* **1944**, *34*, 267–344.
17. Faria, A.F.; de Rosso, V.V.; Mercadante, A.Z. Carotenoid composition of jackfruit (*Artocarpus heterophyllus*), determined by HPLC-PDA-MS/MS. *Plant Food Hum. Nutr.* **2009**, *64*, 108–115.
18. Faria, A.F.; Hasegawa, P.N.; Chagas, E.A.; Pio, R.; Purgatto, E.; Mercadante, A.Z. Cultivar influence on carotenoid composition of loquats from Brazil. *J. Food Compos. Anal.* **2009**, *22*, 196–203.
19. Schuep, W.; Schierle, J. Astaxanthin: Determination of Stabilized, Added Astaxanthin in Fish Feeds and Pre-mixes. In *Carotenoids: Isolation and Analysis*; Britton, G., Liaanen-Jensen, S., Pfander, H., Eds.; Birkauser Verlag: Basel, Switzerland, 1995; Volume 1A, pp. 273–276.
20. Eugster, C.H. Chemichal derivatization: Microscale Tests for the Presence of Common Functional Groups in Carotenoids. In *Carotenoids: Isolation and Analysis*; Britton, G., Liaanen-Jensen, S., Pfander, H., Eds.; Birkauser Verlag: Basel, Switzerland, 1995; Volume 1A, pp. 71–80.

Samples Availability: Available from the authors.

Paper 3

A gas chromatography–mass spectrometry multi-target method for the simultaneous analysis of three classes of metabolites in marine organisms

David M. Pereira, *Juliana Vinholes, Paula Guedes de Pinho, Patrícia Valentão, Teresa Mouga, Natércia Teixeira, Paula B. Andrade,*

Talanta, 2012, 100, 391–400

Talanta 100 (2012) 391–400

Contents lists available at SciVerse ScienceDirect

Talanta

journal homepage: www.elsevier.com/locate/talanta

A gas chromatography–mass spectrometry multi-target method for the simultaneous analysis of three classes of metabolites in marine organisms

David M. Pereira [a], Juliana Vinholes [a], Paula Guedes de Pinho [b], Patrícia Valentão [a], Teresa Mouga [c], Natércia Teixeira [d,e], Paula B. Andrade [a,*]

[a] REQUIMTE/Laboratório de Farmacognosia, Departamento de Química, Faculdade de Farmácia, Universidade do Porto, Rua de Jorge Viterbo Ferreira n.º 228, 4050-313 Porto, Portugal
[b] REQUIMTE/Laboratório de Toxicologia, Departamento de Ciências Biológicas, Faculdade de Farmácia, Universidade do Porto, Rua de Jorge Viterbo Ferreira n.º 228, 4050-313 Porto, Portugal
[c] GIRM—Marine Resources Research Group, School of Tourism and Maritime Technology, Polytechnic Institute of Leiria, Santuário N.ª Sra. dos Remédios, Apartado 126, 2524-909 Peniche, Portugal
[d] Laboratório de Bioquímica, Departamento de Ciências Biológicas, Faculdade de Farmácia, Universidade do Porto, Rua de Jorge Viterbo Ferreira n.º 228, 4050-313 Porto, Portugal
[e] IBMC—Instituto de Biologia Molecular e Celular, Universidade do Porto, 4150-180 Porto, Portugal

ARTICLE INFO

Article history:
Received 2 April 2012
Received in revised form
3 August 2012
Accepted 3 August 2012
Available online 18 August 2012

Keywords:
Multi-target GC–MS
Marine organisms
Marthasterias glacialis Linnaeus
Amino acids
Fatty acids
Sterols

ABSTRACT

In this work a fast and simple multi-target gas chromatography–mass spectrometry (GC–MS) method for the simultaneous detection and absolute quantification of amino acids, fatty acids, sterols and lupanes in marine organisms is proposed. The methodology was applied to the characterization of the echinoderm *Marthasterias glacialis* Linnaeus spiny sea star extracts. The main factors influencing the extraction of target compounds were evaluated by using different extraction procedures, solvent systems and temperature conditions and a comparison with a reference technique was performed. The most suitable procedure, capable of successfully extract the three classes of target compounds, was ethanol as solvent at 40 °C under magnetic stirring. Good analytical parameters were obtained since calibrations curves for the 40 compounds under analysis (15 amino acids, 16 fatty acids, 6 sterols and 3 lupanes) showed regression coefficients (r^2) ranging from 0.9844 to 0.9978, with low RSD (from 0.00 to 9.45%), and detection limits varying from 0.03 to 15.40 μg/L. The RSD values for intra- and interday variations studies were also good (RSD < 13.5%, for both) and recoveries were higher than 92%. Variation in samples from different harvests and origins and their chemical composition during the year is reported. The fact that no previous treatment of samples is required can make this a useful technique for metabolite profiling in marine organisms, among others, both in biomedical and nutritional studies. Moreover, due to the fast and robust character of the proposed method it seems to be suitable for the implementation as routine analysis.

1. Introduction

Nowadays multi-target approaches have been increasingly used, thus allowing the identification of several classes of compounds in different matrices [1–3]. Gas chromatography–mass spectrometry (GC–MS) is a popular preference since it provides powerful structural and quantitative information [4]. Adequate extraction procedures are critical for obtaining a chemical profile that is representative of the original sample, both qualitatively and quantitatively. Techniques such as microwave assisted extraction [5], accelerated solvent extraction [6] and supercritical fluid extraction [7,8] have been developed and different derivatization procedures tested. Derivatizing agents are responsible for the increment of volatility of less volatile and non-volatile compounds and, consequently, a higher sensitivity and resolution can be obtained by GC–MS analysis. Currently, silylation is widely used as derivatization method for GC–MS metabolic profile studies, since it allows the determination of metabolites from different classes. Among silylation agents, *N*-methyl-*N*-(trimethylsilyl)-trifluoroacetamide (MSTFA) has been increasingly used due to its ability to react with primary amines and amides, alcohols, phenols, carbohydrates and carboxylic groups [9,10].

Marine organisms have been paving their way as an interesting source of bioactive molecules for biomedical research, as well as alternative foodstuffs for nutrition. In both cases, the use of these organisms must be guided by elevated standards in quality control and hence analytical techniques for fast metabolite profiling are required. Among the metabolites present in marine species, lipids are growing in interest, especially by their content

* Corresponding author. Tel.: +351 220428654; fax: +351 226093390.
E-mail address: pandrade@ff.up.pt (P.B. Andrade).

0039-9140/$ - see front matter © 2012 Elsevier B.V. All rights reserved.
http://dx.doi.org/10.1016/j.talanta.2012.08.004

Table 1
Validation parameters for amino acids, fatty acids, sterols and lupanes.

Compound	Concentration range (μg/mL)	Slope (±SD)	Interception (±SD)	Correlation coefficient (±SD)	LOD (μg/mL)	LOQ (μg/mL)	RSD
Amino acids							
Alanine	12.00–120.00	0.0086 (0.0001)	0.0035 (0.0092)	0.9952 (0.0260)	0.36	1.12	0.10
Glycine	20.00–200.00	0.0130 (0.0002)	0.0193 (0.0247)	0.9974 (0.0696)	1.75	5.83	0.77
Valine	1.50–150.00	0.0631 (0.0007)	0.1612 (0.0588)	0.9978 (0.1659)	0.13	0.43	0.27
Leucine	1.50–88.00	0.0727 (0.0012)	−0.0290 (0.0581)	0.9958 (0.1544)	0.18	0.61	0.45
Isoleucine	1.50–150.00	0.0523 (0.0005)	0.0183 (0.0368)	0.9978 (0.0978)	0.22	0.75	0.38
Proline	12.00–120.00	0.0588 (0.0012)	−0.0726 (0.0892)	0.9938 (0.2135)	0.03	0.11	0.06
Serine	12.00–120.00	0.0125 (0.0002)	−0.0079 (0.0155)	0.9958 (0.0371)	2.51	8.35	1.04
Threonine	5.00–170.00	0.0375 (0.0005)	−0.0290 (0.0365)	0.9972 (0.0970)	0.58	1.94	0.73
Aspartic acid	12.50–200.00	0.0574 (0.0010)	−0.1894 (0.1217)	0.9972 (0.1100)	1.77	5.89	3.10
trans-4-Hydroxyproline	15.00–150.00	0.0180 (0.0004)	−0.0254 (0.0334)	0.9940 (0.0799)	1.67	5.55	1.00
Cysteine	28.00–140.00	0.0440 (0.0013)	0.0041 (0.1016)	0.9888 (0.2424)	2.68	8.92	3.93
Methionine	12.50–200.00	0.0661 (0.0019)	0.5070 (0.2064)	0.9898 (0.1923)	1.46	4.85	1.52
Phenylalanine	13.00–130.00	0.0330 (0.0010)	−0.1386 (0.0761)	0.9864 (0.1822)	0.54	1.81	2.19
Glutamic acid	6.25–200.00	0.0381 (0.0001)	0.1066 (0.0623)	0.9940 (0.0241)	0.61	2.03	1.75
Lysine	12.50–200.00	0.0730 (0.0016)	−0.7400 (0.1570)	0.9926 (0.0450)	0.97	3.27	2.09
Fatty acids							
Pelargonic	20.00–100.00	0.0054 (0.0001)	−0.0216 (0.0078)	0.9910 (0.0188)	4.61	15.36	0.83
Capric	40.00–200.00	0.0039 (0.0001)	−0.0123 (0.0117)	0.9902 (0.0281)	7.86	26.21	1.02
Lauric	5.00–130.00	0.0057 (0.0001)	−0.0276 (0.0115)	0.9886 (0.0275)	0.61	2.04	0.11
Myristic	25.00–500.00	0.0027 (0.0001)	0.1516 (0.0229)	0.9938 (0.0382)	2.71	9.05	0.26
Pentadecanoic	10.00–250.00	0.0052 (0.0001)	−0.0003 (0.0150)	0.9914 (0.0362)	2.27	7.58	0.38
Palmitic	60.00–300.00	0.0056 (0.0001)	0.0613 (0.0264)	0.9891 (0.0633)	7.72	25.75	1.44
Margaric	10.00–120.00	0.0106 (0.0003)	−0.0153 (0.0191)	0.9920 (0.0457)	2.02	6.73	0.71
Oleic	10.00–140.00	0.0004 (0.0000)	−0.0012 (0.0009)	0.9866 (0.0022)	0.14	0.48	0.00
Linoleic	10.00–100.00	0.0104 (0.0003)	−0.0521 (0.0180)	0.9901 (0.0430)	1.34	4.45	0.71
Linolenic	10.00–500.00	0.0003 (0.0000)	−0.0045 (0.0026)	0.9941 (0.0058)	1.77	5.91	0.02
Stearic	10.00–176.00	0.0094 (0.0003)	0.0215 (0.0373)	0.9953 (0.0892)	0.31	1.02	0.10
Arachidonic	10.00–500.00	0.0065 (0.0002)	−0.0259 (0.0541)	0.9932 (0.1294)	3.18	10.61	0.07
Eicosapentaenoic	40.00–200.00	0.0138 (0.0003)	−0.1064 (0.0413)	0.9903 (0.0989)	6.54	21.81	3.01
*cis*11-Eicosenoic	60.00–300.00	0.0002 (0.0000)	−0.0091 (0.0013)	0.9909 (0.0019)	8.35	27.84	0.06
Eicosanoic	28.00–140.00	0.0136 (0.0002)	0.0249 (0.0203)	0.9951 (0.0485)	4.68	15.59	2.12
Docosahexaenoic	30.00–180.00	0.0094 (0.0002)	−0.0642 (0.0385)	0.9947 (0.0866)	4.95	16.48	1.55
Sterols and lupanes							
Cholesta-3,5-diene	14.00–70.00	0.0170 (0.0006)	−0.0478 (0.0265)	0.9844 (0.0596)	3.22	10.73	1.82
Cholesterol	30.00–250.00	0.0108 (0.0004)	−0.0397 (0.0359)	0.9913 (0.0807)	4.17	13.88	1.54
Cholestanol	5.00–100.00	0.0265 (0.0007)	−0.0683 (0.0436)	0.9932 (0.0981)	0.27	0.89	0.23
Ergosterol	76.00–380.00	0.0103 (0.0003)	−0.1466 (0.0684)	0.9903 (0.1538)	15.40	51.34	5.29
Fucosterol	6.25–200.00	0.0146 (0.0002)	−0.0383 (0.0191)	0.9963 (0.0574)	0.95	3.17	9.45
Betuline	6.25–200.00	0.0170 (0.0003)	−0.0903 (0.0294)	0.9937 (0.0882)	0.97	3.24	5.48
Lupeol	6.25–200.00	0.0154 (0.0003)	−0.0743 (0.0269)	0.9935 (0.0854)	0.80	2.68	7.43
Lupeol acetate	6.25–200.00	0.0178 (0.0003)	−0.1000 (0.0257)	0.9956 (0.0771)	0.83	2.74	8.94
β-Sitosterol	10.40–52.00	0.0178 (0.0005)	−0.0201 (0.0168)	0.9896 (0.0377)	1.61	5.37	0.46

in polyunsaturated fatty acids that are important to human health and nutrition. The fatty acids (FA) composition of marine organisms is often characteristic for each species and genus, but also depends on environmental conditions [11–13]. Several protocols have been established for the extraction and analysis of FA, and recent reviews on this topic are available [11,14]. However, in most cases, the protocol includes extensive pre-treatment for the elimination of interferents [1,15] and quantification is not always possible. Separation of polar and apolar constituents is also common.

Other two classes of compounds with nutritional interest found in marine organisms are amino acids and sterols. The first is generally analyzed by GC–MS, GC-FID [16,17] or HPLC-UV/DAD [18,19], while techniques for sterol analysis can be performed either by HPLC-DAD/MS [20,21] or GC–MS [22]. However, pre-treatment of samples is usually required for both classes, which can result in high losses of analyte and low recovery rates.

In this work, a methodology for the simultaneous assessment of the four classes of compounds (amino acids, fatty acids, sterols and lupanes) in marine organisms was developed. The proposed method includes the derivatization of a crude extract and further identification and quantification by GC–MS, in 25 min chromatographic run, without sample pre-treatment or the use of hazard extraction solvents.

2. Experimental

2.1. Standards and reagents

Arginine (≥98%), asparagine (≥98%), aspartic acid (≥98%), cysteine (≥98%), glutamic acid (≥98%), glutamine (≥98%), histidine (≥98%), lysine (≥98%), methionine (≥98%), tryptophan (≥98%), tyrosine (≥98%), alanine (≥98%), glycine (≥99%), valine (≥98%), leucine (≥98%), isoleucine (≥98%), proline (≥99%), serine (≥99%), threonine (≥98%), *trans*-4-hydroxyproline (≥98%), phenylalanine (≥98%), norvaline (≥99%), methyl linolelaidate (≥99%), cholesta-3,5-diene (≥95%), cholesterol (≥95%), cholestanol (≥99%), ergosterol (≥95%) *β*-sitosterol (≥97%), desmosterol (≥85%), fucosterol (≥95%), betulin (≥95%), lupeol (≥95%), lupeol acetate (≥95%), *N*-methyl-*N*-(trimethylsilyl) trifluoroacetamide (MSTFA), as well as pelargonic (≥99%), decanoic (≥99%), capric (≥99%), lauric (≥95%), myristic (≥99%), pentadecanoic (≥99%), palmitic (≥99%), margaric

(≥98%), stearic (≥99%), oleic (≥99%), linoleic (≥99%), linolenic (≥99%), arachidonic (≥99%), 5,8,11,14,17-eicosapentaenoic (EPA) (≥99%), *cis*11,14-eicosadienoic (≥98%), *cis*11-eicosaenoic (≥99%), docosahexaenoic (DHA) (≥98%) and eicosanoic acids (≥97%) and dichloromethane were from Sigma (St. Louis, MO, USA). The *n*-alkane series (C_8-C_{40}) and boron trifluoride (BF_3) 10% methanolic solution were from Supelco (Bellefonte, PA, USA). Chloroform, methanol, anhydrous sodium sulfate and isooctane were from Panreac Quimica SA (Barcelona, Spain). Potassium hydroxide was obtained from Pronalab (Lisboa, Portugal).

2.2. Preparation of standard solutions

Stock solutions of amino acids, fatty acids, sterols and lupanes and the internal standards (IS) norvaline, methyl linolelaidate and desmosterol were prepared individually in ethanol and kept at −20 °C until analysis. Calibration solutions were then prepared by mixing and diluting each stock solution in appropriate amounts with ethanol to achieve the concentration range discriminated in Table 1.

2.3. Marine organisms

Marthasterias glacialis Linnaeus individuals were collected at the rocky coast at Cabo Carvoeiro, west Portugal, in July and September of 2009 and at Praia do Baleal and Praia da Consolação in February of 2010 (Fig. 1). The organisms were placed on ice and immediately transported to the laboratory in ice-boxes. The macro-invertebrates were then cleaned and washed with sea water and kept at −20 °C, prior to their freeze-drying in a Labconco 4.5 Freezone apparatus (Kansas City. MO. USA). The dried material was powdered and sifted (<910 μm) before extraction. Each sample corresponds to a mixture of three individuals.

2.4. GC–MS system and data acquisition

2.4.1. GC–MS general conditions

In all cases, analysis was performed with a Varian CP-3800 gas chromatograph coupled to a Varian Saturn 4000 mass selective ion trap detector (USA) and a Saturn GC–MS workstation software version 6.8. A VF-5 ms (30 m × 0.25 mm × 0.25 μm) column (VARIAN) was used. A CombiPAL automatic autosampler (Varian, Palo Alto, CA) was used for all experiments. The injector port was heated to 250 °C. Injections were performed in split mode, with a ratio of 1/40. The carrier gas was helium C-60 (Gasin, Portugal), at a constant flow of 1 ml/min. The ion trap detector was set as follows: transfer line, manifold and trap temperatures were 280, 50, and 180 °C, respectively. The mass ranged from 50 to 600 *m/z*, with a scan rate of 6 scan/s. The emission current was 50 μA and the electron multiplier was set in relative mode to auto tune procedure. The maximum ionization time was 25.000 μs, with an ionization storage level of 35 *m/z*. The injection volume was 2 μL and the analysis was performed in Full Scan mode.

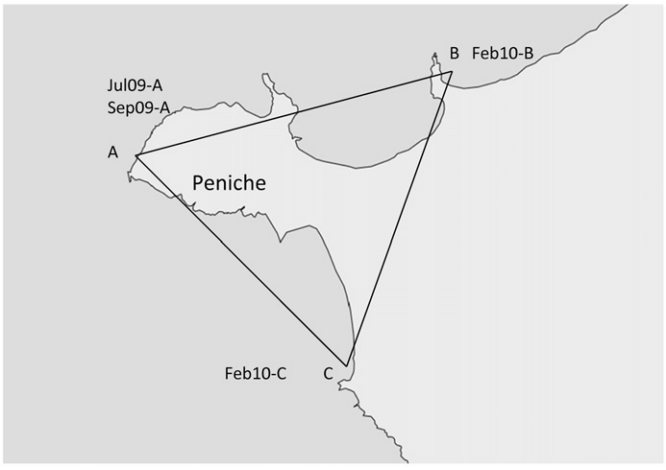

Fig. 1. Collection sites of the organisms used in this study (west Portugal) and respective sample identification.

2.4.2. GC conditions for trimethylsilyl (TMS) derivatives analysis

The oven temperature was set at 100 °C for 1 min, then increasing 20 °C/min to 250 °C and held for 2 min, 10 °C/min to 300 °C and held for 10 min. All mass spectra were acquired in electron impact (EI) mode. Ionization was maintained off during the first 4 min to avoid solvent overloading. For quantification purposes, each sample was injected in triplicate and the amount of metabolites present in samples was achieved from the calibration curves of the respective TMS derivatives. All compounds were quantified in Full Scan mode, with the exceptions of linoleic (*m/z* 262, 337 and 352), linolenic (*m/z* 191, 335 and 350), and oleic (*m/z* 264, 339 and 354) derivatives that were quantified by the area obtained from the re-processed chromatogram, using the characteristic *m/z* fragments. Identification of compounds was achieved by comparisons of their retention time and mass spectra with those of pure standards TMS derivatives prepared and injected under the same conditions, and from NIST 05 MS Library Database. In addition, the retention index (RI) was experimentally calculated and the values were compared with those reported in the literature for GC columns with 5%-Phenyl-95%-dimethylpolysiloxane (Table 6). For the RI determination, an *n*-alkanes series C_8-C_{40} was used.

2.4.3. GC conditions for fatty acids methyl esters (FAMEs) analysis

For comparison purposes, we have used chromatographic conditions published before [23]. The oven temperature was set at 40 °C for 1 min, then increasing 5 °C/min to 250 °C, 3 °C/min to 300 °C and held for 15 min. The injection volume for liquid extracts was 1 μL and the analysis was performed in Full Scan mode. Identification of compounds was achieved by comparisons

Table 2
Recovery values for representative amino acids, fatty acids and sterols. For each compound, three different concentration levels were tested.

Compounds	Concentration (μg/mL)	Recovery (%)
Isoleucine	2.00	94
	4.00	94
	20.00	99
trans-4-Hydroxyproline	10.00	96
	50.00	97
	150.00	103
Palmitic acid	15.00	95
	30.00	93
	150.00	95
Arachidonic acid	40.00	95
	80.00	96
	300.00	94
Cholesta-3,5-diene	10.00	92
	20.00	95
	80.00	98
Cholestanol	7.50	106
	15.00	95
	34.00	101

Table 3
Values of intra- and interday reproducibility for amino acids.

Compounds	Concentration (μg/mL)	Intraday (RSD)	Interday (RSD)
Alanine	12.00	4.87	12.94
	72.00	3.30	7.76
	120.00	0.49	7.30
Glycine	20.00	2.30	7.82
	120.00	1.57	5.91
	400.00	3.11	4.67
Valine	1.50	2.89	6.82
	90.00	0.06	5.49
	150.00	0.20	8.14
Leucine	1.50	0.41	6.55
	66.00	3.67	8.26
	88.00	2.27	3.66
Isoleucine	15.00	2.77	5.91
	90.00	1.86	4.83
	120.00	1.31	7.63
Proline	24.00	0.05	4.00
	72.00	2.50	7.01
	120.00	0.81	4.69
Serine	24.00	2.48	8.43
	72.00	4.17	8.70
	120.00	0.62	12.82
Threonine	17.00	1.17	5.14
	102.00	3.26	5.55
	136.00	1.04	7.22
Aspartic acid	12.50	3.10	7.17
	50.00	4.18	6.18
	200.00	1.57	8.75
trans-4-Hydroxyproline	30.00	2.17	11.65
	90.00	4.26	4.34
	150.00	0.11	6.68
Cysteine	26.00	2.19	7.27
	78.00	4.01	8.35
	130.00	0.58	8.27
Methionine	1.52	1.52	6.73
	5.06	2.73	3.69
	2.45	2.45	8.68
Phenylalanine	13.00	1.92	9.19
	78.00	2.29	10.61
	130.00	2.73	8.22
Glutamic acid	6.25	1.75	9.89
	50.00	1.05	8.15
	200.00	2.06	8.06
Lysine	6.25	2.09	4.24
	50.00	6.80	7.36
	200.00	4.99	9.22

Table 4
Values of intra- and interday reproducibility for fatty acids.

Compounds	Concentration (μg/mL)	Intraday (RSD)	Interday (RSD)
Lauric acid	26.00	3.73	9.87
	78.00	0.60	6.74
	130.00	3.72	8.16
Myristic acid	25.00	1.31	5.15
	300.00	2.46	7.80
	500.00	0.98	9.71
Pentadecanoic acid	10.00	2.87	9.32
	150.00	2.42	10.57
	250.00	2.97	10.44
Palmitic acid	60.00	3.25	3.93
	180.00	3.16	9.41
	300.00	1.96	4.74
Margaric acid	10.00	8.70	8.73
	72.00	6.64	10.12
	120.00	1.93	8.88
Linoleic acid	10.00	7.85	10.77
	40.00	5.47	7.13
	100.00	0.77	5.54
Linolenic acid	10.00	9.92	11.51
	300.00	2.76	10.83
	500.00	3.11	8.02
Oleic acid	10.00	8.64	12.53
	84.00	3.25	4.82
	140.00	2.19	4.62
Stearic acid	10.00	3.74	10.18
	132.00	3.25	9.20
	220.00	0.99	9.98
Arachidonic acid	100.00	1.85	8.62
	300.00	3.66	8.05
	500.00	2.95	6.24
Eicosapentaenoic acid	40.00	4.88	7.29
	120.00	2.66	11.93
	200.00	2.76	7.38
*cis*11-Eicosenoic acid	60.00	4.02	11.81
	180.00	3.61	9.81
	300.00	3.00	11.58
Eicosanoic acid	28.00	5.67	10.64
	84.00	2.96	3.76
	140.00	2.65	7.74
Docosahexaenoic acid	30.00	10.45	11.96
	180.00	4.86	12.37
	300.00	2.54	8.68

of their retention time and mass spectra with those from pure standards injected under the same conditions, and from NIST 05 MS Library Database.

2.5. Metabolites extraction and derivatization

2.5.1. Procedure for TMS derivatives

In order to establish the most suitable method for the extraction and quantification of metabolites present in marine samples,

Table 5
Values of intra- and interday reproducibility for sterols and lupanes.

Compounds	Concentration (μg/mL)	Intraday (RSD)	Interday (RSD)
Cholesta-3,5-diene	14.00	0.54	7.39
	42.00	3.56	10.49
	70.00	8.63	12.47
Cholesterol	30.00	1.29	9.27
	90.00	4.12	9.74
	150.00	11.48	13.67
Cholestanol	5.00	5.70	11.51
	80.00	1.84	13.39
	100.00	1.95	10.97
Ergosterol	150.00	3.46	6.90
	228.00	6.40	9.64
	380.00	2.16	8.73
Fucosterol	6.25	6.55	6.63
	50.00	3.76	4.79
	200.00	0.45	6.69
β-Sitosterol	10.40	3.87	9.30
	31.20	1.72	10.51
	52.00	2.75	10.99
Betuline	6.25	5.25	6.28
	50.00	1.63	5.42
	200.00	4.91	6.96
Lupeol	6.25	5.68	7.24
	50.00	4.50	5.90
	200.00	4.97	5.19
Lupeol acetate	6.25	8.94	9.89
	50.00	3.66	6.21
	200.00	1.50	5.30

different extracts from *M. glacialis* (sample Sep09-A) were prepared. Briefly, 100.00 ± 1.00 mg of dried sample was transferred to a glass vial and the internal standards were added: 80 μL of norvaline (0.30 mg/mL), 20 μL of methyl linolelaidate (10.00 mg/mL), and 80 μL of desmosterol (2.00 mg/mL). The volume was then completed to 2.00 mL with either ethanol or a solution of choloroform:methanol, according to the experiment being carried.

Extractions with ethanol were performed at different temperatures (40, 50 and 60 °C) by incubating for 20 min under magnetic stirring (200 rpm). Ultra-sonication with ethanol was also performed and all extracts were compared with the extraction with chloroform/methanol (2:1) [24] incubated for 20 min under magnetic stirring 200 rpm. Samples were then filtered through a 0.45 μm membrane (Millipore). Extractions were carried out in triplicate.

An aliquot of 50 μL of extract was transferred to a glass vial, the solvent was evaporated under nitrogen stream and 50 μL of the derivatization reagent (MSTFA) was added to the dried residue. The vial was capped, vortexed and heated for 20 min in a dry block heater maintained at 40 °C. All analyses were performed in triplicate.

2.5.2. Procedure for FAMES

Methyl esters derivatives were obtained as described by Ribeiro et al. [23], with some modifications: 100 mg of the powdered sample plus 20 μL of methyl linolelaidate (10.00 mg/mL) ethanol solution (internal standard) were mixed with chloroform: methanol (2:1) (2 × 2 mL) with magnetic stirring (500 rpm), for 10 min, at 40 °C. The resulting extract was filtered, concentrated to dryness under reduced pressure (40 °C) and redissolved in 2 mL of ethanol. Derivatization was assured by treatment with 1 mL of BF_3 methanolic solution (10%), at 90 °C, for 10 min. Derivatives were purified with 2 × 6 mL of isooctane and anhydrous sodium sulfate was added to assure the total absence of water. The extract was then evaporated under a stream of nitrogen and redissolved in 200 μL of isooctane.

2.6. Method validation

At least six concentration levels of compounds' trimethylsilyl (TMS) derivatives were analyzed. Each calibration solution contained norvaline, methyl linolelaidate and desmosterol as internal standards, at a final concentration of 12.00, 100.00 and 80 μg/mL, respectively. The ratios of the peak areas of compounds *versus* those of IS were plotted against the corresponding concentration to obtain the calibrations graphs. The derivatization procedure was carried out as described in 2.5.1., using 50 μL of calibration solution instead of the extract.

2.6.1. Linearity

Method linearity was determined by evaluation of the regression curve (ratio of analyte peak area/IS area *versus* analyte concentration) and expressed by the correlation coefficient. The linearity range of the method was analyzed by performing calibration curves using at least six different concentration levels of the analytes, according to the range of concentrations present in the samples (Table 1).

2.6.2. Limits of detection and of quantification

Limit of detection (LOD) and limit of quantification (LOQ) were determined from calibration curve data and were obtained by the following formula [25]:

$$\mathrm{LOD} = (3.3 \times \mathrm{SD})/b \text{ and } \mathrm{LOQ} = (10 \times \mathrm{SD})/b$$

where SD is the residual standard deviation of the linear regression, and b is the slope of the regression line.

2.6.3. Precision, accuracy and recovery tests

Precisions and accuracies were determined using intra- and interday assays at three different concentrations (low, medium and high) and are expressed as coefficients of variation (CV). Recovery tests were performed by spiking *M. glacialis* (sample Sep09-A) with two compounds representative of each class: isoleucine (2.00, 4.00 and 20.00 μg/mL), *trans*-4-hydroxyproline (10.00, 50.00 and 150.00 μg/mL), palmitic (15.00, 30.00 and 150.00 μg/mL) and arachidonic acids (40.00, 80.00 and 300.00 μg/mL), cholesta-3,5-diene (10.00, 20.00, and 80.00 μg/mL) and cholestanol (7.50, 15.00 and 34.00 μg/mL).

3. Results and discussion

3.1. Optimization of the extraction procedure

For the development of the method, sample Sep09-A was selected. A preliminary screening revealed that fatty acids were the predominant compounds in *M. glacialis*. Given the fact that fatty acids were important compounds in the samples, both from a qualitative and quantitative point of view, we applied a methodology available in the bibliography that is currently used for the analysis of this class of metabolites derivatives (Folch

Table 6
Quantification of amino acids, fatty acids and sterols in *M. glacialis* samples.

Peak	RI^{Exp}	RI^{Lit}	Compound	*Marthasterias glacialis*			
				Jul09-A	***Sep09-A***	***FeB10-B***	***Feb10-C***
Amino acids				Average mg/100 **g (± SD)**			
1	1096	1095 [41]	Alanine	–	279.34 (19.87)	319.46 (1.20)	956.50 (73.61)
2	1115		Glycine	957.46 (89.13)	1520.42 (85.48)	1213.07 (251.30)	1969.08 (218.50)
3	1210	1210 [42]	Valine	18.14 (0.01)	30.36 (0.11)	23.80 (3.47)	105.94 (5.22)
4	1250	1262 [43]	Leucine	40.26 (5.26)	57.20 (2.60)	52.16 (1.08)	94.30 (3.39)
5	1274	1290 [41]	Isoleucine	20.08 (0.87)	25.63 (2.33)	28.71 (0.97)	57.61 (5.21)
6	1286	1299 [42]	Proline	48.91 (1.04)	29.28 (0.20)	23.91 (6.33)	–
7	1352	1343 [43]	Serine	100.57 (1.45)	69.62 (6.01)	56.24 (16.28)	–
8	1364	1367 [43]	Threonine	21.44 (0.72)	30.30 (4.19)	21.25 (3.47)	25.10 (3.79)
9	1500		*trans*-4-Hydroxyproline	94.88 (1.43)	131.26 (9.17)	37.79 (4.64)	–
10	1619	1622 [43]	Phenylalanine	11.22 (0.16)	38.94 (4.01)	33.80 (8.02)	65.46 (15.67)
Total				**1312.96 (94.75)**	**2212.34 (133.98)**	**1810.19 (231.29)**	**3273.99 (269.27)**
Fatty acids							
11	1837	1843 [43]	Myristic	316.46 (5.53)	96.15 (1.68)	23.87 (7.89)	334.74 (9.97)
12	1938	1943 [43]	Pentadecanoic	141.37 (0.73)	71.53 (6.03)	74.64 (18.25)	147.69 (2.90)
13	2043	2040 [43]	Palmitic	538.31 (68.28)	293.98 (4.68)	180.96 (14.99)	288.06 (10.37)
14	2147		Margaric	73.78 (0.33)	48.21 (0.43)	14.36 (0.20)	26.83 (0.21)
15	2214	2212 [44]	Linoleic	< LOQ	–	< LOQ	–
16	2225	2218 [44]	Linolenic	–	–	27.35 (2.20)	27.85 (0.32)
17	2238	2248 [44]	Oleic	27.76 (0.69)	44.49 (9.19)	21.73 (2.68)	19.63 (0.38)
18	2253	2234 [44]	Stearic	251.87 (0.88)	157.56 (0.92)	62.55 (0.69)	124.04 (0.66)
19	2389	2373 [43]	Arachidonic	444.20 (10.23)	267.82 (0.35)	425.13 (16.61)	602.34 (7.05)
20	2398	2380 [44]	Eicosapentaenoic	240.48 (9.14)	144.30 (1.04)	215.26 (5.52)	303.84 (5.30)
21	2404	2413 [39]	*cis*11,14-Eicosedienoic[a]	213.42 (18.77)	144.26 (7.12)	137.86 (3.96)	239.51 (22.14)
22	2425		*cis*11-Eicosenoic isomer[a]	438.09 (38.03)	243.24 (2.74)	190.45 (11.84)	252.09 (17.61)
23	2430	2420 [39]	*cis*11-Eicosenoic	374.67 (48.09)	265.36 (11.90)	181.42 (8.67)	207.19 (6.18)
24	2585	2562 [43]	Docosahexaenoic	63.28 (3.25)	117.89 (3.89)	99.72 (3.79)	72.19 (2.58)
Total				**3132.60 (23.82)**	**1895.12 (9.94)**	**1653.33 (14.10)**	**2645.16 (6.78)**
Sterols							
25	2938		Cholesta-3,5-diene	–	34.72 (0.22)	–	51.57 (0.50)
26	3176		M^+ 458 *m/z* (73(100), 369(88), 330(82), 75(75), 95(74), 129(72), 458(70), 81(51), 146(49), 91(48))[b]	–	–	22.29 (2.25)	90.16 (0.11)
27	3181		M^+ 456 *m/z* (344(100), 73(83), 81(70), 118(68), 95(60), 69(59), 148(58), 97(54), 75(54), 256(52))[b]	–	< LOQ	27.81 (2.65)	–
28	3190		M^+ 462 *m/z* (75(100), 216(88), 217(51), 446(38), 93(30), 356(28), 148(25), 55(25), 202(25), 81(24))[b]	–		29.24 (0.02)	64.05 (2.07)
29	3197		Cholesterol	–	< LOQ	40.69 (3.40)	44.28 (2.12)
30	3207		Cholestanol	–	13.05 (0.20)		–
31	3249		M+ 460 *m/z* (460(100), 75(45), 255(45), 444(38), 460(35), 213(32), 133(25), 73(25)147(23), 145(23))[b]	89.87 (4.29)	84.65 (4.94)	169.80 (6.09)	–
32	3271	3232 [45]	Ergosterol	64.18 (2.66)	45.96 (0.29)	90.14 (5.02)	65.61 (2.06)
33	3353		M^+ 474 *m/z* (472(100), 214(45), 75(39), 55(38), 91(37), 79(34), 119(33), 57(32), 149(30), 256(29))[c]	–	42.63 (1.23)	70.16 (4.48)	97.60 (1.04)
34	3443		M^+ 488 *m/z* (344(100), 75(80), 256(58), 487(55), 387(49), 93(41), 345(41), 81(36), 55(36), 214(33))[d]	–	22.80 (0.89)	29.25 (4.42)	44.05 (1.60)
35	3454		M^+ 488 *m/z* (344(100), 387(44), 75(38), 345(37), 254(33), 69(28), 55(21), 214(18), 73(18), 93(17))[d]	–	< LOQ	25.71 (3.68)	–
Total				**152.17 (4.29)**	**241.89 (7.04)**	**505.09 (31.95)**	**457.31 (0.14)**

n.i.: not identified.

[a] Quantified as *cis*11-eicosenoic acid.
[b] Quantified as cholesterol.
[c] Quantified as ergosterol.
[d] Quantified as β-sitosterol. RI^{Exp}—Retention Index obtained in this experiments; RI^{Lit}—Retention Index described in literature.

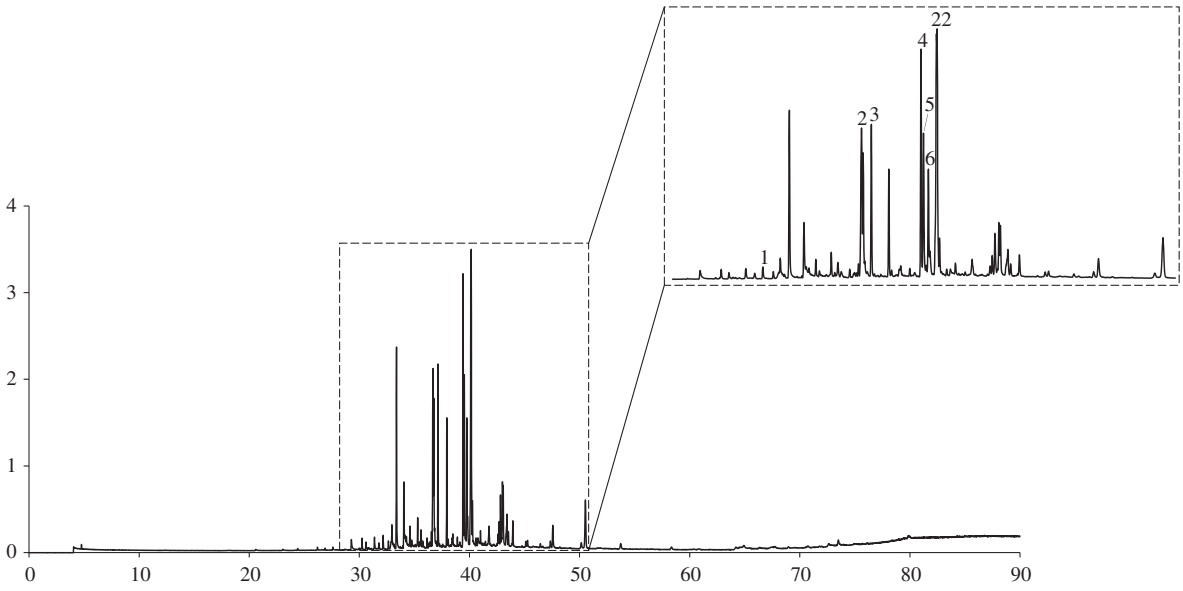

Fig. 2. GC–MS profile of *M. glacialis* using a previously described method [23]. Identity of peaks as in Table 6.

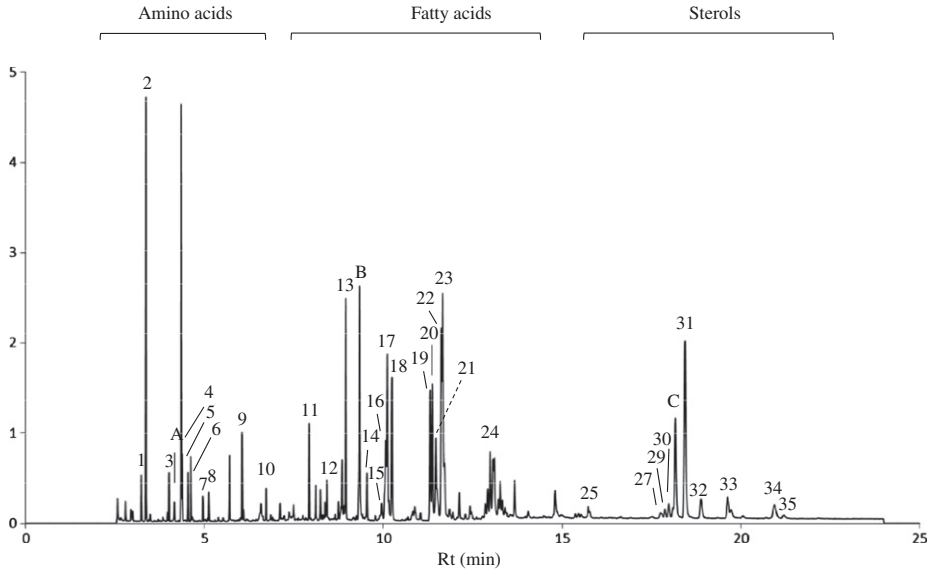

Fig. 3. GC–MS profile of *M. glacialis* using the method developed in this work. Amino acids, fatty acids and sterols are clearly separated in different areas of the chromatogram. Identity of compounds as in Table 6. IS (Internal Standard): A-norvaline, B-methyl linolelaidate, C-desmosterol.

method for the extraction and GC–MS analysis of FAME) [23]. Fig. 2 displays the resulting chromatogram, where it can be seen that, in addition to the absence of amino acids and sterols, only 6 compounds were identified. On the other hand, when the method proposed herein was used, about 16 fatty acids were determined.

Afterwards we used ethanol as extraction solvent, followed by TMS derivatization, in order to verify if the qualitative and quantitative profile would be affected. As shown in Fig. 3, ethanol effectively extracted amino acids, fatty acids and sterols. From a quantitative point of view, the amounts of fatty acids extracted exceeded those obtained with chloroform:methanol (Fig. 4). Water:-ethanol (1:1) was also tested as extraction solvent, but the high lipidic content caused insolubilization in water and, for this reason, this solvent was not used. Given the fact that our ethanol extraction and chromatographic conditions allowed the simultaneous identification of amino acids, fatty acids and sterols, we used them in subsequent studies. In addition, it has the advantage of using a cheap and non-hazard solvent (ethanol). Also, derivatization with MSTFA allows the use of mild temperatures (40 °C), while standard boron trifluoride method requires temperatures around 90 °C [23].

After this point, we studied the effect of the temperature in the extraction efficiency of ethanol: 40 °C, 50 °C and 60 °C were tested. As it can be seen in Fig. 4, extraction at 40 °C was the most effective for amino acids. The highest temperature assayed, 60 °C, resulted in high standard deviation indicating that some loss or reaction took place.

Regarding fatty acids, no major differences were noticed between different temperatures (Fig. 4). In the case of sterols, efficiency of extraction was highly affected by temperature, 40 °C being the most suitable one. After confirming that ethanol at 40 °C with magnetic stirring at 200 rpm was the most effective extraction procedure, we investigated the contribution of ultra-sonication (US) to the total amount of metabolites extracted. Although US clearly increased the level of extracted fatty acids, its low efficiency concerning both sterols and amino acids (Fig. 4) prevented its use and hence, all the

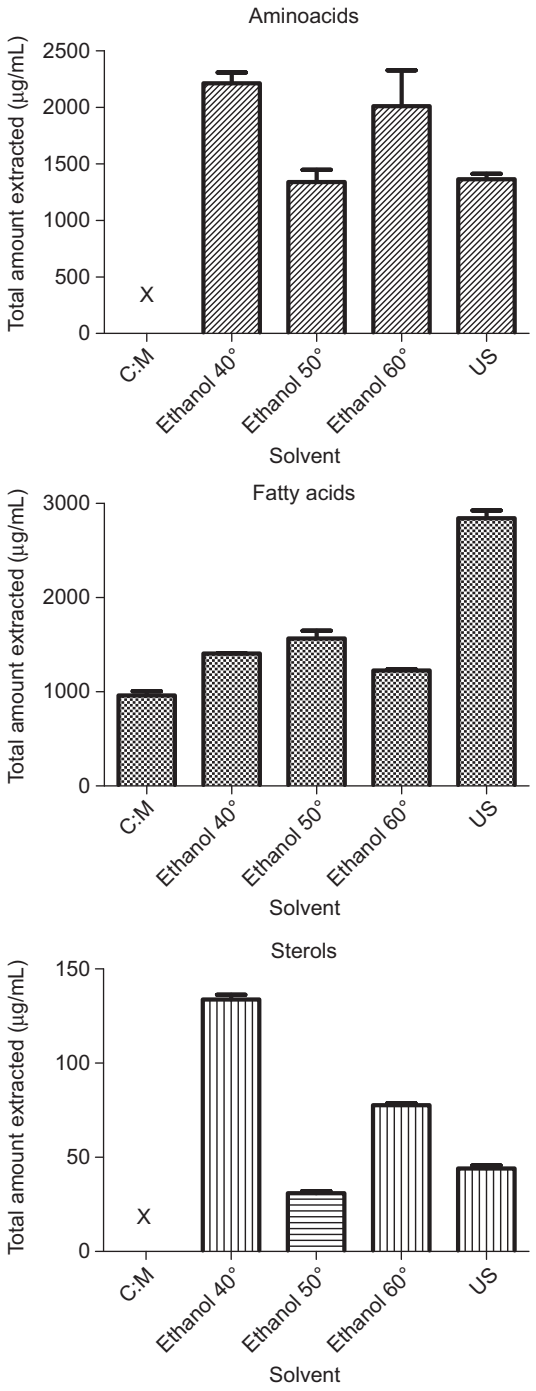

Fig. 4. Comparison of total amounts of amino acids, fatty acids and sterols extracted with different experimental conditions. C:M, chloroform:methanol (2:1); US, ultra-sonication. Data are means ± SD (n=3).

remaining analysis for validation parameters were conducted using ethanol as extraction solvent, at 40 °C, for 20 min, with a magnetic stirrer set at 200 rpm. This procedure represents an advantage when compared with other methods for fatty acids [7], amino acids [4,19] and sterols [5,23] that are time-consuming and employ high temperatures, which can result in the advent of artifacts or loss of analytes.

3.2. Method performance

In this work we developed a method for a quick screening analysis that renders both identification and quantification of three distinct classes of metabolites, useful for routine analysis and comparisons of samples. For this reason, among the several experimental conditions assayed, we selected the one that represented a compromise between the three classes. In this matter, ethanol at a temperature of 40 °C was the one that scored better results for 2 out of 3 classes.

3.2.1. Linearity

The linearity of the method was tested using calibration solutions prepared as described in the Experimental section. Internal standards for each class of compounds were used in order to account for analyte losses and matrix effect. Calibration curves were constructed by plotting the analyte/IS peak areas ratio obtained against the concentration values.

Good linearity for the concentration range studied was obtained for all compounds from the different chemical classes, as can be observed in Table 1, with correlations coefficients higher than 0.9844. Among the three classes, amino acids were those with best results (Table 1).

3.2.2. Recovery, precision and reproducibility

Ideally, all compounds addressed should be tested for recovery values. However, this becomes increasingly harder as the number of metabolites to be analyzed rises. Due to the diversity and complexity of metabolites present, in metabolomics of natural matrices it is not usual to determine the efficiency of the extraction of all of the compounds and the most abundant or more characteristic of each class are selected [26,27]. For this reason, and taking into account that we describe the identification and quantification of over 40 compounds, we decided to use two compounds of each class: isoleucine and *trans*-4-hydroxyproline for amino acids, palmitic acid and arachidonic acid for saturated and unsaturated fatty acids, respectively, and cholesta-3,5-diene and cholestanol for sterols, although we also tested other compounds, for example eicosapentaenoic acid (40 μg/ml—91% recovery; 80 μg/ml—95% recovery and 200 μg/ml—92% recovery) in order to check whether the method was acceptable.

Given the fact that over 15 fatty acids can be analyzed with this method, it is difficult to choose an internal standard that represents all compounds present equally. Furthermore, the fact that about 40 compounds are eluted in a 25 min run turns this issue even more difficult. For this reason, we choose methyl linolelaidate as internal standard for fatty acids as it was not present in the samples and did not co-elutes with any of the compounds.

Table 2 summarizes the results obtained for the analysis, in triplicate, of three concentrations levels. As can be observed, in the case of amino acids best recoveries were obtained for *trans*-4-hydroxyproline when compared to isoleucine. Similar recovery values were obtained for both palmitic and arachidonic acids (higher than 93%). Finally, sterols also showed good recoveries, varying between 92 and 106%.

Results for accuracy and precision can be found in Tables 3–5. The intraday variations (RSD) for the standard compounds ranged from 0.05 to 13.19% (n=3), being generally lower than those of the interday studies. Among the four classes, amino acids presented the smaller variations regarding both accuracy and precision.

3.2.3. Limit of detection and limit of quantification

In general, amino acids were the class yielding the lowest LOD and LOQ. LOD ranged between 0.03 and 2.68 μg/mL, for proline and cysteine, respectively. LOQ varied from 0.11 to 8.92 μg/mL for the same compounds, respectively (Table 1). Recently, a GC–MS method for the analysis of several amino acids was described [28].

That method presented very low detection limits and employed methyl chloroformate derivatization; however, quantification was obtained by applying deuterated derivatization reagents and, for this reason, it can be too expensive for routine screening analysis.

Regarding fatty acids, oleic acid was the compound with lower LOD and LOQ, 0.14 μg/mL and 0.48 μg/mL, respectively. Some recent works report the fatty acids profile of marine organisms [29–32]. Nevertheless, in most cases no complete validation data is available, which renders direct comparison difficult. Furthermore, quantification is frequently presented as percentage and not as absolute amounts [29,31,33,34].

3.3. Profiling of the echinoderm M. glacialis

In 2010 it was possible to collect organisms in the same month from two different sites (Praia do Baleal and Praia da Consolação, samples Fev10-B and Fev10-C, respectively) and, for this reason, direct comparison regarding the influence of geographical origin can be established. Sample Fev10-C presented ca. 80% higher amounts of amino acids than that from Baleal (Fev10-B) (Table 6). A similar trend was found for fatty acids, with organisms from Consolação having 40% more when compared to that of Baleal. Unsaturated fatty acids are major compounds in both samples (Table 6). In the case of sterols, no important changes between both locations were noticed (Fig. 5).

For the study of the influence of the season in the chemical composition, samples from the same geographical origin, Cabo Carvoeiro (samples Jul09-A and Set09-A), were used. Overall, samples from September had higher amounts of sterols and amino acids, with both classes displaying an increase of around 70% when compared to their July homologs (Fig. 5). Glycine was always the compound present in higher amounts (Table 6).

In the case of fatty acids, samples from September displayed a decrease in total amounts of around 35%. Both saturated and unsaturated free fatty acids have been described in echinoderms from Asteroidea, Holothuroidea and Echinoidea [35–37]. In the case of sea stars, palmitic acid is frequently the compound present in higher amounts, which may constitute a defense mechanism given its antifouling properties [36]. Our results show that in the case of *M. glacialis* this is only true for samples collected in July and September. As it can be seen in Table 6, in samples collected in February arachidonic acid was the major compound, far exceeding palmitic acid. It should be highlighted that among all samples studied, unsaturated fatty acids were present in higher amounts than saturated ones (Table 6).

Regarding sterols and lupanes, there was a clear distinction between samples from February and July/September, with the former displaying higher amounts of sterols and also greater diversity. Compounds 26 and 28 were found solely in organisms from February (Table 6). Ergosterol was the only compound present in all analyzed samples, while β-sitosterol, fucosterol, betulin, lupeol and lupeol acetate could not be found in any of them. However, a compound similar to β-sitosterol (34) was present in all samples, excepting in sample Jul09-A. In fact, when analyzing sterols we found several compounds whose mass spectra closely resembled those of cholesterol (compounds 26, 27 and 28), ergosterol (33) and β-sitosterol (compounds 34 and 35). We compared the mass fragmentation of these unknowns with some published MS data for sterols, such as brassicasterol, ergosta-7,22-dienol, ergosta-5,7-dienol, ergosta-7-enol [38], but no matches were found.

Apart from the interest of these metabolites for their bioactivity, the knowledge of the composition of these organisms can also be exploited from a chemico-ecological point of view. For instance, in the case of fatty acids most animals are unable to synthesize longer chain polyunsaturated fatty acids, such as EPA and DHA, obtaining them by preying on organisms from lower trophic levels, like bacteria and phytoplankton [31,39]. The same trend can be found in the case of sterols, which are synthesized by algae and plants [40].

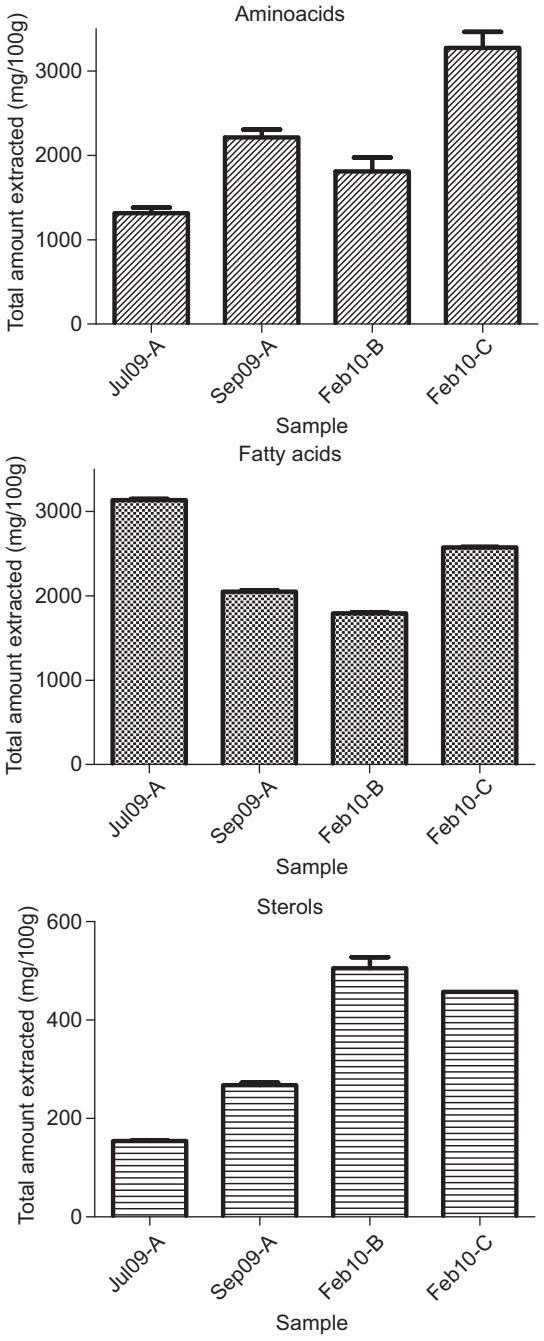

Fig. 5. Comparison of total amounts of amino acids, fatty acids and sterols in different *M. glacialis* samples. Data are means ± SD (n=3).

4. Conclusions

In this work, we report a GC–MS method for metabolite profiling of extracts of marine organisms. This approach constitutes a fast and powerful option for the identification and quantification of amino acids, fatty acids, sterols and lupanes in marine organisms. The extraction procedure is simple and

employs ethanol at mild temperatures, thus preventing degradation of sample or the production of artifacts. Since no purification or pre-treatment of samples are required the loss of analytes is minimized. The extraction method and the analytical method here developed appear to be good analytical tools available to researchers, for other matrices than marine organisms containing amino acids, fatty acids, sterols and lupanes.

Acknowledgments

This work has been supported by the Fundação para a Ciência e a Tecnologia (FCT) through grant no. PEst-C/EQB/LA0006/2011. David M. Pereira is grateful to FCT for the grant (SFRH/BD/62663/2009).

Appendix A. Supporting information

Supplementary data associated with this article can be found in the online version at http://dx.doi.org/10.1016/j.talanta.2012.08.004.

Appendix. Supporting information

References

[1] I. Bonaduce, M. Cito, M.P. Colombini, J. Chromatogr. A 1216 (2009) 5931–5939.
[2] K.N. Jom, T. Frank, K.H. Engel, Metabolomics 7 (2011) 102–117.
[3] S. Kim, M.H. Shin, M.A. Hossain, E.J. Yun, H. Lee, K.H. Kim, Anal. Bioanal. Chem. 399 (2011) 3519–3528.
[4] D.S. Wishart, Trends Food Sci. Tech. 19 (2008) 482–493.
[5] M. Virot, V. Tomao, G. Colnagui, F. Visinoni, F. Chemat, J. Chromatogr. A 1174 (2007) 138–144.
[6] B. Jansen, K.G.J. Nierop, M.C. Kotte, P. de Voogt, J.M. Verstraten, Appl. Geochem. 21 (2006) 1006–1015.
[7] R.B. Johnson, H.J. Barnett, Aquaculture 216 (2003) 263–282.
[8] R.M. Couto, J. Fernandes, M.D.R.G. da Silva, P.C. Simoes, J. Supercritical Fluid 51 (2009) 159–166.
[9] D. Saraiva, R. Semedo, C. Castilho Mda, J.M. Silva, F. Ramos, J Chromatogr. B Anal. Technol. Biomed. Life Sci. 879 (2011) 3806–3811.
[10] C. Schummer, O. Delhomme, B.M. Appenzeller, R. Wennig, M. Millet, Talanta 77 (2009) 1473–1482.
[11] D.M. Pereira, P.B. Andrade, J. Vinholes, G. Correia-da-Silva, P. Valentão, N. Teixeira, Curr. Pharm. Anal. 7 (2011) 108–119.
[12] V.M. Dembitsky, M. Srebnik, Prog. Lipid Res. 41 (2002) 315–367.
[13] C. Djerassi, W.K. Lam, Acc. Chem. Res. 24 (1991) 69–75.
[14] G.L. Wei, E.Y. Zeng, TrAC–Trend Anal. Chem. 30 (2011) 1429–1436.
[15] J. Giacometti, A. Milosevic, C. Milin, J. Chromatogr. A 976 (2002) 47–54.
[16] E. Boselli, M.F. Caboni, A.G. Sabatini, G.L. Marcazzan, G. Lercker, Apidologie 34 (2003) 129–137.
[17] V.A. Isidorov, A.G. Isidorova, L. Szczepaniak, U. Czyżewska, Food Chem. 115 (2009) 1056–1063.
[18] I. Molnar-Perl, J. Chromatogr. A 891 (2000) 1–32.
[19] A.P. Oliveira, D.M. Pereira, P.B. Andrade, P. Valentão, C. Sousa, J.A. Pereira, A. Bento, M.A. Rodrigues, R.M. Seabra, B.M. Silva, J. Agric. Food Chem. 56 (2008) 5216–5221.
[20] F. Igarashi, J. Hikiba, M.H. Ogihara, T. Nakaoka, M. Suzuki, H. Kataoka, Anal. Biochem. 419 (2011) 123–132.
[21] G. Lopes, C. Sousa, J. Bernardo, P.B. Andrade, P. Valentão, F. Ferreres, T. Mouga, J. Phycol. 47 (2011) 1210–1218.
[22] J. Porschmann, J. Plugge, R. Toth, J. Chromatogr. A 909 (2001) 95–109.
[23] B. Ribeiro, P.G. de Pinho, P.B. Andrade, P. Baptista, P. Valentão, Microchem. J. 93 (2009) 29–35.
[24] J. Folch, M. Lees, G.H.S. Stanley, J. Biol. Chem. 226 (1957) 497–509.
[25] FDA, in, 2000, pp. 752–777.
[26] M. Rodriguez-Palmero, M.C. Lopez-Sabater, A.I. Castellote-Bargallo, M.C. De la Torre-Boronat, M. Rivero-Urgell, J. Chromatogr. A 778 (1997) 435–439.
[27] S.N. Tan, J.W. Yong, C.C. Teo, L. Ge, Y.W. Chan, C.S. Hew, Talanta 83 (2011) 891–898.
[28] H.F. Kvitvang, T. Andreassen, T. Adam, S.G. Villas-Boas, P. Bruheim, Anal. Chem. 83 (2011) 2705–2711.
[29] M. Aydin, H. Sevgili, B. Tufan, Y. Emre, S. Kose, Int. J. Food Sci. Tech. 46 (2011) 500–508.
[30] T. Dincer, S. Cakli, Crit. Rev. Food Sci. 47 (2007) 21–26.
[31] J.C. Drazen, C.F. Phleger, M.A. Guest, P.D. Nichols, Comp. Biochem. Phys. B 151 (2008) 79–87.
[32] I. Martínez-Pita, F.J. García, M.L. Pita, J. Shellfish Res. 29 (2010) 517–525.
[33] J. Wen, C. Hu, S. Fan, J. Sci. Food Agric. 90 (2010) 2469–2474.
[34] S. Zlatanos, K. Laskaridis, A. Sagredos, Int. J. Food Sci. Tech. 44 (2009) 1590–1594.
[35] J.C. Drazen, C.F. Phleger, M.A. Guest, P.D. Nichols, Comp. Biochem. Physiol. B Biochem. Mol. Biol. 151 (2008) 79–87.
[36] J. Guenther, A.D. Wright, K. Burns, R. De Nys, Mar. Ecol.—Prog. Ser. 385 (2009) 137–149.
[37] S. Zlatanos, K. Laskaridis, A. Sagredos, Int. J. Food Sci. Tech. 44 (2009) 1590–1594.
[38] K.M. Phillips, D.M. Ruggio, R.L. Horst, B. Minor, R.R. Simon, M.J. Feeney, W.C. Byrdwell, D.B. Haytowitz, J. Agric. Food Chem. 59 (2011) 7841–7853.
[39] J.K. Volkman, S.W. Jeffrey, P.D. Nichols, G.I. Rogers, C.D. Garland, J. Exp. Mar. Biol. Ecol. 128 (1989) 219–240.
[40] J.K. Volkman, Appl. Microbiol. Biotechnol. 60 (2003) 495–506.
[41] T. Shepherd, G. Dobson, S.R. Verrall, S. Conner, D.W. Griffiths, J.W. McNicol, H.V. Davies, D. Stewart, Metabolomics 3 (2007) 475–488.
[42] E.H. Meyer, T. Tomaz, A.J. Carroll, G. Estavillo, E. Delannoy, S.K. Tanz, I.D. Small, B.J. Pogson, A.H. Millar, Plant Physiol. 151 (2009) 603–619.
[43] NIST, in, 2011.
[44] V.A. Isidorov, V.T. Vinogorova, Z. Naturforsch. C 58 (2003) 355–360.
[45] N.S. Radulovic, N.D. Dordevic, J. Serbian Chem. Soc. 76 (2011) 1471–1483.

Paper 4

Amino acids, fatty acids and sterols profile of some marine organisms from Portuguese waters

David M. Pereira, *Patrícia Valentão, Natércia Teixeira, Paula B. Andrade*

Food Chemistry, 2013, 141, 2412–2417

Food Chemistry 141 (2013) 2412–2417

Contents lists available at SciVerse ScienceDirect

Food Chemistry

journal homepage: www.elsevier.com/locate/foodchem

Amino acids, fatty acids and sterols profile of some marine organisms from Portuguese waters

David M. Pereira [a], Patrícia Valentão [a], Natércia Teixeira [b,c], Paula B. Andrade [a,*]

[a] REQUIMTE/Laboratório de Farmacognosia, Departamento de Química, Faculdade de Farmácia, Universidade do Porto, Rua de Jorge Viterbo Ferreira n.° 228, 4050-313 Porto, Portugal
[b] Laboratório de Bioquímica, Departamento de Ciências Biológicas, Faculdade de Farmácia, Universidade do Porto, Rua de Jorge Viterbo Ferreira n.° 228, 4050-313 Porto, Portugal
[c] IBMC – Instituto de Biologia Molecular e Celular, Universidade do Porto, 4150-180 Porto, Portugal

ARTICLE INFO

Article history:
Received 17 January 2013
Received in revised form 11 March 2013
Accepted 26 April 2013
Available online 10 May 2013

Keywords:
Paracentrotus lividus
Holothuria forskali
Aplysia spp.
Amino acids
Fatty acids
Sterols

ABSTRACT

Marine organisms have been increasingly regarded as good sources of new drugs for human therapeutics and also as nutrients for human diet. The amino acids, fatty acids and sterols profiles of the widely consumed echinoderms *Paracentrotus lividus* Lamarck (sea urchin), *Holothuria forskali* Chiaje (sea cucumber), the gastropod molluscs *Aplysia fasciata* Poiret and *Aplysia punctata* Cuvier (sea hares), from Portuguese waters, were established by GC–MS analysis. Overall, 10 amino acids, 14 fatty acids and 4 sterols were determined. In general, all species presented the 10 amino acids identified, with the exceptions of *H. forskali*, in which no glycine, proline, *trans*-4-hydroxy-proline or phenylalanine were found, and of *A. fasciata* which did not contain proline. Unsaturated fatty acids were predominant compounds, with those from the ω-6 series, being in higher amounts than their ω-3 homologues, and cholesterol being the main sterol. The amino acids, fatty acids and sterols qualitative and quantitative composition of *A. fasciata, A. punctata* and *H. forskali* is reported here for the first time.

1. Introduction

Marine organisms have been increasingly regarded as a promising source of new bioactive molecules for the pharmaceutical industry. In addition, many echinoderms and molluscs are regarded as excellent sources of nutritionally important compounds, such as fatty acids (Latyshev, Kasyanov, Kharlamenko, & Svetashev, 2009; Ozogul, Duysak, Ozogul, Özkütük, & Türeli, 2008; Usydus, Szlinder-Richert, Adamczyk, & Szatkowska, 2011), amino acids (Hamdi, 2011; Xu, Yan, & Xu, 2012; Zarai et al., 2011) and sterols (Kanazawa, 2001; Kandyuk, 2006; Zhukova, 2007).

Fatty acids are essential for life, due to their pivotal role as a source of energy, membrane constituents, as well as metabolic and signalling mediators. Compounds with two or more double bonds are named polyunsaturated fatty acids (PUFA) and the position of the first double bound is given by the (*n*–*x*) notation, counting the number of carbon atoms from the methyl group (the ω end). A review on the chemistry and distribution of fatty acids, in marine animals, was recently published (Pereira et al., 2011). Due to their positive impact on human health, alternative sources of PUFA are being pursued, with marine sources being increasingly regarded as good alternatives. Within PUFA, ω-3 compounds are particularly relevant, as they have already proved to have a positive impact on human health (Miles, Banerjee, & Calder, 2004; Miles & Calder, 2012; Rees et al., 2006). For example, ω-3 fatty acids have been shown to ameliorate some inflammatory conditions (Calder, 2008) and to improve cardiovascular status (Cawood et al., 2010; Studer, Briel, Leimenstoll, Glass, & Bucher, 2005).

Amino acids are determinant metabolites in the homeostasis of an organism, mainly due to their role as protein building blocks, in the regulation of several cellular processes and also as precursors of other molecules, such as hormones and nitrogenous bases (Wu, 2009). Given the fact that some of these compounds (essential amino acids) cannot be synthesised by humans, a diet rich in this class of metabolites is mandatory for a healthy organism.

The term sterol refers to a compound with a fused cyclopentanophenanthrene ring with a 3-hydroxyl moiety. These compounds have been regarded to have a positive impact on human health, mainly due to their hypocholesterolemic activity, that arises from their marked similarity with cholesterol, thus competing for absorption (Plat et al., 2012; Vanstone, Raeini-Sarjaz, Parsons, & Jones, 2002;Ostlund, 2002).

In a previous work, we have developed a method for the simultaneous determination of several classes of metabolites in marine organisms, including amino acids, fatty acids and sterols (Pereira et al., 2012). In the present work, four macro invertebrates were analysed. The metabolic profile of two molluscs (*Aplysia fasciata* Poiret and *Aplysia punctata* Cuvier) is reported here for the first time. Two echinoderms, *Holothuria forskali* Chiaje and

* Corresponding author. Tel.: +351 220428654; fax: +351 226093390.
E-mail address: pandrade@ff.up.pt (P.B. Andrade).

0308-8146/$ - see front matter © 2013 Elsevier Ltd. All rights reserved.
http://dx.doi.org/10.1016/j.foodchem.2013.04.120

Paracentrotus lividus Lamarck, were also studied and the metabolic profile of the former is described here for the first time; some studies are available regarding the latter (Arafa, Chouaibi, Sadok, & El Abed, 2012; Martínez-Pita, García, & Pita, 2010; Mol, Baygar, Varlik, & Tosun, 2008), but, to our knowledge, no absolute quantification has been reported. These echinoderms are consumed worldwide (Andrew et al., 2002; FAO, 2008) and a detailed knowledge of their chemical composition is needed.

2. Material and methods

2.1. Standards and reagents

Nonanoic acid (⩾99%), decanoic acid (⩾99%), lauric acid (⩾95%), myristic acid (⩾99%), pentadecanoic acid (⩾99%), palmitic acid (⩾99%), margaric acid (⩾98%), stearic acid (⩾99%), arachidonic acid (⩾99%), linolenic acid (⩾99%), methyl linolelaidate (⩾99%), oleic acid (⩾99%), 5,8,11,14,17-eicosapentaenoic acid (EPA) (⩾99%), *cis*-11,14-eicosadienoic acid (⩾98%), *cis*-11-eicosaenoic acid (⩾99%), docosahexaenoic acid (DHA) (⩾98%), arachidic acid (⩾97%), arginine (⩾98%), asparagine (⩾98%), aspartic acid (⩾98%), cysteine (⩾98%), glutamic acid (⩾98%), glutamine (⩾98%), histidine (⩾98%), lysine (⩾98%), methionine (⩾98%), tryptophan (⩾98%), tyrosine (⩾98%), alanine (⩾98%), glycine (⩾99%), valine (⩾98%), leucine (⩾98%), isoleucine (⩾98%), proline (⩾99%), serine (⩾99%), threonine (⩾98%), *trans*-4-hydroxy-proline (⩾98%), phenylalanine (⩾98%), norvaline (⩾99%), cholestan-3,5-diene (⩾95%), 5-α-cholestan-3-ol (⩾95%), cholestanol (⩾99%), ergosterol (⩾95%), β-sitosterol (⩾97%), desmosterol (⩾85%) and *N*-methyl-*N*-(trimethylsilyl) trifluoroacetamide (MSTFA) were from Sigma and ethanol was from Panreac.

2.2. Organisms

Samples were from Portuguese waters: *H. forskali* and *P. lividus* were collected in the area of Peniche (west Portugal coast), in September 2009; *A. fasciata* was collected in October, 2009 and *A. punctata* in July, 2010, both in the Óbidos lagoon (Foz do Arelho). Specimens were placed on ice and transported to the laboratory. The organisms were then cleaned and washed with sea water. In the case of *P. lividus*, individuals were cracked and the coelomic fluid and gonads collected. Samples were kept at −20 °C, prior to freeze-drying in a Labconco 4.5 Freezone apparatus (Kansas City, MO, USA). The dried material was powdered and sifted (<910 μm) before extraction. Each sample corresponds to a mixture of 2–4 individuals.

2.3. Metabolites extraction

Each sample (100 ± 1.00 mg) was transferred to a glass vial and the internal standards for amino acids (norvaline), fatty acids (methyl linolelaidate) and sterols (desmosterol) were added. The volume was then made up to 2 ml with ethanol. The mixture was stirred at 200 rpm, for 20 min, at 40 °C. The extract was filtered and 50 μl was transferred to a glass vial. The solvent was evaporated under a nitrogen stream and 50 μl of the derivatization reagent, MSTFA, was added to the residue. The vial was capped, vortexed and heated for 20 min in a dry block heater, maintained at 40 °C. All extractions and analysis were performed in triplicate.

2.4. GC–MS analysis

The GC–MS conditions used herein were the ones used by Pereira et al. (2012). A Varian CP-3800 gas chromatograph coupled to a Varian Saturn 4000 mass selective ion trap detector (USA) and a Saturn GC/MS workstation software version 6.8 was used, with a VF-5 ms (30 m × 0.25 mm × 0.25 μm) column (VARIAN). A CombiPAL automatic autosampler (Varian, Palo Alto, CA) was used for all experiments. The injector port was heated to 250 °C and the injections were performed in split mode, with a ratio of 1/40. The carrier gas was helium C-60 (Gasin, Portugal), at a constant flow of 1 ml/min. The Ion Trap detector was set as follows: transfer line, manifold and trap temperatures were 280, 50, and 180 °C, respectively. The mass ranged from 50 to 600 *m*/*z*, with a scan rate of 6 scan/s. The emission current was 50 μA and the electron multiplier was set in relative mode to an auto tune procedure. The maximum ionisation time was 25.000 μs, with an ionisation storage level of 35 *m*/*z*. The injection volume was 2 μl and the analysis was performed in Full Scan mode. The oven temperature was set at 100 °C for 1 min, then increasing 20 °C/min to 250 °C, held for 2 min, 10 °C/min to 300 °C and held for 10 min. All mass spectra were acquired in the electron impact (EI) mode. Identification of compounds was achieved by comparison of their mass spectra, with those from pure standards analysed under the same conditions, and from the NIST05 MS Library Database.

For quantification purposes, each sample was injected in triplicate and the amount of metabolites was determined from the calibration curves of the respective trimethylsilyl (TMS) standards. All compounds were quantified in Full Scan mode, with the exception of linoleic (*m*/*z* 262, 337 and 352), linolenic (*m*/*z* 191, 335 and 350) and oleic (*m*/*z* 264, 339 and 354) acids that were quantified, by the area obtained from the re-processed chromatogram, using the characteristic *m*/*z* fragments.

3. Results and discussion

The technique used in this study was first validated with the echinoderm *Marthasterias glacialis* L. (Pereira et al., 2012). For this reason, in our work, recovery experiments for the analysed species were conducted (Table 1). Representative compounds of the three classes studied were used: isoleucine (amino acids), hexadecanoic acid (fatty acids) and 5-α-cholestan-3-ol (sterols). Two different concentrations were tested, one lower and the other higher, and the values of recovery were in the ca. 89–117% range, with the exception of the lower concentration of hexadecanoic acid in *H. forskali*, which corresponded to ca. 65%. However, this low value of recovery was found solely for *H. forskali* and for this particular compound, which could be a consequence of a matrix effect and not be related to the technique itself. Recovery for isoleucine was in the range ca. 93–112% and 5-α-cholestan-3-ol was ca. 92–117%.

3.1. Amino acids

The majority of the 10 amino acids detected (Fig. 1), could be found in all samples, with the exception of glycine, *trans*-4-hydroxy-proline and phenylalanine, which were not detected in *H. forskali*, and of proline which was not found in neither this species or in *A. fasciata* (Table 2). *A. punctata* contained the highest amount of amino acids, followed by *P. lividus* (Table 2).

In both *Aplysia* species and in *H. forskali* the major amino acid was alanine, which accounted for over 49% of the determined amino acids. In contrast to this, in the echinoderm *P. lividus* glycine was the major amino acid (Table 2), a trend that has already been reported in the echinoderm *M. glacialis*, collected in different seasons and in locations similar to those of the sample used herein (Pereira et al., 2012).

Threonine was the amino acid present in lower amounts in *Aplysia* sp., whilst in the echinoderms *P. lividus* and *H. forskali*, phenylalanine and valine were the minor amino acids, respectively (Table 2).

Table 1
Recovery values (%) ± standard deviation obtained for representative compounds of amino acids, fatty acids and sterols.

Compound	Concentration, μg/ml	Mollusca	Echinodermata	
		A. punctata	*H. forskali*	*P. lividus*
Isoleucine	1.66	93.7 ± 6.8	94.5 ± 1.2	99.9 ± 0.6
	18.8	92.9 ± 1.7	113 ± 4.0	112 ± 5.8
Hexadecanoic acid	15.9	95.6 ± 8.6	64.6 ± 14.3	104 ± 3.7
	110	117 ± 10.3	98.9 ± 2.3	88.6 ± 1.9
5-α-Cholestan-3-ol	7.41	117 ± 10.7	107 ± 15.1	98.9 ± 0.1
	34.1	92.3 ± 1.5	92.3 ± 1.4	96.8 ± 8.7

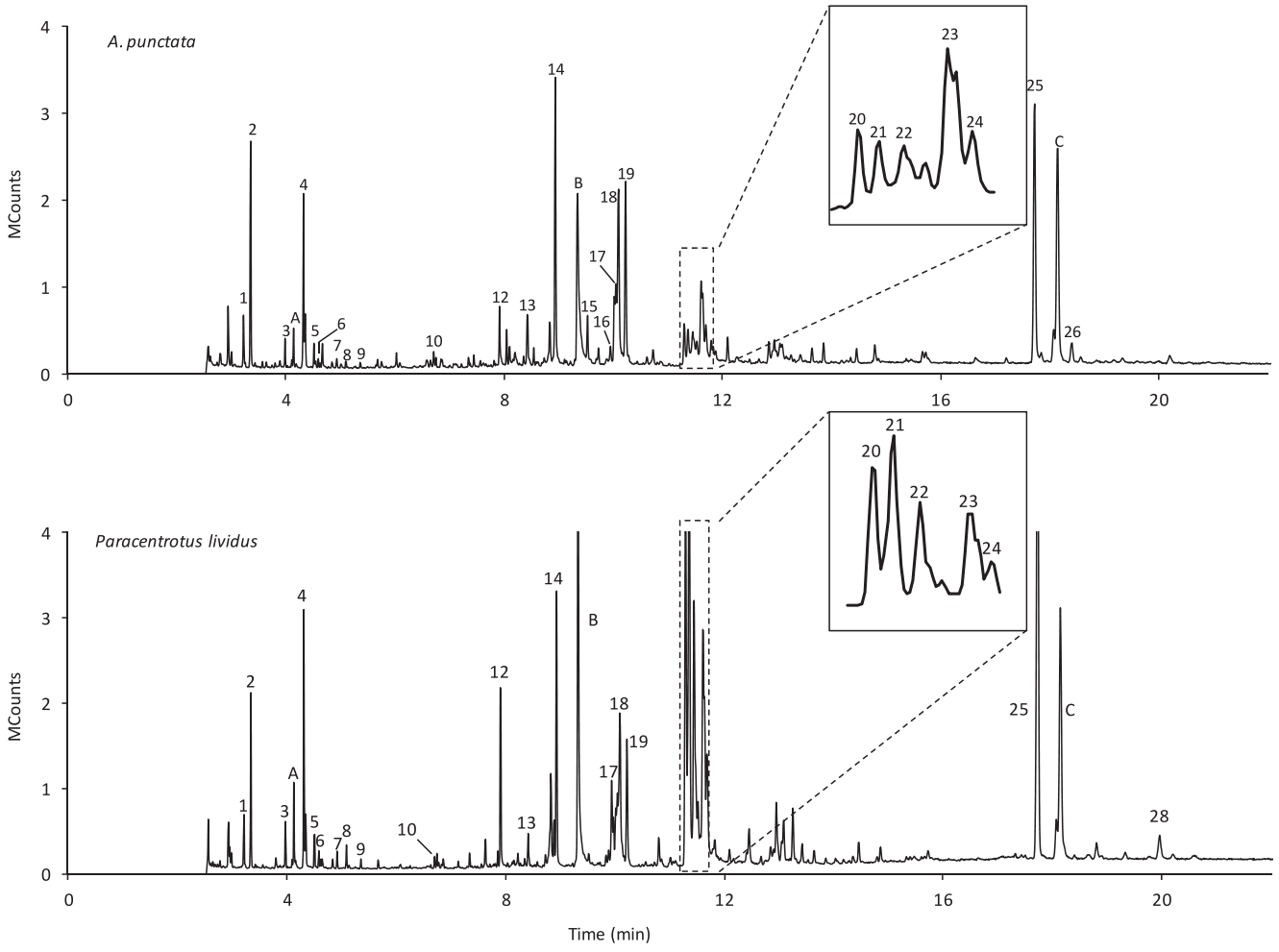

Fig. 1. GC–MS profile of *A. punctata* and *P. lividus*. Peak identification as in Tables 2 and 3. A, norvaline; B, methyl linolelaidate; C, desmosterol.

3.2. Fatty acids

Regarding fatty acids, amongst all species studied, 14 compounds were identified and 12 of them could be quantified (Fig. 1, Table 2).

Differences between the four analysed species were found. *A. punctata*, *P. lividus* and *H. forskali* displayed higher amounts of unsaturated fatty acids when compared with saturated derivatives. In contrast to this, in *A. fasciata* saturated fatty acids exceeded unsaturated ones. In all samples, ω-6 fatty acids were predominant comparatively to ω-3 compounds (Fig. 2). *P. lividus* was the species with higher amounts of fatty acids, and also with the highest unsaturated/saturated compounds ratio (Fig. 2, Table 2). *H. forskali* was the species with the lowest fatty acids content.

Some work regarding the identification and quantification of saturated fatty acids in sea cucumbers is available (Aydin, Sevgili, Tufan, Emre, & Kose, 2011), although none addressed the species studied herein (*H. forskali*). Aydin et al. (2011) evaluated the fatty acids composition of *Holothuria tubulosa* Gmelin, *Holothuria poli* Delle Chiaje and *Holothuria mammata* Grube, and found that palmitic and stearic acids, were the saturated fatty acids present in higher levels. The results were expressed as a percentage and no absolute quantification was reported. Our results confirmed this trend in *H. forskali* (Table 2). Regarding unsaturated fatty acids, we found that *cis*-11-eicosaenoic and arachidonic acids were the two compounds present in higher quantities in *H. forskali* (Table 2). The former is not reported in *H. tubulosa*, *H. poli* and *H. mammata*; however, it has been described before in *Holothuria fuscogilva*

Table 2
Primary metabolites in Mollusca and Echinodermata species analysed in this work (mg/100 g).[a]

Peak		Compound	Mollusca				Echinodermata			
			A. fasciata		*A. punctata*		*H. forskali*		*P. lividus*	
			Mean	STD	Mean	STD	Mean	STD	Mean	STD
		Amino acids								
1		Alanine	340	46.0	353	30.6	181	22.9	199	41.8
2		Glycine	71.1	4.59	98.5	0.10	–	–	323	14.0
3		Valine	35.5	2.81	19.7	1.90	7.74	0.91	15.9	0.14
4		Leucine	46.3	6.51	50.0	1.27	68.7	2.26	29.3	5.49
5		Isoleucine	17.0	0.29	17.5	2.82	14.7	2.61	18.3	2.00
6		Proline	–	–	19.8	2.42	–	–	22.1	12.8
7		Serine	33.5	2.26	37.0	2.42	31.7	0.17	41.9	7.71
8		Threonine	9.92	1.36	16.2	1.00	7.87	1.49	18.2	0.40
9		*trans*-4-Hydroxy-proline	26.2	1.81	68.5	11.1	–	–	18.1	0.40
10		Phenylalanine	27.8	6.34	34.3	8.04	–	–	10.9	0.60
		Total	608	54.1	714	30.2	311	25.9	697	82.3
		Fatty acids								
11	12:0	Dodecanoic	–	–	–	–	<LoQ	–	–	–
12	14:0	Tetradecanoic	<LoQ	–	<LoQ	–	<LoQ		144	17.0
13	15:0	Pentadecanoic	61.1	1.07	49.6	5.36	<LoQ	–	<LoQ	–
14	16:0	Palmitic	136	2.48	152	1.60	69.1	0.45	155	16.5
15	17:0	Heptadecanoic	24.9	1.46	15.7	0.54	–	–	<LoQ	–
16	18:2	Linoleic	<LoQ	–	<LoQ	–	–	–	<LoQ	–
17	18:3	Linolenic	44.6	1.23	44.6	1.23	–	–	29.4	0.81
18	19:1	Oleic	19.0	1.18	30.9	1.20	16.8	0.32	31.8	3.63
19	18:0	Stearic	55.5	1.84	91.8	0.66	50.4	10.0	60.1	2.07
20	20:4	Arachidonic	59.5	5.00	76.2	4.50	81.0	8.32	296	23.2
21	20:5	5,8,11,14,17-Eicosapentaenoic	<LoQ	–	42.4	1.95	<LoQ	–	229	17.1
22	20:2	*cis*-11,14-Eicosadienoic	64.0	5.45	83.7	8.42	<LoQ	–	199	13.4
23	20:1	*cis*-11-Eicosaenoic	84.3	5.86	153	11.2	83.4	4.04	105	2.91
24	22:6	Docosahexaenoic	<LoQ	–	63.5	0.96	<LoQ	–	56.4	2.28
		Total	529	9.62	711	12.2	301	14.4	1375	140

[a] Compounds listed correspond to their TMS derivatives and quantification results from three determinations. STD: standard deviation. LoQ: Limit of quantification.

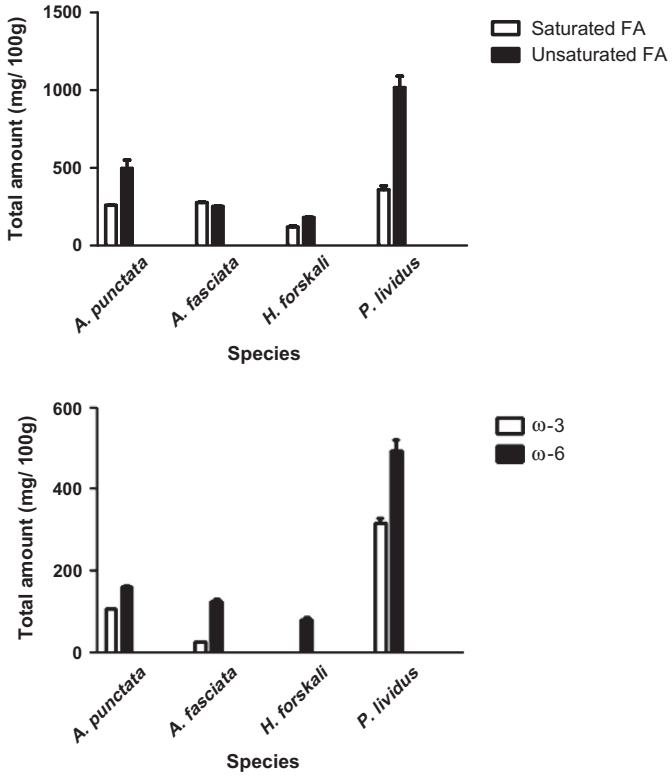

Fig. 2. Ratio of saturated/unsaturated fatty acids and ω-3/ω-6 compounds in the studied species.

Cherbonnier and in *Holothuria fuscopunctata* Jaeger, although it was found not to be the major compound (Wen, Hu, & Fan, 2010). In the case of arachidonic acid, the available studies point this compound as the predominant unsaturated fatty acid, in all of the above-mentioned species (Aydin et al., 2011; Wen et al., 2010).

To our knowledge, the work presented herein is the first to address the absolute quantification of fatty acids in *P. lividus*. Previous work concerning the fatty acid composition of this species, collected in several locations, described palmitic, stearic and tetradecanoic acids as the predominant saturated fatty acids (Kalogeropoulos, Mikellidi, Nomikos, & Chiou, 2012; Zlatanos, Laskaridis, & Sagredos, 2009). Other studies, focused on the influence of the season on the fatty acids composition of this organism, found that although the proportion of unsaturated/saturated fatty acids varied during the year, the major compounds were usually the same and indicated tetradecanoic and palmitic acids as the major saturated fatty acids (Arafa et al., 2012; Mol et al., 2008). We have confirmed this trend in our samples, collected in the Atlantic sea, along the coast of Portugal.

Regarding the unsaturated fatty acids, we found arachidonic, EPA and cis-11,14-eicosadienoic acids to be the predominant compounds in *P. lividus*. Whilst a number of studies are in harmony with these results (Arafa et al., 2012; Kalogeropoulos et al., 2012), EPA was found to be the major compound in a study carried out by Mol et al. (2008), but no arachidonic acid was reported. Instead, oleic and 13,16-docosadienoic acids were found to be the major unsaturated fatty acids.

Little is known about the chemical composition of the species from the *Aplysia* genus. Some bioactive compounds have been characterised (Ortega, Zubía, & Salvá, 1997; Spinella et al., 1992), but, as far as we are aware, the fatty acids composition of *A. fasciata*

Table 3
Sterols in Mollusca and Echinodermata species analysed in this work (mg/100 g).[a]

Peak	Compound	Molluska				Echinodermata			
		A. fasciata		*A. punctata*		*H. forskali*		*P. lividus*	
		Mean	STD	Mean	STD	Mean	STD	Mean	STD
25	Cholesterol	177	11.8	202	7.55	<LoQ	–	400	48.1
26	Cholesterol derivative[b]	–	–	26.4	3.75	–	–	–	–
27	Choleste-7-ene-3-ol	–	–	–	–	<LoQ	–	–	–
28	β-Sitosterol	–	–	–	–	–	–	17.7	1.72
	Total	177	11.8	228	3.80	–	–	418	49.8

[a] Compounds listed correspond to their TMS derivatives and quantification results from three determinations. STD: standard deviation. LoQ: limit of quantification.
[b] Tentatively identified based on its mass fragmentation.

and *A. punctata* has not been addressed before. The chromatographic profile of these two species revealed a marked similarity, both from qualitative and quantitative points of view. Fatty acids were present in higher amounts in *A. punctata*, although in both species, palmitic acid was the main saturated fatty acid and cis-11-eicosaenoic acid the predominant unsaturated fatty acid (Table 2).

3.3. Sterols

In the past few years, the chemistry of marine sterols has grown steadily, with the identification of several compounds with remarkable chemical diversity. Over 200 "classical" sterols, displaying a 3β-hydroxy-Δ5-cholestane nucleus and a C8–C10 side chain, have been described (Goad, 1978). New classes of compounds have been reported, remarkably in sponges (Sarma, Sri Rama Krishna, & Ramakrishna Rao, 2005). Sterols are widespread compounds in marine organisms due to their biological importance, namely as components of membranes, but also as a chemical defence against predation and environmental conditions (Bernsdorff & Winter, 2003; Chen & Tripp, 2012; Edidin, 2003).

In general, only cholesterol, β-sitosterol and one cholesterol derivative could be quantified in the analysed species. One minor compound, choleste-7-ene-3-ol, was found in *H. forskali* (Fig. 1, Table 3). The species with the highest sterols content was *P. lividus*.

Many other compounds were searched, including ergosterol and its derivatives, stigmasterol, campsterol and other cholesterol derivatives, though none could be found. The presence of high amounts of cholesterol, in marine organisms, has been proved to constitute a chemical defence, due to the antifouling properties of this compound (Guenther, Wright, Burns, & de Nys, 2009).

4. Conclusion

The amino acids, fatty acids and sterols composition of two molluscs and two echinoderms has been investigated. Twenty-eight compounds were identified and quantified. To our knowledge, this is the first report on the amino acids and fatty acids composition of *Aplysia* spp. and *H. forskali*. Regarding *P. lividus*, our data confirms most of the compounds identified previously and, in addition to this, we provide the first quantification of these compounds.

This work shows that these species may constitute alternative sources of molecules, with nutritional and biomedical interest. In particular, the species presented herein can be interesting candidates to be part of diets rich in amino acids and polyunsaturated fatty acids.

Acknowledgements

This work has been supported by Fundação para a Ciência e a Tecnologia (FCT) through grant No. PEst-C/EQB/LA0006/2011. David M. Pereira is grateful to FCT for the grant (SFRH/BD/62663/2009).

References

Andrew, N. L., Agatsuma, Y., Ballesteros, E., Bazhin, A. G., Creaser, E. P., Barnes, D. K. A., et al. (2002). Status and management of world sea urchin fisheries. In R. N. Gibson, M. Barnes, & R. J. A. Atkinson (Eds.). *Oceanography and marine biology – An annual review* (Vol. 40, pp. 343–425). CRC Press.

Arafa, S., Chouaibi, M., Sadok, S., & El Abed, A. (2012). The influence of season on the gonad index and biochemical composition of the sea urchin *Paracentrotus lividus* from the golf of Tunis. *The Scientific World Journal*.

Aydin, M., Sevgili, H., Tufan, B., Emre, Y., & Kose, S. (2011). Proximate composition and fatty acid profile of three different fresh and dried commercial sea cucumbers from Turkey. *International Journal of Food Science & Technology, 46*, 500–508.

Bernsdorff, C., & Winter, R. (2003). Differential properties of the sterols cholesterol, ergosterol, β-sitosterol, trans-7-dehydrocholesterol, stigmasterol and lanosterol on DPPC Bilayer Order. *Journal of Physical Chemistry B, 107*, 10658–10664.

Calder, P. C. (2008). Session 3: Joint Nutrition Society and Irish Nutrition and Dietetic Institute Symposium on 'Nutrition and autoimmune disease' PUFA, inflammatory processes and rheumatoid arthritis. *Proceedings of the Nutrition Society, 67*, 409–418.

Cawood, A. L., Ding, R., Napper, F. L., Young, R. H., Williams, J. A., Ward, M. J., et al. (2010). Eicosapentaenoic acid (EPA) from highly concentrated n-3 fatty acid ethyl esters is incorporated into advanced atherosclerotic plaques and higher plaque EPA is associated with decreased plaque inflammation and increased stability. *Atherosclerosis, 212*, 252–259.

Chen, C., & Tripp, C. P. (2012). A comparison of the behavior of cholesterol, 7-dehydrocholesterol and ergosterol in phospholipid membranes. *Biochimica et Biophysica Acta, 1818*, 1673–1681.

Edidin, M. (2003). The state of lipid rafts: From model membranes to cells. *Annual Review of Biophysics and Biomolecular Structure, 32*, 257–283.

FAO (2008). Sea cucumbers: A global review of fisheries and trade. In V. Toral-Granda, A. Lovatelli, & M. Vasconcellos (Eds.), *FAO fisheries and aquaculture technical paper No. 516*.

Goad, L. J. (1978). The sterols of marine invertebrates: Composition, biosynthesis and metabolites. In P. J. Scheuer (Ed.). *Marine natural products: Chemical and biological perspectives* (Vol. II, pp. 76–172). New York: Academic Press.

Guenther, J., Wright, A. D., Burns, K., & de Nys, R. (2009). Chemical antifouling defences of sea stars: Effects of the natural products hexadecanoic acid, cholesterol, lathosterol and sitosterol. *Marine Ecology Progress Series, 385*, 137–149.

Hamdi, S. A. H. (2011). Muscle and exoskeleton extracts analysis of both fresh and marine crustaceans *Procambarus clarkii* and *Erugosquilla massavensis*. *African Journal of Pharmacy and Pharmacology, 5*, 1589–1597.

Kalogeropoulos, N., Mikellidi, A., Nomikos, T., & Chiou, A. (2012). Screening of macro- and bioactive microconstituents of commercial finfish and sea urchin eggs. *LWT – Food Science and Technology, 46*, 525–531.

Kanazawa, A. (2001). Sterols in marine invertebrates. *Fisheries Science, 67*, 997–1007.

Kandyuk, R. P. (2006). Sterols and their functional role in Mollusks (a review). *Hydrobiological Journal, 42*, 56–66.

Latyshev, N. A., Kasyanov, S. P., Kharlamenko, V. I., & Svetashev, V. I. (2009). Lipids and fatty acids of edible crabs of the north-western Pacific. *Food Chemistry, 116*, 657–661.

Martínez-Pita, I., García, F. J., & Pita, M. L. (2010). The effect of seasonality on gonad fatty acids of the sea urchins *Paracentrotus lividus* and *Arbacia lixula* (echinodermata: Echinoidea). *Journal of Shellfish Research, 29*, 517–525.

Miles, E. A., Banerjee, T., & Calder, P. C. (2004). The influence of different combinations of gamma-linolenic, stearidonic and eicosapentaenoic acids on the fatty acid composition of blood lipids and mononuclear cells in human volunteers. *Prostaglandins Leukotrienes and Essential Fatty Acids, 70*, 529–538.

Miles, E. A., & Calder, P. C. (2012). Influence of marine n-3 polyunsaturated fatty acids on immune function and a systematic review of their effects on clinical outcomes in rheumatoid arthritis. *British Journal of Nutrition, 107*, S171–S184.

Mol, S., Baygar, T., Varlik, C., & Tosun, Ş. Y. (2008). Seasonal variations in yield, fatty acids, amino acids and proximate compositions of sea urchin (*Paracentrotus lividus*) Roe. *Journal of Food and Drug Analysis, 16*, 68–74.

Ortega, M. J., Zubía, E., & Salvá, J. (1997). 3-Epi-aplykurodinone B, a new degraded sterol from *Aplysia fasciata*. *Journal of Natural Products, 60*, 488–489.

Ostlund, R. E. Jr., (2002). Phytosterols in human nutrition. *Annual Review of Nutrition, 22*, 533–549.

Ozogul, Y., Duysak, O., Ozogul, F., Özkütük, A. S., & Türeli, C. (2008). Seasonal effects in the nutritional quality of the body structural tissue of cephalopods. *Food Chemistry, 108*, 847–852.

Pereira, D. M., Andrade, P. B., Vinholes, J., Correia-da-Silva, G., Valentão, P., & Teixeira, N. (2011). Fatty acids in marine organisms: In the pursuit of bioactive agents. *Current Pharmaceutical Analysis, 7*, 108–119.

Pereira, D. M., Vinholes, J., Guedes de Pinho, P., Valentão, P., Mouga, T., Teixeira, N., et al. (2012). A gas chromatography–mass spectrometry multi-target method for the simultaneous analysis of three classes of metabolites in marine organisms. *Talanta, 100*, 391–400.

Plat, J., Mackay, D., Baumgartner, S., Clifton, P. M., Gylling, H., Jones, P. J. H., et al. (2012). Progress and prospective of plant sterol and plant stanol research: Report of the Maastricht meeting. *Atherosclerosis, 225*, 521–533.

Rees, D., Miles, E. A., Banerjee, T., Wells, S. J., Roynette, C. E., Wahle, K. W., et al. (2006). Dose-related effects of eicosapentaenoic acid on innate immune function in healthy humans: A comparison of young and older men. *The American Journal of Clinical Nutrition, 83*, 331–342.

Sarma, N. S., Sri Rama Krishna, M., & Ramakrishna Rao, S. (2005). Sterol ring system oxidation pattern in marine sponges. *Marine Drugs, 3*, 84–111.

Spinella, A., Gavagnin, M., Crispino, A., Cimino, G., Martinez, E., Ortea, J., et al. (1992). 4-Acetylaplykurodin B and aplykurodinone B, two ichthyotoxic degraded sterols from the Mediterranean mollusk *Aplysia fasciata*. *Journal of Natural Products, 55*, 989–993.

Studer, M., Briel, M., Leimenstoll, B., Glass, T. R., & Bucher, H. C. (2005). Effect of different antilipidemic agents and diets on mortality: A systematic review. *Archives of Internal Medicine, 165*, 725–730.

Usydus, Z., Szlinder-Richert, J., Adamczyk, M., & Szatkowska, U. (2011). Marine and farmed fish in the Polish market: Comparison of the nutritional value. *Food Chemistry, 126*, 78–84.

Vanstone, C. A., Raeini-Sarjaz, M., Parsons, W. E., & Jones, P. J. (2002). Unesterified plant sterols and stanols lower LDL-cholesterol concentrations equivalently in hypercholesterolemic persons. *The American Journal of Clinical Nutrition, 76*, 1272–1278.

Wen, J., Hu, C., & Fan, S. (2010). Chemical composition and nutritional quality of sea cucumbers. *Journal of the Science of Food and Agriculture, 90*, 2469–2474.

Wu, G. (2009). *Amino acids: Metabolism, functions, and nutrition* (Vol. 37). Vienna: Springer.

Xu, X. H., Yan, B. L., & Xu, J. T. (2012). Comparison on nutrient composition and amino acid and fatty acid profile of muscle in wild and farmed prawn, *Penaeus japonicus*. *Applied Mechanics and Materials, 140*, 286–290.

Zarai, Z., Frikha, F., Balti, R., Miled, N., Gargouri, Y., & Mejdoub, H. (2011). Nutrient composition of the marine snail (*Hexaplex trunculus*) from the Tunisian Mediterranean coasts. *Journal of the Science of Food and Agriculture, 91*, 1265–1270.

Zhukova, N. V. (2007). Lipid classes and fatty acid composition of the tropical nudibranch mollusks *Chromodoris* sp. and *Phyllidia coelestis*. *Lipids, 42*, 1169–1175.

Zlatanos, S., Laskaridis, K., & Sagredos, A. (2009). Determination of proximate composition, fatty acid content and amino acid profile of five lesser-common sea organisms from the Mediterranean Sea. *International Journal of Food Science & Technology, 44*, 1590–1594.

Paper 5

GC-MS/MS Lipidomic Profiling of the Echinoderm *Marthasterias glacialis* and Screening for Bioactivity Against Human Cancer and Non-cancer Cell Lines

David M. Pereira, *Georgina Correia-da-Silva, Patrícia Valentão, Natércia Teixeira, Paula B. Andrade*

GC-MS/MS Lipidomic Profiling of the Echinoderm *Marthasterias glacialis* and Screening for Bioactivity Against Human Cancer and Non-cancer Cell Lines

David M. Pereira[1], Georgina Correia-da-Silva[2,3], Patrícia Valentão[1], Natércia Teixeira[2,3], Paula B. Andrade*[,1]

[1] *REQUIMTE/Laboratório de Farmacognosia, Departamento de Química, Faculdade de Farmácia, Universidade do Porto, Rua de Jorge Viterbo Ferreira n.º 228, 4050-313 Porto, Portugal*
[2] *Laboratório de Bioquímica, Departamento de Ciências Biológicas, Faculdade de Farmácia, Universidade do Porto, Rua de Jorge Viterbo Ferreira n.º 228, 4050-313 Porto, Portugal*
[3] *IBMC - Instituto de Biologia Molecular e Celular, Universidade do Porto, 4150-180 Porto, Portugal*

* Address correspondence to this author at REQUIMTE/Laboratório de Farmacognosia, Departamento de Química, Faculdade de Farmácia, Universidade do Porto, Rua de Jorge Viterbo Ferreira n.º 228, 4050-313 Porto, Portugal; Tel: + 351 220428654; Fax: + 351 226093390; E-mail: pandrade@ff.up.pt

Abstract: Marine organisms have been increasingly regarded as an excellent source of bioactive molecules for human health. As part of an on-going study to elucidate the chemical composition and biological activity of this organism, we report here the lipidomic profile of this organism and screening for anticancer activity. Two classes of biologically active metabolites were identified and quantified by a GC-MS optimized for screening several classes of metabolites in a single run. Free fatty acids and sterols were found, including ergosterol, β-sitosterol and cholesterol derivatives, some of which are reported in this species for the first time. The extract was screened for its ability to affect cell viability (MTT), membrane integrity (LDH) and cell density (SRB) of three human cancer cell lines: human oestrogen receptor-positive (ER^+) breast cancer (MCF-7), human neuroblastoma (SH-SY5Y) and human colon cancer (Caco-2). Differential activity towards the three cancer cell lines was found, with the SH-SY5Y cell line being the most susceptible. No activity was found for Caco-2 cell line. Non-cancer cell lines (human dermal fibroblasts and human foreskin fibroblasts) were also tested and revealed to be less susceptible. This work establishes *M. glacialis* as a potential source of bioactive molecules for further studies.

Keywords: *Marthasterias glacialis* L., GC-MS, breast cancer, neuroblastoma, sterols, fatty acids

2. INTRODUCTION

Natural sources have been very important from an historical point of view, given the fact that they were the origin of the first drugs and medicines used in human health [1]. Even today they play a relevant role in providing new molecules, which is easily pictured if we consider that nearly 60% of all drugs introduced in therapy between 1981 and 2006 were first identified or inspired in natural products [2].

Nowadays marine resources are paving their way as alternative sources of novel chemical entities with biological activities [3-6]. In fact, some drugs have already been approved to be used in human therapy [7, 8], a trend that is expected to increase in the next few years as a consequence of the high number of molecules that are currently involved in clinical trials. The most frequent bioactivities reported include anticancer, antibacterial, anti-inflammatory and immune modulation [4, 6, 9, 10].

Marthasterias glacialis (spiny sea-star) is an asteroid echinoderm, a group that has demonstrated to play one of the most influential roles in benthic ecosystems on a variety of scales [11]. During the 70's-80's this species received great attention, mainly due to its asterosaponins [12, 13].

In a previous work developing a non-targeted approach, we have demonstrated that extracts of *M. glacialis* contained appreciable amounts of carotenoids and other lipids and an inhibitory effect upon the growth of two murine cell lines was shown [14, 15]. Given the fact that these preliminary studies showed the interest of this matrix from a biological point of view, the chemical composition and biological effects were further studied.

In this work a purification process optimized for lipophilic compounds was used and characterized using gas chromatography coupled to mass spectrometry (GC-MS). The biological effects of the resulting extract on viability, membrane integrity and cell density were investigated in three human cancer cell lines: colon cancer (Caco-2), oestrogen receptor-positive (ER^+) breast cancer (MCF-7) and neuroblastoma (SH-SY5Y). In addition, in order to investigate the selective effect of the extract, non-tumour cells were used, namely human dermal fibroblasts (HDF) and human foreskin fibroblasts (HFF).

3. MATERIALS AND METHODS

2.1. Standards and Reagents

All GC-MS standards, as well as (trimethylsilyl) trifluoroacetamide (MSTFA), were of chromatographic grade and purchased to Sigma (St. Louis, MO, USA). Ergosta-7,22-dien-3-ol was from BioBioPha Co., Ltd (China). Chloroform, methanol, anhydrous sodium sulphate and isooctane were from Panreac Quimica SA (Barcelona, Spain). Potassium hydroxide was obtained from Pronalab (Lisboa, Portugal). Dulbecco's Modified Eagle Medium (DMEM), foetal bovine serum (FBS), phosphate buffer saline (PBS) and antibiotic were from GIBCO (Invitrogen, UK). Tris-base, acetic acid and trichloroacetic acid were from Merck (Germany). LDH CytoTox 96 non-radioactive assay kit was from Promega (Madison, WI, USA).

2.2. Animal Material

M. glacialis individuals were collected in Cabo Carvoeiro, west Portugal, in September 2009. Samples were immediately frozen, transported to the laboratory, lyophilized (Labconco 4.5 Freezone apparatus, Kansas City, MO) and powdered using an electric blender.

2.3. Extract Preparation

Acetone:methanol (7:3) was used for extraction of 15 g of lyophilized powder. The extraction was repeated as many times as necessary to render the powder colourless. Partial evaporation of the solvent was used in order to concentrate the extract. Afterwards, the extract was added to a separating funnel with equal amount (20 mL) of an ether:hexane mixture (1:1). An equivalent volume of 5% NaCl was then added. The mixture was separated into two phases and the aqueous hypophase was collected and re-extracted with the ether:hexane mixture until no further pigment could be extracted. The organic epiphases were then collected and washed with water in order to remove all traces of acetone and evaporated until dryness in a rotary evaporator. All procedures were conducted under low light conditions, at room temperature and the final residue was kept at -80 ^{o}C in an inert atmosphere (nitrogen).

Table 1 GC-MS Metabolite Profiling of the Lipophilic Purified Extract from *M. glacialis* (Trimethylsilyl Derivatives)

Peak	Compound	Concentration (µM)[1]
	Fatty Acids	
1	Dodecanoic acid	<LoQ
2	Tetradecanoic acid	<LoQ
3	Pentadecanoic acid	50.6±12.4
4	Palmitic acid	124.0±14.2
5	Linoleic acid	<LoQ
6	Linolenic acid	<LoQ
7	Oleic acid	74.2±11.8
8	Stearic acid	46.4±6.5
9	Arachidonic acid	75.3±17.26
10	Eicosapentaenoic acid	36.3±6.7
11	*cis* 11,14-Eicosadienoic acid	83.8±2.9
12	*cis* 11-Eicosenoic acid	182.2±23.8
	Sterols	
13	Cholesterol	101.7±7.47
14	Cholesterol derivative[b]	64.4±1.0
15	Cholestanol	45.4±3.1
16	Cholesten-7-en-3-ol*	1139.0±78.7
17	Ergosta-7,22-dien-3-ol	160.5±16.4
18	Ergosterol derivative[c]	227.9±25.44
19	Ergosta-7-en-3-ol[*]	89.0±14.7
20	β-Sitosterol derivative[d*]	112.1±4.1

[1] Concentration of compound in a 1 mg/mL solution of purified extract; [b] quantified as cholesterol; [c] quantified as ergosta-7,22-dien-3-ol; [d] quantified as β-sitosterol; * Tentative identification based on mass fragmentation pattern. Values represent the mean ± standard deviation of three determinations. LoQ: Limit of quantification.

2.4. Derivatization for GC-MS Analysis

A solution of 1 mg/mL of extract in ethanol was prepared. 50 µL were then transferred to a glass vial, the solvent was evaporated under nitrogen stream and 50 µL of MSTFA were added to the dried residue. The vial was capped, vortexed and heated for 20 minutes in a dry block heater maintained at 40º C. All analyses were performed in triplicate.

2.5. GC-MS Analysis

A method previously developed by our group for the simultaneous analysis of amino acids, fatty acids, steroids and triterpenes was used [15]. All mass spectra were acquired in electron impact (EI) mode. For quantification purposes, triplicate injections were performed and the amount of metabolites was achieved from the calibration curves of the respective trimethylsilyl (TMS) derivatives. All compounds were quantified in Full Scan mode, with the exception of linoleic (*m/z* 262, 337 and 352), linolenic (*m/z* 191, 335 and 350) and oleic (*m/z* 264, 339 and 354) that were quantified by the area obtained from the re-processed chromatogram, using the characteristic *m/z* fragments.

2.6. Cell Culture

MCF-7 cell line was maintained in MEM media with 1 mmol/L pyruvate and glutamine, while SH-SY5Y, Caco-2, HDF and HFF cell lines were cultured in DMEM. Heat-

inactivated FBS (10%) and 2% penicillin-streptomycin (2%) was used in all cases. Caco-2 and SH-SY5Y cell lines were additionally cultured with 1% non-essential amino acids and also with human transferrin in the case of the Caco-2 cell line. Cells were maintained in an incubator at 37 °C and atmosphere of 5% CO_2.

2.7. Cell Density Assay

The sulphorhodamine B (SRB) method used was described before [16]. Briefly, cells were seeded in 96-well plates with a density of $20x10^4$ cells/well for SH-SY5Y and MCF-7 cell lines and $30x10^4$ cells/well for Caco-2 cell line. Cells were allowed to attach for 24 hours, after which the purified extract was added (76–1250 µg/mL).

After 24, 48 and 72 hours of incubation, media was removed, cells were washed with PBS, 100 µL of cold 40% trichloroacetic acid was added and plates maintained at 4°C for 60 minutes. After this time, cells were washed, dried and incubated with 0.4% SRB (50 µL) in 1% acetic acid, for 30 minutes at 4°C. After the incubation period, cells were washed with 1% acetic acid to remove unbound dye and tris-base (100 µL) was added. The absorbance was read at 492 nm and OD values were plotted against concentration. Three independent assays were conducted, each one of them in triplicate. Media was used as a negative control.

2.8. Viability Assay

Cells were cultured in 96-well plates with the density mentioned above for SRB assay and allowed to attach for 24 hours. After this period, cells were cultured for 24, 48 or 72 hours in the presence or absence of purified extract (76–1250 µg/mL) or palmitic acid (15-30 µM). After incubation, (3-(4,5-dimethylthiazol-2-yl)-2,5-diphenyltetrazolium bromide (MTT) (0.5 mg/ml final concentration) was added to each well and the plate was incubated for 2 hours at 37 °C. The formazan was dissolved by addition of a DMSO:isopropanol mixture (3:1) and quantified spectrophotometrically at 540 nm. The results of cell viability correspond to the mean of three independent experiments performed in triplicate and are expressed as percentage of the untreated control cells.

2.9. Membrane Integrity

Lactate dehydrogenase (LDH) release was measured after 24, 48 and 72 hours in culture media supernatant using CytoTox 96 non-radioactive cytotoxicity assay kit (Promega, Madison, WI, USA) according to the manufacturer's protocol. Absorbance was read in a multiplate reader at 492 nm. The results correspond to the mean of three independent experiments performed in triplicate and expressed as fold increase of absorbance in treatments *versus* untreated control cells, expressed as arbitrary units.

2.10. Statistical Analysis

Comparisons of data from different groups, controls and treatments, were performed using a one-way ANOVA test. Dunnet's post-test was used. A *P* value lower than 0.05 was considered statistically significant.

3. RESULTS AND DISCUSSION

3.1. Fatty Acids and Sterols in the Lipidome of *M. glacialis*

The first report regarding the chemical composition of *M. glacialis* addressed its carotenoid composition using organisms collected in the Adriatic Sea [17]. Subsequent works confirmed lutein, zeaxanthin and astaxanthin and some isomers as major carotenoids in samples from the Atlantic Ocean as well [14, 18]. Recently, other metabolites were described in crude extracts, namely amino acids, fatty acids and sterols [15].

In the present work, we used a lipophilic extract and subjected the sample to GC-MS analysis in order to deepen our knowledge on the extract's chemical composition. Using a technique previously developed by our group [15], it was possible to identify and quantify fatty acids (saturated and unsaturated) and sterols. Amino acids were searched, however they were not detected, which is in line with the lipophilic nature of the extract. Fig. **1** shows a representative GC-MS chromatogram of the purified extract of *M. glacialis*. When compared with the previously published crude extract, in addition to amino acids, the fatty acid composition was also altered, as unsaturated fatty acids were found to be predominant compounds, while crude extracts exhibited similar amounts of saturated and unsaturated fatty acids [15].

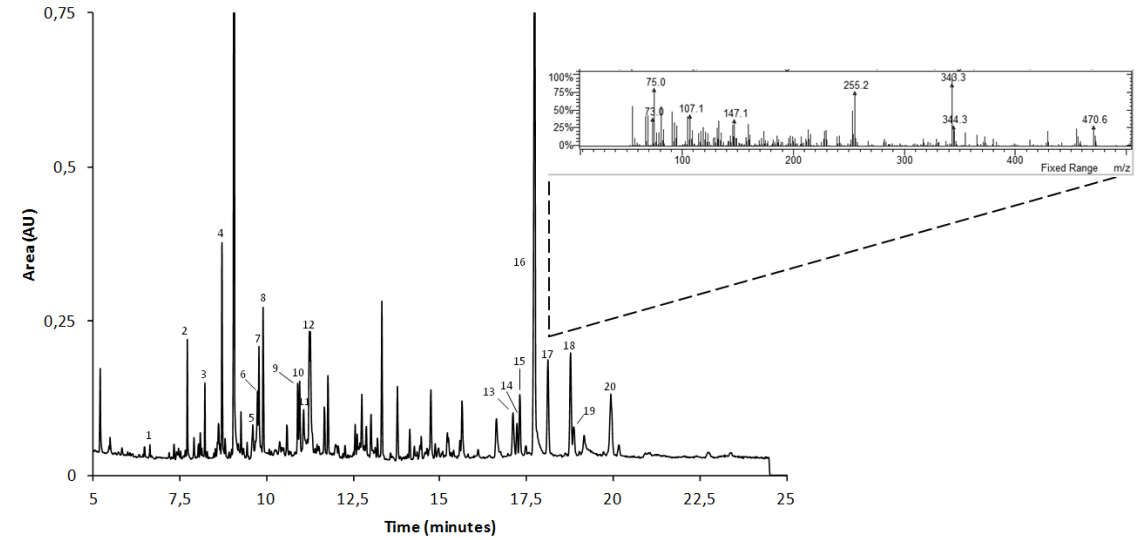

Fig. (1). GC-MS chromatogram of the *M. glacialis* purified extract. Identity of peaks as in Table 1.

Palmitic acid (peak **4**) was the major saturated fatty acid, while *cis*-11 eicosenoic acid (peak **12**) was the unsaturated one present in higher amounts. In the case of sterols, eight compounds could be found.

The compound present in higher amounts, peak **16**, displayed *m/z* 458 as molecular ion and *m/z* 353, 255 and 213 as the most representative fragments, which is compatible to a silylated derivative of cholesterol with an unsaturation in the B or C ring (Fig. **1**, Table **1**) [19]. The presence of the ion at *m/z* 255 and the absence of *m/z* 229 point to a double bound in position 7 instead of 8-14 and thus this compound was identified as [choleste-7-ene-3-oxy]trimethylsilane. The precursor compound, cholesterol, was also found (peak **13**), albeit in lower amounts. Peak **15** displayed the molecular ion at *m/z* 460, which is compatible with a trimethylsilane di-hydro derivative of cholesterol. By comparison of its mass spectra and co-elution experiments, the compound was identified as cholestanol. Compound **17** presented a molecular ion at 470 *m/z* and other prominent fragments at *m/z* 455, 343, 255 and 229. This fragmentation pattern is in line with that described for [ergosta-7,22-dien-3-oxy]trimethylsilane, both regarding diagnostic ions and their relative amounts [19, 20] and was later confirmed by comparison with an authentic standard.

In the case of peak **19**, the fragmentation pattern was similar to that of ergosta-7,22-dien-3-ol trimethylsilane, though the molecular ion was found at *m/z* 472, which is compatible with a trimethylsilane di-hydro derivative of 18, tentatively [ergosta-7-en-3-oxy] trimethylsilane.

Other sterols, such as stigmasterol, β-sitosterol and campsterol were searched however they were not found. In addition, some representative triterpenes with lupane scaffolds were searched, though they were not detected.

Due to the lipophilic nature of the extract, carotenoids, which have been described before in this species, were also present in the extract. In concordance with previous reports [14, 18], astaxanthin, lutein and zeaxanthin were major compounds in the purified extract of *M. glacialis*. Lutein, zeaxanthin and astaxanthin were present in concentrations around 74, 42 and 2 µM, respectively, in a solution of 1 mg/mL of extract. In a general way, in the working concentrations of the extract, no biological effect could be noticed (data not shown).

3.2. Effect of the Extract in Caco-2 Cell Line

The effect of the extract in all cell lines was studied at different times (24, 48 and 72 hours) and concentrations, ranging from 76 to 1250 µg/mL. Different techniques were used to study the biological effect of the extract on cells, namely MTT for evaluation of cell viability, SRB for cell density and LDH for membrane integrity.

Among all cell lines tested, Caco-2 cells were the most resistant to the extract tested herein (Fig. **2**). In fact, in a general way, only the highest concentration (1250 µg/mL) displayed a reduction of cell viability and

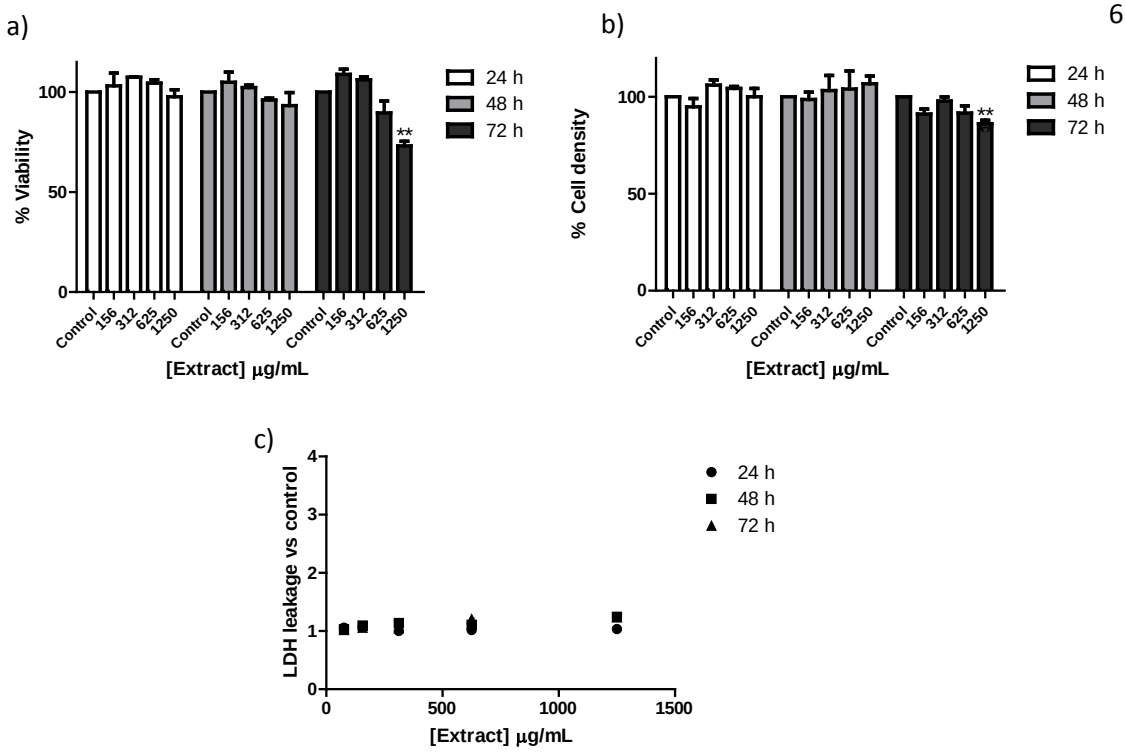

Fig. (2). Effect of *M. glacialis* purified extract on a) viability, b) density and c) membrane integrity of Caco-2 cells. The results correspond to the mean of three independent experiments performed in triplicate. * $P<0.05$; ** $P<0.01$.

density after 72 hours. No LDH release was detected.

Although Caco-2 cells were originally derived from a human colon adenocarcinoma, they display several metabolic and morphological traits of enterocytes, namely efflux transporters, phase II conjugation enzymes and microvillus transporters [21, 22]. The high activity of proteins, such as glycoprotein *P*, usually results in an innate resistance of these cells against many drugs and, for this reason, low bioavailability of the extract inside the cell cannot be ruled out.

3.3. Effect of the Extract in MCF-7 Cell Line

The purified extract reduced MCF-7 cells' viability in a time- and dose-dependent manner (Fig. **3**). In both MTT and SRB assays, in concentrations in the range 312-1250 µg/mL, the effect was time- and concentration-dependent, with a concentration of 625 µg/mL causing a decrease in 50% of viability after 72 hours (Fig. **3a**). At 24 hours of incubation only the highest concentration, 1250 µg/mL, caused a reduction of cell density, although lower concentrations were already affecting viability. However, with the extension of the time of treatment, lower concentrations also induced a decrease in cell viability, 625 µg/mL for 48 hours and to 312 µg/mL at 72 hours, a trend that was noticed equally in the IC_{50} of the MTT assay (916 and 602 µg/mL at 48 and 72 hours, respectively). Regarding membrane integrity, LDH release was observed for the first time after 48 hours of incubation with the highest concentration.

3.4. Effect of the Extract in SH-SY5Y, HDF and HFF Cell Lines

In the case of SH-SY5Y cells, only a concentration-dependent effect was found (Fig. **4**), with a reduction of cell viability and cell density more pronounced than that detected for MCF-7 cells (Fig. **3**). A maximum of activity was found for 625 µg/mL and, for this reason, no data regarding higher concentrations is presented. In a general way, for any given concentration, no significant time-dependent effect was noticed, as shown by the similar values of IC_{50} in the MTT assay at 24, 48 and 72 hours (206, 219 and 195 µg/mL, respectively). After 24 hours of incubation the concentration of 156 µg/mL caused a decrease of 30 and 20% in cell viability (Fig. **4a**) and density (Fig. **4b**), respectively. LDH release was not observed even for the higher concentrations and incubation times (Fig. **4c**).

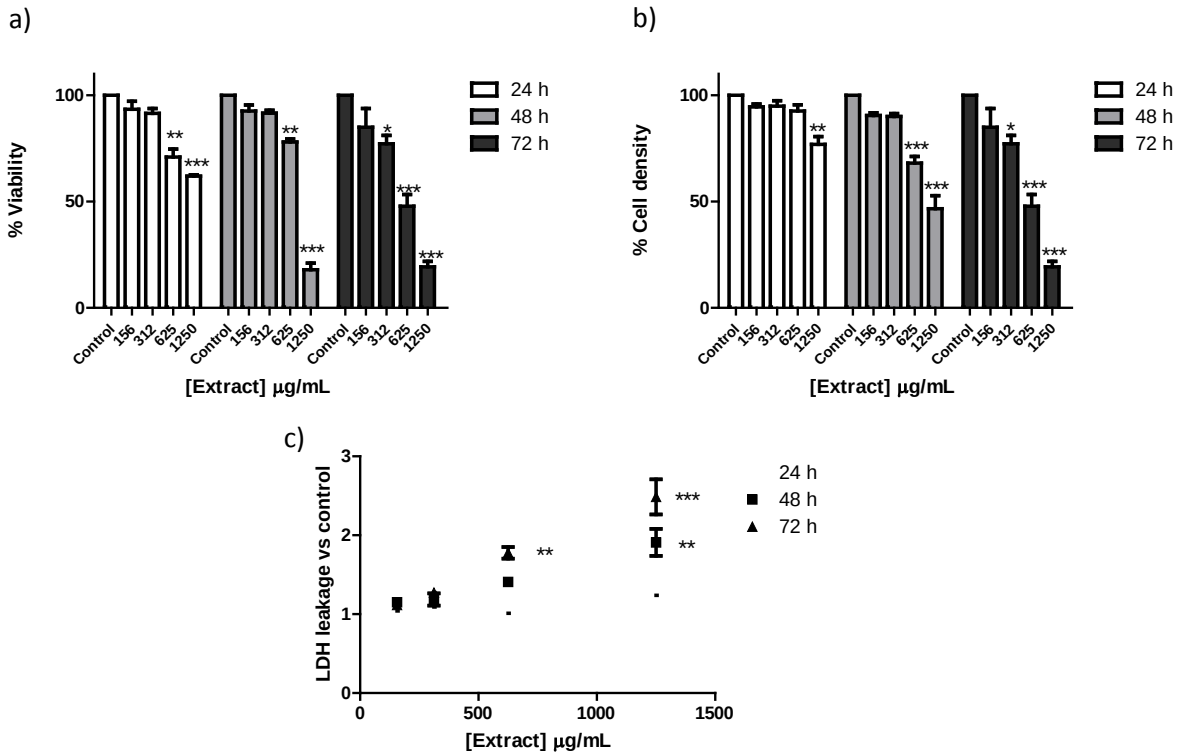

Fig. (3). Effect of *M. glacialis* purified extract on a) viability, b) density and c) membrane integrity of MCF-7 cells. The results correspond to the mean of three independent experiments performed in triplicate. * P<0.05 ; ** P<0.01; *** P<0.001.

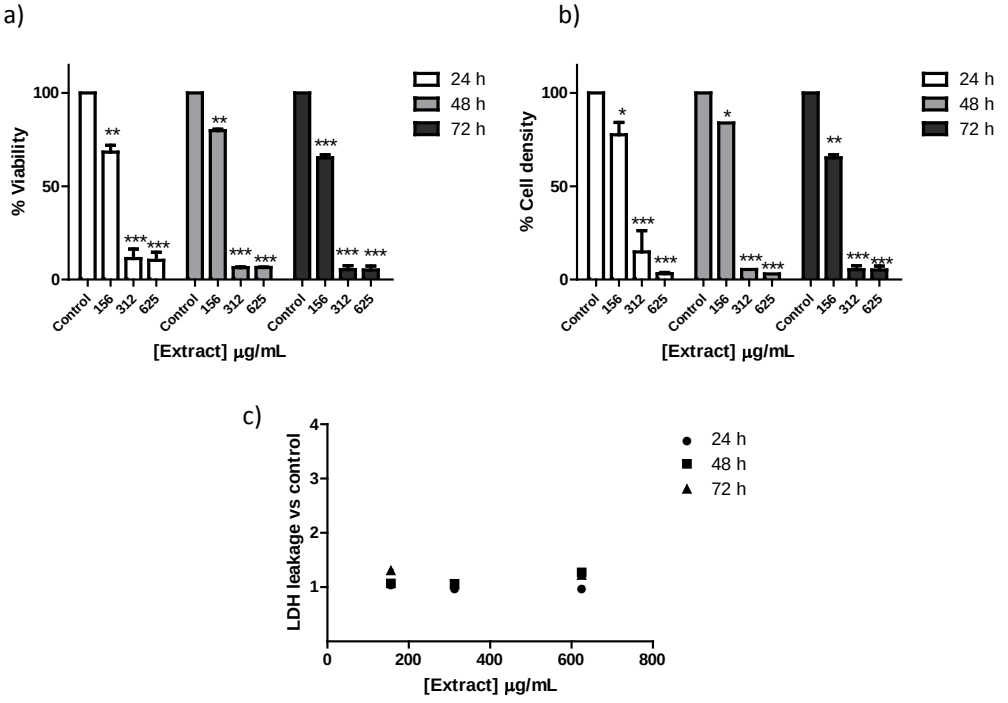

Fig. (4). Effect of *M. glacialis* purified extract on a) viability, b) cell density and c) membrane integrity of SH-SY5Y cells. The results correspond to the mean of three independent experiments performed in triplicate. * P<0.05 ; ** P<0.01; *** P<0.001.

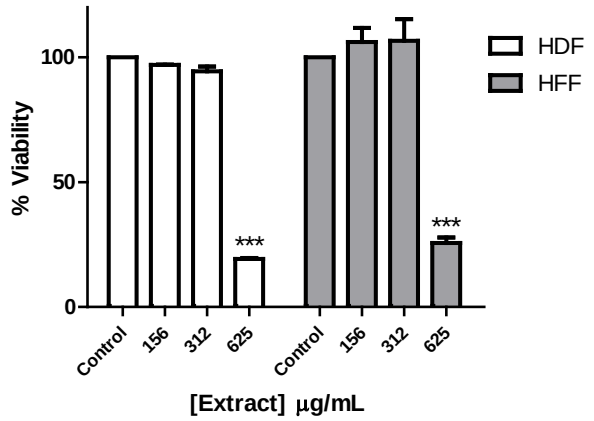

Fig. (5). Effect of purified extract from *M. glacialis* on the viability of the human non-tumour cell lines HDF and HFF (24 hours). The results correspond to the mean of three independent experiments performed in triplicate *** $P<0.001$.

4. CONCLUSIONS

In this work we investigated the chemical composition and biological activity of a purified fraction of the lipidome of *M. glacialis*. Fatty acids and sterols were identified and quantified and the presence of ergosta-7,22-diene-3-ol and cholestan-7-ene-3-ol was confirmed for the first time in this species.

From a biological point of view, we have tested this matrix in a panel of three human cancer cell lines: colon cancer, neuroblastoma and breast cancer. Overall, the extract displayed different activities against the different cells, with no significant activity being found for Caco-2 cells. In the case of the breast cancer MCF-7 and neuroblastoma SH-SY5Y cell lines, inhibitory activity was found and cells displayed different susceptibilities: while MCF-7 required higher incubation periods and concentrations, the SH-SY5Y cell line required lower concentrations and incubation periods and no loss of membrane integrity took place, which points to a process of regulated cell death.

CONFLICT OF INTEREST

The authors confirm that this article content has no conflict of interest.

ACKNOWLEDGMENTS

The authors thank Fundação para a Ciência e a Tecnologia (FCT) for grant no. PEst-C/EQB/LA0006/2011. David M. Pereira is grateful to FCT for the grant (SFRH/BD/62663/2009).

REFERENCES

1. Pelt, J. M., *Les nouveaux remedes naturels*. Fayard Ed.: Paris, 2001.

2. Newman, D. J.; Cragg, G. M. Natural products as sources of new drugs over the last 25 years. *Journal of Natural Products* **2007**, *70*(3), 461-477.

3. Chakraborty, C.; Hsu, C. H.; Wen, Z. H.; Lin, C. S. Anticancer drugs discovery and development from marine organisms. *Curr. Top. Med. Chem.* **2009**, *9*(16), 1536-1545.

4. Mayer, A. M. S.; Rodríguez, A. D.; Berlinck, R. G. S.; Fusetani, N. Marine pharmacology in 2007-8: Marine compounds with antibacterial, anticoagulant, antifungal, anti-inflammatory, antimalarial, antiprotozoal, antituberculosis, and antiviral activities; Affecting the immune and nervous system, and other miscellaneous mechanisms of

action. *Comp. Biochem. Phys. C* **2011**, *153*(2), 191-222.
5. Newman, D. J.; Cragg, G. M.; Battershill, C. N. Therapeutic agents from the sea: Biodiversity, chemo-evolutionary insight and advances to the end of Darwin's 200th year. *Diving Hyperb. Med.* **2009**, *39*(4), 216-225.
6. Pereira, D. M.; Correia-da-Silva, G.; Valentão, P.; Teixeira, N.; Andrade, P. B., In *OMICS: Biomedical Perspectives and Applications* Barh, D., Ed. CRC Press: 2011.
7. Martínez-Serra, J.; Maffiotte, E.; Martín, J.; Bex, T.; Navarro-Palou, M.; Ros, T.; Plazas, J. M.; Vögler, O.; Gutiérrez, A.; Amat, J. C.; Ramos, R.; Saus, C.; Ginés, J.; Alemany, R.; Diaz, M.; Besalduch, J. Yondelis® (ET-743, Trabectedin) sensitizes cancer cell lines to CD95-mediated cell death: New molecular insight into the mechanism of action. *Eur. J. Pharmacol.* **2011**, *658*(2-3), 57-64.
8. Murti, Y.; Agrawal, T. Marine derived pharmaceuticals- development of natural health products from marine biodiversity. *Int. J. Chem.Tech. Res.* **2010**, *2*(4), 2198-2217.
9. Blunt, J. W.; Copp, B. R.; Munro, M. H. G.; Northcote, P. T.; Prinsep, M. R. Marine natural products. *Nat. Prod. Rep.* **2011**, *28*(2), 196-268.
10. Hughes, C. C.; Fenical, W. Antibacterials from the sea. *Chem-Eur. J.* **2010**, *16*(42), 12512-12525.
11. Verling, E.; Crook, A. C.; Barnes, D. K.; Harrison, S. S. Structural dynamics of a sea-star (*Marthasterias glacialis*) population. *J. Mar. Biol. Assoc. UK* **2003**, *83*(3), 583-592.
12. De Simone, F.; Dini, A.; Finamore, E.; Minale, L.; Pizza, C.; Riccio, R. Starfish saponins—IV. Sapogenins from the starfish *Astropecten aurantiacus* and *Marthasterias glacialis*. *Comp. Biochem. Phys. B* **1979**, *64*(1), 25-32.
13. Dini, A.; Mellon, F.; Minale, L.; Pizza, C.; Riccio, R.; Self, R.; Zollo, F. Starfish saponins—XI. Isolation and partial characterization of the saponins from the starfish *Marthasterias glacialis*. *Comp. Biochem. Phys. B* **1983**, *76*(4), 839-844.
14. Ferreres, F.; Pereira, D. M.; Gil-Izquierdo, A.; Valentao, P.; Botelho, J.; Mouga, T.; Andrade, P. B. HPLC-PAD-atmospheric pressure chemical ionization-MS metabolite profiling of cytotoxic carotenoids from the echinoderm *Marthasterias glacialis* (spiny sea-star). *J. Sep. Sci.* **2010**, *33*(15), 2250-2257.
15. Pereira, D. M.; Vinholes, J.; Guedes de Pinho, P.; Valentão, P.; Mouga, T.; Teixeira, N.; Andrade, P. B. A gas chromatography-mass spectrometry multi-target method for the simultaneous analysis of three classes of metabolites in marine organisms. *Talanta* **2012**, *100*, 391-400.
16. Pereira, D. M.; Cheel, J.; Areche, C.; San-Martín, A.; Rovirosa, J.; Silva, L. R.; Valentão, P.; Andrade, P. B. Anti-proliferative activity of meroditerpenoids isolated from the brown alga *Stypopodium flabelliforme* against several cancer cell lines. *Mar. Drugs* **2011**, *9*, 952-962.
17. Czeczuga, B. Investigations of carotenoids in some animals of the Adriatic Sea V. Echinodermata. *Hydrobiologia* **1977**, *54*(2), 177-180.
18. Mariutti, L. R. B.; Pereira, D. M.; Mercadante, A. Z.; Valentão, P.; Teixeira, N.; Andrade, P. B. Further insights on the carotenoid profile of the echinoderm *Marthasterias glacialis L. Mar. Drugs* **2012**, *10*(7), 1498-1510.
19. NIST NIST Chemistry WebBook. http://webbook.nist.gov/chemistry.
20. Phillips, K. M.; Ruggio, D. M.; Horst, R. L.; Minor, B.; Simon, R. R.; Feeney, M. J.; Byrdwell, W. C.; Haytowitz, D. B. Vitamin D and sterol composition of 10 types of mushrooms from retail suppliers in the United States. *J. Agric. Food Chem.* **2011**, *59*(14), 7841-7853.
21. Artursson, P. Cell cultures as models for drug absorption across the intestinal mucosa. *Crit. Rev. Ther. Drug.* **1991**, *8*(4), 305-330.
22. Press, B.; Di Grandi, D. Permeability for intestinal absorption: Caco-2 assay and

related issues. *Curr. Drug Metab.* **2008**, *9*(9), 893-900.

Paper 6

The anti-inflammatory effect of unsaturated fatty acids and ergosta-7,22-dien-3-ol from the echinoderm *Marthasterias glacialis* involves prevention of CHOP pathway-mediated ER-stress and NF-κB activation

David M. Pereira, *Georgina Correia-da-Silva, Patrícia Valentão, Natércia Teixeira, Paula B. Andrade*

Synergic anti-inflammatory effect of fatty acids and ergosta-7,22-dien-3-ol from *Marthasterias glacialis*: prevention of CHOP-mediated ER-stress and NF-κB activation

David M. Pereira[1], Georgina Correia-da-Silva[2, 3,] Patrícia Valentão[1], Natércia Teixeira[2], [3*], Paula B. Andrade[1*]

1 REQUIMTE/Laboratório de Farmacognosia, Departamento de Química, Faculdade de Farmácia, Universidade do Porto, Rua de Jorge Viterbo Ferreira, nº 228, 4050-313 Porto, Portugal. **2** Laboratório de Bioquímica, Departamento de Ciências Biológicas, Faculdade de Farmácia, Universidade do Porto, Rua de Jorge Viterbo Ferreira, nº 228, 4050-313 Porto, Portugal. **3** IBMC –Instituto de Biologia Molecular e Celular, Universidade do Porto, 4150-180 Porto, Portugal

Corresponding authors: pandrade@ff.up.pt (Paula B. Andrade); natercia@ff.up.pt

Keywords: Marthasterias glacialis L.; Anti-inflammatory; CHOP; IKB-α; Ergosta-7,22-dien-3-ol

Abstract

There has been increasing awareness to the potential interest of drug discovery from marine natural products to treat several pathological conditions, including inflammation. In this work we describe the anti-inflammatory activity of several compounds present in the echinoderm *Marthasterias glacialis* (spiny sea-star) in an inflammatory model using RAW 264.7 cells challenged with LPS.

Lipidomic profiling of the organism revealed two major classes of compounds: fatty acids and sterols. Among these, the predominant compounds *cis* 11-eicosenoic and *cis* 11,14 eicosadienoic acids and the unsaturated sterol ergosta-7,22-dien-3-ol were evaluated.

The mechanism of action of the compounds was distinct as they modulated different levels of the inflammation pathway. Classical inflammatory markers such as COX-2, iNOS, IL-6 and NF-κB were evaluated. We also studied the contribution of the CHOP pathway-mediated ER-stress to the inflammatory process.

Overall, the sterol ergosta-7,22-dien-3-ol was the most active compound, however maximum activity was obtained when all compounds were tested in combination, thus suggestion a synergic activity of both classes of metabolites.

This work establishes the echinoderm *M. glacialis* as an interested source of anti-inflammatory molecules.

1. Introduction

Inflammation is a complex process occurring in many animals and constitutes one of the first lines of defense against a number of stimuli that are perceived as harmful, such as bacteria, trauma and irritants. While acute inflammatory processes may serve to protect the organism, deregulated or chronic inflammatory processes are the base of a number of pathological conditions that include asthma, rheumatoid arthritis, cardiovascular diseases, among many others.

In the continuous search of new molecules to counter and treat inflammatory conditions, Nature has been a prolific source of such compounds for many years. Recently, much interest has been given to anti-inflammatory compounds from non-conventional environments, with marine micro and macroorganisms being very important. Several compounds of marine origin have been

described in the last few years, such as avarol, cycloamphilectenes 1-6 , cavernolide and the lead compound manoalide [1], among many others. Some of these compounds are already in advanced stages of clinical trials.

Several factors are known to modulate the inflammatory process. Among these, NF-κB plays a pivotal role [2,3]. When free from its cytoplasmatic inhibitor proteins, the IκB family, it translocates to the nucleus, where it binds to the promoter region of several genes, thus exerting a number of actions. Target genes codify proteins that include cytokines, cyclooxygenase-2 (COX-2), inducible nitric oxide synthase (iNOS), proteases and many others [4].

Marthasterias glacialis L., also known as spiny sea-star, is an echinoderm that can be found in several ecosystems. Previous works have addressed the chemical composition of this organism and several classes of compounds important in human diet were found, namely carotenoids [5-7], fatty acids, sterols and amino acids [8,9]. Some biological properties were also evaluated, namely its anticancer activity against both non-human [6] and human cells [8]. In this work the anti-inflammatory effect of a lipophilic extract and its mains compounds was evaluated in the LPS-induced RAW 264.7 macrophages model of inflammation. The effect of the extract on several inflammatory markers was assessed.

2. Materials and methods

2.1. Chemicals

Lipopolysaccharide (LPS), acridine orange (AO), Triton X-100, sulphanilamide, dichlorodihydrofluorescein diacetate (DCDHF-DA), 3-(4,5-dimethylthiazolyl- 2)-2,5-diphenyltetrazolium bromide (MTT), palmitic acid, *cis* 11-eicosenoic acid (≥99%) and *cis* 11,14-eicosadienoic acid (≥98%) were from Sigma-Aldrich. Ergosta-7,22-dien-3-ol was from BioBioPha Co., Ltd (China). Sodium nitroprusside dehydrate (SNP) from Riedel-de-Haën (Seelze, Germany). *N*-(1-naphtyl)-ethylene-diamine dihydrochloride were obtained from Merck (Darmstadt, Germany). Dulbecco's Modified Eagle Medium (DMEM), foetal bovine serum (FBS), Dulbecco's phosphate buffer saline (DPBS), Hank's balanced salt solution (HBSS) and antibiotic were from GIBCO (Invitrogen, UK). COX-2, iNOS, IKB-α, β-tubulin and CHOP primary antibodies, as well as anti-rabbit secondary antibody were from Santa Cruz, USA. IL-6 ELISA kit was from AbCam, UK.

2.2. Sample preparation

M. glacialis individuals were collected in west Portugal (Cabo Carvoeiro) in September 2009. Samples were frozen, transported to the laboratory, lyophilized (Labconco 4.5 Freezone apparatus, Kansas City, MO) and powdered using an electric blender. Lyophilized powder (15 g) were extracted with acetone:methanol (7:3) and the extraction was repeated as many times as necessary to render the powder colourless. Afterwards, the extract was added to a separating funnel with equal amount (20 mL) of an ether:hexane mixture (1:1). An equivalent volume of 5% NaCl was then added. The mixture was separated into two phases and the aqueous hypophase was collected and re-extracted with the ether:hexane mixture until no further pigment could be extracted. The organic epiphases were then collected and washed with water in order to remove all traces of acetone and evaporated until dryness in a rotary evaporator. All procedures were conducted under low light conditions, at room temperature and the final residue was kept at -80 ºC in an inert atmosphere (nitrogen).

2.3. Derivatization and GC-MS analysis

A solution of 1 mg/mL of extract in ethanol was prepared. An aliquot of 50 µL was then transferred to a glass vial, the solvent was evaporated under nitrogen stream and 50 µL of MSTFA were added to the dried residue. The vial was capped, vortexed and heated for 20 minutes at 40 ºC. All analysis were performed in triplicate. GC-MS conditions were as described previously by our group [9].

2.4. Cell culture

RAW 264.7 macrophages were maintained in DMEM supplemented with 10% FBS and 1% penicillin/streptomycin and grown in an incubator at 37 °C and 5% CO_2.

For the Wright staining cells were seeded at a density of $3x10^5$ cells/well in 24-well plates. After incubation with different concentrations of the extract at different times, cells were washed twice with PBS. After fixation with cold methanol, at 4°C for 30 minutes, cells were stained with Wright solution. Cells were then mounted with DPX.

2.5. Cell viability

Cells were cultured in 96-well plates ($2x10^4$ cells/well) and allowed to attach for 24 hours. After this period, cells were treated with LPS, with or without pre-incubation with the extract/compounds for 2 hours. After incubation (24 hours), MTT (0.5 mg/ml final concentration) was added to each well and the plate was incubated for 2 hours at 37 °C.

The formazan was dissolved by addition of a DMSO:isopropanol mixture (3:1) and quantified spectrophotometrically at 560 nm. The results of cell viability correspond to the mean of three independent experiments performed in triplicate and are expressed as percentage of the untreated control cells. LDH release was measured after 24 hours in culture media supernatant using CytoTox 96 non-radioactive cytotoxicity assay kit (Promega, Madison, WI, USA) according to the manufacturer's protocol. Absorbance was read in a multiplate reader at 492 nm. All the results correspond to the mean ± SD of three independent experiments performed in triplicate and expressed as fold increase of absorbance in treatments *versus* untreated control cells, expressed as arbitrary units.

2.6. Acridine orange

Cells were incubated as described before with LPS, with or without pre-incubation with the extract/pure compounds. After this period, cells were washed with HBSS and incubated with a 0.1 µg/mL solution of acridine orange (AO) for 15 minutes. After this period cells were washed with HBSS and observed in a fluorescence microscope equipped with a 490 nm band-pass blue excitation filter and a 515-nm long pass-barrier filter.

2.7. Nitric oxide scavenging activity and NO determination

The ability of the extract to scavenge nitric oxide radical generated in a cell-free system was evaluated according to the method previously described [10]. A dilution series (five different concentrations of extract) was prepared in a 96-well plate. The reaction mixtures in the sample wells consisted of 156 µg/mL extract and SNP. The plates were incubated at 25 ºC for 60 min under light.

Nitrite was quantified by mixing 50 µl of either extract solution or culture media with an equal volume of Griess reagent (1% sulphanilamide and 0.1% naphthylethylenediamine dihydrochloride in 2% H_3PO_4) and incubated for 10 minutes in the dark, after which absorbance was read in a multiplate reader set at 540 nm.

2.8. Intracellular reactive oxygen species

Cells were seed in 96-well black plates according to the above mentioned conditions for the MTT assay and exposed to LPS for 24 hours, with or without pre-incubation with *M. glacialis* purified extract for 2 hours. Cells were washed with HBSS 30 minutes before the end of the incubation period, followed by incubation with a solution of DCDHF-DA (25 µM in HBSS) for 30 minutes. Afterwards they were mounted with VectaShield mounting media (Vector, UK). For the quantification of intracellular ROS the plate was read using fluorescence multiplate reader (Excitation: 490 nm excitation; Emission: 520 nm) following incubation with DCDHF-DA. Cells in HBSS were used as negative control and LPS was used as a positive control.

2.9. IL-6

IL-6 levels were determined by ELISA in culture media as *per* the manufacturer's instructions.

2.10. Western-Blot

Cells were seeded in 6-well plates with a density of $3{,}5x10^5$ cells/well. Cells were treated for 24 hours with LPS, with or without pre-incubation with extract or pure compounds for 2 hours. After this period, macrophages were washed with PBS, scraped and incubated with a lysis solution with protease inhibitors for 20 minutes on ice. After this period the solution was centrifuged at 14,000 *g* for 15 minutes and the supernatant collected and protein content determined by the Bradford method. Samples (40 µg) were subjected to 10% SDS-PAGE and proteins were transferred onto nitrocellulose membranes and blocked for one hour at room temperature with a solution of 5% non-fat milk in 0.1% Triton X-100. Overnight incubation at 4°C were performed with antibodies anti-COX-2 (1:1000), anti-iNOS (1:100), anti-CHOP (1:100), anti-IKB-α (1000), anti-tubulin (1:1000) and then with peroxidase-conjugated secondary antibody (1:3000) at room temperature for 1 hour. β-Tubulin was used as a loading control. Finally blots were subjected to a chemiluminescence detection kit (Super Signal West Pico; Pierce, Rockford, USA).

2.11. Statistical analysis

Comparisons of data from different groups, controls and treatments, were performed using a one-way ANOVA test. Dunnet's post-test was used. A *p* value lower than 0.05 was considered statistically significant. All experiments were performed in triplicate.

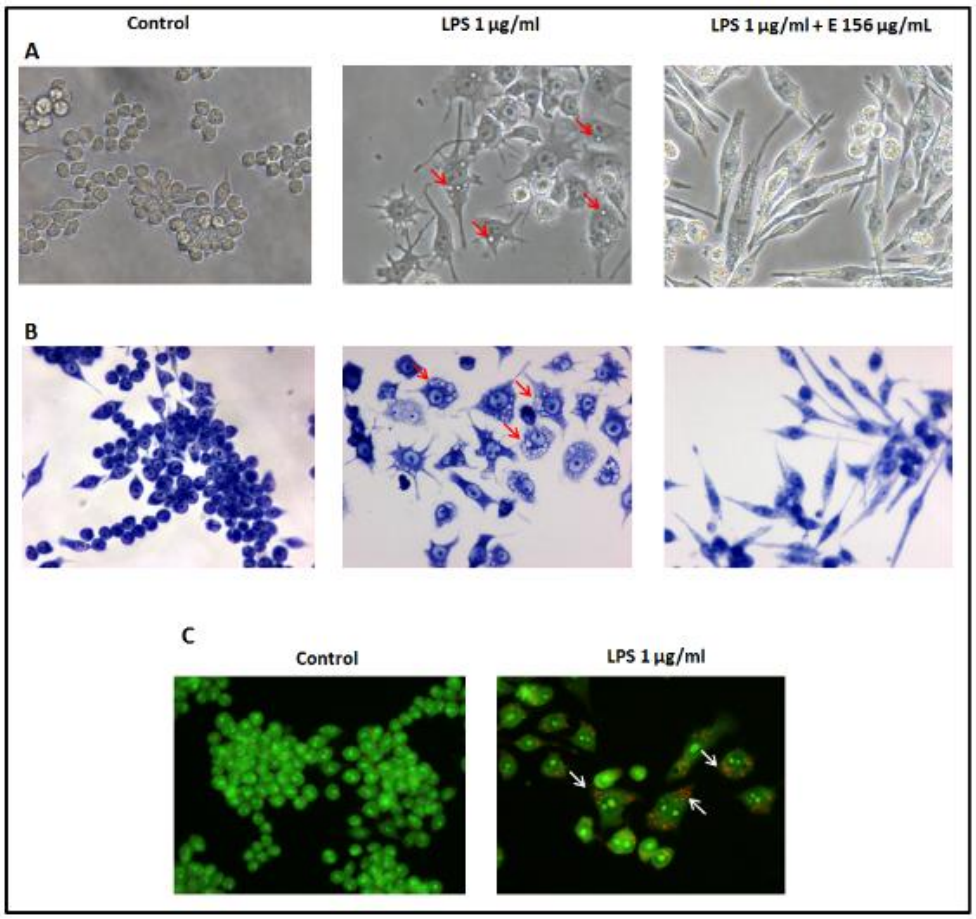

Figure 1 - Evaluation of the effect of LPS and LPS+extract on cell morphology: **A** – phase contrast, **B** – Wright staining. Red arrows: cytoplasmatic vesicles. **C** - Acridine orange staining of control and LPS-treated macrophages. White arrows: autophagosomes. Incubation with LPS causes the characteristic morphology of activated macrophages, which includes the advent of autophagosomes. Pre-incubation with the extract attenuates the number of autophagosomes. Original magnification: 400x.

3. Results

3.1. Extract concentration screening and impact on cell morphology

Given the fact that at the concentration of 312 µg/ml a decrease of about 20% of cell viability was noticed (data not shown), in subsequent experiments lower concentrations (156 µg/mL) were used for testing the anti-inflammatory activity. LDH was not present in culture supernatants in any concentration tested (data not shown).

LPS treatment induced characteristic macrophage-like morphology (Fig. 1). Cytoplasmatic vesicles were noticed and were compatible with autophagosomes described as a result of toll-like receptor 4 (TLR 4) activation by LPS in macrophages [11]. In order to confirm the identity of these autophagosomes, acridine orange was used to confirm their acidic nature (Fig. 1C). As it can be found in Fig. 1A, pre-incubation of macrophages with the extract caused changes in cell morphology and reduced the number of visible autophagossomes.

After this point we evaluated the potential anti-inflammatory activity of the extract by screening its ability to prevent/ameliorate LPS-induced increase in IL-6. As it can be seen in Fig. 2, LPS caused a marked increase in IL-6 levels, which were lowered by about 30% in the presence of the extract.

3.2. Effect of LPS and *M. glacialis* extract / pure compounds upon macrophage viability

LPS challenge resulted in a decrease to 70% of cell viability when compared to control. This effect was prevented by pre-incubation with the extract at a concentration of 156 µg/mL for 2 hours, which restored cell viability of LPS-treated cells to control levels (Fig. 3A). After this, we tested the individual effect of several compounds present in the extract on cell viability.

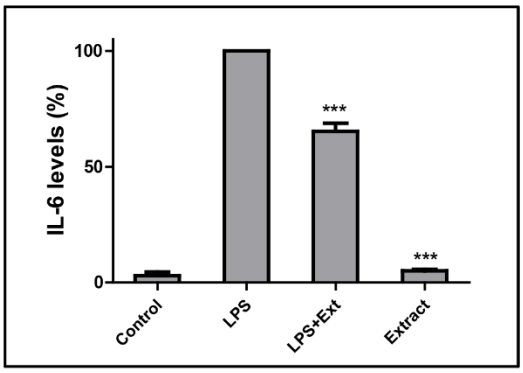

Figure 2 - IL-6 levels determined in culture media. Challenge with LPS causes a marked increase in IL-6 levels, which are partly prevented by pre-incubation with the extract (156 µg/mL) for 2 hours. **Ext**: extract (156 µg/mL). The results correspond to the mean ± SD of three independent experiments performed in triplicate. *** $P<0.001$ (*vs* LPS).

Previous studies have identified and quantified major fatty acids and sterols in *M. glacialis* [9]. We used the same method for the determination of major compounds present in the purified extract used herein. Fatty acids and sterols were major classes in the extract and, at the concentration 156 µg/mL, the major candidates to exert a biological effect were palmitic acid (20 µM), *cis* 11-eicosenoic acid (30 µM), *cis* 11,14-eicosadienoic acid (10 µM) and µM ergosta-7,22-dien-3-ol (25 µM).

All compounds tested individually had no effect in cell viability after 24 hours treatment as assed by the MTT assay (Fig. 3A). When compounds were tested in the presence of LPS, distinct behaviors were found. While *cis* 11-eicosenoic acid had no effect in cell viability, *cis*-11,14- eicosadienoic acid and ergosta-7,22-dien-3-ol had a moderate reduction on LPS-induced loss of viability. Incubation with palmitic acid in a concentration of 20 µM resulted in a marked increase in LPS-induced toxicity. When all compounds were tested together, cell viability was restored to 90% of the control.

3.3. *M. glacialis* extract/pure compounds modulate NO levels *via* down-regulation of iNOS expression

NO was quantified in culture media after challenge with LPS for 24 hours with or without pre-incubation with the extract for 2 hours. NO was present in control samples in negligible amounts and, for this reason, NO production following LPS incubation was considered 100%.

The extract (156 µg/mL) lowered the values of NO by about 50% of those obtained with LPS (Fig. 3B). After this, we investigated the contribution of the three major compounds: *cis*-11-eicosenoic acid, *cis*-11,14-eicosadienoic acid and ergosta-7,22,dien-3-ol. Palmitic acid was not tested isolated due to its above-mentioned impact in cells (70% loss of viability) although it was included in the mixture of major compounds used to mimic the extract. *cis* 11-Eicosenoic acid successfully caused a 10% reduction of NO levels, while *cis* 11,14-eicosadienoic acid and ergosta-7,22,dien-3-ol were capable of lowering NO levels by 20%. When all compounds were incubated together, a 30% decrease in LPS-induced NO levels was found (Fig. 3B).

Several natural products have displayed NO-scavenging capacity and, for this reason, the NO scavenging activity of the extract was evaluated. NO radical was generated in a cell-free chemical system, as described before [12]. Several concentrations were tested and up to a concentration of 625 µg/mL, far higher than the ranges used in cells, no NO scavenging capacity was found (data not shown). We evaluated the effect of the extract on iNOS levels, the major enzyme responsible for the production of NO. While LPS induced a marked increase on iNOS levels, the extract was able to partially prevent this up-regulation (Fig. 4A). *cis*-11-Eicosenoic and *cis*-11,14-eicosadienoic acids were able to reduce LPS-induced increase in iNOS, albeit in low extent (Fig. 4B). The sterol ergosta-7,22-dien-3-ol had a marked effect in iNOS protein levels, being able to revert those to near-control levels, a behavior also found for the combination of all compounds (Fig. 4B).

3.4. *M. glacialis* extract / pure compounds down-regulate COX-2

The study of COX-2 levels after LPS elicitation revealed a marked increase in the expression of this enzyme (Fig. 4A), which is in line with the pro-inflammatory effects described for LPS. When LPS was co-incubated with the extract the levels of COX-2 were significantly reduced, a trend that had already been noticed with iNOS protein expression (Fig. 4A). The study of the contribution of the major components of the extract revealed that, although some compounds had a significant activity, notably ergosta-7,22-dien-3-ol, only the combination of all compounds was able to revert the levels of COX-2 to those of control cells (Fig. 4B).

3.5. *M. glacialis* extract / pure compounds lower LPS-induced ROS

We evaluated the effect of both LPS and the extract upon intracellular levels of ROS in RAW 264.7 cells. Initially, cells were incubated with either media, media with LPS or media with LPS after pre-incubation with the extract and cells were then observed in a fluorescence microscope.

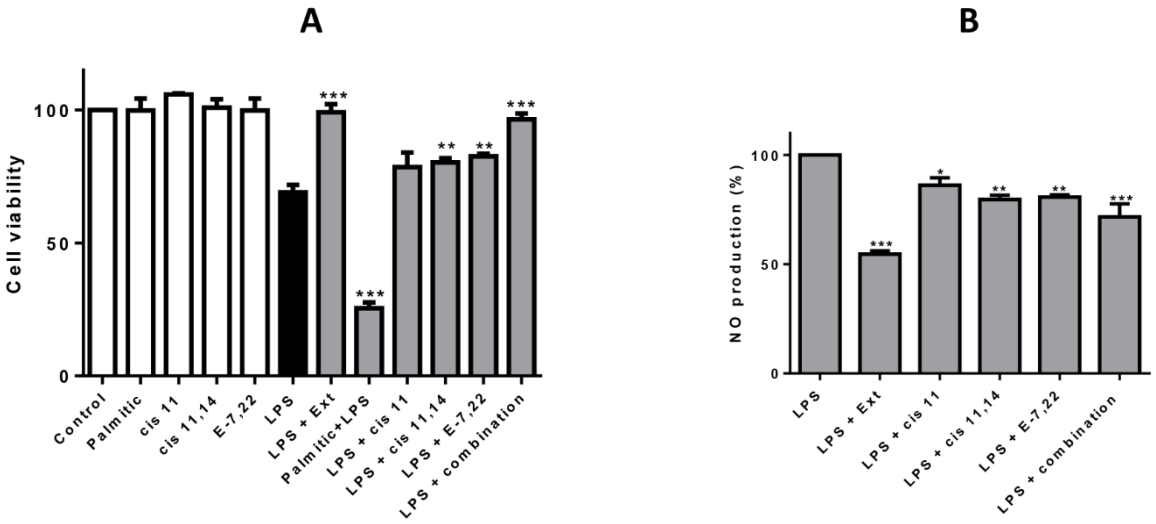

Figure 3 - A - Viability of macrophages after treatment with purified extract or individual compounds with or without LPS after 24 hours of incubation.
B - NO production in RAW 264.7 cells in the presence of a purified extract and of the major compounds in the extract, isolated and in combination after 24 hours of incubation. Compounds were used in the concentrations at which they occur in the extract; ***cis* 11**: 35 µM *cis* 11-eicosenoic acid; ***cis* 11,14**: 10µM *cis* 11,14-eicosadienoic acid; **E-7,22**: 25 µM ergosta-7,22-dien-3-ol. **Ext**: extract (156 µg/mL); **combination**: Palmitc acid + *cis* 11-eicosenoic acid + *cis* 11,14-eicosadienoic + ergosta-7,22-dien-3-ol.The results correspond to the mean ± SD of three independent experiments performed in triplicate. * $P<0.05$; ** $P<0.01$; *** $P<0.001$ (*vs* LPS).

As it can be seen in Fig. 5A, LPS caused an increase in total intracellular ROS when compared with control cells. Co-incubation of LPS with the extract resulted in a partial reversion of this behavior. These qualitative results were then confirmed by quantification of the signal in a fluorescent multi-plate reader. As shown in Fig. 5B, the extract was capable of preventing LPS-induced generation of ROS by around 50%, an effect that could be mimicked by the combination of all compounds tested. Interestingly, the sterol ergosta-7,22-dien-3-ol had no effect on ROS levels at the incubation time studied herein, with the unsaturated fatty acids causing partial reduction of ROS levels.

3.6. *M. glacialis* extract / pure compounds prevent LPS-induced CHOP pathway-mediated ER stress

ER stress has been increasingly implied as a potential source and aggravation of inflammatory processes and CHOP is one of the most commonly used markers of ER-stress [13]. An increase in CHOP expression levels following incubation with LPS was observed, an effect significantly prevented by the extract (Fig. 4A). Unsaturated fatty acids *cis* 11-eicosenoic and *cis* 11,14-eicosadienoic acids were unable to reduce CHOP expression levels in LPS-challenged cells. When cells were incubated in the presence of ergosta-7,22-dien-3-ol CHOP expression was similar to untreated cells (Fig. 4B).

3.7. *M. glacialis* extract / pure compounds prevents NF-κB activation by avoiding IκB-α degradation

NF-κB is usually found in its inactive form in cytoplasm by action of the inhibitory protein IκB-α (Fig. 6). As it can be found in Fig. 5, incubation with LPS caused a decrease in the levels of IκB-α, which can explain all the classical traits of inflammatory process, namely the increase of COX-2, iNOS and IL-6 levels. When cells were pre-incubated with the extract, LPS was unable to cause a reduction in IκB-α levels (Fig. 4A). This protective effect was also found when all compounds tested were evaluated in combination (Fig. 4B). These results show that some of the above-presented findings may result from inhibition of the NF-κB pathway.

4. Discussion

LPS treatment induced the characteristic morphology of activated macrophages. As a result of TLR4 activation by LPS, the advent of autophagosomes is known to occur. We demonstrated that incubation with the purified extract from *M. glacialis* lowered the number of autophagosomes.

The use of LPS as a pro-inflammatory stimulus resulted in a loss of cell viability of about 30%, which could be prevented by pre-incubation with the extract. When the major compounds of the extract were tested individually, no impact on cell viability was found: *cis* 11,14 and ergosta-7,22-dien-3-ol had a protective effect and palmitic acid exacerbated LPS-induced loss of viability. This result

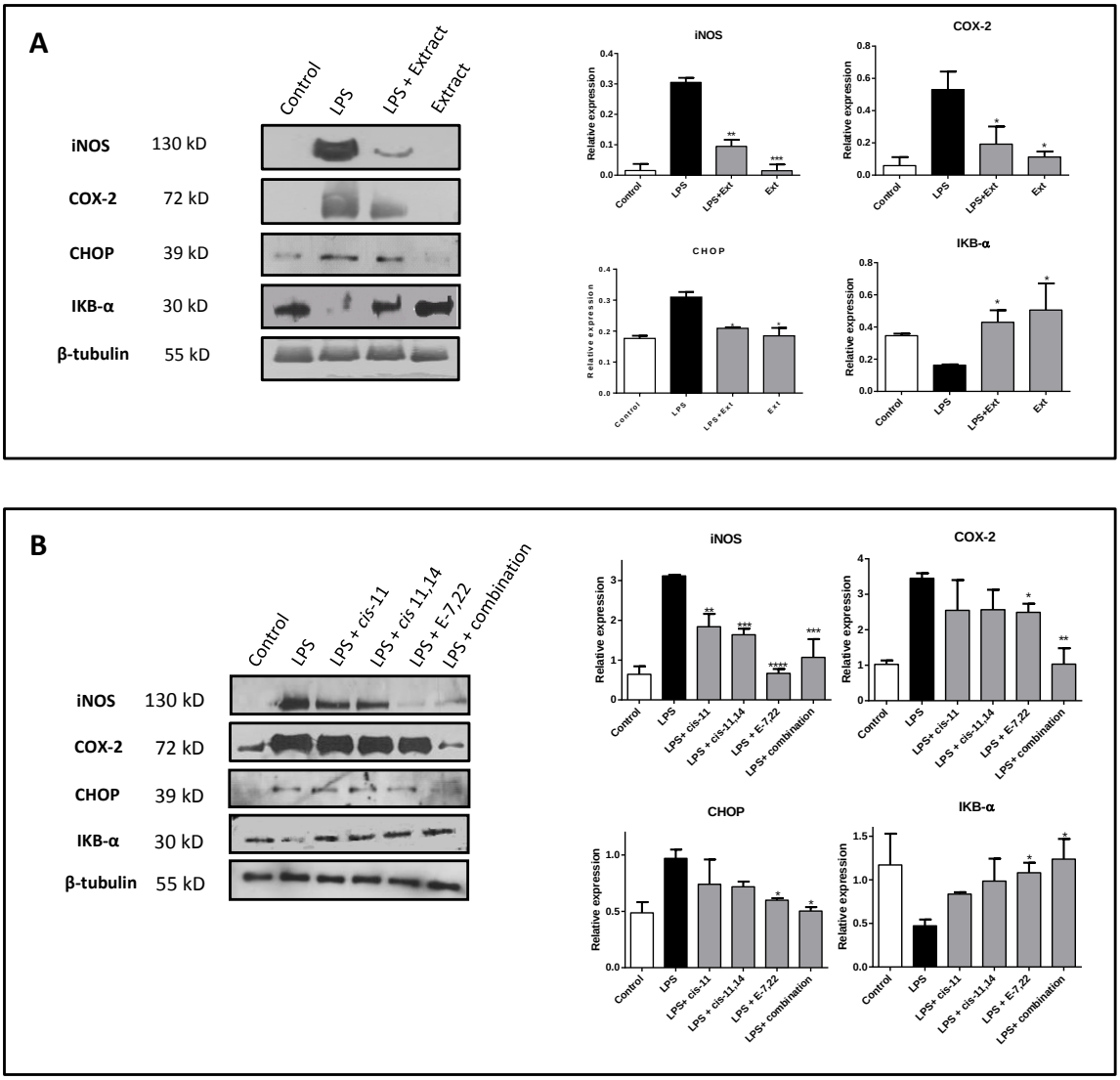

Figure 4 - Effect of **A**) purified extract (156 µg/mL) from *M. glacialis* and **B**) major compounds in the extract in the expression of iNOS, COX-2, CHOP and IKB-α in LPS-treated RAW 264.7 cells. Densitometric analysis of the studied proteins after normalisation to β-tubulin levels. Results are expressed as mean ± SD of three experiments. * $P<0.05$; ** $P<0.01$; *** $P<0.001$ (*vs* LPS). **Ext**: extract (156 µg/mL); **PA**: 20 µM palmitic acid; ***cis* 11**: 35 µM *cis* 11-eicosenoic acid; ***cis* 11,14**: 10µM *cis* 11,14-eicosadienoic acid; **E-7,22**: 25 µM ergosta-7,22-dien-3-ol. **combination**: Palmitic acid + *cis* 11-eicosenoic acid + *cis* 11,14-eicosadienoic + ergosta-7,22-dien-3-ol.

suggests a synergic pro-inflammatory effect of palmitic acid with LPS, which is in line with previous reports that describe palmitic acid as an activator of TLR 4, the same target activated by LPS [14]. When all compounds were combined, reversion of LPS-induced loss of viability occurred, as it had been found for the extract treatment.

The inflammatory marker NO is synthesized from the conversion of arginine to citrulline by nitric oxide synthases, the inducible isoform (iNOS) being the main responsible for the large amounts of NO found in inflammatory processes [15,16]. On the other hand, excessive iNOS activity is known to be related with a number of pathological conditions, such as asthma, psoriasis, neurodegenerative diseases and can lead to NO-induced apoptosis in several cell lines [17-19]. We showed that the extract was able to significantly lower the levels of LPS-induced NO as a result of down-regulation of iNOS, an effect for which all compounds tested contributed, notably ergosta-7,22-dien-3-ol.

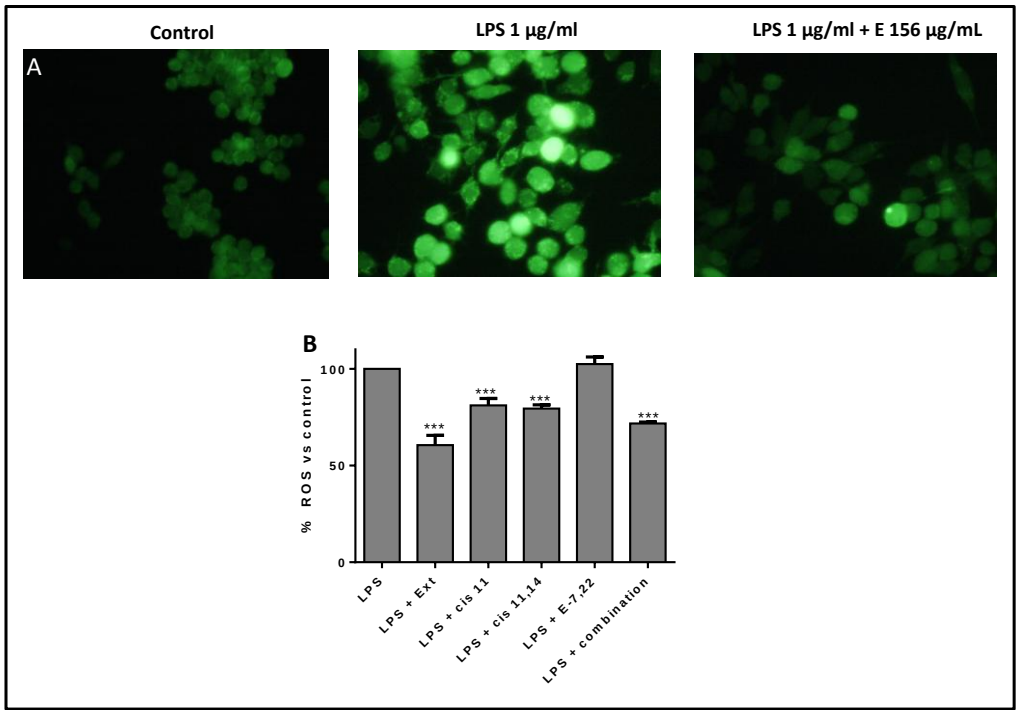

Figure 5 - Evaluation of intracellular ROS assessed by the fluorescent probe DCDHF-DA. **A** – Fluorescence microscopy, qualitative evaluation of the effect of the extract in LPS-activated cells. **B** – Quantitative evaluation of the effect of the extract and its main compounds in LPS-challenged cells. The results correspond to the mean ± SD of three independent experiments performed in triplicate. *** $P<0.001$ (vs LPS). **Ext**: extract (156 µg/mL); ***cis* 11**: 35 µM *cis* 11-eicosenoic acid; ***cis* 11,14**: 10µM *cis* 11,14-eicosadienoic acid; **E-7,22**: 25 µM ergosta-7,22-dien-3-ol. **combination**: Palmitic acid + *cis* 11-eicosenoic acid + *cis* 11,14-eicosadienoic + ergosta-7,22-dien-3-ol.

Three isoforms of cyclooxygenase are known: COX-1, COX-2 and COX-3. In the inflammatory context the inducible isoform, COX-2, is the most significant. We evaluated the effect of both the extract and its compounds in LPS-induced up-regulation of COX-2. As it had been found in the case of iNOS, pre-incubation with the extract prevented LPS-induced increase of the expression levels by over 50%. However, while in the case of iNOS one compound, ergosta-7,22-dien-3ol, was found to be responsible for this activity, in the case of COX-2 no single compound could explain this activity. Instead, the combination of all compounds tested showed higher capacity to prevent LPS-induced up-regulation of COX-2.

ROS are known to play a pivotal role in early stages of inflammation and in the particular case of LPS, the increase in ROS generation has been shown to be an upstream event taking place following exposure to this positive elicitor [20]. We demonstrated that the purified extract from *M. glacialis* prevented LPS-induced increase in ROS levels by about 50%. Differently from what had been found for other inflammatory markers, ergosta-7,22-dien-3-ol had no effect in ROS levels. However, when all compounds were tested together, the activity was comparable to that found for the extract, a trend that had already been found for COX-2 expression levels.

From a cellular point of view, activation of the NF-κB pathway is one of the most important events that trigger the inflammatory response. By studying the levels of the inhibitory protein IκB-α, we showed that the extract and some of its constituents successfully prevented the activation of the NF-κB pathway. Several cellular events, some of them caused by LPS challenge, may trigger the activation of this pathway and among these, ROS and ER-stress are particularly relevant. As we referred above, prevention of ROS generation by the extract and its components can contribute, at least in part, to the anti-inflammatory activity found.

In order to evaluate the other possible causative agent of NF-κB activation, we studied ER-stress status by evaluating the expression of the endpoint protein of the CHOP pathway, which is known to be involved in the pathogenesis of inflammation [21], although the details and sequence of events are not completely understood [13,22]. At this point it is important to highlight that the contribution of CHOP to the fate of RAW 264.7 cells is largely influenced by the type of pro-inflammatory *stimuli* used. When LPS is used alone, CHOP-mediated ER stress alters several metabolic and biochemical traits, though no apoptosis is

detected. Differently, when LPS and IFN-γ are used in combination, NO-induced apoptosis takes place. Further studies showed that these differences are a consequence of a delay in the induction of CHOP by LPS, which takes place only after the activation of ER-protective factors, such as BiP, p58IPK, EDEM, derlin-1 and derlin-2 and, for this reason, an incomplete activation of the CHOP pathway takes place and does not lead to apoptosis. Full activation of ER-stress pathway *via* ER-stress inducers, such as thapsigargin or tunicamycin, is known to induce apoptosis in RAW 264.7 cells [23]. We demonstrated that CHOP expression levels were increased following exposure to LPS, an effect partly reverted by the extract and its components. As so, the attenuation of ER stress that we describe herein for several compounds can contribute, at least in part, to the inhibition of the NF-κB pathway. In addition, due to the established contribution of ROS to further propagate the inflammatory response, namely NF-κB activation and subsequent expression of some inflammatory markers, the above-mentioned capacity of the extract and some of its compounds to attenuated oxidative stress may contribute to the anti-inflammatory activity found.

In summary, in this work we addressed the anti-inflammatory activity of a purified extract and individual compounds present in the spiny sea-star *M. glacialis*. Several markers for inflammation were tested. Overall, the extract reversed LPS-induced loss of viability in RAW 264.7 cells and increase of ROS and NO levels, as well as of the expression of COX-2, iNOS and the ER-stress marker protein CHOP. A proposed mechanism for the anti-inflammatory activity found can be seen in Fig. 6.

A combination of the unsaturated fatty acids *cis*-11-eicosenoic and *cis*-11,14 eicosadienoic acids and the sterol ergosta-7,22-dien-3-ol was able to mimic the anti-inflammatory effect displayed by the extract, although different compounds were active against distinct inflammatory parameters. For example, ergosta-7,22-dien-3-ol was effective against iNOS, CHOP and IKB-α expression, while its importance for the reduction of COX-2 or ROS was limited or null, respectively. As so, we establish the importance of synergism between different classes of metabolites in order to mimic the protective effect of the extract. In addition, besides describing the anti-inflammatory activity of the extract, this is the first report regarding the anti-inflammatory properties of the sterol ergosta-7,22-dien-3-ol, as well as of the unsaturated fatty acids *cis*-11-eicosenoic and *cis*-11,14-eicosadienoic acids.
We suggest that *M glacialis* may be a good source of nutraceuticals with application in inflammatory conditions.

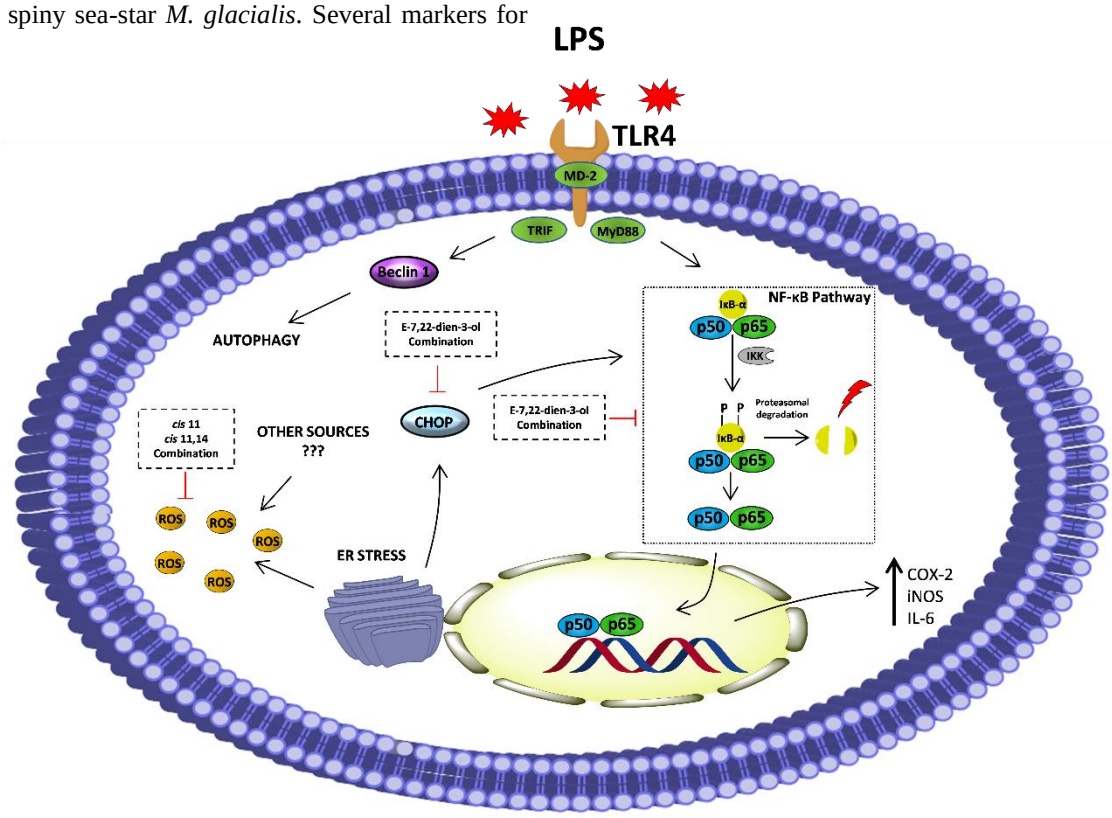

Figure 6 - Proposed mechanism for the anti-inflammatory activity of different compounds present in *M. glacialis.*

The authors thank Fundação para a Ciência e a Tecnologia (FCT) for grant no. PEst-C/EQB/LA0006/2011. David M. Pereira is grateful to FCT for the grant (SFRH/BD/62663/2009).

References

1. Pereira DM, Valentão P, Andrade PB (2013) Lessons from the Sea: Distribution, SAR and Molecular Mechanisms of Anti-inflammatory Drugs from Marine Organisms. In: Atta-ur-Rahman, editor. Studies in Natural Products Chemistry (Bioactive Natural Products). The Netherlands: Elsevier Science Publishers.
2. Dolcet X, Llobet D, Pallares J, Matias-Guiu X (2005) NF-kB in development and progression of human cancer. Virchows Archiv 446: 475-482.
3. Lin Y, Bai L, Chen W, Xu S (2010) The NF-κB activation pathways, emerging molecular targets for cancer prevention and therapy. Expert Opin Ther Tar 14: 45-55.
4. Evans PC (2005) Regulation of pro-inflammatory signalling networks by ubiquitin: identification of novel targets for anti-inflammatory drugs. Expert Rev Mol Med 7: 1-19.
5. Czeczuga B (1977) Investigations of carotenoids in some animals of the Adriatic Sea V. Echinodermata. Hydrobiologia 54: 177-180.
6. Ferreres F, Pereira DM, Gil-Izquierdo A, Valentao P, et al. (2010) HPLC-PAD-atmospheric pressure chemical ionization-MS metabolite profiling of cytotoxic carotenoids from the echinoderm *Marthasterias glacialis* (spiny sea-star). J Sep Sci 33: 2250-2257.
7. Mariutti LRB, Pereira DM, Mercadante AZ, Valentão P, et al. (2012) Further insights on the carotenoid profile of the echinoderm *Marthasterias glacialis*. Mar Drugs 10: 1498-1510.
8. Pereira DM, Correia-da-Silva G, Valentão P, Mouga T, et al. (2013) GC-MS/MS lipidomic profiling of the echinoderm *Marthasterias glacialis* and screening for bioactivity against human cancer and non-cancer cell lines. Submitted.
9. Pereira DM, Vinholes J, Guedes de Pinho P, Valentão P, et al. (2012) A gas chromatography-mass spectrometry multi-target method for the simultaneous analysis of three classes of metabolites in marine organisms. Talanta 100: 391-400.
10. Pereira DM, Noites A, Valentao P, Ferreres F, et al. (2009) Targeted metabolite analysis and biological activity of *Pieris brassicae* fed with *Brassica rapa* var. *rapa*. J Agric Food Chem 57: 483-489.
11. Xu Y, Jagannath C, Liu X-D, Sharafkhaneh A, et al. (2007) Toll-like Receptor 4 is a sensor for autophagy associated with innate immunity. Immunity 27: 135-144.
12. Ferreres F, Pereira DM, Valentão Pc, Andrade PB, et al. (2008) New phenolic compounds and antioxidant potential of *Catharanthus roseus*. J Agric Food Chem 56: 9967-9974.
13. Zhang K, Kaufman RJ (2008) From endoplasmic-reticulum stress to the inflammatory response. Nature 454: 455-462.
14. Shi H, Kokoeva MV, Inouye K, Tzameli I, et al. (2006) TLR4 links innate immunity and fatty acid–induced insulin resistance. J Clin Invest 116: 3015-3025.
15. Alderton WK, Cooper CE, Knowles RG (2001) Nitric oxide synthases: structure, function and inhibition. Biochem J 357: 593-615.
16. Kleinert H, Schwarz PM, Forstermann U (2003) Regulation of the expression of inducible nitric oxide synthase. Biol Chem 384: 1343-1364.
17. Chae I-H, Park K-W, Kim H-S, Oh B-H (2004) Nitric oxide-induced apoptosis is mediated by Bax/Bcl-2 gene expression, transition of cytochrome c, and activation of caspase-3 in rat vascular smooth muscle cells. Clin Chim Acta 341: 83.
18. Oyadomari S, Takeda K, Takiguchi M, Gotoh T, et al. (2001) Nitric oxide-induced apoptosis in pancreatic β cells is mediated by the endoplasmic reticulum stress pathway. P Natl Acad Sci Usa 98: 10845-10850.
19. Takada K, Hirose J, Yamabe S, Uehara Y, et al. (2013) Endoplasmic reticulum stress mediates nitric oxide-induced chondrocyte apoptosis. Biomed Rep 1: 315-319.
20. Asehnoune K, Strassheim D, Mitra S, Kim JY, et al. (2004) Involvement of Reactive Oxygen Species in Toll-Like Receptor 4-Dependent Activation of NF-κB. J Immunol 172: 2522-2529.
21. Endo M, Mori M, Akira S, Gotoh T (2006) C/EBP Homologous Protein (CHOP) is crucial for the induction of caspase-11 and the pathogenesis of lipopolysaccharide-induced inflammation. J Immunol 176: 6245-6253.
22. Liu X-D, Ko S, Xu Y, Fattah EA, et al. (2012) Transient aggregation of ubiquitinated proteins is a cytosolic unfolded

protein response to inflammation and endoplasmic reticulum stress. J Biol Chem 287: 19687-19698.
23. Nakayama Y, Endo M, Tsukano H, Mori M, et al. (2010) Molecular mechanisms of the LPS-induced non-apoptotic ER stress-CHOP pathway. J Biochem 147: 471-483.

Paper 7

Palmitic acid and ergosta-7,22-dien-3-ol contribute to the apoptotic effect and cell cycle arrest of an extract from *M. glacialis* in neuroblastoma cells

David M. Pereira, *Georgina Correia-da-Silva, Patrícia Valentão, Natércia Teixeira, Paula B. Andrade*

Article

Palmitic acid and ergosta-7,22-dien-3-ol contribute to the ER-stress-mediated apoptotic effect and cell cycle arrest of an extract from *Marthasterias glacialis* L. in neuroblastoma cells

David M. Pereira[1], Georgina Correia-da-Silva[2,3], Patrícia Valentão[1], Natércia Teixeira[2,3*], Paula B. Andrade[1*]

[1] REQUIMTE/Laboratório de Farmacognosia, Departamento de Química, Faculdade de Farmácia, Universidade do Porto, Rua de Jorge Viterbo Ferreira, nº 228, 4050-313 Porto, Portugal.
E-Mails: david.ffup@gmail.com (DMP); valentao@ff.up.pt (PV); pandrade@ff.up.pt (PBA)

[2] Laboratório de Bioquímica, Departamento de Ciências Biológicas, Faculdade de Farmácia, Universidade do Porto, Rua de Jorge Viterbo Ferreira, nº 228, 4050-313 Porto, Portugal.
E-mails: george@ff.up.pt (GCS); natercia@ff.up.pt (NT)

[3] IBMC –Instituto de Biologia Molecular e Celular, Universidade do Porto, 4150-180 Porto, Portugal

* Authors to whom corresponde

nce should be addressed. E-Mails: pandrade@ff.up.pt (PBA), Tel: + 351 220428654; natercia@ff.up.pt (NT), Tel: + 351 220428560

Received: / Accepted: / Published:

Abstract: We describe the effect of a chemically characterized lipophilic extract obtained from *Marthasterias glacialis* L. against human breast cancer (MCF-7) and human neuroblastoma (SH-SY5Y) cell lines. Evaluation of DNA synthesis revealed that both cell lines were markedly affected in a concentration-dependent way, SH-SY5Y cell line being more susceptible. Cell cycle arrest was observed, an effect induced by the sterol ergosta-7,22-dien-3-ol present in the extract. Morphological evaluation of treated cells showed the advent of lipid droplets and chromatin condensation compatible with apoptosis, which was confirmed by the evaluation of caspase-3 and -9 activities. Palmitic acid was the main compound responsible for this apoptotic effect by a ceramide-independent mechanism that involved activation of the CHOP-mediated ER-stress pathway.

Keywords: *Marthasterias glacialis* L.; Palmitic acid; ER-stress; CHOP; Apoptosis

---

1. Introduction

Nature is an indisputable source of drugs for human pharmacotherapeutical arsenal [1-3]. In the recent years, marine-derived drugs have received great attention, with a steady increase in the number of molecules in clinical trials [4-7].

The chemical composition of *Marthasterias glacialis* L. has been described before and amino acid, fatty acids, carotenoids and sterols have been identified [8-10]. In addition, the effect of a purified extract upon several human cancer and non-cancer cells was reported [8, 11], though the mechanism responsible for the anticancer activity has not been investigated.

Nowadays, there has been increasing awareness regarding the role of the endoplasmic reticulum (ER) in the homeostasis of the cell. When ER homeostasis is disturbed, the unfolded protein response (UPR) can be activated and the ER stress associated is known to be the basis of several cellular aggressions, namely apoptosis. In order to monitor ER status, three stress sensor proteins are known: double-stranded RNA-dependent protein kinase PKR-like ER kinase (PERK), inositol-requiring 1α (IRE1α) and activating transcription factor 6 (ATF6). In the particular case of PERK, its active form phosphorylates eIF2, which inhibits protein translation. In this branch of UPR, the DNA-damage-inducible gene 153 (GADD153), also known as C/EBP homologous protein (CHOP, a member of the C/EBP transcription factor family that heterodimerizes with other C/EBPs), is upregulated and, for this reason, it is a widely used marker of ER-stress [12-14]. Increased levels of CHOP have been associated with pro-apoptotic effects in several cancer cell lines, an effect attributed to CHOP-mediated repression of BCL2 gene family.

In this work we evaluated the activity of a purified lipophilic extract from *M. glacialis* on the cancer cell lines MCF-7 (estrogen receptor positive human breast cancer cells) and SH-SY5Y (human neuroblastoma cells) and investigated the mechanism involved in cell death and cell cycle arrest. The contribution of the main compounds present in the extract is discussed.

2. Results and Discussion

2.1. Screening of M. glacialis lipophilic extract effect on cell morphology and DNA synthesis

We evaluated the effect of a broad range of concentrations (78-625 µg/mL) of *M. glacialis* lipophilic extract in DNA synthesis. As it can be seen in **Figure 1**, the extract caused a concentration-dependent reduction of DNA synthesis in both cell lines. However, in neuroblastoma cells the effect was stronger and time-independent, while in MCF-7 it was time-dependent. These results are in line with previous reports that point to a similar behavior in what regards to cell viability [11]. The lowest concentrations that elicited a biological effect were selected for morphological studies, 156 and 312 µg/mL for SH-SY5Y and MCF-7 cell lines, respectively.

Figure 1. Rate of DNA synthesis in MCF-7 and SH-SY5Y cells treated with the extract (78-625 µg/mL for 24 or 48 hours) by the ^{3}H-thymidine incorporation assay. The results correspond to the mean ± standard deviation of three independent experiments performed in triplicate.

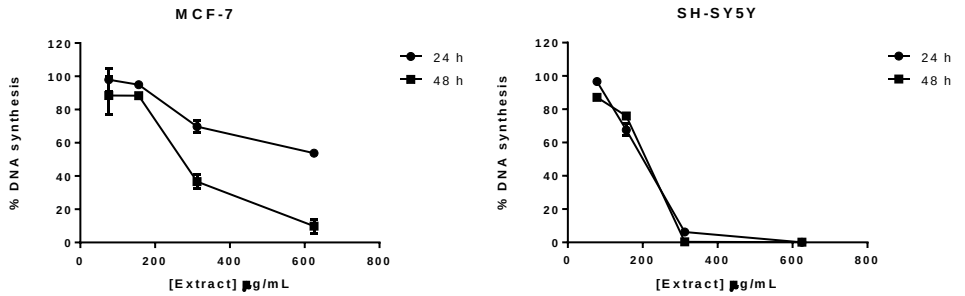

Several techniques were employed for the study of the effect of *M. glacialis* extract on cytoplasmic and nuclear morphology. Both Giemsa and Hoechst 33342 stainings showed chromatin condensation in MCF-7 and SH-SY5Y cells after incubation with the extract for 48 and 24 hours, respectively (**Figures 2** and **3**). In both cell lines, exposure to the extract resulted in cytoplasmic vesicles. Given the lipophilic nature of the extract we hypothesized that these vesicles could be the result of the accumulation of lipid compounds in the cell. For this reason, the Oil Red O staining was performed. As it can be seen in **Figures 2** and **3**, Oil Red O successfully stained the cytoplasmic vesicles, which is compatible with lipid droplets. This result was further confirmed by transmission electron microscopy, which showed that these structures displayed the homogeneous grey opacity commonly found in lipid-containing organelles (**Figure 2**).

As SH-SY5Y cell line showed higher susceptibility, it was selected for subsequent studies.

2.2. Ergosta-7,22-dien-3-ol is responsible for cell cycle arrest

In light of the results from the thymidine incorporation assay, we evaluated the impact of the *M. glacialis* lipophilic extract and of the pure compounds that were present in higher amounts in the extract on the neuroblastoma cells cell cycle. At a concentration of 156 µg/mL, the purified extract caused a G0/G1 arrest, which resulted in an increase of 10% of the number of cells in this phase (**Figure 4**).

In a previous work, we have established the identity of major compounds and their concentrations in the purified extract from *M. glacialis* [11]. At the working concentration of 156 µg/mL, major candidates to exert a biological effect were palmitic acid (20 µM), *cis* 11-eicosenoic acid (30 µM), *cis* 11,14-eicosadienoic acid (10 µM) and ergosta-7,22-dien-3-ol (25 µM). In order to evaluate the compounds responsible for the cell cycle arrest capacity of the extract, these compounds were evaluated individually and in combination after 24 hours of incubation (**Figure 4**). None of the fatty acids tested showed significant effect in these values, while the sterol ergosta-7,22-dien-3-ol was able to cause an effect similar to that of the extract. When all compounds were tested in combination, similar values were found. Our data show that cell cycle arrest caused by the extract can be mostly attributed to the sterol ergosta-7,22-dien-3-ol.

Figure 2. Morphological assessment of MCF-7 cells (control *vs* treatment, 48 hours of incubation). Giemsa and Hoechst 33342 stainings show chromatin condensation (red and white arrows, respectively) following incubation with the extract. Cytoplasmic vesicles, visible in Giemsa staining, proved to harbor lipophilic compounds, as shown with Oil Red O staining and transmission electron microscopy (green arrows).

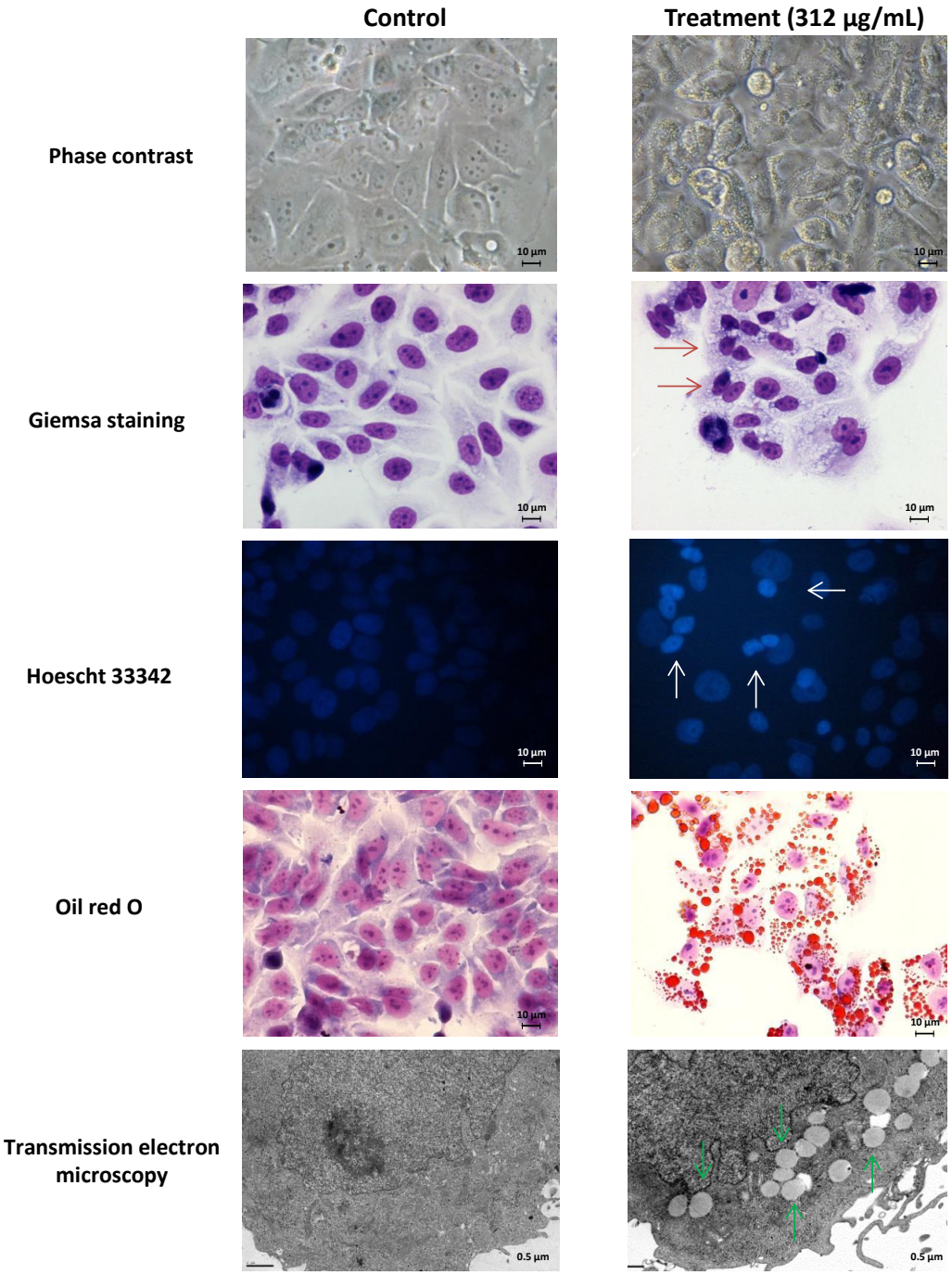

Figure 3. Morphological assessment of SH-SY5Y cells (control *vs* treatment, 24 hours of incubation). Giemsa and Hoechst 33342 stainings show chromatin condensation and fragmentation (red and white arrows). The advent of lipophilic cytosolic vesicles is demonstrated by the Oil Red O staining and transmission electron microscopy (TEM) micrographs.

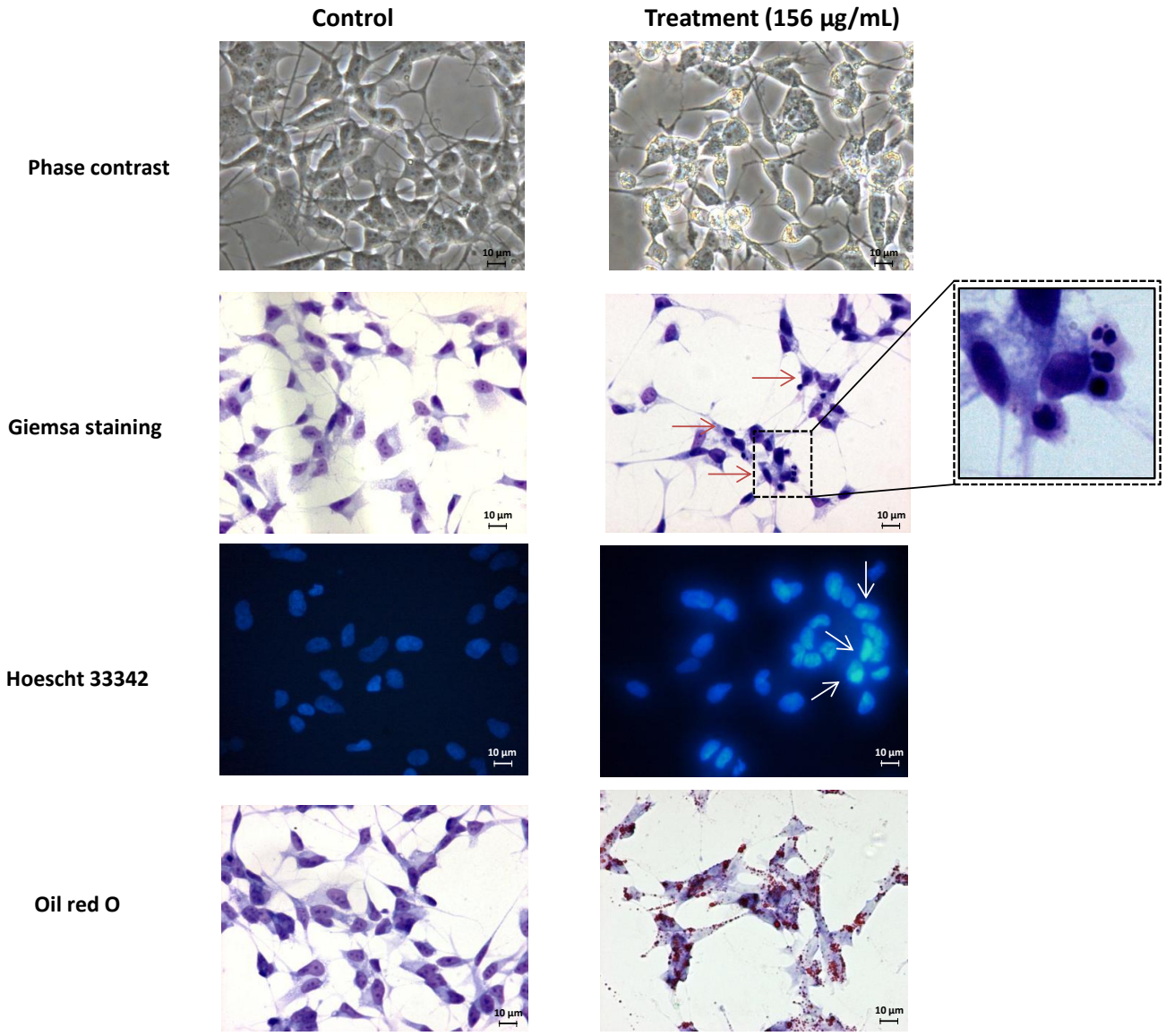

Figure 4. Representative histograms of the effect of *M. glacialis* lipophilic extract and pure compounds on SH-SY5Y cell cycle. The extract caused a cell cycle arrest in the G0/G1 phase, an effect attributed to ergosta-7,22-dien-3-ol. Other major compounds found in the extract had no appreciable effect. Results are expressed as mean ± standard deviation of three experiments. * $P<0.05$; ** $P<0.01$; *** $P<0.001$ (*vs* control). **PA**: 20 µM palmitic acid; ***cis* 11**: 35 µM *cis* 11-eicosenoic acid; ***cis* 11,14**: 10µM *cis* 11,14-eicosadienoic acid; **E-7,22**: 25 µM ergosta-7,22-dien-3-ol; **combination**: palmitic acid + *cis* 11-eicosenoic acid + *cis* 11,14-eicosadienoic + ergosta-7,22-dien-3-ol.

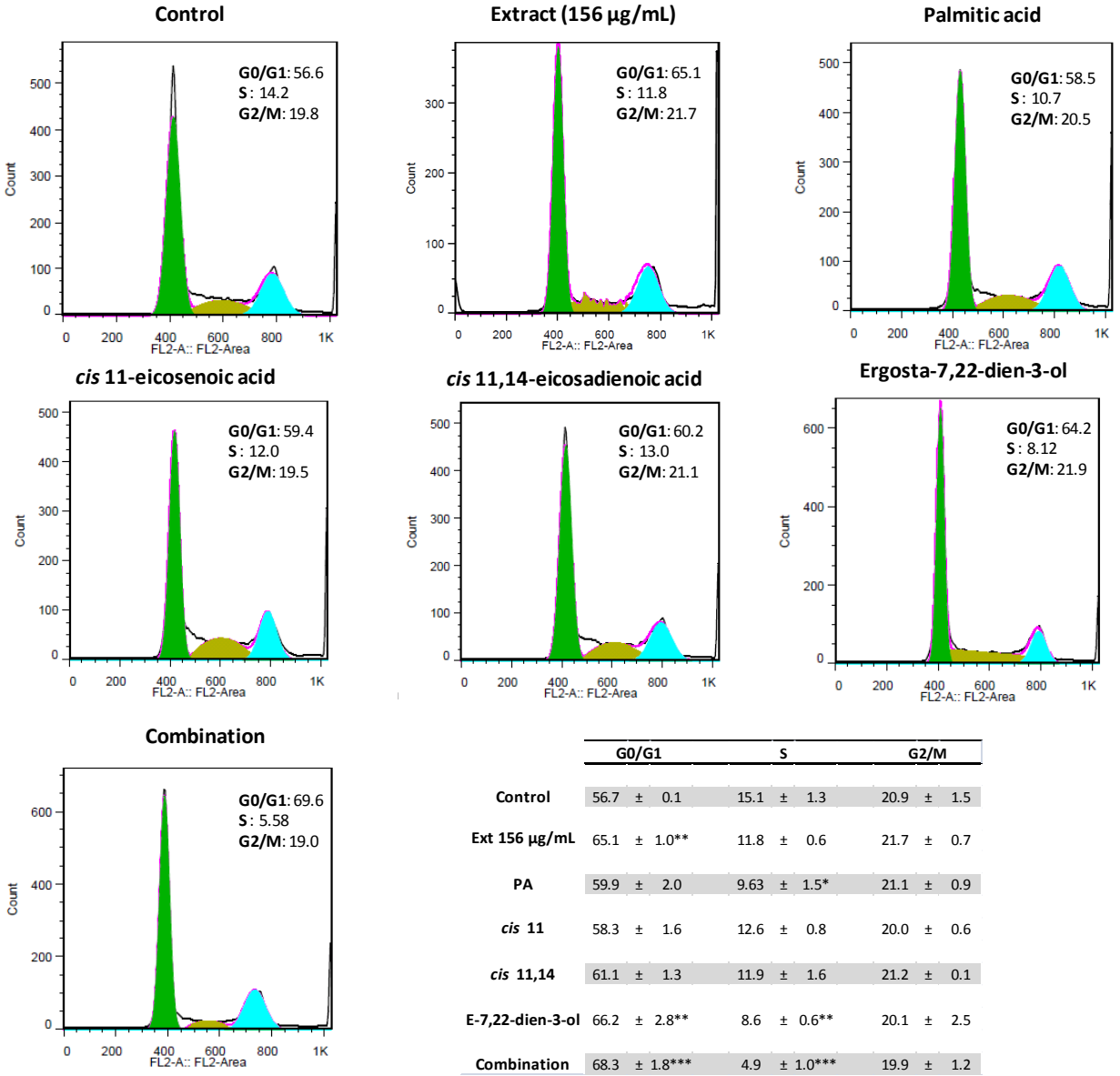

	G0/G1	S	G2/M
Control	56.7 ± 0.1	15.1 ± 1.3	20.9 ± 1.5
Ext 156 µg/mL	65.1 ± 1.0**	11.8 ± 0.6	21.7 ± 0.7
PA	59.9 ± 2.0	9.63 ± 1.5*	21.1 ± 0.9
cis 11	58.3 ± 1.6	12.6 ± 0.8	20.0 ± 0.6
cis 11,14	61.1 ± 1.3	11.9 ± 1.6	21.2 ± 0.1
E-7,22-dien-3-ol	66.2 ± 2.8**	8.6 ± 0.6**	20.1 ± 2.5
Combination	68.3 ± 1.8***	4.9 ± 1.0***	19.9 ± 1.2

2.3. Palmitic acid is responsible for the extract-induced ceramide-independent apoptosis via the intrinsic pathway

In a previous work, we have described the impact of the purified lipophilic extract from *M. glacialis* in cell density, viability and membrane integrity of SH-SY5Y cells. At the concentration of 156 µg/mL, the extract elicited about 30% of reduction in cell viability. Palmitic acid was the likely candidate for this activity however the mechanism of action was not investigated. In the work herein,

we confirmed these results and showed that, apart from palmitic acid, the other compounds had no impact in cell viability (**Figure 5**).

Figure 5. Cell viability was evaluated following incubation with the compounds present in the extract for 24 hours. **PA** - palmitic acid (20 µM); **Cis 11** - *cis* 11-eicosenoic acid (30 µM); **Cis 11,14** - *cis* 11,14-eicosadienoic acid (10 µM); **E-7,22** - ergosta-7,22-dien-3-ol (25 µM). Results are expressed as mean ± standard deviation of 3 experiments. *** $P<0.001$ (*vs* control).

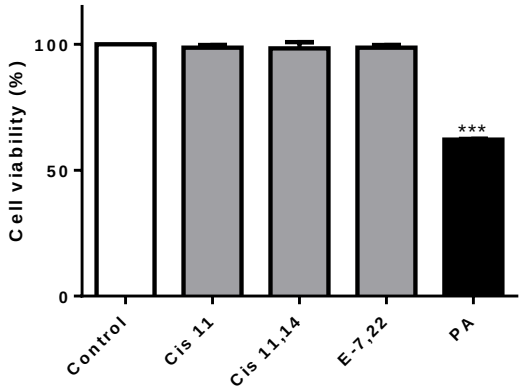

In addition, the morphological assays, by both Giemsa and Hoechst 33342 stainings, showed the appearance of chromatin condensation and the advent of structures compatible with apoptotic bodies. In order to confirm that apoptosis was taking place, we evaluated the activity of caspase-3/7, and -9. After 24 hours of incubation, the extract caused an increase of about 30% in both caspase-3/7 and -9 activity (**Figure 6**). While *cis* 11-eicosenoic and *cis* 11-14,eicosadienoic acids and ergosta-7-22-dien-3-ol had no impact on caspases activity (data not shown), palmitic acid elicited an increase in caspase-9 and -3/7 activity of approximately 12 and 20%, respectively. However, when all compounds were tested in combination, higher values,closer to those displayed by the extract (18 and 25%, respectively),were found. Taken together, these results suggest that, although palmitic acid is the main compound responsible for the pro-apoptotic activity of the extract, its effect is enhanced by the presence of the unsaturated fatty acids and sterol.

Palmitic acid plays several physiological roles in cells, from energy production to structural support in membranes. In addition, it can be the biosynthetic precursor of ceramide. Ceramide is an intra-cellular lipid signaling molecule that is involved in several cellular processes, including differentiation, growth arrest and apoptosis [15, 16]. This process has been widely studied in neuronal cells [17, 18]. Ceramide can be synthesized from palmitic acid *via* the *de novo* pathway, by the action of serine-palmitoyl transferase (SPT) and also from sphyngomyelin, by the enzyme sphingomyelinase [19]. The importance of ceramide to the pro-apoptotic effects of palmitic acid is still in discussion and two distinct mechanisms are known: ceramide-mediated/caspase-3-independent cell death and ceramide-independent/caspase-3-dependent apoptosis [18]. We hypothesized that the high amount of palmitate in the purified extract could induce an increase of intra-cellular levels of ceramide, thus explaining the pro-apoptotic effect of the extract. In order to test this hypothesis, we evaluated the effect of two inhibitors of the key enzymes involved in the *de novo* biosynthesis of ceramide: L-cycloserine and fumonisin B1. As it can be found in **Figure 7**, the co-incubation of the extract with the

two inhibitors had no significant impact on viability and hence we can conclude that the effects of palmitic acid are ceramide-independent. Taken together, these results show that the mechanism of cell death taking place is ceramide-independent and caspase-dependent.

Figure 6. Caspase-3/7 and -9 activity. **Ext -** 156 µg/mL extract; **PA -** palmitic acid (20 µM); **Combination:** PA (20 µM) + *cis* 11-eicosenoic acid (30 µM) + *cis* 11,14-eicosadienoic acid (10 µM) + ergosta-7,22-dien-3-ol (25 µM). Results are expressed as mean ± standard deviation of 3 experiments. ** P<0.01; *** P<0.001 (*vs* control).

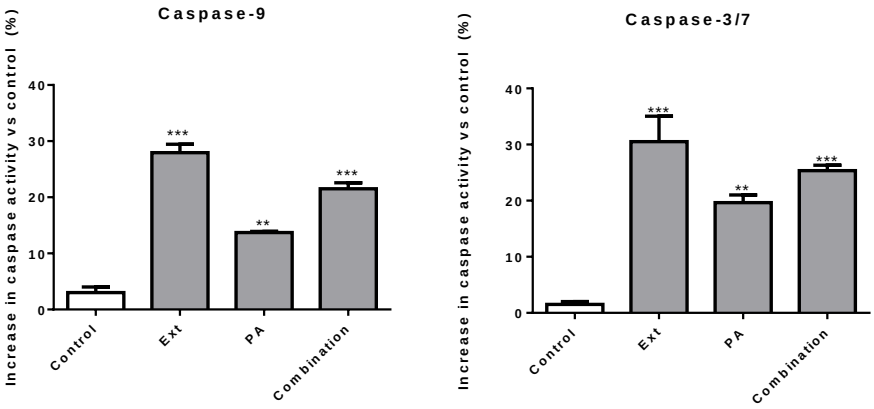

Figure 7. Cell viability of SH-SY5Y cells treated with the extract (Ext, 156 µg/mL) for 24 hours. The ability of L-cycloserine (CSer, 500 µM) and fumonisin B1 (FumB1, 50 µM) to prevent the extract-induced loss of viability was evaluated. Both inhibitors were not cytotoxic. Results are expressed as mean ± standard deviation of 3 experiments. * *P*<0.05(*vs* control).

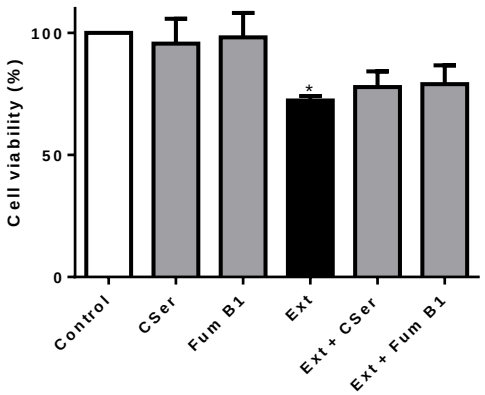

2.4. The extract and palmitic acid cause ER-stress via the CHOP pathway

There has been increasing awareness regarding the role of the ER in the homeostasis of the cell. In particular, ER stress is known to be the basis of several cellular aggressions, namely apoptosis. In order to monitor ER status, CHOP was used due to its role in ER-stress [12-14].

The effect of the extract in the expression of this stress marker was evaluated. As it can be found in **Figure 8**, incubation with the extract resulted in a marked increase of CHOP levels. Palmitic acid has been associated with ER-stress and apoptosis *via* ER-stress in pancreatic β-cells [20], liver cells [21] and Schwann cells [18]. Given the presence of this compound in the extract, it was also tested and, as seen in **Figure 8**, the levels of CHOP protein were residual in control cells and rose significantly in palmitic acid-treated cells.

Figure 8. Effect of the extract (Ext, 156 µg/mL) and palmitic acid (PA, 20 µM) on the expression of CHOP by western blot.

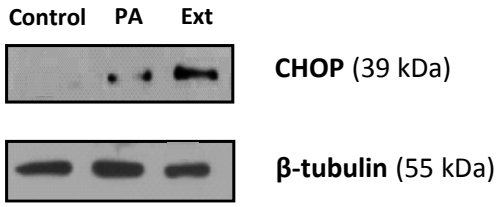

Nowadays the link between ER stress and apoptosis has been established, however the precise mechanisms underlying is not completely understood. Several studies suggest that CHOP-triggered apoptosis is a result of repression of the BCL2 gene family, thus favouring pro-apoptotic proteins, which ultimately led to the activation of caspase-9 and, subsequently, caspase-3. This result is in line with the caspase activation reported above and, for this reason, we suggest that extract/palmitic acid-induced apoptosis is a consequence of ER-stress *via* the CHOP pathway (**Figure 9**). Another player, caspase-12, has been implicated before in mice, however the fact that most humans do not possess an active caspase-12 gene [22, 23] hinders our current understanding of its importance in ER-mediated apoptosis.

Figure 9. Proposed mechanism for the effect of the purified extract from *M. glacialis*. The anti-proliferative effect is caused by ergosta-7,22-dien-3ol, which triggers cell cycle arrest. Palmitic acid is not involved in ceramide biosynthesis. Instead, it causes ER-stress, as depicted by the increase in CHOP expression levels. This protein then triggers apoptosis by interacting with mitochondrial proteins. **SPT** - Serine palmitoyl transferase; **CERase** - ceramidase; **SM** - sphingomyelin; **SM synthase** – sphingomyelin synthase; **CS** – ceramide synthase; **SMase** – Sphingomyelinase.

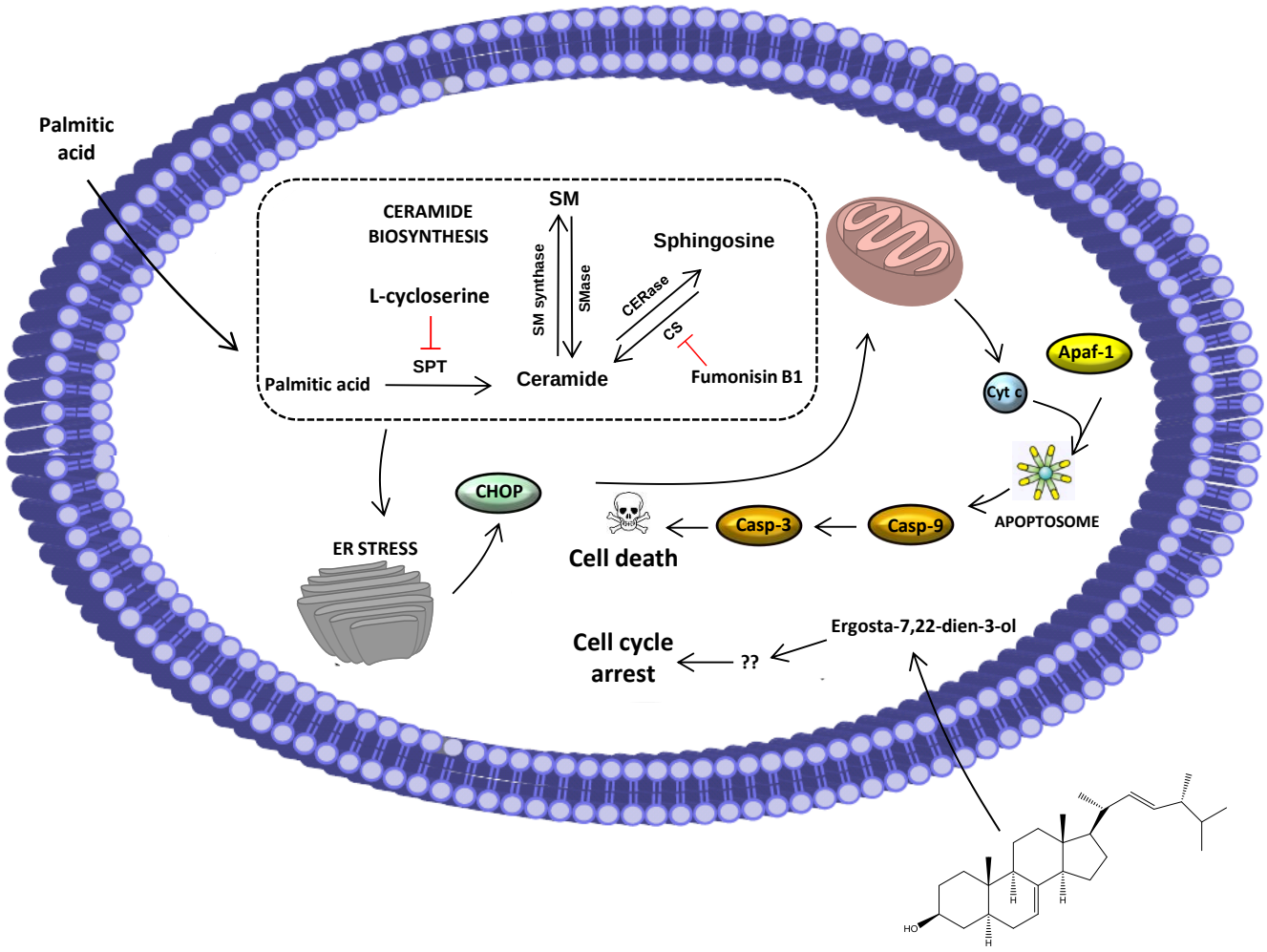

3. Experimental Section

3.1. Reagents and standards

Dulbecco's Modified Eagle Medium (DMEM), trypsin, fetal bovine serum (FBS), phosphate buffer saline (PBS), fungizone and penicillin were from GIBCO (Invitrogen, UK). Oil Red O, glutaraldehyde, *p*-formaldehyde, DNase-free RNase A, palmitic acid (≥99%), *cis* 11-eicosenoic acid (≥99%), *cis* 11,14-eicosadienoic acid (≥98%), Triton X-100 and propidium iodide were from Sigma-Aldrich (St. Louis, MO, USA). Thymidine was from PerkinElmer (Massachusetts, USA). Ergosta-7,22-dien-3-ol (≥98%) was from BioBioPha Co., Ltd (China). L-cycloserine, fumonisin B1, CHOP and β-tubulin primary antibodies, as well as anti-rabbit secondary antibody, were from Santa Cruz (Heidelberg, Germany).

3.2. Extract preparation

M. glacialis individuals were collected in Cabo Carvoeiro, Portugal, in September 2009. Samples were frozen, transported to the laboratory, lyophilized (Labconco 4.5 Freezone apparatus, Kansas City, MO) and powdered using an electric blender.

The lyophilized powder (15 g) was extracted with acetone:methanol (7:3) and the extract was added to a separating funnel with 20 mL of an ether:hexane mixture (1:1). An equivalent volume of 5% NaCl was then added. The mixture was separated into two phases and the aqueous hypophase was collected and re-extracted with the ether:hexane mixture. The organic epiphases were then collected, washed with water in order to remove traces of acetone and evaporated until dryness in a rotary evaporator. All procedures were conducted at room temperature and the final residue was kept at -80 ºC in an inert atmosphere (nitrogen).

3.3. Cell Culture

SH-SY5Y and MCF-7 cells were maintained in DMEM and MEM, respectively, with 10% FBS and 1% penicillin/streptomycin. In the case of SH-SY5Y cells media was also supplemented with 1% non-essential amino acids. All cells were grown in an incubator at 37 °C and 5% CO_2.

3.4. Morphological studies

For Giemsa staining cells were seeded at a density of 2×10^4/well /well in 24-well plates. After incubation with different concentrations of the extract, cells were washed twice with PBS and fixed with cold methanol, at 4°C, for 30 minutes. Diluted Giemsa dye (1:10) was then added and kept for 20 minutes, after which cells were repeatedly washed and then mounted in DPX.

Changes in nuclear morphology were studied by employing the Hoëchst 33342 staining. Cells were fixed as described for Giemsa staining, but 4% *p*-formaldehyde was used as fixing agent. Cells were exposed to 0.5 mg/mL Hoëchst 33342 for 20 minutes at room temperature and mounted in Vectashield mounting medium. Preparations were examined under a fluorescence microscope (Eclipse E400, Nikon, Japan), equipped with an excitation filter with maximum transmission at 360/400 nm, and processed by Nikon ACT-2U image software.

In order to study lipid bodies, methanol-fixed cells were rinsed with propylene glycol and exposed to Oil Red O (0.7% in propylene glycol) for 7 minutes, with agitation. Oil red O solution was

removed and 85% propylene glycol was added and maintained for 3 minutes, after which cells were washed with distilled water and mounted with aqueous mounting media.

For electron microscopy studies, cells were harvested by trypsinization after 24 and 48 hours incubation with the extract, washed with phosphate buffer fixed with 1.25% glutaraldehyde/4% *p*-formaldehyde and preserved at 4°C for further processing. The cells were post-fixed in 1% osmium tetroxide in the same buffer, dehydrated in graded alcohols and embebed in Epon 812. Ultra-thin sections obtained with a Reichert Supra Nova ultra-microtome were collected on copper grids, stained with uranyl acetate/lead citrate and examined in a Zeiss 902A transmission electron microscope.

3.5. ^{3}H-Thymidine incorporation assay

Cells were seeded in 96-well plates (2×10^{4}/well) and incubated with different concentrations of extract. Incubations were maintained for 24–48 hours and, for each exposure time, ^{3}H-thymidine (0.5 μCi) was added to each well and incubated at 37 °C in 5% CO_2 for the last 8 hours. After two cycles of freezing/thawing, cells were harvested using a cell harvester (Skatron Instruments, Norway) and 1 ml scintillation cocktail was added. Incorporated ^{3}H-thymidine was determined in a scintillation counter (LS 6500, Beckman Instruments, CA, USA). Assays were carried out in triplicate and results are representative of three independent experiments.

3.6. Cell cycle analysis

Cell cycle analysis was performed by flow cytometry. Cells were seeded in 6-well plates (7×10^{5}/well) and cultured with or without extract at different concentrations or with the compounds. After 48 hours of treatment, cells were harvested using 0.25% trypsin in EDTA, washed twice with PBS and fixed in 70% cold ethanol.Fixed cells were finally re-suspended in 0.5 ml DNA staining solution (5 μg/ml PI, 0.1% Triton X-100 and 200 μg/ml DNase-free RNase A in PBS) and kept 30 min at room temperature, in the dark.

Flow cytometric analysis of DNA content was based on the acquisition of 20.000 events in a Becton Dickinson FACSCalibur (San Jose, CA, U.S.A) equipped with CELLQuest Pro software. Debris, cell doublets and aggregates were gated out using a two parameter plot of FL-2-Area to FL-2-Width of PI fluorescence. Detectors for forward (FSC) and side (SSC) light scatter and the three fluorescence channels (FL-1, FL-2 and FL-3) were set on a linear scale. Cell cycle histograms were analyzed using FlowJo Software (Tree Star, Inc). Assays were carried out in triplicate and results are representative of three independent experiments.

3.7. Cell viability

Cells were cultured in 96-well plates ($2x10^{4}$ cells/well) and allowed to attach for 24 hours. Cells were pre-incubated with the extract/compounds for 2 hours, after which LPS was added and further incubated for 24 hours. After incubation, MTT (0.5 mg/mL, final concentration) was added to each well and incubated for 2 hours at 37 °C. The formazan was dissolved by addition of a DMSO:isopropanol mixture (3:1) and quantified spectrophotometrically at 560 nm. The results of cell viability correspond to the mean of three independent experiments performed in triplicate and are expressed as percentage of the untreated control cells.

3.8. Caspase-3/7 and -9 activity assay

For the evaluation of caspase-3/7 and -9 activity the luminescent assay kits Caspase-GloH 9, and Caspase-GloH 3/7 (Promega Corporation) were used. Cells were seeded in white 96-well plates in the conditions reported above for MTT. As positive control, cells were incubated with STS (1 μM) for 12 hours. Luminescence was measured in a 96-well Microplate Luminometer (BioTek Instruments) and presented as relative light units (RLU). Assays were carried out in triplicate and results are representative of three independent experiments.

3.9. Western blot

Cells were seeded in 6-well plates with a density of $3.5x10^5$ cells/well. Cells were treated for 24 hours with the extract or palmitic acid. After this period, cells were washed with PBS, scraped and incubated with a lysis solution with protease inhibitors for 20 minutes on ice. The solution was then centrifuged at 14,000 *g* for 15 minutes, the supernatant was collected and protein content was determined by the Bradford method. Samples (40 μg) were subjected to 10% SDS-PAGE and proteins were transferred onto nitrocellulose membranes and blocked for one hour at room temperature with a solution of 5% non-fat milk in 0.1% Triton X-100. Overnight incubation at 4°C was performed with anti-CHOP (1:100) and anti-tubulin (1:1000) and then with peroxidase-conjugated secondary antibody (1:3000) at room temperature for 1 hour. β-Tubulin was used as a loading control. Finally blots were subjected to a chemiluminescence detection kit (Super Signal West Pico; Pierce, Rockford, USA).

4. Conclusions

In this work we described the effect of a lipophilic extract obtained from *M. glacialis* against the human cancer cell lines MCF-7 and SH-SY5Y. Evaluation of DNA synthesis revealed that both cell lines were markedly affected in a concentration-dependent way, the latter being more susceptible. We showed that the extract was responsible for two distinct effects: cell cycle arrest and caspase-dependent apoptosis. We evaluated the contribution of the main compounds and demonstrated that while ergosta-7-dien-3-ol was responsible for the cell cycle arrest, palmitic acid was responsible for the apoptotic effect *via* CHOP-mediated pathway of ER-stress. A proposed mechanism for the activity displayed by the extract can be found in **Figure 9**.

Acknowledgments

This work has been supported by Fundação para a Ciência e a Tecnologia (FCT) through grant no. PEst-C/EQB/LA0006/2011. David M. Pereira is grateful to FCT for the grant (SFRH/BD/62663/2009).

Samples Availability: Available from the authors.

References

1. Altmann, K.-H.; Gertsch, J., Anticancer drugs from nature—natural products as a unique source of new microtubule-stabilizing agents. *Nat. Prod. Rep.* **2007**, *24*, 327-357.
2. Itokawa, H.; Morris-Natschke, S. L.; Akiyama, T.; Lee, K.-H., Plant-derived natural product research aimed at new drug discovery. *J. Nat. Med.-Tokyo* **2008**, *62*, 263-280.
3. Pereira, D. M.; Valentão, P.; Correia-da-Silva, G.; Teixeira, N.; Andrade, P. B., Plant secondary metabolites in cancer chemotherapy: Where are we? *Curr. Pharm. Biotechno.* **2012**, *13*, 632-650.
4. Mayer, A.; Glaser, K. B.; Cuevas, C.; Jacobs, R. S.; Kem, W.; Little, R. D.; McIntosh, J. M.; Newman, D. J.; Potts, B. C.; Shuster, D. E., The odyssey of marine pharmaceuticals: a current pipeline perspective. *Trends Pharmacol. Sci.* **2010**, *31*, 255-265.
5. Montaser, R.; Luesch, H., Marine natural products: a new wave of drugs? *Future Med. Chem.* **2011**, *3*, 1475-1489.
6. Pereira, D. M.; Valentão, P.; Andrade, P. B., Lessons from the Sea: Distribution, SAR and Molecular Mechanisms of Anti-inflammatory Drugs from Marine Organisms. In *Studies in Natural Products Chemistry (Bioactive Natural Products)*, Atta-ur-Rahman, Ed. Elsevier Science Publishers: The Netherlands, 2013.
7. Schumacher, M.; Kelkel, M.; Dicato, M.; Diederich, M., Gold from the sea: marine compounds as inhibitors of the hallmarks of cancer. *Biotechnol. Adv.* **2011**, *29*, 531-547.
8. Ferreres, F.; Pereira, D. M.; Gil-Izquierdo, A.; Valentão, P.; Botelho, J.; Mouga, T.; Andrade, P. B., HPLC-PAD-atmospheric pressure chemical ionization-MS metabolite profiling of cytotoxic carotenoids from the echinoderm *Marthasterias glacialis* (spiny sea-star). *J. Sep. Sci.* **2010**, *33*, 2250-2257.
9. Mariutti, L. R. B.; Pereira, D. M.; Mercadante, A. Z.; Valentão, P.; Teixeira, N.; Andrade, P. B., Further insights on the carotenoid profile of the echinoderm *Marthasterias glacialis*. *Mar. Drugs* **2012**, *10*, 1498-1510.
10. Pereira, D. M.; Vinholes, J.; Guedes de Pinho, P.; Valentão, P.; Mouga, T.; Teixeira, N.; Andrade, P. B., A gas chromatography-mass spectrometry multi-target method for the simultaneous analysis of three classes of metabolites in marine organisms. *Talanta* **2012**, *100*, 391-400.
11. Pereira, D. M.; Correia-da-Silva, G.; Valentão, P.; Mouga, T.; Teixeira, N.; Andrade, P. B., A lipidomic approach to drug discovery from marine organisms: Effect of a purified fraction of the lipidome of the echinoderm *Marthasterias glacialis* L. against human cancer cells. *Unplublished results* **2013**.
12. Ron, D.; Walter, P., Signal integration in the endoplasmic reticulum unfolded protein response. *Nat. Rev. Mol. Cell Bio.* **2007**, *8*, 519-529.
13. Schroder, M.; Kaufman, R. J., The mammalian unfolded protein response. *Annu. Rev. Biochem.* **2005**, *74*, 739-789.
14. Zhang, K.; Kaufman, R. J., From endoplasmic-reticulum stress to the inflammatory response. *Nature* **2008**, *454*, 455-462.

15. Kolesnick, R.; Hannun, Y. A., Ceramide and apoptosis. *Trends Biochem. Sci.* **1999**, *24*, 224-225.
16. Morad, S. A. F.; Cabot, M. C., Ceramide-orchestrated signalling in cancer cells. *Nat. Rev. Cancer* **2013**, *13*, 51-65.
17. Movsesyan, V. A.; Yakovlev, A. G.; Dabaghyan, E. A.; Stoica, B. A.; Faden, A. I., Ceramide induces neuronal apoptosis through the caspase-9/caspase-3 pathway. *Biochem. Biophys. Res. Commun.* **2002**, *299*, 201-207.
18. Suzuki, J.; Akahane, K.; Nakamura, J.; Naruse, K.; Kamiya, H.; Himeno, T.; Nakamura, N.; Shibata, T.; Kondo, M.; Nagasaki, H.; Fujiya, A.; Oiso, Y.; Hamada, Y., Palmitate induces apoptosis in Schwann cells via both ceramide-dependent and independent pathways. *Neuroscience* **2011**, *176*, 188-198.
19. Holland, W. L.; Summers, S. A., Sphingolipids, insulin resistance, and metabolic disease: new insights from *in vivo* manipulation of sphingolipid metabolism. *Endocr. Rev.* **2008**, *29*, 381-402.
20. Karaskov, E.; Scott, C.; Zhang, L.; Teodoro, T.; Ravazzola, M.; Volchuk, A., Chronic palmitate but not oleate exposure induces endoplasmic reticulum stress, which may contribute to INS-1 pancreatic β-cell apoptosis. *Endocrinology* **2006**, *147*, 3398-3407.
21. Wei, Y.; Wang, D.; Topczewski, F.; Pagliassotti, M. J., Saturated fatty acids induce endoplasmic reticulum stress and apoptosis independently of ceramide in liver cells. *Am. J. Physiol-Endoc. M.* **2006**, *291*, E275-E281.
22. Saleh, M.; Vaillancourt, J. P.; Graham, R. K.; Huyck, M.; Srinivasula, S. M.; Alnemri, E. S.; Steinberg, M. H.; Nolan, V.; Baldwin, C. T.; Hotchkiss, R. S., Differential modulation of endotoxin responsiveness by human caspase-12 polymorphisms. *Nature* **2004**, *429*, 75-79.
23. Yavari, M.; Brinkley, G.; Klapstein, K.; Hartwig, W.; Rao, R.; Hermel, E., Presence of the functional CASPASE-12 allele in Indian subpopulations. *Int J Immunogenet* **2012**, *39*, 389-393.

PART III
DISCUSSION AND CONCLUSION

4.1. Chemical composition of *M. glacialis*

The chemical composition of *M. glacialis* had been addressed for the first time in 1977, in a work by Czeczuga et al (164). At the time, the only class of metabolites investigated was carotenoids, which were studied by TLC. In that work, astaxanthin, lutein and zeaxanthin were major compounds.

In the work presented herein, the chemical composition of this organism was revisited and studied using HPLC-DAD and APCI/LC-MS. Identification and confirmation of the presence of several compounds was achieved, astaxanthin, zeaxanthin and lutein being the major carotenoids identified. However, many of the compounds previously described (β-carotene, cryptoxanthin, echinenone, lutein 5,6-epoxide, among others) could not be found (**Paper 1**). At this point, it is important to consider the geographical origin of the sample. While the original 1977 report used organisms collected in the Baltic sea, in the present work samples were collected along the coast of Portugal. Given the fact that animals are, in a general way, unable to synthesize carotenoids, their presence is a consequence of predation upon lower trophic levels. Thus, it is highly probable that organisms collected in distinct sites present different chemical compositions. As several carotenoid peaks could not be identified at the time, a different method, in which HPLC-DAD-APCI-MS/MS was equipped with a C30 column instead of a C18, was used. This approach rendered the identification of twenty compounds, eight of them reported for the first time in this marine organism. Differentiation of carotenoid isomers was also achieved (**Paper 2**).

After carotenoids, the chemical characterization of other classes of metabolites, namely FA, was pursued. In this regard, the need and opportunity to develop a GC-MS technique for a fast and cost-effective analysis of these compounds in marine organisms was identified. During the development of the method, not only saturated and unsaturated FA but also amino acids, sterols and triterpenes were included in the list of metabolites covered by the method. The main factors influencing the extraction of target compounds were evaluated by using different extraction procedures, solvent systems and temperature conditions and a comparison with a reference technique was performed. The most suitable procedure, capable of successfully extract the three classes of target compounds, was ethanol as solvent, at 40 °C under magnetic stirring. Good analytical parameters were obtained for the 40 compounds under analysis (15 amino acids, 16 FA, 6 sterols and 3 lupanes) (**Paper 3**).

Overall, the method proved to be fast (25 minutes run), reproducible and employing cheap and non-hazard solvents (ethanol), contrarily to the classic technique for

the analysis of FA, which requires several organic solvents, high temperatures and longer chromatographic runs. Crude ethanolic extracts of several individuals of *M. glacialis*, collected in different temporal and geographical points, were used for validating this technique and allowed a deeper knowledge of the chemical composition of *M. glacialis* (**Paper 3**).

This method was later used in other marine organisms from Portuguese waters, the echinoderms *Paracentrotus lividus* (sea urchin) and *Holothuria forskali* (sea cucumber), the gastropod molluscs *Aplysia fasciata* and *Aplysia punctata* (sea hares). In general, all species presented all the ten amino acids identified, with the exceptions of *H. forskali*, in which no glycine, proline, *trans* 4-hydroxy-proline or phenylalanine were found, and of *A. fasciata* which did not contain proline. Unsaturated FA were predominant compounds, being those from the ω-6 series in higher amounts than their ω -3 homologues, with the exception of A. fasciata, in which saturated FA were predominant.

In what regards sterols, cholesterol, β-sitosterol and one unidentified cholesterol derivative were the only compounds found. Several other compounds, including ergosterol, stigmasterol and campesterol were searched using their molecular weight and fragmentation spectra, however none were found. The species with the highest sterol content was *P. lividus*, with cholesterol being the sterol in higher amounts in all species studied. (**Paper 4**).

4.2. Anti-inflammatory activity

Several marine organisms have been the source of anti-inflammatory molecules (9). In light of the recognized capacity of some FA and molecules with a steroid backbone to act as anti-inflammatory compounds, the purified extract from *M. glacialis* was evaluated for its potential anti-inflammatory effect (**Paper 6**).

In order to assess the potential anti-inflammatory effect of an extract *M. glacialis* and of its components, the murine macrophage cell line RAW 264.7 was used as a model of inflammation. This *Mus musculus* derived cell line was established from cells of a BAB/14 mouse tumor induced by Abelson murine leukemia virus (MuLV) in 1978 (248). In the particular case of this cell line, following LPS binding to TLR4 receptor and to its co-receptors, CD14 and MD-2, the adaptor protein myeloid differentiation factor 88 (MyD88) is recruited to the Toll/IL-1 receptor (TIR) domain (249, 250). The interaction of TIR and MyD88 leads to the activation of NF-κB. In fact, activation of TLR4/CD14/MD2 receptor complex (251), is sufficient to induce NF-κB activation in several cell types, notably macrophages and microglia (252, 253).

In the structure of LPS, it is important to highlight the lipid A moiety, which has been demonstrated to be the most relevant chemical trait to its pro-inflammatory effect (254). Taking into account the structure of the LPS molecule, it has been hypothesized that saturated FA can, *per si*, induce some pro-inflammatory factors.

Upon LPS treatment, RAW 264.7 respond by activating the NF-κB pathway and rising the levels of some inflammatory markers, like COX-2, iNOS, IL-6, TNF-α, IL-1 and ROS (53, 249, 250, 252, 255).

For the evaluation of the anti-inflammatory activity of the purified lipophilic extract from *M. glacialis*, studies were conducted with a concentration of 156 µg/mL, which was determined by screening studies and presented palmitic, *cis* 11-eicosenoic and *cis* 11,14-eicosadienoic acids and ergosta-7,22-dien-3-ol as main compounds. Incubation with the extract for 24 hours was able to prevent the characteristic morphology of activated macrophages and the LPS-induced autophagosomes. Initial screening assays also showed a reduction of about 30% in the IL-6 levels elicited by LPS.

In this model of inflammation, incubation with the pro-inflammatory *stimuli* LPS resulted in a reduction in cell viability of 30%. This effect was completely prevented by the extract and, from this point, the role of the individual compounds to the activity displayed by the lipophilic extract was studied. Among the compounds tested, none displayed any impact on the viability of unchallenged cells. After this point, the impact of *M. glacialis* extract and isolated compounds in several classical markers of the inflammatory process, like NO and ROS production as well as COX-2 and iNOS expression, was investigated.

The inflammatory mediator NO, synthesized from the conversion of arginine to citrulline by nitric oxide synthases, was quantified in culture media after challenge with LPS for 24 hours with or without pre-incubation with the extract for 2 hours. The extract reduced NO levels produced by LPS-challenged cells by around 50%. *cis* 11-Eicosenoic acid caused a 10% reduction of NO levels, while *cis* 11,14-eicosadienoic acid and ergosta-7,22,dien-3-ol decreased NO levels by 20%. When all compounds were incubated together, a 30% decrease in LPS-induced NO levels were found. This impact on NO levels was shown to be a result of the down-regulation of iNOS, the major enzyme responsible for the production of NO. The extract was able to lower LPS-induced iNOS by about 50%, an effect to which *cis*-11-eicosenoic, *cis*-11,14-eicosadienoic and ergosta-7,22-dien-3-ol contributed, being the latter the most relevant compound for this effect.

In the case of COX-2 the extract was found to lower LPS-induced expression levels of this enzyme by about 50%. However, differently to what was found for iNOS, in which ergosta-7,22-dien-3-ol was responsible for most of the activity, in COX-2 only the combination of all compounds tested was able to achieve maximum inhibition. This result

demonstrates the importance of using a mixture comprising several compounds that act in an additive or synergic way.

ROS are known to play a pivotal role in several physiological and pathological processes, being increased in early stages of inflammation and apoptosis. The purified extract from *M. glacialis* also prevented LPS-induced increase in ROS levels by about 50%. Differently from what had been found for the other inflammatory markers, ergosta-7,22-dien-3-ol had no effect in ROS levels. However, when all compounds were tested together, the activity was comparable to that found for the extract. Several cellular organelles can be the source of these ROS, in particular the ER and mitochondria when undergoing stress (227, 231).

ER stress has been increasingly pointed out as a potential source and aggravation of inflammatory processes, being CHOP one of the most commonly used endpoint markers of ER stress. In accordance to previous studies (237), an increase in CHOP expression levels following incubation with LPS was observed, an effect significantly prevented by the extract. The unsaturated FA *cis* 11-eicosenoic and *cis* 11,14-eicosadienoic acids were unable to reduce CHOP expression levels in LPS-challenged cells. However, when cells were pre-incubated with ergosta-7,22-dien-3-ol CHOP expression was similar to untreated cells, suggesting that this compound was the main responsible for the effect induced by the extract.

On the other hand, it is known that the NF-κB pathway is a key orchestrator that can trigger and modulated the inflammatory response. Thus, by evaluating the levels of the main NF-κB protein inhibitor, IκB-α, the capacity of the extract and some of its constituents in preventing the activation of the NF-κB pathway was demonstrated. Several cellular events, some of them caused by LPS challenge, may trigger the activation of this pathway and among these, ROS and ER stress are particularly relevant. As referred above, prevention of ROS generation and down regulation of CHOP expression by the extract and its components can contribute, at least in part, to the anti-inflammatory activity found. As so, the attenuation of ER stress that we describe herein for several compounds can contribute to the inhibition of the NF-κB pathway. In addition, due to the established contribution of ROS to further propagate the inflammatory response, namely NF-κB activation and subsequent expression of some inflammatory markers, the above-mentioned capacity of the extract and of some of its compounds to attenuate oxidative stress may contribute to the anti-inflammatory activity observed.

4.3. Pro-apoptotic activity

In a preliminary study using a crude extract it was demonstrated that there was selectivity towards cancer cells when compared to non-cancer ones. The IC_{25} obtained for a lipophilic fraction rich in carotenoids was 268 µg/mL in the RBL-2H3 cancer cell line against 411 µg/mL in the non-cancer cell line V79 (**Paper 1**).

In a subsequent study, using the purified and fully characterized lipophilic extract, the effect in cell viability, as well as membrane integrity, was evaluated against a panel of 5 cell lines: 3 cancer cell lines (SH-Sy5Y, human neuroblastoma; MCF-7, human estrogen receptor positive breast cancer and Caco-2, human colon cancer) and 2 non-cancer cell lines (HDF, human dermal fibroblasts and HFF, human foreskin fibroblasts) (**Paper 5**). The effect of the extract in all cell lines was studied at different times (24, 48 and 72 hours) and concentrations ranging from 76 to 1250 µg/mL. Among all cell lines tested, Caco-2 cell line was the most resistant as only the highest concentration, 1250 µg/mL, displayed a reduction of cell viability after 72 hours with no LDH release detected.

In the case of the breast cancer cell line, MCF-7, a time- and dose-dependent reduction of cell viability was found. The concentration of 625 µg/mL caused a decrease in 50% in cell viability after 72 hours. However, regarding membrane integrity, LDH release was already observed after 48 hours of incubation for the highest concentration.

When SH-SY5Y cells were used, only a concentration-dependent effect was found. The reduction of cell viability was more pronounced than that detected for MCF-7 cells. After 24 hours of incubation the concentration of 156 µg/mL caused a decrease of 30% in cell viability. The extract was also tested against the non-cancer cell lines, HDF and HFF, and up to the concentration of 312 µg/mL, which elicited about 80% of cell viability loss in the neuroblastoma cell line, no effect could be noticed.

FA are possible candidates for some of the effects reported herein due to their established role in several physiological and pathological processes. In particular, palmitic acid, the major FA present in the extract, has been reported as a potent inducer of apoptosis in several cell lines. In that way, the effect of palmitic acid in the viability of SH-SY5Y cells, at the concentrations present in the extract, was evaluated. At the extract concentrations of 156 and 312 µg/mL, the concentration of palmitic acid was 15 and 30 µM, respectively. Palmitic acid at 15 µM caused about 20% of cell viability loss in the neuroblastoma cell line, while the extract at 156 µg/mL induced a decrease of approximately 30% of. At higher concentrations, the behaviour was markedly different. While 312 µg/mL caused around 80% of viability loss, the concentration of palmitic acid present in this extract (30 µM), induced only a decrease of 40%. These results suggest that, although palmitic acid has a relevant contribution to the activity displayed by the extract, at higher concentrations the effect of other compounds must be considered.

After this preliminary screening had shown the ability of the extract to lower cancer cells' viability (**Paper 5**), the underlying mechanisms were further explored (**Paper 7**).

Initial studies addressed the effect of the extract on cell morphology. Incubation with the extract caused chromatin condensation and the advent of cytoplasmic structures that were shown, by Oil Red O staining and TEM, to be lipid droplets. These results indicate that the lipophilic compounds identified and quantified in the extract were able to enter the cells and to accumulate in the cytosol.

In light of the biochemical basis of the (3-(4,5-dimethylthiazol-2-yl)-2,5-diphenyltetrazolium bromide (MTT) assay, lower levels of reduced MTT in treated cells can have two possible explanations: decreased cell proliferation or occurrence of cell death. In order to elucidate the underlying mechanism, the effect of the extract in DNA synthesis in MCF-7 and SH-SY5Y cells was evaluated by taking into consideration the extract concentrations previously established. In both cell lines, the extract caused a concentration-dependent reduction in DNA synthesis, although different responses were registered. In the SH-SY5Y cells this effect was more potent and time-independent, while in the MCF-7 cell this effect was time-dependent. The reduction on DNA synthesis was further investigated only in the SH-SY5Y cells, as they showed higher susceptibility. The purified extract, at a concentration of 156 µg/mL, elicited a G0/G1 cell cycle arrest which resulted in an increase of about 10% in the number of cells in this phase. The FA tested showed no effect in cell cycle, while the sterol ergosta-7,22-dien-3-ol was able to cause an effect similar to that of the extract. When all compounds were tested in combination, the same values were found. For this reason, it is concluded that the cell cycle arrest caused by the extract can be attributed solely to the sterol ergosta-7,22-dien-3-ol. Several targets can be responsible for this cell cycle arrest, such as p53, CDK2 and CDK4 (163).

Although it was demonstrated that the extract was causing a decrease in proliferation *via* G0/G1 cell cycle arrest, its ability to trigger cell death was also investigated. Morphological data had already showed that one of the traits of apoptosis, chromatin condensation, was present and, for this reason, caspase 3/7 and -9 activities were evaluated. Incubation with the extract induced an increase in caspase-9 and 3/7 activities of 25% and 30%, respectively, thus showing the intervention of the mitochondrial pathway, an effect for which palmitic acid was responsible. As palmitic acid can be a ceramide precursor, a potent pro-apoptotic molecule, the relevance of this pathway to the effect displayed by the extract was evaluated. In that way, the ability of inhibitors of the key enzymes of ceramide biosynthesis to prevent palmitic acid-induced loss of cell viability was assessed. Experiments conducted with L-cycloserine (inhibitor of serine palmitoyltransferase) and fumonisin B1 (inhibitor of ceramide synthase) showed

that this effect was ceramide-independent. In this research area, there are contradicting reports regarding the role of ceramide in palmitate-induced apoptosis. Recently, a study addressing this topic in Schwann cells showed that, although inhibition of *de novo* ceramide biosynthesis could ameliorate palmitate-induced apoptosis, the effect was only partial. For this reason, the authors suggested that palmitate may induce apoptosis in a ceramide-dependent and –independent way (256).

Due to the fact that palmitic acid has been implicated in ER stress (257, 258), and that there is a crosstalk between ER-stress and apoptosis, CHOP expression was analyzed. CHOP is an endpoint product in most of the mechanisms that are associated to ER stress, thus being generally used as a marker for ER stress. Results showed that both the extract and palmitic acid elicited an increase in CHOP expression levels, which were absent in control cells.

Taken together, these results suggest that the effect exhibited by the extract involves ergosta-7,22-dien-3-ol-mediated cell cycle arrest and palmitic acid-caused activation of the intrinsic pathway of apoptosis by a ceramide-independent way. In addition, this effect is associated to ER stress. Although not addressed in the work herein, the investigation of the contribution of caspase-4/12 to ER stress-derived apoptosis could also be a valuable tool. In these regards, it is important to highlight that the role of caspase-12 in ER stress-mediated apoptosis is not unanimous. Some authors report that this caspase can, *per si*, trigger the apoptotic process, while others refer its importance in propagating and increasing the response of caspases-3 and -9 (239, 240). In addition, if we consider that most humans do express caspase-12, all together these information clearly highlight the importance of continuing to study the pathways involved in ER-mediated apoptosis (241, 242).

Several concluding remarks can be drawn from all the data obtained in this research project.

Instrumental techniques for a fast and multi-target analysis of marine organisms were developed and their application across several taxonomic groups was demonstrated. In addition, the potential application of marine-derived molecules in several pathological conditions was confirmed. By conjugating metabolomic analysis with biological evaluation, several bioactive molecules were described and their effects in cancer and inflammation were demonstrated and, additionally, the mechanisms of action involved were elucidated. In both model systems, ER stress was shown to play an important role, although the effect of the extract and its components was distinct. Thus, while in cancer cells ER-stress was induced, hence triggering apoptosis, in the case of macrophages the anti-inflammatory effect was associated with ER protection.

PART IV
BIBLIOGRAPHY

1. Samuelsson G. Drugs of natural orign: a textbook of pharmacognosy. Stockholm: Swedish Pharmaceutical Press; 2004.
2. Kingston DGI. Tubulin-interactive natural products as anticancer agents. Journal of Natural Products. 2009;72(3):507-15.
3. Costantino L, Barlocco D. Privileged structures as leads in medicinal chemistry. Current Medicinal Chemistry. 2006;13(1):65-85.
4. Cragg GM, Newman DJ. Nature: a vital source of leads for anticancer drug development. Phytochemistry Reviews. 2009;8(2):313-31.
5. Li JW-H, Vederas JC. Drug discovery and natural products: end of an era or an endless frontier? Science. 2009;325(5937):161-5.
6. Albericio F, Álvarez M, Cuevas C, Francesch A, Pla D, Tulla-Puche J. The sea as a source of new drugs. Molecular imaging for integrated medical therapy and drug development: Springer; 2010. p. 237-49.
7. Jha RK, Zi-rong X. Biomedical compounds from marine organisms. Marine drugs. 2004;2(3):123-46.
8. Pereira DM, Correia-da-Silva G, Valentão P, Teixeira N, Andrade PB. Marine metabolomics in cancer chemotherapy. In: Barh D, editor. OMICS: Biomedical Perspectives and Applications CRC Press; 2011.
9. Pereira DM, Valentão P, Andrade PB. Lessons from the sea: distribution, SAR and molecular mechanisms of anti-inflammatory drugs from marine organisms. In: Atta-ur-Rahman, editor. Studies in Natural Products Chemistry (Bioactive Natural Products). The Netherlands: Elsevier Science Publishers; 2013.
10. Pereira DM, Vinholes J, Correia-da-Silva G, Valentao P, Teixeira N, Andrade PB. Fatty acids in marine organisms: in the pursuit of bioactive agents. Current Pharmaceutical Analysis. 2011;7(2):108-19.
11. Poulos A. Very Long-Chain Fatty-acids in higher animals - a review. Lipids. 1995;30(1):1-14.
12. Dewick PM. Medicinal Natural Products: A Biosynthetic Approach. 3rd ed: John Wiley & Sons Ltd; 2009.
13. Barnathan G. Non-methylene-interrupted fatty acids from marine invertebrates: Occurrence, characterization and biological properties. Biochimie. 2009;91(6):671-8.
14. Berge JP, Barnathan G. Fatty acids from lipids of marine organisms: Molecular biodiversity, roles as biomarkers, biologically active compounds, and economical aspects. Advances in Biochemical Engineering/Biotechnology. 2005;96:49-125.
15. Carballeira NM, Alicea J. The first naturally occurring α-methoxylated branched-chain fatty acids from the phospholipids of *Amphimedon complanata*. Lipids. 2001;36(1):83-7.

16. Carballeira NM, Pagan M. New methoxylated fatty acids from the Caribbean sponge *Callyspongia fallax*. Journal of Natural Products. 2001;64(5):620-3.
17. Lobo AM, Lourenço AM. Metabolitos derivados do ácido acético. In: Lobo AM, Lourenço AM, editors. Biossíntese de produtos naturais: IST Press; 2007. p. 77-118.
18. Tvrdik P, Westerberg R, Silve S, Asadi A, Jakobsson A, Cannon B, et al. Role of a new mammalian gene family in the biosynthesis of very long chain fatty acids and sphingolipids. Journal of Cell Biology. 2000;149(3):707-17.
19. Cinti DL, Cook L, Nagi MN, Suneja SK. The fatty-acid chain elongation system of mammalian endoplasmic-Reticulum. Progress in Lipid Research. 1992;31(1):1-51.
20. Folch J, Lees M, Sloane Stanley GH. A simple method for the isolation and purification of total lipides from animal tissues. Jornal of Biological Chemistry. 1957;226(1):497-509.
21. Bligh EG, Dyer WJ. A rapid method of total lipid extraction and purification. Canadian Journal of Biochemistry and Physiology. 1959;37(8):911-7.
22. Lacaze JP, Stobo LA, Turrell EA, Quilliam MA. Solid-phase extraction and liquid chromatography-mass spectrometry for the determination of free fatty acids in shellfish. Journal of Chromatography A. 2007;1145(1-2):51-7.
23. Mu H, Sundin P, Wesén C. Halogenated fatty acids II. Methods of determination in lipids. Trac - Trend Anal Chem. 1997;16(5):274-86.
24. Sato D, Ando Y, Tsujimoto R, Kawasaki K. Identification of novel nonmethylene-interrupted fatty acids, 7E,13E-20 : 2, 7E,13E,17Z-20 : 3, 9E,15E,19Z-22 : 3, and 4Z,9E,15E,19Z-22 : 4, in Ophiuroidea (brittle star) lipids. Lipids. 2001;36(12):1371-5.
25. Arao K, Inagaki M, Higuchi R. Constituents of crinoidea. 2. Isolation and structure of the novel type gangliosides from the feather star *Comanthus japonica*. Chemical and Pharmaceutical Bulletin. 2001;49(6):695-8.
26. Copeman LA, Parrish CC. Marine lipids in a cold coastal ecosystem: Gilbert Bay, Labrador. Marine Biology. 2003;143(6):1213-27.
27. Drazen JC, Phleger CF, Guest MA, Nichols PD. Lipid, sterols and fatty acid composition of abyssal holothurians and ophiuroids from the North-East Pacific Ocean: food web implications. Comparative Biochemistry and Physiology Part B - Biochemistry and Molecular Biology. 2008;151(1):79-87.
28. Inagaki M, Shiizaki M, Hiwatashi T, Miyamoto T, Higuchi R. Constituents of Crinoidea. 5. Isolation and structure of a new glycosyl inositolphosphoceramide-type ganglioside from the feather star *Comanthina schlegeli*. Chemical and Pharmaceutical Bulletin. 2007;55(11):1649-51.

29. Takagi T, Kaneniwa M, Itabashi Y, Ackman RG. Fatty-Acids in Echinoidea - unusual *cis*-5-olefinic acids as distinctive lipid components in sea-urchins. Lipids. 1986;21(9):558-65.
30. Meier S, Mjos SA, Joensen H, Grahl-Nielsen O. Validation of a one-step extraction/methylation method for determination of fatty acids and cholesterol in marine tissues. Journal of chromatography A. 2006;1104(1-2):291-8.
31. Saraiva D, Semedo R, Castilho Mda C, Silva JM, Ramos F. Selection of the derivatization reagent--the case of human blood cholesterol, its precursors and phytosterols GC-MS analyses. Journal of Chromatography B - Analytical Technologies in Biomedical and Life Sciences. 2011;879(32):3806-11.
32. Schummer C, Delhomme O, Appenzeller BM, Wennig R, Millet M. Comparison of MTBSTFA and BSTFA in derivatization reactions of polar compounds prior to GC/MS analysis. Talanta. 2009;77(4):1473-82.
33. Andersson BÅ. Mass spectrometry of fatty acid pyrrolidides. Progress in the Chemistry of Fats and other Lipids. 1978;16(C):279-308.
34. Christie WW. Gas chromatography mass spectrometry methods for structural analysis of fatty acids. Lipids. 1998;33(4):343-53.
35. Dobson G, Christie WW. Structural analysis of fatty acids by mass spectrometry of picolinyl esters and dimethyloxazoline derivatives. TrAC-Trends in Analytical Chemistry. 1996;15(3):130-7.
36. Dobson G, Christie WW. Mass spectrometry of fatty acid derivatives. European Journal of Lipid Science and Technology. 2002;104(1):36-43.
37. Das UN. Essential Fatty Acids: Biochemistry and Physiology. Metabolic Syndrome Pathophysiology: Wiley-Blackwell; 2010. p. 181-200.
38. Dowhan W. Molecular basis for membrane phospholipid diversity: Why are there so many lipids? Annual Review of Biochemistry. 1997;66:199-232.
39. Bergsson G, Arnfinnsson J, Steingrimsson O, Thormar H. In vitro killing of *Candida albicans* by fatty acids and monoglycerides. Antimicrobial Agents and Chemotherapy. 2001;45(11):3209-12.
40. Carballeira NM. New advances in fatty acids as antimalarial, antimycobacterial and antifungal agents. Progress in Lipid Research. 2008;47(1):50-61.
41. Kabara JJ, Swieczko.Dm, Truant JP, Conley AJ. Fatty-acids and derivatives as antimicrobial agents. Antimicrobial agents and Chemotherapy. 1972;2(1):23-&.
42. Brown DA, London E. Functions of lipid rafts in biological membranes. Annual Review of Cell and Development Biology. 1998;14:111-36.
43. Lingwood D, Simons K. Lipid rafts as a membrane-organizing principle. Science. 2010;327(5961):46-50.

44. Simons K, Sampaio JL. Membrane organization and lipid rafts. Cold Spring Harbor Perspectives in Biology. 2011;3(10).
45. Simons K, Toomre D. Lipid rafts and signal transduction. Nature Reviews Molecular Cell biology. 2000;1(1):31-9.
46. Schrick K, Mayer U, Martin G, Bellini C, Kuhnt C, Schmidt J, et al. Interactions between sterol biosynthesis genes in embryonic development of Arabidopsis. The Plant journal : for cell and molecular biology. 2002;31(1):61-73.
47. Xu XL, Bittman R, Duportail G, Heissler D, Vilcheze C, London E. Effect of the structure of natural sterols and sphingolipids on the formation of ordered sphingolipid/sterol domains (rafts). Journal of Biological Chemistry. 2001;276(36):33540-6.
48. Lee JY, Sohn KH, Rhee SH, Hwang D. Saturated fatty acids, but not unsaturated fatty acids, induce the expression of cyclooxygenase-2 mediated through Toll-like receptor 4. J Biol Chem. 2001;276(20):16683-9.
49. Calder PC. n-3 polyunsaturated fatty acids, inflammation, and inflammatory diseases. American Journal of Clinical Nutrition. 2006;83(6 Suppl):1505S-19S.
50. Simopoulos AP. Importance of the ratio of omega-6/omega-3 essential fatty acids: evolutionary aspects. World Review of Nutrition and Dietetics. 2003;92:1-22.
51. Wall R, Ross RP, Fitzgerald GF, Stanton C. Fatty acids from fish: the anti-inflammatory potential of long-chain omega-3 fatty acids. Nutrition Reviews. 2010;68(5):280-9.
52. Simopoulos AP. Essential fatty acids in health and chronic diseases. Forum of Nutrition. 2003;56:67-70.
53. Shi H, Kokoeva MV, Inouye K, Tzameli I, Yin H, Flier JS. TLR4 links innate immunity and fatty acid–induced insulin resistance. Journal of Clinical Investigation. 2006;116(11):3015-25.
54. Chambrier C, Bastard JP, Rieusset J, Chevillotte E, Bonnefont-Rousselot D, Therond P, et al. Eicosapentaenoic acid induces mRNA expression of peroxisome proliferator-activated receptor γ. Obesity Research. 2002;10(6):518-25.
55. Draper E, Reynolds CM, Canavan M, Mills KH, Loscher CE, Roche HM. Omega-3 fatty acids attenuate dendritic cell function via NF-κB independent of PPARγ. The Journal of Nutritional Biochemistry. 2011;22(8):784-90.
56. Loscher CE, Draper E, Leavy O, Kelleher D, Mills KH, Roche HM. Conjugated linoleic acid suppresses NF-κB activation and IL-12 production in dendritic cells through ERK-mediated IL-10 induction. The Journal of Immunology. 2005;175(8):4990-8.

57. Giovannucci E, Goldin B. The role of fat, fatty acids, and total energy intake in the etiology of human colon cancer. American Journal of Clinical Nutrition. 1997;66(6 Suppl):1564S-71S.
58. Terry P, Lichtenstein P, Feychting M, Ahlbom A, Wolk A. Fatty fish consumption and risk of prostate cancer. Lancet. 2001;357(9270):1764-6.
59. Cheng J, Ogawa K, Kuriki K, Yokoyama Y, Kamiya T, Seno K, et al. Increased intake of n-3 polyunsaturated fatty acids elevates the level of apoptosis in the normal sigmoid colon of patients polypectomized for adenomas/tumors. Cancer Letters. 2003;193(1):17-24.
60. Roynette CE, Calder PC, Dupertuis YM, Pichard C. n-3 polyunsaturated fatty acids and colon cancer prevention. Clinical Nutrition. 2004;23(2):139-51.
61. Roynette CE, Calder PC, Dupertuis YM, Pichard C. n-3 polyunsaturated fatty acids and colon cancer prevention. Clinical nutrition. 2004;23(2):139-51.
62. Hossain Z, Hosokawa M, Takahashi K. Growth inhibition and induction of apoptosis of colon cancer cell lines by applying marine phospholipid. Nutrition and Cancer. 2009;61(1):123-30.
63. Slagsvold JE, Pettersen CHH, Follestad T, Krokan HE, Schonberg SA. The antiproliferative effect of EPA in HL60 cells is mediated by alterations in calcium homeostasis. Lipids. 2009;44(2):103-13.
64. Carballeira NM, Betancourt JE, Orellano EA, Gonzalez FA. Total synthesis and biological evaluation of (5Z,9Z)-5,9-hexadecadienoic acid, an inhibitor of human topoisomerase I. Journal of Natural Products. 2002;65(11):1715-8.
65. Mizushima T, Natori S, Sekimizu K. Inhibition of *Escherichia coli* DNA topoisomerase-I activity by phospholipids. Biochemical Journal. 1992;285:503-6.
66. Suzuki K, Shono F, Kai H, Uno T, Uyeda M. Inhibition of topoisomerases by fatty acids. Journal of Enzyme Inhibition. 2000;15(4):357-66.
67. Carballeira NM, Sanabria D, Oyola D. An improved synthesis for the (Z)-14-methyl-9-pentadecenoic acid and its topoisomerase I inhibitory activity. Arkivoc. 2007;2007(8):49-57.
68. Mizushina Y, Tsuzuki T, Eitsuka T, Miyazawa T, Kobayashi K, Ikawa H, et al. Inhibitory action of conjugated C18-fatty acids on DNA polymerases and DNA topoisomerases. Lipids. 2004;39(10):977-83.
69. Yonezawa Y, Tsuzuki T, Eitsuka T, Miyazawa T, Hada T, Uryu K, et al. Inhibitory effect of conjugated eicosapentaenoic acid on human DNA topoisomerases I and II. Archives of Biochemistry and Biophysics. 2005;435(1):197-206.

70. Nemoto T, Ojika M, Sakagami Y. Amphimic acids, novel unsaturated C28 fatty acids as DNA topoisomerase I inhibitors from an Australian sponge *Amphimedon* sp. Tetrahedron Letters. 1997;38(32):5667-70.
71. Harada H, Yamashita U, Kurihara H, Fukushi E, Kawabata J, Kamei Y. Antitumor activity of palmitic acid found as a selective cytotoxic substance in a marine red alga. Anticancer Research. 2002;22(5):2587-90.
72. Bruneton J. Farmacognosia: Fitoquímica, Plantas Medicinales: Acribia, Editorial, S.A. ; 2001.
73. Eisenreich W, Rohdich F, Bacher A. Deoxyxylulose phosphate pathway to terpenoids. Trends in Plant Science. 2001;6(2):78-84.
74. Eisenreich W, Schwarz M, Cartayrade A, Arigoni D, Zenk MH, Bacher A. The deoxyxylulose phosphate pathway of terpenoid biosynthesis in plants and microorganisms. Chemistry & Biology. 1998;5(9):R221-R33.
75. Baker CH, Matsuda SPT, Liu DR, Corey EJ. Molecular-cloning of the human gene encoding lanosterol synthase from a liver cDNA library. Biochemical and Biophysical Research Communications. 1995;213(1):154-60.
76. Sung CK, Shibuya M, Sankawa U, Ebizuka Y. Molecular cloning of cDNA-encoding human lanosterol synthase. Biol Pharm Bull. 1995;18(10):1459-61.
77. Corey EJ, Matsuda SPT, Bartel B. Molecular-cloning, characterization, and overexpression of Erg7 the *Saccharomyces cerevisiae* gene encoding lanosterol synthase. Proceedings of the National Academy of Sciences USA. 1994;91(6):2211-5.
78. Shi Z, Buntel CJ, Griffin JH. Isolation and characterization of the gene encoding 2,3-oxidosqualene-lanosterol cyclase from *Saccharomyces cerevisiae*. Proceedings of the National Academy of Sciences USA. 1994;91(15):7370-4.
79. Heintz R, Benveniste P. Plant sterol metabolism. Enzymatic cleavage of the 9beta, 19beta-cyclopropane ring of cyclopropyl sterols in bramble tissue cultures. Journal of Biological Chemistry. 1974;249(13):4267-74.
80. Laguarda MJ, Garcia-Llata G, Farré G. Analysis of phytosterols in food. Journal of Pharmaceutical and Biomedical Analysis. 2006;40:1486-96.
81. Phillips KM, Ruggio DM, ASHRAF-KHORASSANI M. Analysis of steryl glucosides in foods and dietery supplements by solid-phase extraction and gas chromatography. Journal of Food Lipids. 2005;12(2):124-40.
82. Phillips KM, Ruggio DM, Toivo JI, Swank MA, Simpkins AH. Free and esterified sterol composition of edible oils and fats. Journal of Food Composition and Analysis. 2002;15(2):123-42.

83. Taylor SL, King JW. Optimization of the extraction and fractionation of corn bran oil using analytical supercritical fluid instrumentation. Journal of Chromatographic Science. 2000;38(3):91-4.
84. Laakso P. Analysis of sterols from various food matrices. European Journal of Lipid Science and Technology. 2005;107(6):402-10.
85. Ahmida H, Bertucci P, Franzò L, Massoud R, Cortese C, Lala A, et al. Simultaneous determination of plasmatic phytosterols and cholesterol precursors using gas chromatography–mass spectrometry (GC–MS) with selective ion monitoring (SIM). Journal of Chromatography B - Analytical Technologies in Biomedical and Life Sciences. 2006;842(1):43-7.
86. Acimovic J, Lövgren-Sandblom A, Monostory K, Rozman D, Golicnik M, Lutjohann D, et al. Combined gas chromatographic/mass spectrometric analysis of cholesterol precursors and plant sterols in cultured cells. Journal of Chromatography B - Analytical Technologies in Biomedical and Life Sciences. 2009;877(22):2081-6.
87. Pereira DM, Vinholes J, De Pinho PG, Valentão P, Mouga T, Teixeira N, et al. A gas chromatography-mass spectrometry multi-target method for the simultaneous analysis of three classes of metabolites in marine organisms. Talanta. 2012;100:391-400.
88. Goh EH, Colles SM, Otte KD. HPLC analysis of desmosterol, 7-dehydrocholesterol, and cholesterol. Lipids. 1989;24(7):652-5.
89. Ruan B, Gerst N, Emmons G, Shey J, Schroepfer G. Sterol synthesis. A timely look at the capabilities of conventional and silver ion high performance liquid chromatography for the separation of C27 sterols related to cholesterol biosynthesis. Journal of Lipid Research. 1997;38(12):2615-26.
90. Oliveira AP, Silva LR, Andrade PB, Valentao P, Silva BM, Goncalves RF, et al. Further insight into the latex metabolite profile of *Ficus carica*. Journal of Agricultural and Food Chemistry. 2010;58(20):10855-63.
91. Nagy K, Jakab A, Pollreisz F, Bongiorno D, Ceraulo L, Averna MR, et al. Analysis of sterols by high-performance liquid chromatography/mass spectrometry combined with chemometrics. Rapid Communications in Mass Spectrometry. 2006;20(16):2433-40.
92. Tian Q, Failla ML, Bohn T, Schwartz SJ. High-performance liquid chromatography/atmospheric pressure chemical ionization tandem mass spectrometry determination of cholesterol uptake by Caco-2 cells. Rapid Communications in Mass Spectrometry. 2006;20(20):3056-60.

93. Honda A, Yamashita K, Miyazaki H, Shirai M, Ikegami T, Xu G, et al. Highly sensitive analysis of sterol profiles in human serum by LC-ESI-MS/MS. Journal of Lipid Research. 2008;49(9):2063-73.
94. Clouse SD. Arabidopsis mutants reveal multiple roles for sterols in plant development. The Plant Cell. 2002;14(9):1995-2000.
95. Schaller H. The role of sterol in plant growth and development. Progress in Lipid Research. 2003.
96. Saenz JP, Sezgin E, Schwille P, Simons K. Functional convergence of hopanoids and sterols in membrane ordering. Proceedings of the National Academy of Sciences USA. 2012;109(35):14236-40.
97. Schaller H. New aspects of sterol biosynthesis in growth and development of higher plants. Plant Physiology and Biochemistry. 2004;42(6):465-76.
98. Barenholz Y. Cholesterol and other membrane active sterols: from membrane evolution to “rafts”. Progress in Lipid Research. 2002;41(1):1-5.
99. Boutte Y, Grebe M. Cellular processes relying on sterol function in plants. Current Opinion in Plant Biology. 2009;12(6):705-13.
100. Luo M, Xiao Y, Li X, Lu X, Deng W, Li D, et al. GhDET2, a steroid 5alpha-reductase, plays an important role in cotton fiber cell initiation and elongation. The Plant journal : for cell and molecular biology. 2007;51(3):419-30.
101. Schrick K, Fujioka S, Takatsuto S, Stierhof YD, Stransky H, Yoshida S, et al. A link between sterol biosynthesis, the cell wall, and cellulose in Arabidopsis. The Plant Journal : for Cell and Molecular Biology. 2004;38(2):227-43.
102. Schrick K, Mayer U, Horrichs A, Kuhnt C, Bellini C, Dangl J, et al. FACKEL is a sterol C-14 reductase required for organized cell division and expansion in Arabidopsis embryogenesis. Genes & Development. 2000;14(12):1471-84.
103. Peterson DW. Effect of soybean sterols in the diet on plasma and liver cholesterol in chicks. Proceedings of the Society of Experimental Biology and Medicine. 1951;78(1):143-7.
104. Pollak OJ. Reduction of blood cholesterol in man. Circulation. 1953;7(5):702-6.
105. Katan MB, Grundy SM, Jones P, Law M, Miettinen T, Paoletti R, editors. Efficacy and safety of plant stanols and sterols in the management of blood cholesterol levels. Mayo Clinic Proceedings; 2003: Elsevier.
106. Ostlund RE, Jr. Phytosterols in human nutrition. Annual Review of Nutrition. 2002;22:533-49.
107. Blair SN, Capuzzi DM, Gottlieb SO, Nguyen T, Morgan JM, Cater NB. Incremental reduction of serum total cholesterol and low-density lipoprotein cholesterol with the

addition of plant stanol ester-containing spread to statin therapy. American Journal of Cardiology. 2000;86(1):46-52.

108. Devaraj S, Autret BC, Jialal I. Reduced-calorie orange juice beverage with plant sterols lowers C-reactive protein concentrations and improves the lipid profile in human volunteers. The American Journal of Clinical Nutrition. 2006;84(4):756-61.
109. Jones P, Demonty I, Chan Y-M, Herzog Y, Pelled D. Fish-oil esters of plant sterols differ from vegetable-oil sterol esters in triglycerides lowering, carotenoid bioavailability and impact on plasminogen activator inhibitor-1 (PAI-1) concentrations in hypercholesterolemic subjects. Lipids in Health and Disease. 2007;6(1):28.
110. Nashed B, Yeganeh B, HayGlass KT, Moghadasian MH. Antiatherogenic effects of dietary plant sterols are associated with inhibition of proinflammatory cytokine production in Apo E-KO mice. The Journal of Nutrition. 2005;135(10):2438-44.
111. Kim S-J, Jeong H-J, Yi B-J, Kang T-H, An N-H, Lee E-H, et al. Transgenic *Panax ginseng* inhibits the production of TNF-α, IL-6, and IL-8 as well as COX-2 expression in human mast cells. The American journal of Chinese medicine. 2007;35(02):329-39.
112. Kobori M, Yoshida M, Ohnishi-Kameyama M, Shinmoto H. Ergosterol peroxide from an edible mushroom suppresses inflammatory responses in RAW264. 7 macrophages and growth of HT29 colon adenocarcinoma cells. British Journal of Pharmacology. 2007;150(2):209-19.
113. Bouic P, Etsebeth S, Liebenberg R, Albrecht C, Pegel K, Van Jaarsveld P. Beta-sitosterol and beta-sitosterol glucoside stimulate human peripheral blood lymphocyte proliferation: implications for their use as an immunomodulatory vitamin combination. International Journal of Immunopharmacology. 1996;18(12):693-700.
114. Navarro A, de Las Heras B, Villar A. Anti-inflammatory and immunomodulating properties of a sterol fraction from *Sideritis foetens* Clem. Biological and Pharmaceutical Bulletin. 2001;24(5):470-3.
115. Othman RA, Moghadasian MH. Beyond cholesterol-lowering effects of plant sterols: clinical and experimental evidence of anti-inflammatory properties. Nutrition Reviews. 2011;69(7):371-82.
116. Delgado-Vargas F, Jiménez A, Paredes-López O. Natural pigments: carotenoids, anthocyanins, and betalains—characteristics, biosynthesis, processing, and stability. Critical Reviews in Food Science and Nutrition. 2000;40(3):173-289.
117. Lichtenthaler HK. Chlorophylls and carotenoids - pigments of photosynthetic biomembranes. Method Enzymol. 1987;148:350-82.

118. Goldman M, Horev B, Saguy I. Decolorization of beta-carotene in model systems simulating dehydrated foods - mechanism and kinetic principles. Journal of Food Science. 1983;48(3):751-4.
119. Rodriguez-Amaya DB. Food carotenoids: analysis, composition and alterations during storage and processing of foods. Forum of Nutrition. 2003;56:35-7.
120. Zanoni B, Peri C, Nani R, Lavelli V. Oxidative heat damage of tomato halves as affected by drying. Food Research International. 1998;31(5):395-401.
121. Namitha KK, Negi PS. Chemistry and Biotechnology of Carotenoids. Critical Reviews in Food Science and Nutrition. 2010;50(8):728-60.
122. Melendez-Martinez AJ, Stinco CM, Liu C, Wang X-D. A simple HPLC method for the comprehensive analysis of cis/trans (Z/E) geometrical isomers of carotenoids for nutritional studies. Food Chemistry. 2013;138(2–3):1341-50.
123. Schieber A, Carle R. Occurrence of carotenoid cis-isomers in food: Technological, analytical, and nutritional implications. Trends in Food Science & Technology. 2005;16(9):416-22.
124. Davies BH. Carotenoids. Chemistry and biochemistry of plant pigments. 2. New York: Academic Press; 1976. p. 38-165.
125. Breithaupt DE. Identification and quantification of astaxanthin esters in shrimp (Pandalus, borealis) and in a microalga (*Haematococcus pluvialis*) by liquid chromatography-mass spectrometry using negative ion atmospheric pressure chemical ionization. Journal of Agricultural and Food Chemistry. 2004;52(12):3870-5.
126. Takaichi S, Matsui K, Nakamura M, Muramatsu M, Hanada S. Fatty acids of astaxanthin esters in krill determined by mild mass spectrometry. Comparative Biochemistry and Physiology - B Biochemistry and Molecular Biology. 2003;136(2):317-22.
127. Wingerath T, Sies H, Stahl W. Xanthophyll esters in human skin. Archives of Biochemistry and Biophysics. 1998;355(2):271-4.
128. Goodwin TW. Biochemistry of the carotenoids. New York: Chapman and Hall; 1980.
129. Aman R, Biehl J, Carle R, Conrad J, Beifuss U, Schieber A. Application of HPLC coupled with DAD, APCI-MS and NMR to the analysis of lutein and zeaxanthin stereoisomers in thermally processed vegetables. Food Chemistry. 2005;92(4):753-63.
130. de Rosso VV, Mercadante AZ. Identification and quantification of carotenoids, by HPLC-PDA-MS/MS, from Amazonian fruits. Journal of Agricultural and Food Chemistry. 2007;55(13):5062-72.

131. Emenhiser C, Simunovic N, Sander LC, Schwartz SJ. Separation of geometrical carotenoid isomers in biological extracts using a polymeric C30 column in reversed-phase liquid chromatography. Journal of Agricultural and Food Chemistry. 1996;44(12):3887-93.
132. Oliver J, Palou A. Chromatographic determination of carotenoids in foods. Journal of Chromatography A. 2000;881(1):543-55.
133. Rezanka T, Olsovska J, Sobotka M, Sigler K. The use of APCI-MS with HPLC and other separation techniques for identification of carotenoids and related Compounds. Current Analytical Chemistry. 2009;5(1):1-25.
134. Young AJ, Lowe GM. Antioxidant and prooxidant properties of carotenoids. Archives of Biochemistry and Biophysics. 2001;385(1):20-7.
135. Yemelyanov AY, Katz NB, Bernstein PS. Ligand-binding characterization of xanthophyll carotenoids to solubilized membrane proteins derived from human retina. Experimental Eye Research. 2001;72(4):381-92.
136. Liu C-L, Huang Y-S, Hosokawa M, Miyashita K, Hu M-L. Inhibition of proliferation of a hepatoma cell line by fucoxanthin in relation to cell cycle arrest and enhanced gap junctional intercellular communication. Chemico-Biological Interactions. 2009;182(2):165-72.
137. Stahl W, Sies H. The role of carotenoids and retinoids in gap junctional communication. International Journal for Vitamin and Nutrition Research 1998;68(6):354.
138. Harrison EH. Mechanisms involved in the intestinal absorption of dietary vitamin A and provitamin A carotenoids. Biochimica et Biophysica Acta (BBA)-Molecular and Cell Biology of Lipids. 2012;1821(1):70-7.
139. Nagao A. Absorption and metabolism of dietary carotenoids. Biofactors. 2011;37(2):83-7.
140. von Lintig J. Metabolism of carotenoids and retinoids related to vision. Journal of Biological Chemistry. 2012;287(3):1627-34.
141. Tanaka T, Shnimizu M, Moriwaki H. Cancer chemoprevention by carotenoids. Molecules. 2012;17(3):3202-42.
142. Libby P, Ridker PM, Maseri A. Inflammation and atherosclerosis. Circulation. 2002;105(9):1135-43.
143. Burke JE, Dennis EA. Phospholipase A 2 structure/function, mechanism, and signaling. Journal of Lipid Research. 2009;50(SUPPL.):S237-S42.
144. Garcia-Pastor P, Randazzo A, Gomez-Paloma L, Alcaraz MJ, Paya M. Effects of petrosaspongiolide M, a novel phospholipase A2 inhibitor, on acute and chronic

inflammation. Journal of Pharmacology and Experimental Therapeutics. 1999;289(1):166-72.

145. Monti MC, Casapullo A, Riccio R, Gomez-Paloma L. PLA2-mediated catalytic activation of its inhibitor 25-acetyl-petrosaspongiolide M: serendipitous identification of a new PLA2 suicide inhibitor. FEBS Letters. 2004;578(3):269-74.
146. Monti MC, Chini MG, Margarucci L, Tosco A, Riccio R, Bifulco G, et al. The molecular mechanism of human group IIA phospholipase A2 inactivation by bolinaquinone. Journal of Molecular Recognition. 2009;22(6):530-7.
147. Posadas I, Terencio MC, De Rosa S, Paya M. Cavernolide: a new inhibitor of human sPLA2 sharing unusual chemical features. Life Sciences. 2000;67(24):3007-14.
148. Potts BCM, Faulkner DJ. Phospholipase-A2 inhibitors from marine organisms. Journal of Natural Products. 1992;55(12):1701-17.
149. Kunisawa J, Kiyono H. Immunological function of sphingosine 1-phosphate in the intestine. Nutrients. 2012;4(3):154-66.
150. Bode C, Gräler MH. Immune regulation by sphingosine 1-phosphate and its receptors. Archivum Immunologiae et Therapia Experimentalis. 2012;60(1):3-12.
151. Pinschewer DD, Brinkmann V, Merkler D. Impact of sphingosine 1-phosphate modulation on immune outcomes. Neurology. 2011;76:S15-S9.
152. Simmons DL, Botting RM, Hla T. Cyclooxygenase isozymes: The biology of prostaglandin synthesis and inhibition. Pharmacological Reviews. 2004;56(3):387-437.
153. Warner TD, Mitchell JA. Cyclooxygenases: new forms, new inhibitors, and lessons from the clinic. The FASEB Journal. 2004;18(7):790-804.
154. Chandrasekharan NV, Simmons DL. The cyclooxygenases. Genome Biology. 2004;5(9):241.
155. Kobayashi T, Narumiya S. Function of prostanoid receptors: Studies on knockout mice. Prostaglandins & Other Lipid Mediators. 2002;68-69:557-73.
156. Brash AR. Lipoxygenases: occurrence, functions, catalysis, and acquisition of substrate. Journal of Biological Chemistry. 1999;274(34):23679-82.
157. Boissel JP, Schwarz PM, Forstermann U. Neuronal-type NO synthase: Transcript diversity and expressional regulation. Nitric Oxide: Biology and Chemistry. 1998;2(5):337-49.
158. Alderton WK, Cooper CE, Knowles RG. Nitric oxide synthases: structure, function and inhibition. Biochemical Journal. 2001;357:593-615.
159. Kleinert H, Schwarz PM, Forstermann U. Regulation of the expression of inducible nitric oxide synthase. Biological Chemistry. 2003;384(10-11):1343-64.

160. Okuyama M, Yamaguchi S, Yamaoka M, Nitobe J, Fujii S, Yoshimura T, et al. Nitric oxide enhances expression and shedding of tumor necrosis factor receptor I (p55) in endothelial cells. Arteriosclerosis, Thrombosis and Vascular Biology. 2000;20(6):1506-11.
161. Meini A, Benocci A, Frosini M, Sgaragli G, Pessina G, Aldinucci C, et al. Nitric oxide modulation of interleukin-1β-evoked intracellular Ca 2+ release in human astrocytoma U-373 mg cells and brain striatal slices. Journal of Neuroscience 2000;20(24):8980-6.
162. Gotoh T, Oyadomari S, Mori K, Mori M. Nitric oxide-induced apoptosis in RAW 264.7 macrophages is mediated by endoplasmic reticulum stress pathway involving ATF6 and CHOP. Journal of Biological Chemistry. 2002;277(14):12343-50.
163. Oyadomari S, Takeda K, Takiguchi M, Gotoh T, Matsumoto M, Wada I, et al. Nitric oxide-induced apoptosis in pancreatic β cells is mediated by the endoplasmic reticulum stress pathway. Proceedings of the National Academy of Sciences. 2001;98(19):10845-50.
164. Toku K, Tanaka J, Yano H, Desaki J, Zhang B, Yang L, et al. Microglial cells prevent nitric oxide-induced neuronal apoptosis in vitro. Journal of Neuroscience Research. 1998;53(4):415-25.
165. Dolcet X, Llobet D, Pallares J, Matias-Guiu X. NF-kB in development and progression of human cancer. Virchows Archiv. 2005;446(5):475-82.
166. Ghosh S, May MJ, Kopp EB. NF-κB and rel proteins: Evolutionarily conserved mediators of immune responses. Annual Review of Immunology. 1998;16:225-60.
167. Verma IM, Stevenson JK, Schwarz EM, Van Antwerp D, Miyamoto S. Rel/NF-κB/IκB family: Intimate tales of association and dissociation. Genes & Development. 1995;9(22):2723-35.
168. Evans PC. Regulation of pro-inflammatory signalling networks by ubiquitin: identification of novel targets for anti-inflammatory drugs. Expert Reviews in Molecular Medicine. 2005;7(12):1-19.
169. Gilmore T. Introduction to NF-κB: players, pathways, perspectives. Oncogene. 2006;25(51):6680-4.
170. Lin Y, Bai L, Chen W, Xu S. The NF-κB activation pathways, emerging molecular targets for cancer prevention and therapy. Expert Opinion on Therapeutic Targets. 2010;14(1):45-55.
171. Kota BP, Huang THW, Roufogalis BD. An overview on biological mechanisms of PPARs. Pharmacological Research. 2005;51(2):85-94.

172. Montagner A, Rando G, Degueurce G, Leuenberger N, Michalik L, Wahli W. New insights into the role of PPARs. Prostaglandins, Leukotrienes and Essential Fatty Acids. 2011;85(5):235-43.
173. Martin H. Role of PPAR-gamma in inflammation. Prospects for therapeutic intervention by food components. Mutation Research. 2010;690:57-63.
174. Ohshima K, Mogi M, Horiuchi M. Role of peroxisome proliferator-activated receptor-gamma in vascular inflammation. International Journal Of Vascular Medicine. 2012:9.
175. Chung SW, Kang BY, Kim SH, Pak YK, Cho D, Trinchieri G, et al. Oxidized low density lipoprotein inhibits interleukin-12 production in lipopolysaccharide-activated mouse macrophages via direct interactions between peroxisome proliferator-activated receptor-gamma and nuclear factor-kappa B. Journal of Biological Chemistry. 2000;275(42):32681-7.
176. Sung B, Park S, Yu BP, Chung HY. Modulation of PPAR in aging, inflammation, and calorie restriction. Journals of Gerontology Series A: Biological Sciences. 2004;59(10):997-1006.
177. Lee YH, Lee NH, Bhattarai G, Yun JS, Kim TI, Jhee EC, et al. PPAR gamma inhibits inflammatory reaction in oxidative stress induced human diploid fibloblast. Cell Biochemistry and Function. 2010;28(6):490-6.
178. Yu MK, Lee JC, Kim JH, Lee YH, Jeon JG, Jhee EC, et al. Anti-inflammatory effect of peroxisome proliferator activated receptor gamma on human dental pulp cells. Journal of Endodontics. 2009;35(4):524-8.
179. Mathers CD, Fat DM, Boerma J. The global burden of disease: 2004 update: World Health Organization; 2008.
180. Ferlay J, Shin HR, Bray F, Forman D, Mathers C, Parkin DM. Cancer incidence and mortality worldwide in 2008 2008 [updated 200806/07/2011]. Available from: http://globocan.iarc.fr.
181. Palmero EI, De Campos S, Campos M, De Souza N, Guerreiro I, Carvalho AL, et al. Mechanisms and role of microRNA deregulation in cancer onset and progression. Genetics and Molecular Biology. 2011;34(3):363-70.
182. Voorhoeve PM. MicroRNAs: Oncogenes, tumor suppressors or master regulators of cancer heterogeneity? Biochimica et Biophysica Acta (BBA)-Reviews on Cancer. 2010;1805(1):72-86.
183. Fesik SW. Promoting apoptosis as a strategy for cancer drug discovery. Nature Reviews Cancer. 2005;5(11):876-85.
184. Hanahan D, Weinberg RA. Hallmarks of cancer: the next generation. Cell. 2011;144(5):646-74.

185. Hacker G. The morphology of apoptosis. Cell and Tissue Research. 2000;301(1):5-17.
186. Crompton M. The mitochondrial permeability transition pore and its role in cell death. Biochemical Journal. 1999;341:233-49.
187. Halestrap A. A pore way to die: the role of mitochondria in reperfusion injury and cardioprotection. Biochemical Society Transactions. 2010;38(4):841.
188. Dirsch VM, Muller IM, Eichhorst ST, Pettit GR, Kamano Y, Inoue M, et al. Cephalostatin 1 selectively triggers the release of Smac/DIABLO and subsequent apoptosis that is characterized by an increased density of the mitochondrial matrix. Cancer Research. 2003;63(24):8869-76.
189. Chipuk JE, Moldoveanu T, Llambi F, Parsons MJ, Green DR. The BCL-2 family reunion. Molecular Cell. 2010;37(3):299-310.
190. Ashkenazi A, Herbst RS. To kill a tumor cell: the potential of proapoptotic receptor agonists. Journal of Clinical Investigation. 2008;118(6):1979-90.
191. Ricci M, El-Deiry W. The extrinsic pathway of apoptosis. In: Gewirtz DA, Holt SE, Grant S, editors. Apoptosis, Senescence, and Cancer. Cancer Drug Discovery and Development: Humana Press; 2007. p. 31-54.
192. Wajant H. The Fas signaling pathway: More than a paradigm. Science. 2002;296(5573):1635-6.
193. Brand MD, Affourtit C, Esteves TC, Green K, Lambert AJ, Miwa S, et al. Mitochondrial superoxide: production, biological effects, and activation of uncoupling proteins. Free Radical Biology and Medicine. 2004;37(6):755-67.
194. Bacher G, Beckers T, Emig P, Klenner T, Kutscher B, Nickel B. New small-molecule tubulin inhibitors. Pure and Applied Chemistry. 2001;73(9):1459-64.
195. Pasquier E, Kavallaris M. Microtubules: A dynamic target in cancer therapy. Iubmb Life. 2008;60(3):165-70.
196. Calligaris D, Verdier-Pinard P, Devred F, Villard C, Braguer D, Lafitte D. Microtubule targeting agents: From biophysics to proteomics. Cellular and Molecular Life Sciences. 2010;67(7):1089-104.
197. Blume-Jensen P, Hunter T. Oncogenic kinase signalling. Nature. 2001;411(6835):355-65.
198. Weinstein IB, Joe AK. Mechanisms of Disease: Oncogene addiction - A rationale for molecular targeting in cancer therapy. Nature Clinical Practice Oncology. 2006;3(8):448-57.
199. Zhang JM, Yang PL, Gray NS. Targeting cancer with small molecule kinase inhibitors. Nature Reviews Cancer. 2009;9(1):28-39.

200. Fabbro D, Ruetz S, Buchdunger E, Cowan-Jacob SW, Fendrich G, Liebetanz J, et al. Protein kinases as targets for anticancer agents: from inhibitors to useful drugs. Pharmacologt & Therapeutics. 2002;93(2-3):79-98.

201. Fernand VE, Losso JN, Truax RE, Villar EE, Bwambok DK, Fakayode SO, et al. Rhein inhibits angiogenesis and the viability of hormone-dependent and -independent cancer cells under normoxic or hypoxic conditions in vitro. Chemico-Biological Interactions. 2011;192(3):220-32.

202. Huang YT, Hwang JJ, Lee PP, Ke FC, Huang JH, Huang CJ, et al. Effects of luteolin and quercetin, inhibitors of tyrosine kinase, on cell growth and metastasis-associated properties in A431 cells overexpressing epidermal growth factor receptor. British Journal of Pharmacology. 1999;128(5):999-1010.

203. Joh EH, Kim DH. Kalopanaxsaponin A ameliorates experimental colitis in mice by inhibiting IRAK-1 activation in the NF-κB and MAPK pathways. British Journal of Pharmacology. 2011;162(8):1731-42.

204. Konkimalla VB, Efferth T. Inhibition of epidermal growth factor receptor over-expressing cancer cells by the aphorphine-type isoquinoline alkaloid, dicentrine. Biochemical Pharmacology. 2010;79(8):1092-9.

205. Carmeliet P, Jain RK. Angiogenesis in cancer and other diseases. Nature. 2000;407(6801):249-57.

206. Ferrara N, Hillan KJ, Gerber HP, Novotny W. Discovery and development of bevacizumab, an anti-VEGF antibody for treating cancer. Nature Reviews Drug Discovery. 2004;3(5):391-400.

207. Harris AL. Hypoxia - A key regulatory factor in tumour growth. Nature Reviews Cancer. 2002;2(1):38-47.

208. Bos R, Zhong H, Hanrahan CF, Mommers ECM, Semenza GL, Pinedo HM, et al. Levels of hypoxia-inducible factor-1 alpha during breast carcinogenesis. Journal of the National Cancer Institute. 2001;93(4):309-14.

209. Carpini JD, Karam AK, Montgomery L. Vascular endothelial growth factor and its relationship to the prognosis and treatment of breast, ovarian, and cervical cancer. Angiogenesis. 2010;13(1):43-58.

210. Harris AL. Hypoxia-a key regulatory factor in tumour growth. Nature Reviews Cancer. 2002;2(1):38-47.

211. Holmes K, Roberts OL, Thomas AM, Cross MJ. Vascular endothelial growth factor receptor-2: structure, function, intracellular signalling and therapeutic inhibition. Cellular signalling. 2007;19(10):2003-12.

212. Folkman J, Bach M, Rowe JW, Davidoff F, Lambert P, Hirsch C, et al. Tumor Angiogenesis - Therapeutic Implications. New England Journal of Medicine. 1971;285(21):1182-&.
213. Masson-Gadais B, Houle F, Laferriere J, Huot J. Integrin alpha(v)beta(3) requirement for VEGFR2-mediated activation of SAPK2/p38 and for Hsp90-dependent phosphorylation of focal adhesion kinase in endothelial cells activated by VEGF. Cell Stress and Chaperones. 2003;8(1):37-52.
214. Holmqvist K, Cross M, Riley D, Welsh M. The Shb adaptor protein causes Src-dependent cell spreading and activation of focal adhesion kinase in murine brain endothelial cells. Cellular Signalling. 2003;15(2):171-9.
215. Kitamura T, Asai N, Enomoto A, Maeda K, Kato T, Ishida M, et al. Regulation of VeGF-mediated angiogenesis by the Akt/PKB substrate Girdin. Nature Cell Biology. 2008;10(3):329-U62.
216. Cohen EEW, Seiwert TY. Targeting angiogenesis in head and neck cancer. Seminars in Oncology. 2008;35(3):274-85.
217. Kim ES, William WN, Kies MS, Fossella FV, Liu DD, Gladish G, et al. Phase 2 study of carboplatin, docetaxel, and bevacizumab as frontline teatment for advanced nonsmall-cell lung cancer. Cancer. 2010;116(10):2401-8.
218. Bocca C, Bozzo F, Cannito S, Colombatto S, Miglietta A. CLA reduces breast cancer cell growth and invasion through ER alpha and PI3K/Akt pathways. Chemico-Biological Interactions. 2010;183(1):187-93.
219. Fang J, Xia C, Cao ZX, Zheng JZ, Reed E, Jiang BH. Apigenin inhibits VEGF and HIF-1 expression via PI3K/AKT/p70S6K1 and HDM2/p53 pathways. Faseb Journal. 2005;19(3):342-53.
220. Hasebe Y, Egawa K, Yamazaki Y, Kunimoto S, Hirai Y, Ida Y, et al. Specific inhibition of hypoxia-inducible factor (HIF)-1 alpha activation and of vascular endothelial growth factor (VEGF) production by flavonoids. Biological and Pharmaceutical Bulletin. 2003;26(10):1379-83.
221. Zhang X, Song Y, Wu Y, Dong Y, Lai L, Zhang J, et al. Indirubin inhibits tumor growth by antitumor angiogenesis via blocking VEGFR2-mediated JAK/STAT3 signaling in endothelial cell. International Journal of Cancer. 2011;7(6).
222. Gridelli C, Rossi A, Maione P, Rossi E, Castaldo V, Sacco PC, et al. Vascular disrupting agents: a novel mechanism of action in the battle against non-small cell lung cancer. Oncologist. 2009;14(6):612-20.
223. Kaufman RJ. Stress signaling from the lumen of the endoplasmic reticulum: coordination of gene transcriptional and translational controls. Genes & Development. 1999;13(10):1211-33.

224.Schroder M, Kaufman RJ. The mammalian unfolded protein response. Annu Rev Biochem. 2005;74:739-89.

225.Yoshida H. ER stress and diseases. Febs J. 2007;274(3):630-58.

226.Ron D, Walter P. Signal integration in the endoplasmic reticulum unfolded protein response. Nature Reviews Molecular cell biology. 2007;8(7):519-29.

227.Zhang K, Kaufman RJ. From endoplasmic-reticulum stress to the inflammatory response. Nature. 2008;454(7203):455-62.

228.Szegezdi E, Logue SE, Gorman AM, Samali A. Mediators of endoplasmic reticulum stress-induced apoptosis. EMBO reports. 2006;7(9):880-5.

229.Harding HP, Calfon M, Urano F, Novoa I, Ron D. Transcriptional and translational control in the mammalian unfolded protein response. Annual Review of Cell and Developmental Biology. 2002;18:575-99.

230.Oyadomari S, Mori M. Roles of CHOP/GADD153 in endoplasmic reticulum stress. Cell Death and Differentiation. 2004;11(4):381-9.

231. Pahl HL, Baeuerle PA. Activation of NF-κB by ER stress requires both Ca2+and reactive oxygen intermediates as messengers. FEBS Letters. 1996;392(2):129-36.

232.Tu BP, Weissman JS. Oxidative protein folding in eukaryotes mechanisms and consequences. The Journal of Cell biology. 2004;164(3):341-6.

233.Mathers J, Fraser JA, McMahon M, Saunders RD, Hayes JD, McLellan LI, editors. Antioxidant and cytoprotective responses to redox stress. Biochemical Society Symposia; 2004: London; Portland on behalf of The Biochemical Society; 1999.

234.Endo M, Oyadomari S, Suga M, Mori M, Gotoh T. The ER stress pathway involving CHOP is activated in the lungs of LPS-treated mice. J of Biochemistry. 2005;138(4):501-7.

235.Haze K, Okada T, Yoshida H, Yanagi H, Yura T, Negishi M, et al. Identification of the G13 (cAMP-response-element-binding protein-related protein) gene product related to activating transcription factor 6 as a transcriptional activator of the mammalian unfolded protein response. Biochemical Journal. 2001;355(Pt 1):19.

236.Yoshida H, Okada T, Haze K, Yanagi H, Yura T, Negishi M, et al. ATF6 activated by proteolysis binds in the presence of NF-Y (CBF) directly to the cis-acting element responsible for the mammalian unfolded protein response. Molecular and Cellular Biology. 2000;20(18):6755-67.

237.Nakayama Y, Endo M, Tsukano H, Mori M, Oike Y, Gotoh T. Molecular mechanisms of the LPS-induced non-apoptotic ER stress-CHOP pathway. Journal of Biochemistry. 2010;147(4):471-83.

238.Teske BF, Wek SA, Bunpo P, Cundiff JK, McClintick JN, Anthony TG, et al. A highlights from MBoC Selection: The eIF2 kinase PERK and the integrated stress

response facilitate activation of ATF6 during endoplasmic reticulum stress. Molecular Biology of the Cell. 2011;22(22):4390.

239. Nakagawa T, Yuan J. Cross-talk between two cysteine protease families activation of caspase-12 by calpain in apoptosis. The Journal of Cell Biology. 2000;150(4):887-94.

240. Rao RV, Hermel E, Castro-Obregon S, del Rio G, Ellerby LM, Ellerby HM, et al. Coupling endoplasmic reticulum stress to the cell death program mechanism of caspase activation. Journal of Biological Chemistry. 2001;276(36):33869-74.

241. Saleh M, Vaillancourt JP, Graham RK, Huyck M, Srinivasula SM, Alnemri ES, et al. Differential modulation of endotoxin responsiveness by human caspase-12 polymorphisms. Nature. 2004;429(6987):75-9.

242. Yavari M, Brinkley G, Klapstein K, Hartwig W, Rao R, Hermel E. Presence of the functional CASPASE-12 allele in Indian subpopulations. International Journal of Immunogenetics. 2012;39(5):389-93.

243. Hitomi J, Katayama T, Eguchi Y, Kudo T, Taniguchi M, Koyama Y, et al. Involvement of caspase-4 in endoplasmic reticulum stress-induced apoptosis and Aβ-induced cell death. The Journal of Cell Biology. 2004;165(3):347-56.

244. Puthalakath H, O'Reilly LA, Gunn P, Lee L, Kelly PN, Huntington ND, et al. ER stress triggers apoptosis by activating BH3-only protein Bim. Cell. 2007;129(7):1337-49.

245. Reimertz C, Kögel D, Rami A, Chittenden T, Prehn JH. Gene expression during ER stress–induced apoptosis in neurons induction of the BH3-only protein Bbc3/PUMA and activation of the mitochondrial apoptosis pathway. The Journal of Cell biology. 2003;162(4):587-97.

246. Li J, Lee B, Lee AS. Endoplasmic reticulum stress-induced apoptosis multiple pathways and activation of p53-up-regulated modulator of apoptosis (puma) and noxa by p53. Journal of Biological Chemistry. 2006;281(11):7260-70.

247. Distelhorst CW, McCormick TS. Bcl-2 acts subsequent to and independent of Ca2+ fluxes to inhibit apoptosis in thapsigargin-and glucocorticoid treated mouse lymphoma cells. Cell Calcium. 1996;19(6):473-83.

248. Raschke W, Baird S, Ralph P, Nakoinz I. Functional macrophage cell lines transformed by Abelson leukemia virus. Cell. 1978;15(1):261-7.

249. Medzhitov R. Toll-like receptors and innate immunity. Nature Reviews Immunology. 2001;1(2):135-45.

250. Zuany-Amorim C, Hastewell J, Walker C. Toll-like receptors as potential therapeutic targets for multiple diseases. Nature Reviews Drug Discovery. 2002;1(10):797-807.

251. Poltorak A, He X, Smirnova I, Liu M-Y, Van Huffel C, Du X, et al. Defective LPS signaling in C3H/HeJ and C57BL/10ScCr mice: mutations in Tlr4 gene. Science. 1998;282(5396):2085-8.

252. Bosshart H, Heinzelmann M. Targeting bacterial endotoxin. Annals of the New York Academy of Sciences. 2007;1096(1):1-17.

253. Rhee SH, Hwang D. Murine Toll-like receptor 4 confers lipopolysaccharide responsiveness as determined by activation of NFκB and expression of the inducible cyclooxygenase. Journal of Biological Chemistry. 2000;275(44):34035-40.

254. Raetz CR. Biochemistry of endotoxins. Annual Review of Biochemistry. 1990;59(1):129-70.

255. Nieves D, Moreno JJ. Effect of Arachidonic and Eicosapentaenoic Acid Metabolism on RAW 264.7 Macrophage Proliferation. Journal of Cellular Physiology. 2006;208:428-34.

256. Suzuki J, Akahane K, Nakamura J, Naruse K, Kamiya H, Himeno T, et al. Palmitate induces apoptosis in Schwann cells via both ceramide-dependent and independent pathways. Neuroscience. 2011;176:188-98.

257. Kharroubi I, Ladrière L, Cardozo AK, Dogusan Z, Cnop M, Eizirik DL. Free fatty acids and cytokines induce pancreatic β-cell apoptosis by different mechanisms: role of nuclear factor-κB and endoplasmic reticulum stress. Endocrinology. 2004;145(11):5087-96.

258. Wei Y, Wang D, Topczewski F, Pagliassotti MJ. Saturated fatty acids induce endoplasmic reticulum stress and apoptosis independently of ceramide in liver cells. American Journal of Physiology-Endocrinology and Metabolism. 2006;291(2):E275-E81.